THE UNIVERSITY *of* EDINBURGH

Synthesis and study of novel zwitterionic transition metal complexes and their application as olefin polymerisation catalysts

A thesis submitted for the degree of Doctor of Philosophy by

Michele Melchionna

School of Chemistry
Faculty of Science and Engineering
University of Edinburgh
2006

Declaration

I hereby declare that this thesis has been entirely composed by myself and that the work described herein is my own except where clearly mentioned either in acknowledgement, reference or text. It has not been submitted in whole or in part, for any other degree, diploma or other qualification.

Michele Melchionna

October 2005

This thesis is dedicated to my Dad, whose spirit has always been by my side. Your life and existence have been the greatest teachers I have ever had.

Acknowledgements

Firstly I would like to thank my supervisor Dr. Philip J. Bailey for his guidance and support during my time spent at Edinburgh.

Thanks to Prof. Simon Parsons and his co-workers Dr. Iain Oswald, Dr. Francesca Fabbiani, Dr. Stephen Moggach, Dr. James Davidson, Pete Wood and Fraser White for all their help with the crystallography and for the fantastic work that they have done with all the crystal structures.

Thanks to the technicians and researchers who helped with analytical/structural problem solving: Alan Taylor and Robert Smith (Mass Spec.), John Millar and Dr. Jurai Bella (NMR), Sylvia Williamson (University of St. Andrews) for the CHN analyses, Steve Holding, Catherine Caldecott and Martin Forrest (Rapra Technology) for the GPC analysis. Donald (technician) for his precious help with providing solvents when needed.

I would like to thank the past and present members of my group for their help and for making the time spent in the lab far more pleasant: thanks to Dr. Pedro Pinho, Dr. Chiara McCormack, Dr. Daniel Lorono-Gonzales, Dr. Robert Pfeiffer, Emiliano Clo, Alex Sanchez-Perucha (yeah), Filipa Cavaco and all the Bailey's group "casuals", who are too many to mention.

Thanks to all the wonderful friends I made by working in that "Inorganic Chemistry corridor": Emiliano and Rafa were my initial gurus, Alex (second time mentioned), Iria, Laurent, Pilar, Daniela, Maria, Agostinos, Davide and Chiara (mitici), Andy, Ross, Dot, Robert, the "adopted" (in)organic people Isa, Miriam, Oscar, Pekka, Ewan and Ralph; Costas, Alessandro, Dave and the now far (from Edinburgh) and happy Elaine (bambina, did you really think I would forget you?), Chris and Stuart.

It would be impossible to mention name by name all the other people from the department who have been so important to me; however, a special thank must go to Mike (yo), Maria K. and Andrea.

A special thank also to Lory, for always being there when I needed her, and with whom I shared part of my personal path.

Thanks to all my other friends (whose list is even bigger), especially Emiliano (second time mentioned), Geoff, Olga, Marc, Alessandro, Valeria, Irene, Vassilis, Joana, Drew, Sahar, Cristophe, Wolf, Yavor, Sam, Valentina.

Thanks to my friends down in Italy for their support; again, impossible to mention them all, but especially Tony, Marina, Daniela, Filippo, Enzo, Giuseppe, Dario and Gianluca.

Thanks to the “Kung Funk” members Manu, Arnaud, Ben and Ralph; may other gigs come to prove how funky and talented we are!

Thanks to the “Donkeys’ Sanctuary”…such a bad football team (not always, though), but such a great source of nice friends.

Thanks to all the people from the tango society, for being such nice friends and such nice dancers.

Thanks to the Italian squad for having won the football World Cup 2006! That was particularly special to all the Italians leaving abroad.

I would especially like to thank my family – To my Mom for constantly looking after me in every way (real Italian mom!), to my brother Antonio (hoping he will finally make up his mind about “that one thing”…), my auntie Carmela (tettìiì…), and my two cousins Michela and Antonio, plus all the other members of the family.

Finally thanks to Silvia, for being a little bit everywhere and having the patience to share her days with me…and simply for having appeared in my life.

Abstract

The synthesis, characterization and coordination chemistry of novel zwitterionic late transition metal complexes has been carried out, and an investigation of their ability to act as olefin polymerisation catalysts has been conducted. These systems are based on 6-aminofulvene-2-aldiminate ligands (R_2AFA^-) which are capable of binding metal centres via two nitrogen donors, delocalising the negative charge into their cyclopentadienyl moiety, thus resulting in the formation of neutral zwitterionic complexes. Preparation and characterisation of mono- and di-substituted complexes such as $Ph_2AFACuPPh_3$, $(Ph_2AFA)_2Zn$, $(Ph_2AFA)_2Co$, $(Ph_2AFA)_2Ni$ and $(Ph_2AFA)_2Pd$ have revealed that this type of ligand has enough flexibility to distort upon coordination to the metal depending on geometrical or steric restrictions. As a result, when the ligand coordination involves narrow binding angle of the metal chelate, as it happens in the square-planar species, a severe loss of planarity of the ligand framework is observed, in contrast with the tetrahedral structures where such binding angles are wider.

Although the coordination of the ligand primarily occurs through the nitrogen donors, once they have been occupied by the metal centre, it is possible to exploit the aromatic Cp ring for coordination to a Cp^*Ru^+ unit. In this way, the synthesis and characterisation of two- and tri-metallic complexes $[(Cp^*Ru)(Ph'_2AFA)Pd(\eta^3\text{-}C_3H_5)][BF_4]$ (where Ph'= 2,4,6-trimethylphenyl) and $[(Cp^*Ru)_2(Ph_2AFA)_2Pd][BF4]_2$ has been achieved, featuring the R_2AFA^- molecule acting as an ambidentate ligand, binding the palladium atom in a diimine fashion and the ruthenium centres by means of the C_5 ring. The synthesis of the complex Cp^*RuPh_2AFA where the two N atoms are vacant was also achieved and it was found that this compound acts as a proton sponge in the presence of protic solvents.

In an effort to prepare AFA-metal complexes which could be of potential use in olefin polymerisation catalysis, two novel species, $[(Ph_2AFA)Pd(Me)PPh_3]$ and $[(Ph'_2AFA)Pd(C_3H_5)]$ (where Ph'= 2,4,6-trimethylphenyl) have been synthesised and

characterised, and polymerisation tests with ethylene have been carried out. Some preliminary screening of other molecules as monomers for polymerisation catalysis has also been conducted.

Table of Contents

Table of abbreviations

°	degree
° C	degree centigrade
Å	angstrom
Ar	aryl
AFA	6-aminofulvene-2-aldiminate
AFAH	6-aminofulvene-2-aldimine
ATI	2-aminotroponiminate
Bu	butyl
^{t}Bu	*tert*-butyl
Bz	benzyl
ca.	*circa*
cal	calorie
COD	cyclooctadiene
Cp	cyclopentadienyl
Cp*	pentamethylcyclopentadienyl
Cy	cyclohexyl
DCM	dichloromethane
deg	degree
DFT	Density Functional Theory
DME	Dimethyl ethylene glycol
DMF	Dimethylformamide
DMS	Dimethylsulfate
DMSO	Dimethylsulfoxide
DSSC	Dye-Sensitised Solar Cell
et al.	*et alli* (and others)
EtOH	Ethanol

Et	ethyl
Et_2O	Diethyl ether
EIMS	electron impact mass spectrometry
FABMS	fast atom bombardment mass spectroscopy
FT	Fourier Transform
g	gram
GPC	Gel permeation chromatography
HOMO	Highest Occupied Molecular Orbital
h	hour
Hz	Hertz
IR	infra-red
K	Kelvin
kcal	Kilo calorie
L	Ligand
LLDPE	Linear Low Density Polyethylene
LUMO	Lowest Unoccupied Molecular Orbital
m/z	mass per unit charge
MAO	methylaluminoxane
Me	Methyl
MeCN	Acetonitrile
MeOH	Methanol
min	Minute
ml	Millilitre
MMAO	Modified methylaluminoxane
mmol	milli moles
M_n	Number-average molecular weight
M_w	Weight-average molecular weight
mol	Moles
MS	Mass spectrometry
NMR	Nuclear Magnetic Resonance

Ph	Phenyl
PhCN	Benzonitrile
Py	pyridine
ppm	Parts per million
Pr	propyl
Pr^i	iso-propyl
R	alkyl
T	temperature
THF	tetrahydrofuran
TMA	trimethyaluminium

Chapter 1

Introduction

1.1 Background

It is a common assumption that the structures and reactivities, as well as the catalytic activities, of organometallic transition metal complexes are predominantly governed by dative bonds. Conversely, electrostatic interactions are mainly invoked when biochemical systems and enzymes are considered, leading sometimes to the misleading idea that the two realms are clearly separated and can be individually studied by means of the two different types of interaction.

In reality, the borderline between these two realms is not clear-cut and both the dative bonds and the electrostatic interactions need to be taken into account for an accurate description of the individual system. In the case of metalloenzymes, for example, electrostatic interactions do play the most crucial role, but their models and biomimetic catalysis often require invoking dative interactions with mainly electronegative atoms such as N, O and S.[1] On the other hand, electrostatic interactions with less electronegative atoms such as C, P and H, play a secondary, but definite, role in organometallic complexes. Of significant importance, for example, are the ion-pairing effects in both main group[2] and transition metal[3] organometallic species, especially when catalysis is considered. The role of such ion-paring effects is still somewhat obscure on an intermolecular level and not easily approachable experimentally. By contrast, intramolecular ion-pairing is much more well-defined, and in this context zwitterionic complexes need a special consideration.

By definition, a zwitterion (from German "Zwitter" – "hybrid") is a compound with acidic and basic groups in the same molecule. At neutral pH, most zwitterions are therefore negatively charged anions and positively charged cations at the same time. Due to entropic effects, the disappearance of the charge separation is expected as a consequence of a rearrangement of the molecule; the existence, and even more the isolation, of the *a priori* fragile zwitterionic species is therefore of

considerable significance. Beyond the simple curiosity towards these intriguing molecules, recent research has been moving the studies of zwitterionic systems to a more purposeful level. Over the last decades, the study of zwitterionic species has been aimed at the synthesis of molecules which could have practical uses in an ample range of different areas, spreading from the detergent industry (e.g. CHAPS) [4] to the investigation of non-linear optical responses.[5] One of the areas where zwitterionic species have enjoyed a fast growth is that of homogeneous catalysis, which has witnessed the discovery of novel zwitterionic catalytic systems for a number of different chemical transformations. As far as homogeneous catalysis is concerned, organometallic transition metal complexes are of primary importance. The scope of this chapter is to give a general overview of the recent developments in the synthesis of stable zwitterionic transition metal complexes and their applications in homogeneous catalysis. Because of the ultimate goal of the present research project, particular emphasis is given to zwitterionic species as catalysts for alkene polymerisation and a more detailed discussion of such catalysts is outlined in the introduction to Chapter 4.

1.2. Zwitterionic organometallic complexes

The formulation of an organometallic complex, and in general of a metal complex, as a zwitterion is not a trivial task. In the first instance, contribution from orbital components is normally neglected, so that the situation is conveniently simplified; the through-space electrostatic interaction thus corresponds to the potential energy generated by two opposite unit charges, interacting isotropically. Secondly, the existence of "truly zwitterionic" (or "mesoionic zwitterionic") complexes, where no non-zwitterionic structures can be drawn by resonance of the π-electrons, is not frequently encountered. More commonly, complexes only have a partial zwitterionic character, with the two charges possibly cancelled out by resonance to a non-zwitterionic form. In these cases, the importance of each single resonance form needs to be taken into account in order to appraise the "zwitterionicity" of the molecule. Normally, when one refers to a metal complex as a zwitterionic species, it is actually referring to a complex which is formulated by a main zwitterionic resonance form

and stabilised by secondary non-zwitterionic forms. The most common cases which can be encountered are substantially three: 1) α-dipole, which is the trivial situation corresponding to ionic (A^+, B^-) and semipolar bonds (A^+–B^-), where the charge separation is only formal, being the bonds degenerate by non-zwitterionic resonance forms (A–B, A=B, A↔B). 2) β-dipole, where the two charges are two-bonds separated and the situation can be mesoionic (A^+–B–C^-) or otherwise (A^+=B–C^- ↔ A–B=C); examples are the well studied derivatives of phosphonium ylide complexes M^-–CH_2–$^+PR_3$.[6] 3) ω-dipole, where the charge separation is topologically enhanced, generally leading to a further destabilisation.

Within these three cases a further distinction can be made according to whether the metal is negatively or positively charged.

1.2.1. Zwitterionic complexes with negatively charged metals

Zwitterionic organometallic complexes bearing the negative charge on the metal atom are also known as metallates,[7] which can be divided into mononuclear and dinuclear species. These types of zwitterions constitute in principle a paradox since they feature a negative charge at an electropositive metal centre and their stability is therefore an intriguing issue. This contradiction is relieved by considering that the negative charge is actually more or less delocalised over the metal-ligand fragment, where normally a number of ligands prone to accept electron density (CO, PR_3…) are present.

Most of the examples of this class of zwitterionic complex in the literature are constituted by the above mentioned phosphonium ylides which are typically prepared by substitution of a labile 2-electron ligand. For example, substitution of the labile THF ligand in the vanadium complex in Scheme 1.1 leads to the isolation of the paramagnetic V(III) ylide complex. [8] The same structure is shown by the Ti(III) analogue.

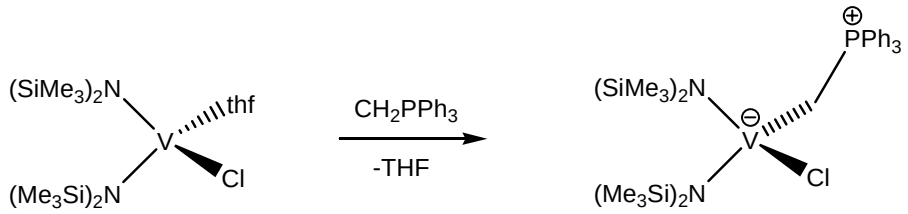

Scheme 1.1. Reaction leading to zwitterionic vanadium(III) complex.

Even more remarkable is the synthesis of the zwitterionic phosphonium carbene metallate $[(R_2N)_2(Cl)Ti^{-}CH^{+}PPh_3]$ (**B**), which is prepared by oxidative coupling of an ylide with the Ti(III) derivative **A** (Scheme 1.2). The presence of the negative charge on the highly electropositive Ti(IV) is particularly intriguing, especially because X-ray analysis shows that the non-zwitterionic form $[(R_2N)_2(Cl)Ti–CH=PPh_3]$ only makes a little contribution to the overall structure and the complex is predominantly zwitterionic.[8]

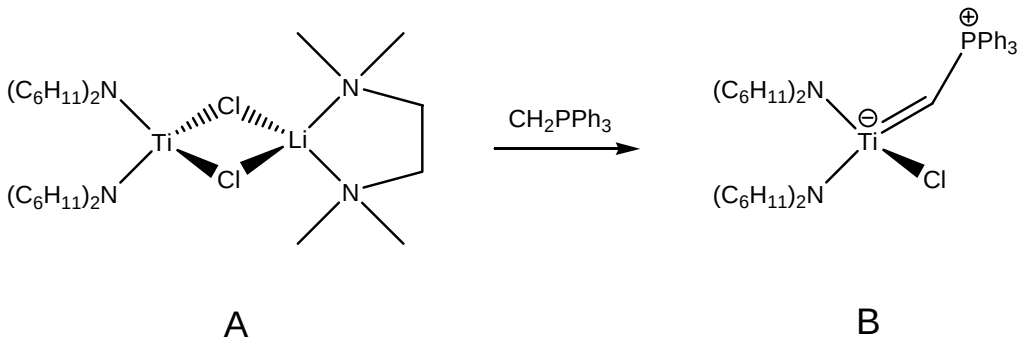

Scheme 1.2. Zwitterionic phosphonium carbene titanium complex (B) prepared by oxidative coupling of an ylide with the Ti(III) derivative A.

The authors rationalised this result by hypothesising a formal negative charge already present in the precursor **A**, which can be formulated as $[(R_2N)_2Ti–Cl_2]^{-}[Li(TMEDA)]^{+}$. Phosphonium zwitterionic complexes with the 2nd row highly electropositive metals such as zirconium have also been reported. For example, [3+2] cycloaddition of the zirconaindene **C** with alkynes provides the phosphoniovinyl zirconate complex **D** (Scheme 1.3).[9] These complexes were described by invoking the existence of two main resonance forms, where the zwitterionic character is determined by means of the two α- and β-phosphonium configuration, so that where

the positive charge is mainly localised on the $-PPh_3$ moiety, the negative charge is delocalised over a bigger metal fragment, imparting more stability to the structure. However, such extra resonance forms are not necessary in terms of stabilization. Isolation of the same type of zirconates featuring one single zwitterionic structure can be obtained by reaction of X=C=S (X = S, NPh) with α-phospholane zirconaindane, leading to the tetracyclic or spyrocyclic complexes **E** and **E'** (Scheme 1.4). [10]

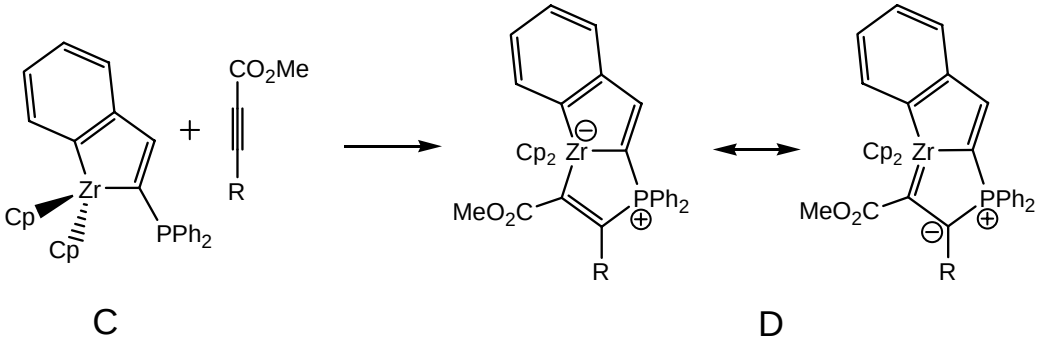

Scheme 1.3. Addition of alkynes to the zirconium derivative C results in the complex D which can be described as a resonance hybrid of two main zwitterionic structures.

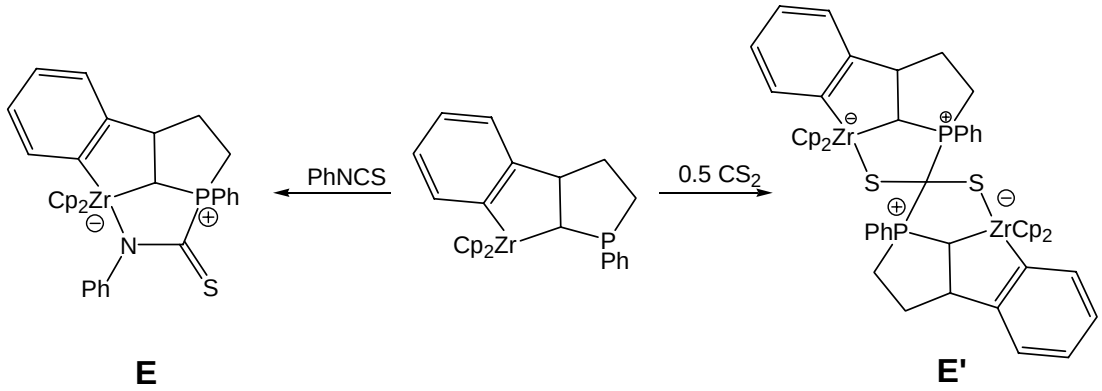

Scheme 1.4. Addition of CS_2 and PhNCS to zirconaindane resulting in bi- (E') and monometallic (E) zwitterionic zirconium complexes.

Phosphonium metallates where the positive and negative charge are several bonds separated have also been reported. These complexes belong to the ω-dipole type and because the larger charge separation leads to greater instability, they are normally stabilised by other resonance forms where the charge separation is decreased. An illustrative example is that of the phosphonium carbene-molybdate complex **F** (Fig

1.1), where the 5-bond separation of the two charges is relieved by additional resonance structures, one of which features an α-ylide form.[11] This is indicated by the short distance of the Mo–C bond, close to those of an alkylidene connection.

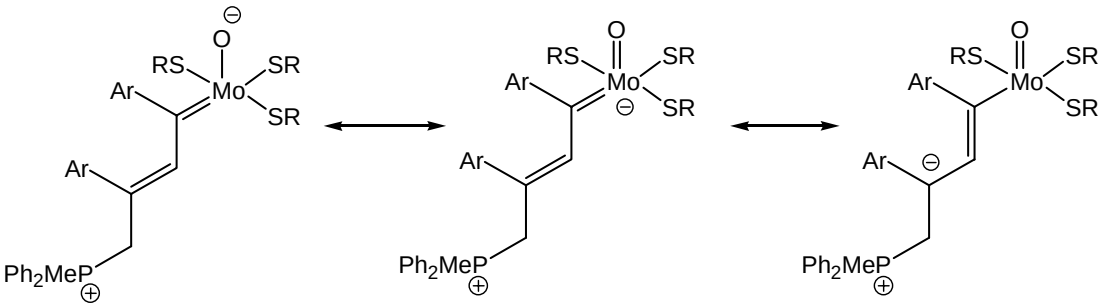

F

Figure 1.1. Three resonance forms for the zwitterionic complex F. The different forms locate the two charges at different distances to each other.

Such a short distance is not found in the related complex **G**, where the Mo–C bond is considerably longer, indicating that neither non-zwitterionic nor ylide resonance forms should be drawn. This is consistent with the higher stabilisation of a zwitterion with a 3-bond charge separation.[11] The same results are found for the Re derivative **H**.[12]

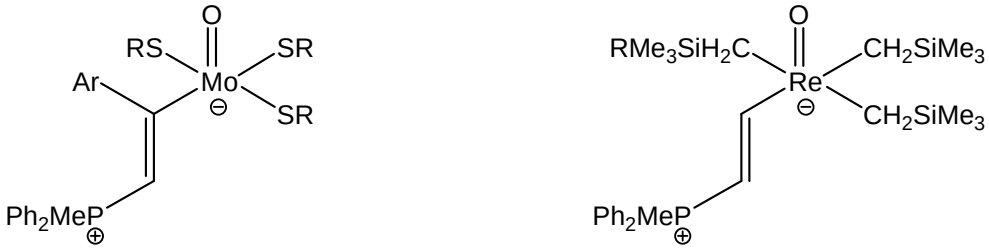

G **H**

Figure 1.2. 3-bonds charge separation occurring in the Mo and Re complexes.

Complexes with a δ charge separation where no other resonance forms intervene to stabilise the structure were recently reported with palladium and platinum metal centres. Such complexes were prepared via an *exo*-nucleophilic attack of α-phosphonium ylides at a cyclooctadiene ligand (Scheme 1.5)[13]

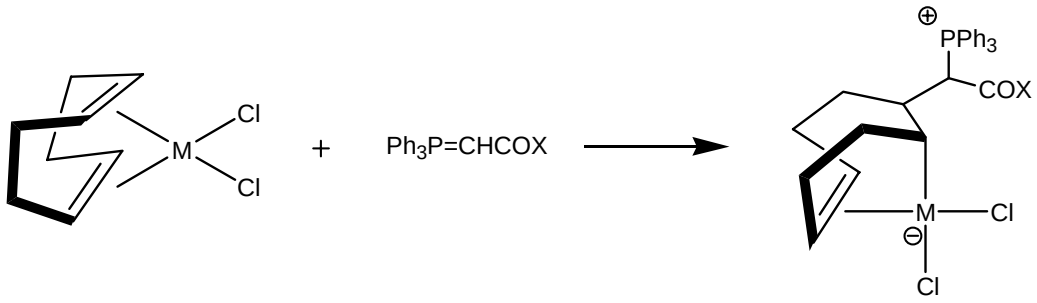

M = Pd, Pt

X = OMe, OEt, NMe_2

Scheme 1.5. δ-charge separation is observed in some Group 10 metal complexes.

Although the phosphonium ylides provide the most common examples of zwitterionic metallates, the occurrence of such species is not limited to them. Other ligands can be suitable for localising the positive charge into a defined region and thus producing an effective charge separation. In this regard, a number of nitrogen-based ligands have been reported to produce zwitterionic species. Several ammonium and iminium metallates are known and their chemistry is currently under investigation. They are generally accessible from Fischer carbenes with cis-azoderivatives and the synthesis works quite well with tungsten derivatives. Sleiman *et al.*, for example, studied the metathesis of the Fischer carbene $(CO)_5W=C(Ph)OCH_3$ with cis-azobenzene and isolated the mesoionic complex **I**.[14] Complex **I** can also be the precursor to the preparation of the corresponding phosphonium species via thermal or photochemical activation and subsequent reaction with PPh_3. [15]

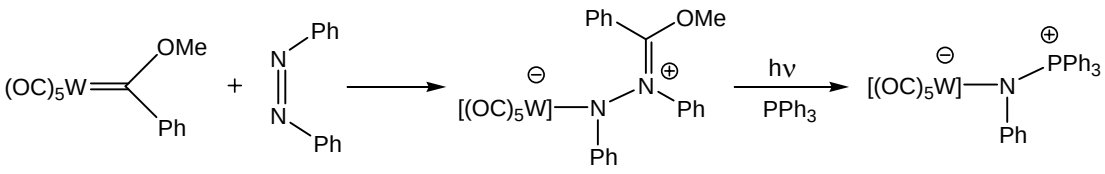

I

Scheme 1.6. Imminium complex with W, formed by reaction of the Fischer carbene $(CO)_5W=C(Ph)OCH_3$ with cis-azobenzene.

McElwee-White et al. showed how the zwitterionic nature of organometallic species can be exploited for synthetic purposes. Under oxidative conditions, **I** represents a precursor for non-zwitterionic imido tungsten complexes, and the main component to the driving force for this reaction is the disappearance of the formal charge separation.[16]

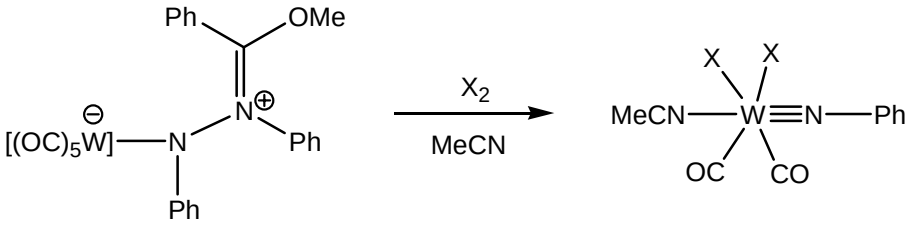

Scheme 1.7. Complex I can lose its zwitterionic character after oxidative addition of halogens.

Pyridinium ylide complexes with metals such as Cr and W have been described, [17] although it is not quite clear whether the stability of such molecules must be ascribed to the aromaticity of the pyridinium moiety, since structural characterisation of non-aromatic 2,5-dihydropyridine has also been reported (Scheme 1.8).[18]

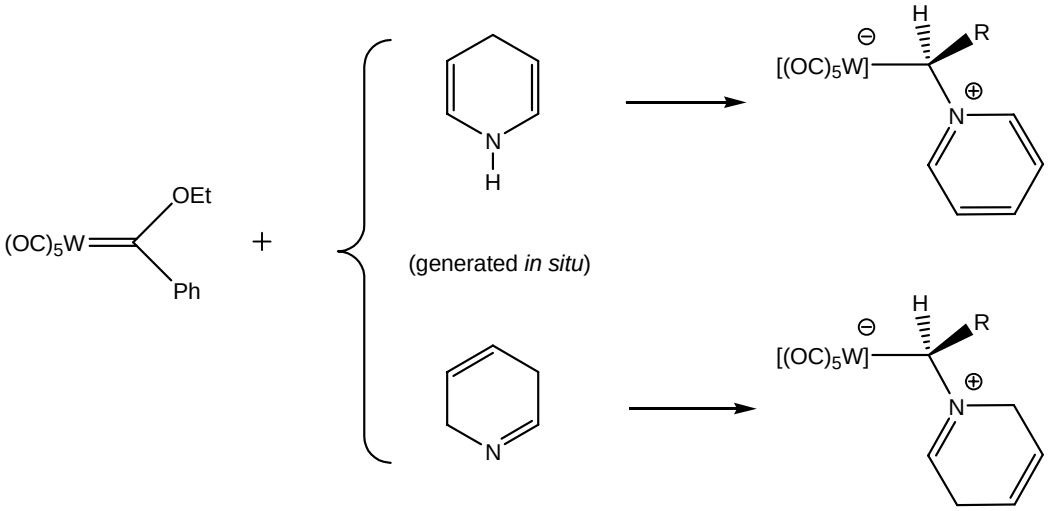

Scheme 1.8. Synthetic route to pyridinium ylide complexes with W.

The preparation and structural characterisation of a novel zwitterionic Re(V) complex with 2-hydroxopyridine has recently been published. In this case the zwitterionic character is intrinsic in the Hhp ligand, for which three resonance forms

can be drawn, and the negative charge is assumed to be transferred to the rhenium centre after coordination leaving a positive charge on the N atom. [19]

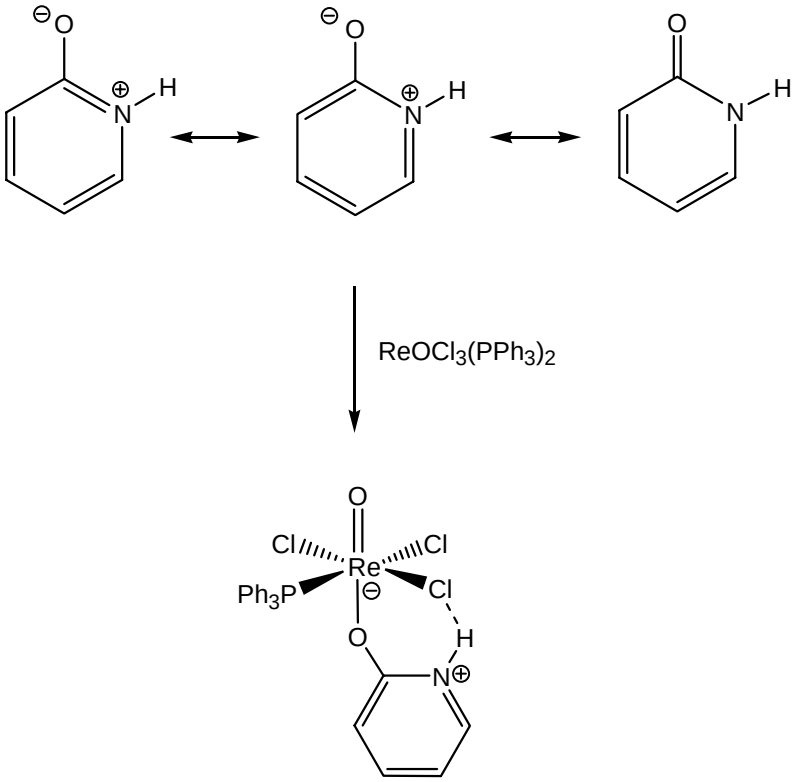

Scheme 1.9. Synthetic route to zwitterionic Re(V) complex with 2-hydroxopyridine.

Indium zwitterionic complexes of the type Br_3InCH_2L where L is a group 15 (N, P, As, Sb) have also been studied, and the novel selenium derivative $Br_3InCH_2SeR^1R^2$ is a related species with particular stability, lacking of any reactivity as ylide carriers by thermal cleavage of the In-C bond. [20]

Finally, special consideration has to be given to that class of transition metal compounds featuring hydrogen bonds of the type $A^{\delta'-}\cdots{}^{\delta+}HX^{\delta-}$. Although hydrogen bonding is generally regarded as electrostatic and does not involve integral formal charges on the A and HX fragments, some examples are given of species where a halide or an oxygen can stabilise, under certain conditions, a truly zwitterionic form where the charge separation is experimentally detectable. For example, formation of the zwitterionic complex **J** (Scheme 1.10) is dictated by strain release produced after insertion of the alkyne into the four-membered metallacycle. The zwitterionic

character is supported by structural data, with the much shorter Ru-O distance in the product in comparison to the starting material and a protonated N atom.[21]

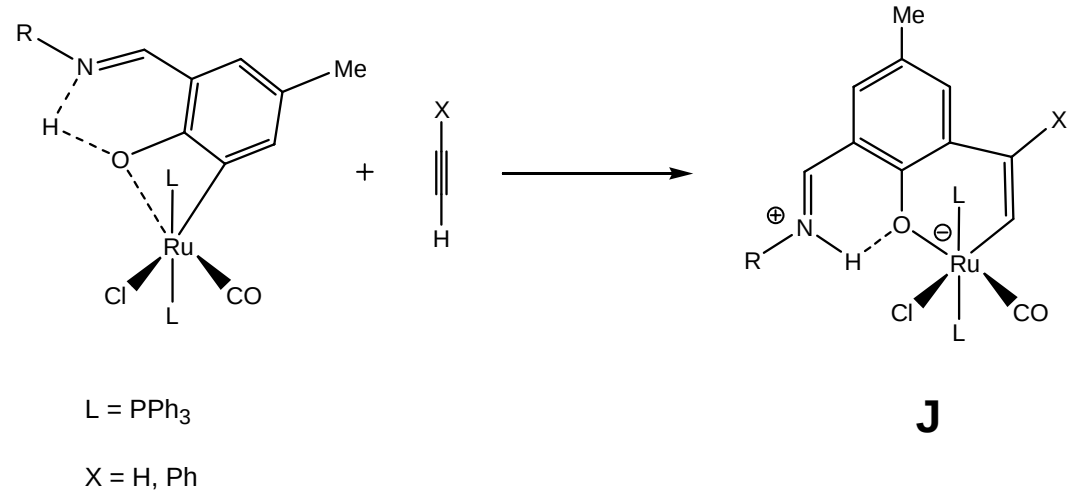

Scheme 1.10. Example of a Ru complex where a H-bond determines the charge separation.

Another interesting example is the one reported by Milstein *et al.*, who described how a non-zwitterionic Pt(IV) complex undergoes a spontaneous stabilisation via intramolecular proton transfer and thus rearranges into the complex **K** (Scheme 1.11). Again, the zwitterionic nature of the product was supported by X-ray analysis. [22]

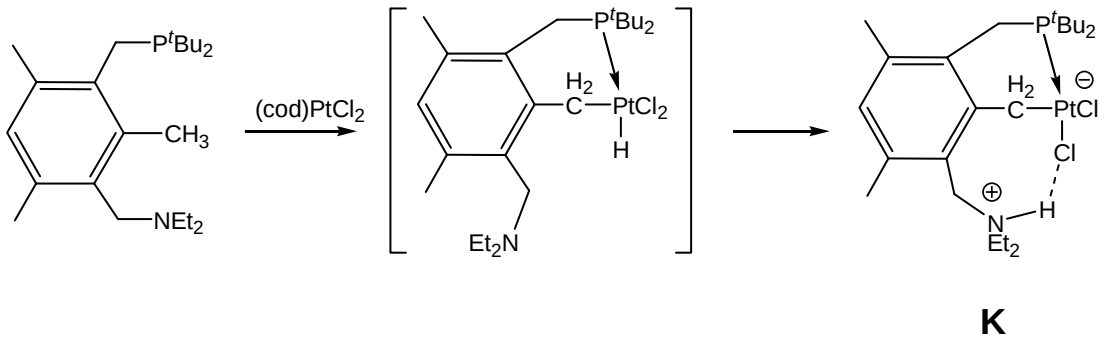

Scheme 1.11. Reaction leading to K. The stability of the product is possible by rearrangement into a zwitterionic species.

Finally, a direct interaction of the hydrogen atom with the metal centre present in a zwitterionic species was described by van Koten, who characterised the platinate(II) complex **L** and established the charge separation via both NMR and X-ray.[23]

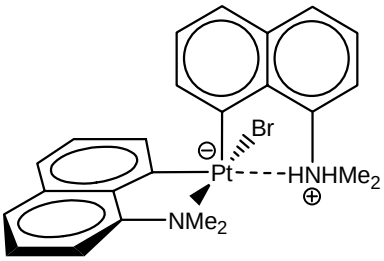

L

Figure 1.3. Zwitterionic platinum complex L, showing the direct interaction of the hydrogen atom with the metal centre.

1.2.2. Zwitterionic complexes with positively charged metals

In contrast with the metallates discussed above, zwitterionic organometallic complexes featuring a positive charge on the metal centre and a negative charge localised in a definite area of the ligand is a more easily justifiable issue. The electropositive metal atom is in principle able to sustain a positive charge, provided that an efficient means to stabilise the negative counter-charge is supplied. There are numerous examples of zwitterionic species with cationic transition metals in the literature and their investigation is mostly driven by potential applications in catalysis. A simple advantage of a neutral charge-separated molecule rather than a salt containing a positively charged metal complex is that its solubility can potentially be exploited either in aqueous than in non-aqueous media. In this regard for example, it is noteworthy to observe that water-soluble catalysts for certain chemical transformations are obtained by tethering ionic functionalities to species known to be effective in organic solvents. Such functionalities would not interfere with the coordination sphere of the positively charged metal centre and serve only to increase the solubility in aqueous media. This potentially allows improvements in catalyst performances, or even afford previously inaccessible transformations. On the other hand, zwitterionic complexes can also be seen as a way to improve the solubility of catalysts in organic media. This case is best represented by homogeneous alkene polymerisation catalysis, which is normally carried out in

organic solvents and where the ionic nature of the active species is sometimes a crucial issue because of its poor solubility. The charge neutrality of zwitterionic analogues would therefore aid catalysis by simply enhancing the concentration of the active species in non-polar solvents, ideally without altering the positively charged environment of the metal centre. Because of the aims of the current research project, zwitterionic complexes for alkene polymerisation catalysis will be discussed in more detail in Chapter 4 and only outlined in the present chapter.

An important class of zwitterionic organometallic complexes featuring cationic metals is that of species bearing borate functionalities, and indeed the main application of such zwitterions is in alkene polymerisation catalysis. The discovery of neutral species where the counter-anion was incorporated within the active species but confined in the periphery relative to the metal centre is only relatively recent, and it can be dated back to the late 80's, when the pioneering work of Hlatky and Turner produced the first examples of zwitterionic zirconium complexes where the negative charge was localised in a tethered borate function (Scheme 1.12).[24]

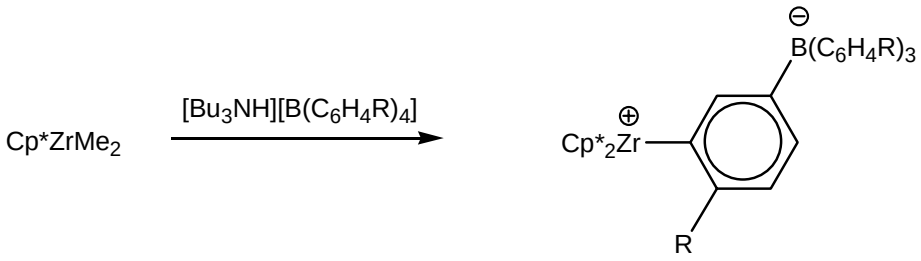

Scheme 1.12. The first example of a zwitterionic zirconium complex with the negative charge localised into a borate fragment.

Since those days, many research groups have focused on the design of zwitterionic Ti, Zr and Hf complexes with borate functionalities which could act as base-free single component polymerisation catalysts, and a number of cyclopentadienyl-containing zwitterionic catalysts of the type shown in Fig 1.4 have periodically been reviewed.[25]

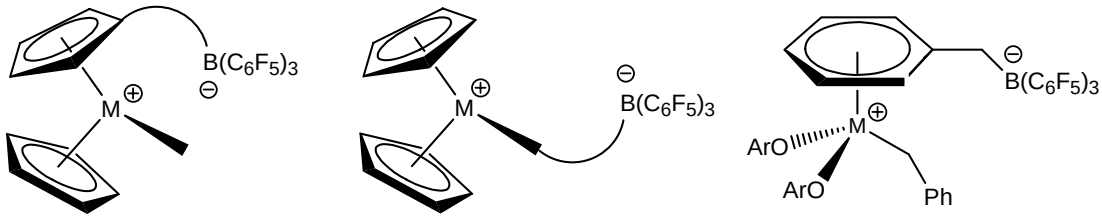

Figure 1.4. Types of zwitterionic complexes active in olefin polymerisation catalysis.

However, this approach has not been limited to group 4 transition metals, but can be used for the preparation of compounds with other metals. In particular, Alper has reported the synthesis of a number of zwitterionic Rh(I) complexes which are successful catalysts for several reactions such as hydroformylation, hydrogenation, polymerisation etc.[26] Complex **M** (Fig 1.5) is a very efficient catalyst for the carbonylation of benzylic and allylic bromides under phase-transfer conditions,[27] whereas the rhodium bis(catecholato)borate complex **N** is used as a catalyst for the hydroboration and diboration of alkenes.[28]

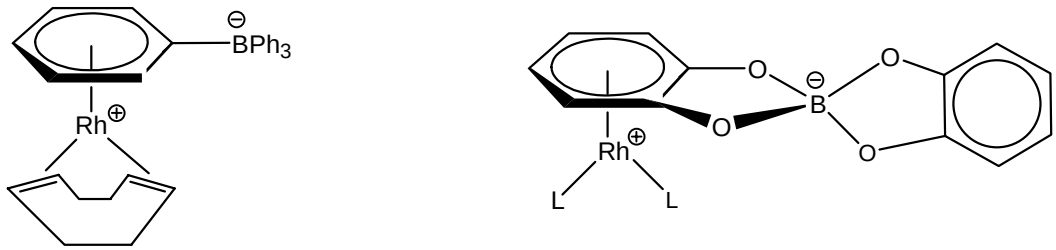

M **N**

Figure 1.5. Zwitterionic rhodium catalysts for the carbonylation of benzylic and allylic bromides (M) and for the hydroboration of alkenes (N).

More recently, reactivity of tantalum derivatives has been exploited to synthesise the cyclopentadienyl tantalum complexes with a borate attached in a girdle position relative to the metal. These species are formed by reaction of the tantalocene methyl methylidene complex with tris(perfluorophenyl)borane $B(C_6F_5)_3$ (Scheme 1.13) and

are shown to be stabilised by ground-state α-agostic interaction of a methylene hydrogen atom.[29]

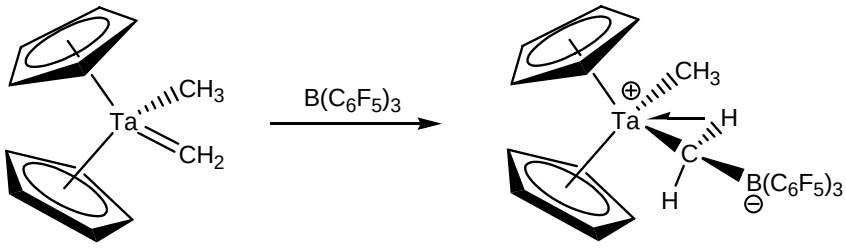

Scheme 1.13. Synthesis of Ta zwitterionic complexes. Stabilisation is possible by α-agostic interaction of a methylene hydrogen with the metal centre.

An extended study of these complexes has shown that a H agostic interaction with a B–H hydrogen is found when the same tantalum derivative is reacted with $HB(C_6F_5)_2$. In this case, if the product is allowed to lose methane in the presence of an excess of the sterically undemanding alkynes of the 2-butyne type, the putative intermediates featuring a borataalkene coordinated in an olefin fashion are trapped in the form of zwitterionic complexes **O**. Such a result is quite striking because it demonstrates the "olefin-like" behaviour of this specific borate ligand despite the flexibility in bonding mode available.[30]

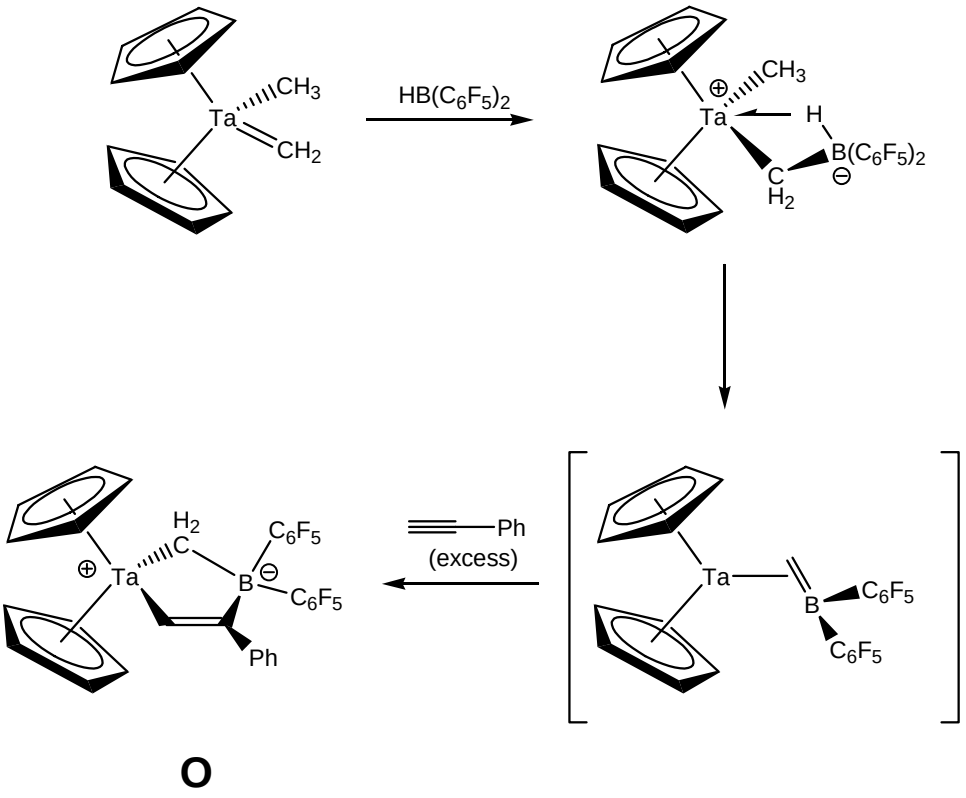

O

Scheme 1.14. B-H agostic interaction with Ta. Loss of methane produces an "olefin-like" borate ligand, which is trapped as a zwitterion (O).

A series of *N*-chelated, zwitterionic complexes with rhodium(I) has been achieved by using the anionic bidentate ligand $[Ph_2B(CH_2NMe_2)_2]^-$. The lithium salt of this anion undergoes facile transmetallation with $[(NBD)RhCl]_2$ (NBD = norbornadiene) to afford the isolation of $[Ph_2B(CH_2NMe_2)_2]Rh(NBD)$.[31] Such a complex is formally zwitterionic and, unlike complexes with the parent (pyrazolyl)borate ligand, there are no simple resonance forms that provide for delocalisation of the anionic borate charge to the nitrogen donors. In the presence of 2 equivalents of phosphine, the bis(phosphine) derivative is obtained, whereas the acetonitrile derivative was provided by using excess of acetonitrile in hydrogenative conditions.

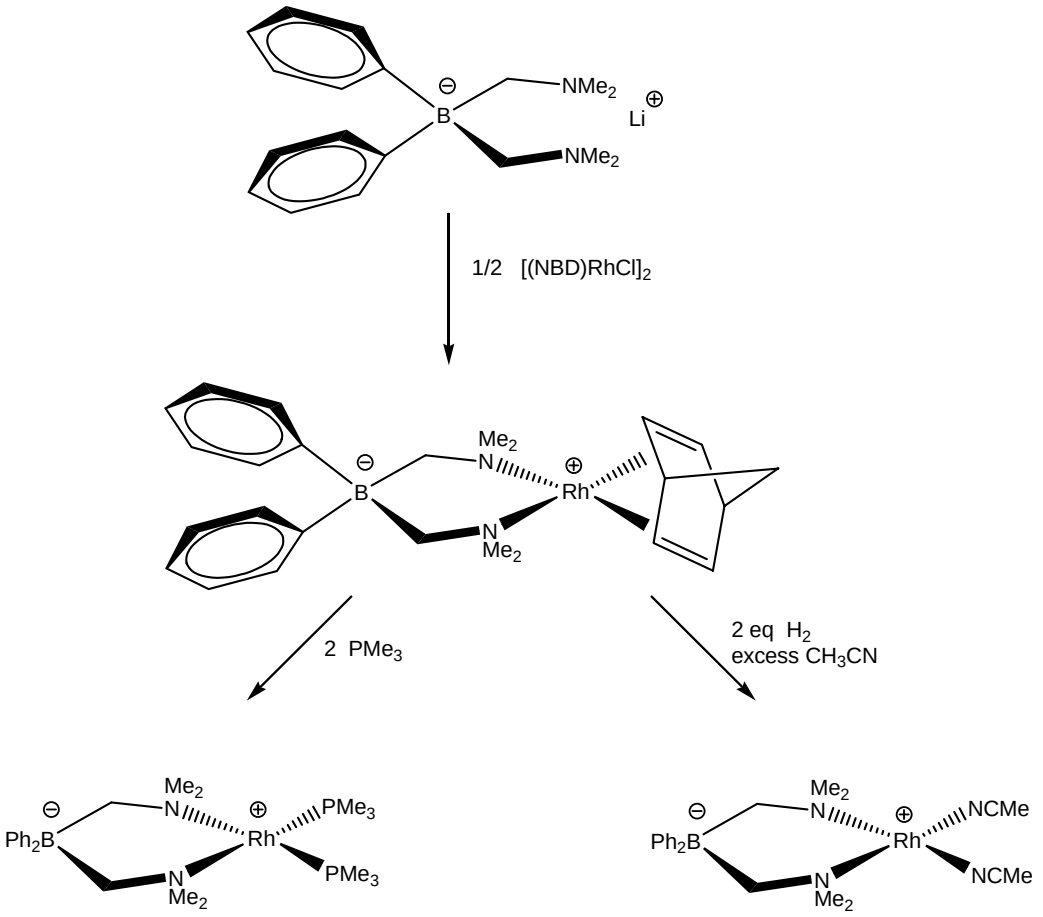

Scheme 1.15. Synthetic routes to *N*-chelated zwitterionic complexes with rhodium(I).

Studies on these zwitterionic systems led to the isolation of several rhodium complexes with phosphorus-based pincers in lieu of the original (dialkylamino)borate, as well as Rh(I) square-planar complexes featuring diverse co-ligand combinations with CO, PMe_3 and CH_3CN. These species constitute the neutral analogues of the well known Osborne and Schrock cationic $[(P\text{-}P)Rh(solv)_2]^+$ complexes[32] and were similarly reported to exhibit catalytic activity for H-E bond addition to olefins (E = C, Si, B).[33]

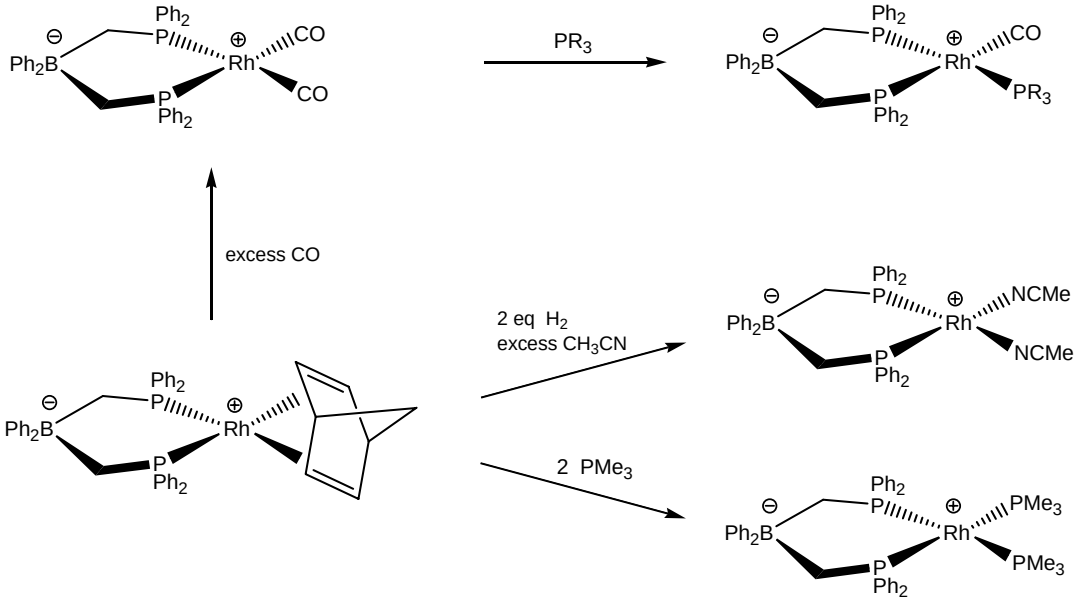

Scheme 1.16. Synthetic routes to *P*-chelated zwitterionic complexes with rhodium(I).

The same type of ligand was also been used in the synthesis of the related zwitterionic palladium complexes displayed in Scheme 1.17 which showed high activity towards CO/ethylene copolymerisation.[34]

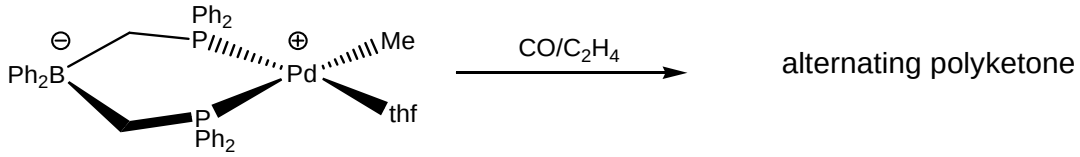

Scheme 1.17. Zwitterionic palladium complex active in CO/C_2H_4 copolymerisation catalysis.

Another way of exploiting a boron atom into the chemistry of transition metal zwitterions is to use a borane cluster. The stanna-*closo*-dodecaborate dianion (Scheme 1.18) reacts with platinum(II)halide complexes, forming the complex **P** where the second negative charge of the dianion is located on the cluster sphere.[35]

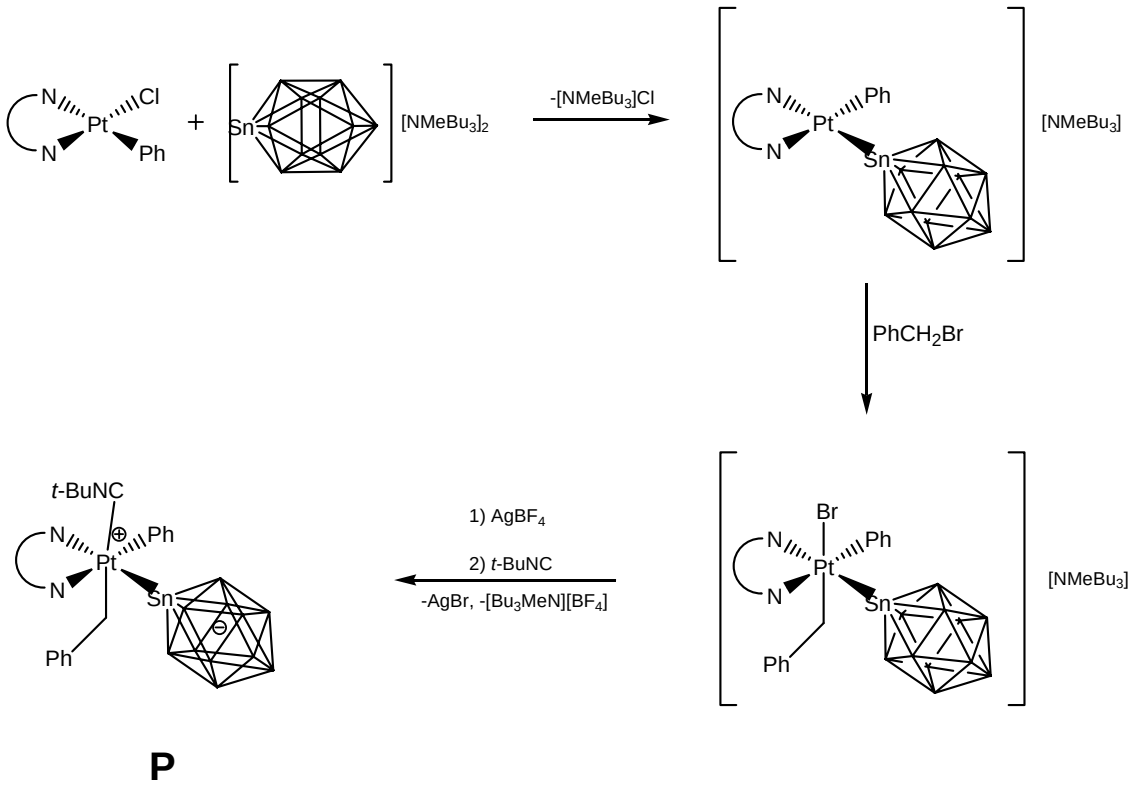

P

Scheme 1.18. Synthetic route to the zwitterionic species P, where one of the negative charge is localises in the borate cluster.

The localisation of the negative charge into a well defined molecule moiety is not a peculiarity of boron-based ligands. Several platinum and palladium complexes with NCN pincers such as those shown in Figure 1.6 combine an organometallic site and with an ionisable M-X bond (X = halide) and an ionic organic group such as $-C\equiv C^-$ or $-SO_3^-$ (counterion Na^+, K^+) in the *para*-position and are therefore potentially zwitterionic.[36]

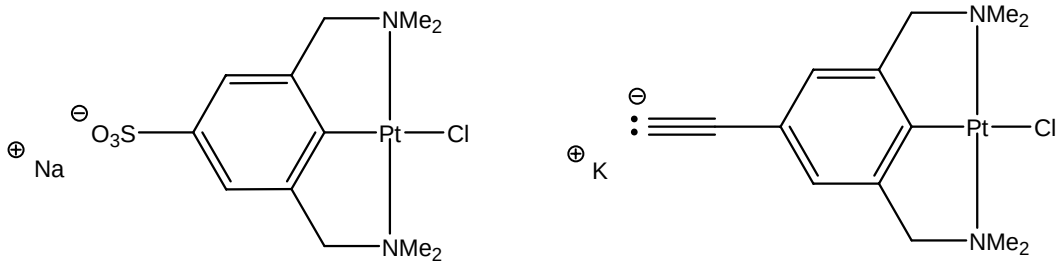

Figure 1.6. Potential zwitterionic platinum complexes.

By selectively removing the counter-ion it is possible to isolate the resulting zwitterionic species; this approach was used to prepare and characterise the arylpalladium (pincer) complex with a tethered sulfato group as *para*-substituent. These complexes are particularly interesting because of the possibility of varying the charge separation by selecting the length of the aliphatic spacers.[37]

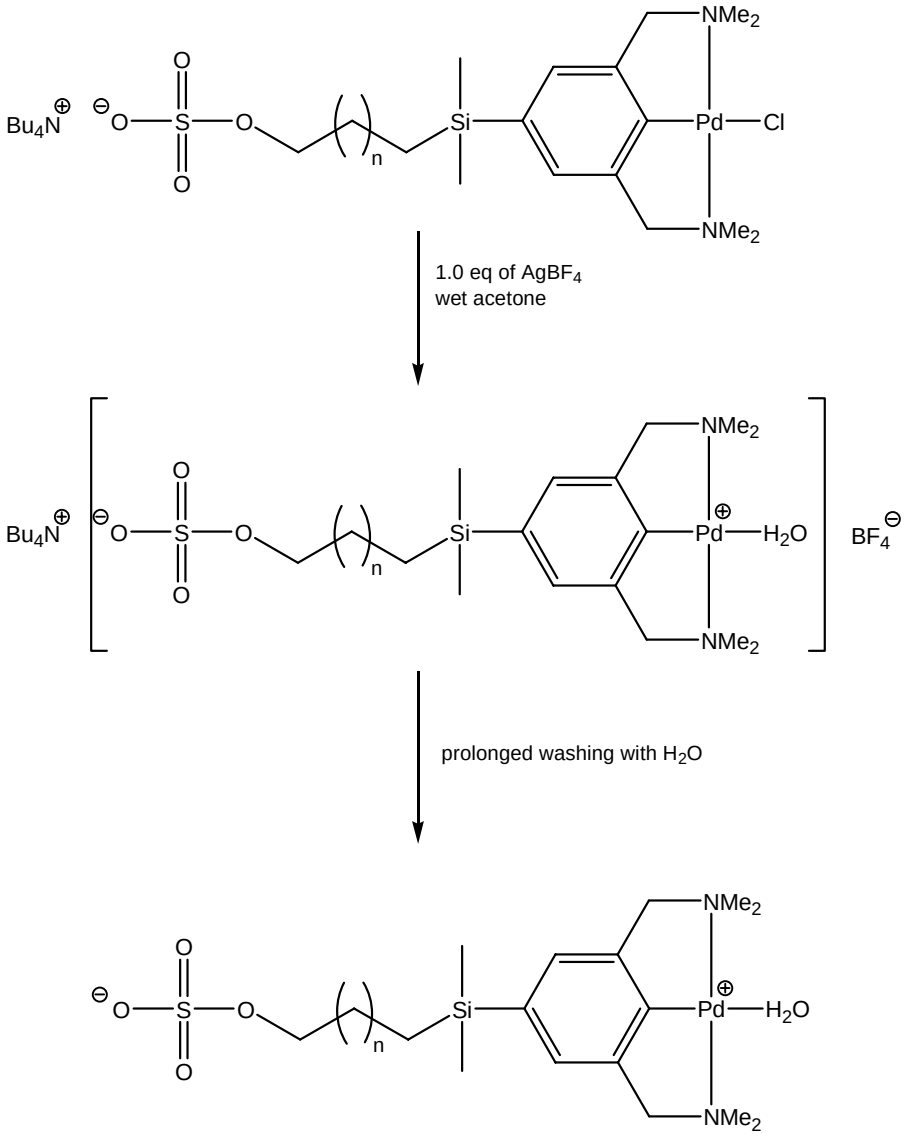

Scheme 1.19. Removal of the counterion generates a zwitterionic Pd complex. The $-(CH_2)_n-$ chain length can be varied leading to different extents of charge separations.

Zwitterionic complexes where the negative charge is localised into a sulphonate groups are also known for rhodium(I) species. Complex **Q** (Fig 1.7) was reported to

be an active catalyst for the liquid-biphase hydrogenolysis of benzo(b)thiophene due to its solubility properties.[38]

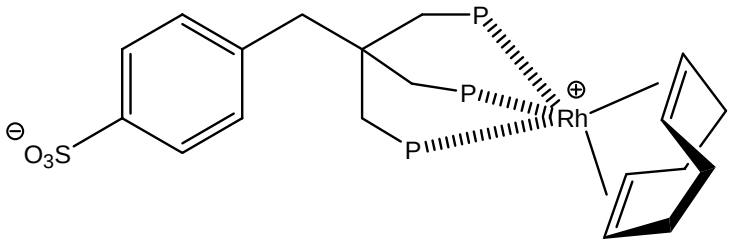

Q

Figure 1.7. Zwitterionic Rh complex showing interesting solubility properties.

The exploitation of ligands which are prone to accommodate the negative charge within their frameworks by delocalisation leading to anionic aromatic structures has also recently been gaining attention. Stradiotto *et al.* have synthesised and studied the zwitterionic Rh(I) complex **R** featuring a κ^2-*P,N* pincer where the negative charge is delocalised into an indenyl moiety;[39] such a complex has been reported to catalyse the dehydrogenative coupling triethylsilane and styrene.[40] The iridium analogue **S** with the same ligand was reported to mediate the hydrogenation of alkenes under mild conditions in a wider range of solvents than the related non-zwitterionic Crabtree's catalyst $[(cod)Ir(PCy_3)(Py)]^+[PF_6]^-$.[41]

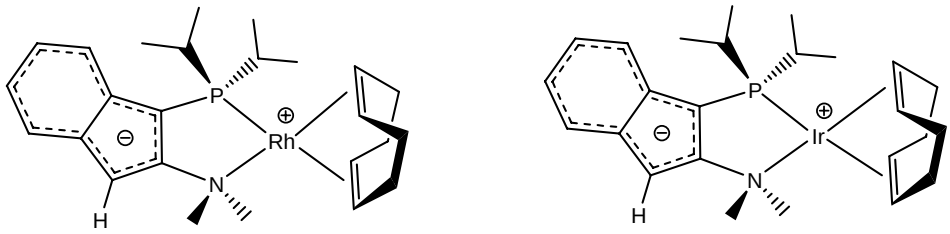

R **S**

Figure 1.8. Stradiotto's complexes of Rh and Ir with indenyl ligands featuring κ^2-*P,N* pincers.

A ruthenium complex with the same ligand was also prepared; however, whereas the CH_3CN-stabilised complex **S** is stable and isolable, the coordinatively unsaturated Ru species rearranges into the isomeric hydridocarbenes **T**.[42]

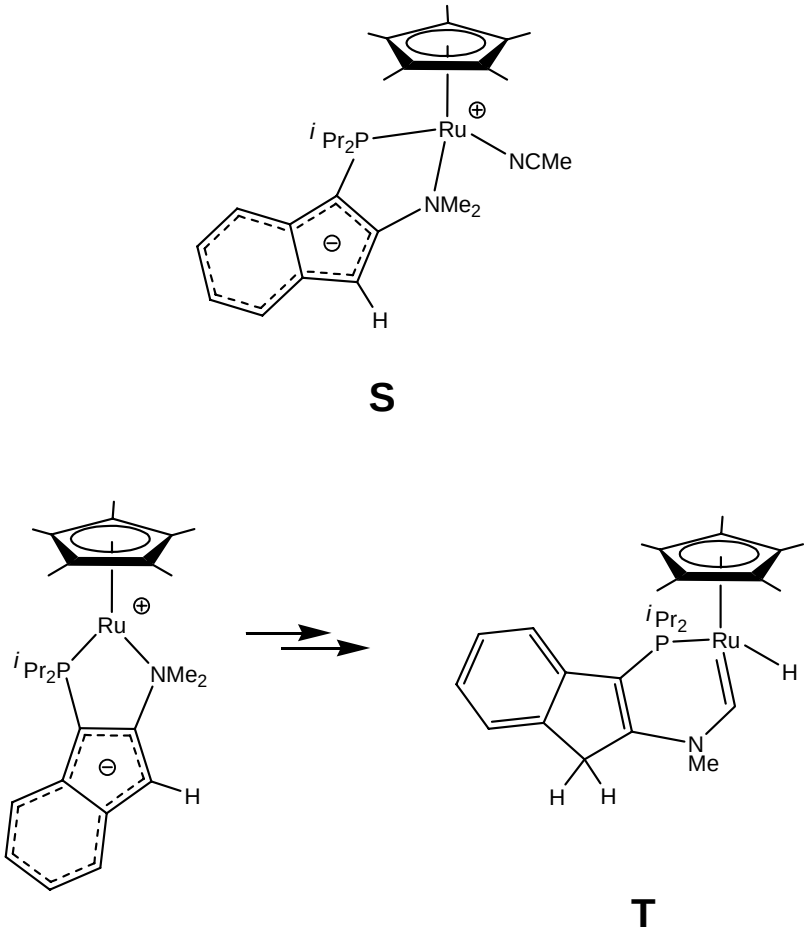

Figure 1.9. The zwitterionic ruthenium complex S is stabilised by a NCMe ligand, whereas the donor-free species rearranges into the isomeric hydridocarbenes T.

The chemistry of these P,N-functionalised indene ligands has recently been extended to Pt(II) and Au(III) metal complexes and the two methyl derivative shown in Fig. 1.10 have been prepared and characterised. However, while the Au(III) complex can be described as a zwitterion, the Pt(II) species contains the neutral ligand and is therefore non-zwitterionic. Moreover, their catalytic utility for the addition of silanes to styrene has been assessed; it was found that whereas the platinum complex reacts in a stoichiometric and catalytic fashion with silanes, the zwitterionic gold analogue showed no reactivity under the same conditions.[43]

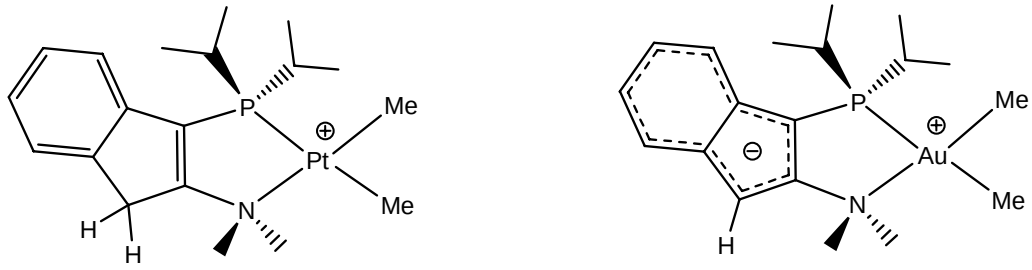

Figure 1.10. Pt and Au analogues of Stradiotto's zwitterions.

In a similar fashion, it is possible to delocalise the negative charge into an aromatic cyclopentadienyl moiety, as described by Stephan et al. for the synthesis of the zwitterionic 1,2-cyclopentadienyl diketimine zirconium complex shown in Fig 1.11.[44]

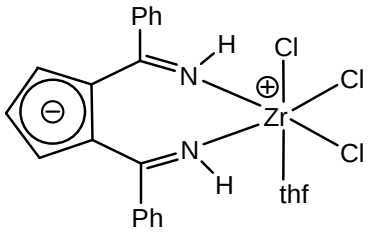

Figure 1.11. Stephan's zwitterionic complex with zirconium. The negative charge is delocalised into the Cp moiety.

Finally, systems where another metal complex fragment is exploited as a charge carrier are also known. In this case, a distinction has to be made according to whether the negative charge is localised on the metal (see next paragraph) or in a defined region of the second metal complex fragment. The latter case is well represented by the recently reported dinuclear Fe-Ru monohydro sesquifulvalene complex shown in Fig 1.12.[45]

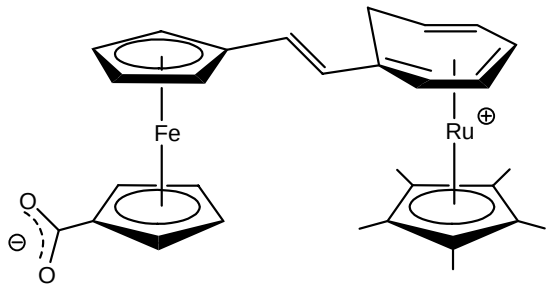

Figure 1.12. Dinuclear Fe-Ru monohydro sesquifulvalene complex.

1.2.3. Zwitterionic complexes with both positively and negatively charged metals

This type of zwitterion is essentially the combination of the two cases just described hitherto in respect to the metal centres. There is a wide range of such bimetallic complexes where one metal centre bears a negative charge and the other one a positive charge, with the two centres linked by means of ligands possessing two distinct binding sites. These complexes can be described by considering a static two-electron transfer from one metal to another and their zwitterionic nature is normally identified on the basis of their structural and spectroscopic features. Because of the extremely wide variety of these species, only a few indicative examples will be given in the present section.

Zwitterionic homo-bimetallic complexes with a number of transition metals are known, although in some cases their zwitterionic nature is still not clearly established. For the zirconium complex shown in Figure 1.13, the charge separation is suggested by electron counting, which indicates two 16-electron Zr(IV) and Zr(II) atoms, and confirmed by the diamagnetism of the molecule,[46]

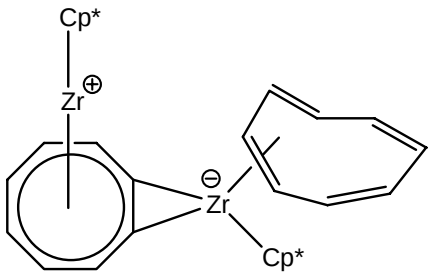

Figure 1.13. Zwitterionic homobimetallic complexes with Zr.

whereas for the rhodium complex (Fig. 1.14), X-ray crystallography supported the zwitterionic character of the compound on the basis of the tetrahedrally coordinated anionic tricarbonylrhodium centre facing a geometrically distorted cationic triphospane rhodium centre without an Rh−Rh bond; the charge separation is sustained by a semi-bridging carbonyl ligand.[47]

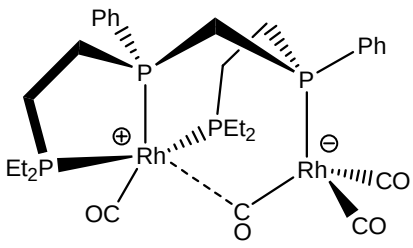

Figure 1.14. Zwitterionic homobimetallic complexes with Rh. The charge separation is possible by means of a semi-bridging carbonyl ligand.

X-ray analysis and IR and NMR spectroscopy also revealed the zwitterionic nature of the dinuclear complexes of Mo and W of the type shown in Scheme 1.20, which can be prepared by several methods from [(fulvalene)$M_2(CO)_6$] and basic phosphines and exhibit different CO vs. phosphine substitution patterns.[48] Interestingly, the molybdenium derivative undergoes ring-slippage to give the η^4-fulvalene complex **U**.

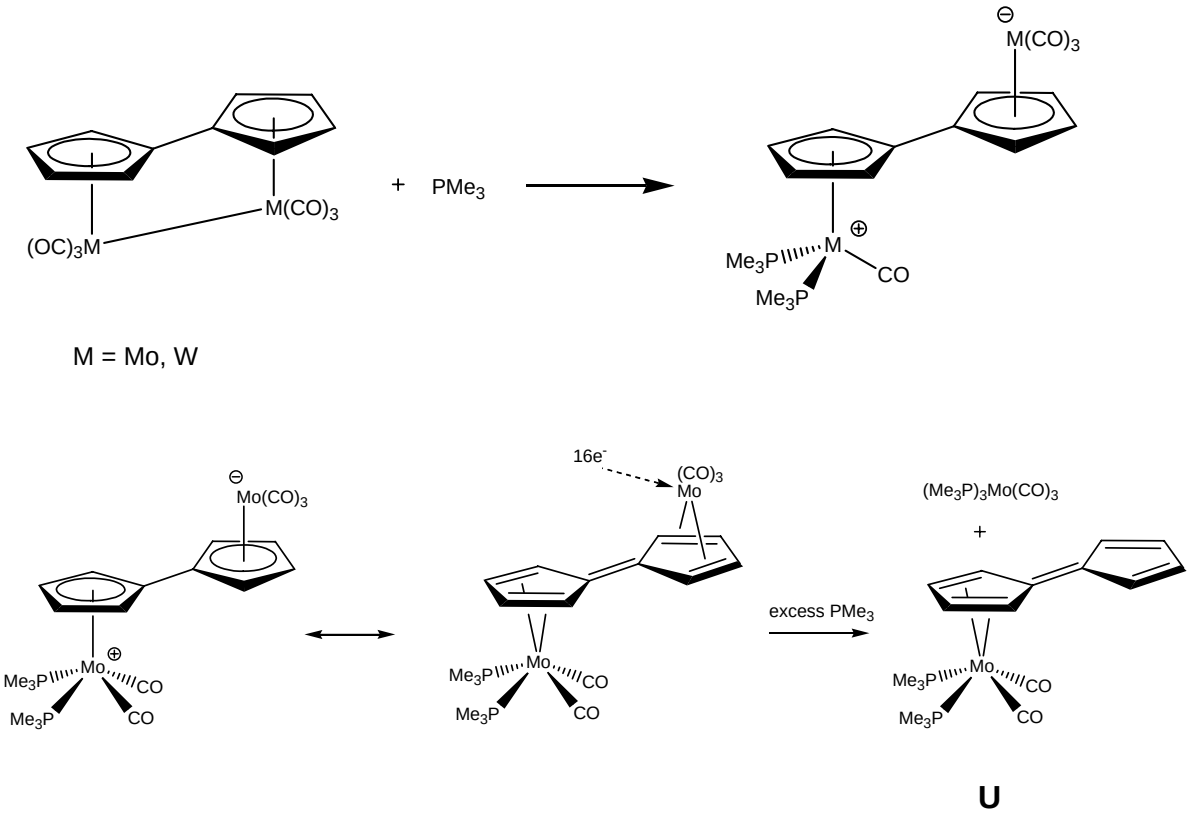

Scheme 1.20. Synthetic routes to Mo and W bimetallic zwitterionic complex. In the presence of an excess of PMe_3, the Mo complex rearranges to a non-zwitterionic monometallic species.

A zwitterionic homobimetallic complex with manganese was reported to be formed upon electrocatalytic conversion under CO, resulting in the cleavage of the Mn−Mn bond and the distortion of the naphthalene ring which is bent to an angle of 45°. Because of the facile and reversible cleavage of such Mn−Mn bond to give a zwitterionic product, the chemistry of the (naphthalene)Mn complexes and the related synthetic methodology might find useful applications in bimetallic catalysis.[49]

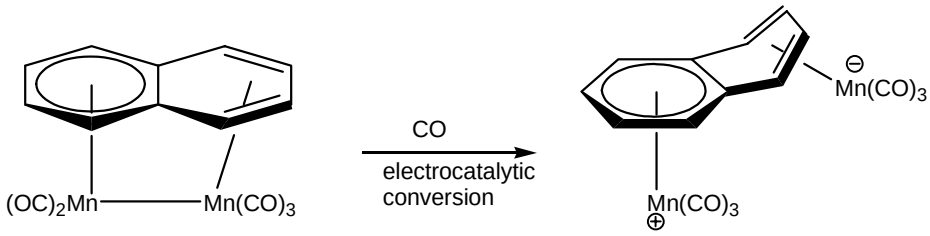

Scheme 1.21. Electrocatalytic conversion of a dimanganese complex to a zwitterionic structure where the Mn−Mn bond has been cleaved.

Heterobimetallic zwitterionic complexes are also well known and find applications in several fields. A particular interest is being gained by transition metals linked by a chain of *sp*-hybridised carbon atoms because of the potential electron-transfer between the two metals under various physicochemical stimuli. In this context, the possibility of having a zwitterionic form that gives a significant contribution to the overall structure is beneficial for the stability of the ground state energy of the molecule; such a zwitterionic contribution can arise when the two metals have different electronegativities. As an example, the Re-Os complex shown in Fig 1.15 seems to possess a zwitterionic form that makes a considerable contribution as opposed to the polyacetylenic form.[50]

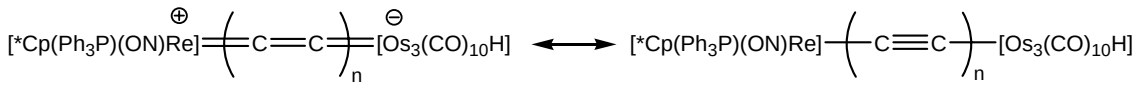

Figure 1.15. Zwitterionic and non-zwitterionic resonance forms of a Re-Os heterobimetallic complex.

An unusual charge separation is observed in complexes formed upon reaction of cationic π-allyl complexes of palladium and platinum with dianionic platinates. The stable anionic bimetallic complex is postulated to have a 2-/+ charge separation with the two metals linked through π-coordination of the alkyne ligand.[51]

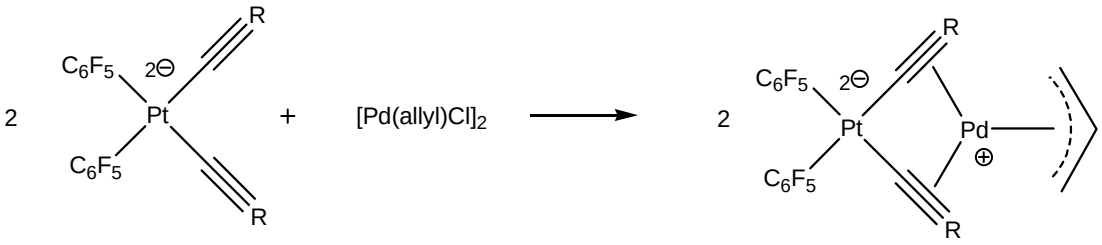

Scheme 1.22. Unusual 2-/+ charge separation in a Pt-Pd bimetallic complex.

However, when the reactant is the dicationic $[Cp^*Ir(PEt_3)(acetone)]^{2+}$ complex, the expected 2-/2+ charge separation is not stable and a non-zwitterionic product is formed via migration of one alkynyl ligand to the iridium.[52] Conversely, a more typical charge separation is observed when the migration of the alkynyl ligand from neutral bis(alkynyl)platinum complexes to neutral platinum or rhodium occurs in the presence of suitable ligands.[53]

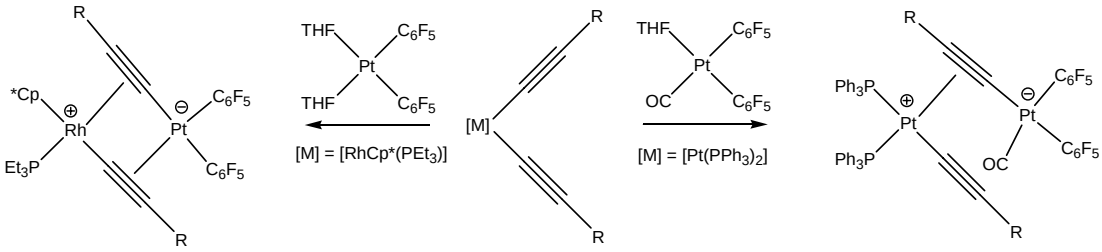

Scheme 1.23. Synthetic routes to Pt-Pt and Pt-Rh zwitterions.

A series of zwitterionic Pt-Rh organometallic compounds have also been recently prepared, featuring bridging ligands of the type μ-PPy_nPh_{3-n} (n = 2, 3; Py = 2-pyridyl), where the P end of the ligand is invariably coordinated to the Pt centre, while the *N*-donor ends chelate the Rh atom, giving metallacycles comparable to the well known Tp'Rh complexes (Tp' = hydridotris(pyrazolyl)borate). These metallacycles adopt two conformations with the Pt complex moiety in either a pseudoaxial position or in a remote position relative to the Rh centre.[54]

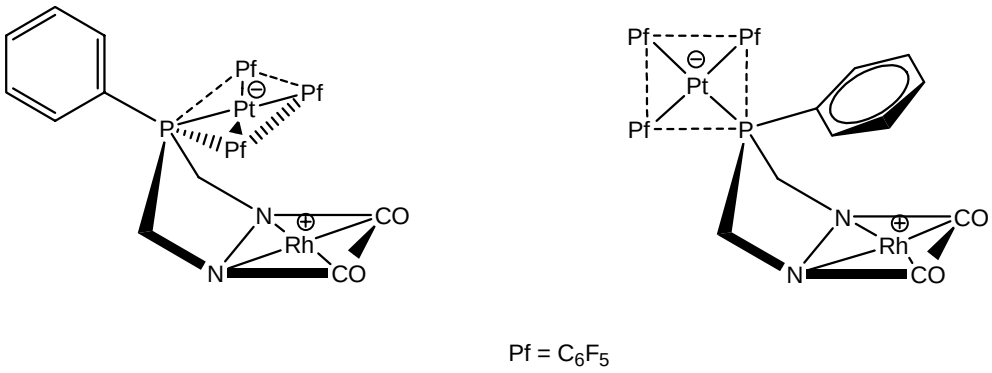

Pf = C_6F_5

Figure 1.16. The two conformations found in the Pt-Rh zwitterion using μ-PPy$_n$Ph$_{3-n}$ (n = 2, 3; Py = 2-pyridyl).

As a last example, zwitterionic bimetallic complexes have also been prepared by using the above mentioned stanna-*closo*-dodecaborate ligand. In the synthesis of the two-metal complex shown in Fig, the $[SnB_{11}H_{11}]^{2-}$ dianion acts as an ambidentate ligand, binding initially a (triphosph)Fe^{2+} fragment using a η^3-(B–H) chelation. The resulting iron complex displays a reduced nucleophilicity at the tin atom and coordination can only be achieved by reacting metal fragments with labile ligands.[55]

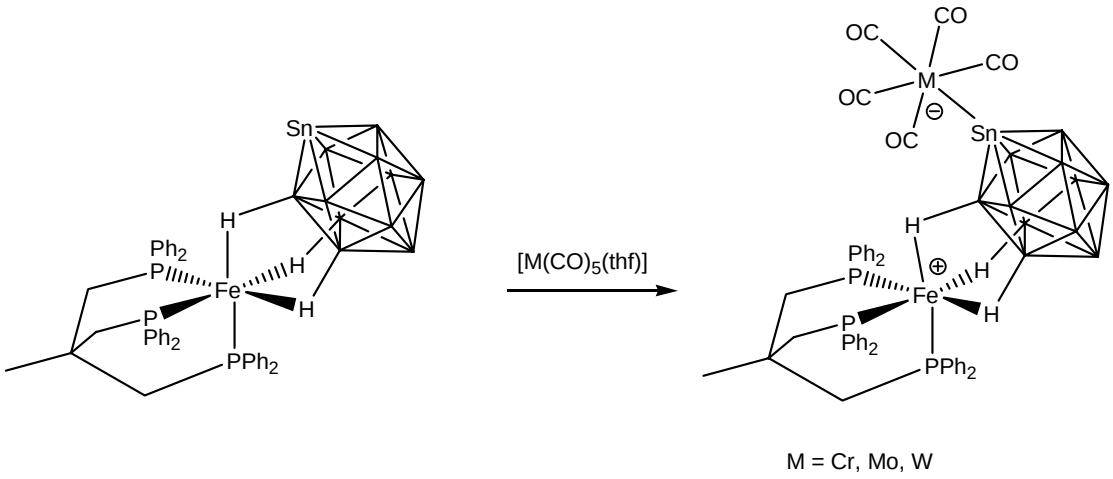

M = Cr, Mo, W

Scheme 1.26. Reaction leading to the Fe-M (M = Cr, Mo, W) zwitterionic complex with the $[SnB_{11}H_{11}]^{2-}$ dianion functioning as an ambidentate ligand.

1. A. E. Shilov, *"Metal Complexes in Biomimetic Chemical Reactions"*, CRC Press, New York, **1997**; A. E. Shilov, *Structure and Bonding* **1997**, vol. *88-91*.

2. C. Lambert, P. von Ragué Schleyer, *Angew. Chem. Int. Ed. Engl.* **1994**, *33*, 1129.
3. J. K. Kochi, T. M. Bockman, *Adv. Organomet. Chem.* **1991**, *33*, 51.
4. U.S. Patent 4372888
5. I. R. Whitewall, A. M. McDonagh, M. G. Humphrey, M. Samoc, *Adv. Organomet. Chem.* **1998**, *42*, 291; S. R. Marder, *Inorganic Material* (Eds.: D. W. Bruce, D. O'Hare), chapt. 3, p. 122, Wiley, New York, **1996**.
6. H. Schmidbaur, *Angew. Chem. Int. Ed. Engl.* **1983**, *22*, 907; U. Belluco, R. A. Michelin, M. Mozzon, R. Bertani, G. Facchin, L. Zanotto, L. Pandolfo, *J. Organomet. Chem.* **1998**, *557*, 37.
7. For a recent review see: R. Chauvin, *Eur. J. Inorg. Chem.* **2000**, 577.
8. P. Berno, S. Gambarotta, S. Kotila, G. Erker, *Chem. Commun.* **1996**, 779.
9. Y. Miquel, A. Igau, B. Donnadieu, J.-P. Majoral, N. Pirio, P. Meunier, *J. Am. Chem. Soc.* **1998**, *120*, 3504.
10. V. Cardieno, M. Zablocka, B. Donnadieu, A. Igau, J.-P. Majoral, *Organometallics* **1999**, *18*, 1882.
11. S. A. Fairhurst, D. L. Hughes, K. Marjani, R. L. Richards, *J. Chem. Soc., Dalton Trans.* **1998**, 1899.
12. D. M. Hoffman, J. C. Huffman, D. Lappas, D. A. Wierda, *Organometallics* **1993**, *12*, 4312.
13. J. Vicente, M.-T. Chicote, C. MacBeath, J. Fernandez-Baeza, D. Bautista, *Organometallics,* **1999**, *18*, 2677.
14. H. F. Sleiman, L. McElwee-White, *J. Am. Chem. Soc.* **1988**, *110*, 8700.
15. H. F. Sleiman, S. Mercer, L. McElwee-White, *J. Am. Chem. Soc.* **1989**, *111*, 8007.
16. N. D. R. Barnett, S. T. Massey, P. C. McGowan, J. J. Wild, K. A. Abboud, L. McElwee-White, *Organometallics* **1996**, *15*, 424; Y. He, P. C. McGowan, K. A. Abboud, L. McElwee-White, *J. Chem. Soc., Dalton Trans.* **1998**, 3373.
17. H. Rudler, M. Audouin, A. Parlier, B. Martin-Vaca, R. Goumont, T. Durand-Réville, *J. Am. Chem. Soc.* **1996**, *118*, 12045.
18. H. Rudler, B. Martin-Vaca, M. Nicolas, M. Audouin, J. Vaissermann, *Organometallics* **1998**, *17*, 361.
19. E. J. de Souza, V. M. Deflon, A. G. de A. Fernandes, S. S. Lemos, A. Hagenbach, U. Abram, *Inorg. Chim. Acta* **2006**, *359*, 1513.
20. F. Molinos de Andrade, W. Massa, C. Peppe, W. Uhl, *J. Organomet. Chem.* **2005**, *690*, 1294.
21. K. Ghosh, S. Pattanayak, A. Chakravorty, *Organometallics* **1998**, *17*, 1956.
22. M. Gandelman, A. Vigalok, L. J. W. Shimon, D. Milstein, *Organometallics* **1997**, *16*, 3981.
23. I. C. M. Wehman-Ooyevaar, D. M. Grove, H. Koijman, P. van der Sluis, A. L. Spek, G. van Koten, *J. Am. Chem. Soc.* **1992**, *114*, 9916.
24. G. G. Hlatky, H. W. Turner, R. R. Eckman, *J. Am. Chem. Soc.* **1989**, *111*, 2728.

25. W. E. Piers, *Chem. Eur. J.* **1998**, *4*, 13; M. Bochmann, *Topics Catal.* **1999**, *7*, 9; W. E. Piers, Y. Sun, L. W. M. Lee, *Topics Catal.* **1999**, *7*, 133; S. Aldridge, C. Bresner, *Coord. Chem. Rev.* **2003**, *244*, 71.
26. I. Amer, H. Alper, J. Am. Chem. Soc. 1990, 112, 3674; J.-Q. Zhou, H. Alper, *Organometallics*, **1994**, *13*, 1586; Z. Zou, B. R. James, H. Alper, *Organometallics*, **1995**, *14*, 4209; Z. Zhou, G. Facey, B. R. James, H. Alper, *Organometallics*, **1996**, *15*, 2496; Y. Goldberg, H. Alper, *J. Chem. Soc., Chem Commun.* **1994**, 1209.
27. S. Amaratunga, H. Alper, *J. Organomet. Chem.* **1995**, *488*, 25.
28. S. A. Westcott, H. P. Blom, T. B. Marder, R. T. Baker, *J. Am. Chem. Soc.* **1992**, *114*, 8863; C. Dai, T. B. Marder, E. G. Robins, D. S. Yufit, J. A. K. Howard, A. J. Scott, W. Clegg, *Chem. Commun.* **1998**, 1983.
29. K. S. Cook, W. E. Piers, S. J. Rettig, R. McDonald, *Organometallics* **2000**, *19*, 2243.
30. K. S. Cook, W. E. Piers, R. McDonald, *J. Am. Chem. Soc.* **2002**, *124*, 5411.
31. T. A. Betley, J. C. Peters, *Inorg. Chem.* **2002**, *41*, 6541.
32. R. R. Schrock, J. A. Osborne, *J. Am. Chem. Soc.* **1971**, *93*, 3091; R. H. Crabtree, *Acc. Chem. Res.* **1979**, *12*, 331.
33. T. A. Betley, J. C. Peters, *Angew. Chem. Int. Ed.* **2003**, *42*, 2385.
34. C. C. Lu, J. C. Peters, *J. Am. Chem. Soc.* **2002**, *124*, 5272.
35. T. Marx, L. Wesemann, S. Dehnen, *Organometallics,* **2000**, *19*, 4653.
36. M. Q. Slagt, R. J. M. Klein Gebbink, M. Lutz, A. L. Spek, G. van Koten, *J. Chem. Soc., Dalton Trans.* **2002**, 2591; M. Q. Slagt, G. Rodriguez, M. M. P. Grutters, R. J. M. Klein Gebbink, W. Klopper, L. W. Jenneskens, M. Lutz, A. L. Spek, G. van Koten, *Chem. Eur. J.* **2004**, *10*, 1331.
37. R. van de Coevering, M. Kuil, A. P. Alfers, T. Visser, M. Lutz, A. L. Spek, R. J. M. Klein Gebbink, G. van Koten, *Organometallics* **2005**, *24*, 6147.
38. C. Bianchini, P. Frediani, V. Sernau, *Organometallics,* **1995**, *14*, 5458; C. Bianchini, A. Meli, V. Pantinec, V. Sernau, R. A. Vizza, *J. Am. Chem. Soc.* **1997**, *119*, 4945.
39. J. Cipot, D. Wechsler, M. Stradiotto, R. McDonald, M. J. Ferguson, *Organometallics* **2003**, *22*, 5185.
40. M. Stradiotto, J. Cipot, R. McDonald, *J. Am. Chem. Soc.* **2003**, *125*, 5618.
41. J. Cipot, R. McDonald, M. Stradiotto, *Chem. Commun.* **2005**, 4932.
42. M. A. Rankin, R. McDonald, M. J. Ferguson, M. Stradiotto, *Organometallics* **2005**, *24*, 4981.
43. B. M. Wile, R. J. Burford, R. McDonald, M. J. Ferguson, M. Stradiotto, *Organometallics* **2006**, *25*, 1028.
44. N. Etkin, C. M. Ong, D. W. Stephan, *Organometallics* **1998**, *17*, 3656.
45. F. Zhang, M. H. Prosenc, J. Heck, *J. Organomet. Chem.* **2006**, *691*, 455.
46. P. J. Sinnema, A. Meetsma, J. H. Teuben, *Organometallics* **1993**, *12*, 184.

47. W. J. Peng, S. G. Train, D. K. Howell, F. R. Fronczek, G. G. Stanley, *Chem. Commun.* **1996**, 2607.

48. M. Tilset, K. P. C. Vollhardt, R. Boese, *Organometallics* **1994**, *13*, 3146; D. S. Brown, M.-H. Delville-Desbois, R. Boese, K. P. C. Vollhardt, D. Astruc, *Angew. Chem. Int. Ed. Engl.* **1994**, *33*, 661; C. Moreno, M. L. Marcos, M. J. Macazaga, R. M. Medina, D. H. Farrar, J. Gonzales-Velasco, S. Delgado, *Organometallics* **1998**, *17*, 4657.

49. J. A. Reingold, K. L. Virkaitis, G. B. Carpenter, S. Sun, D. A. Sweigart, P. T. Czech, K. R. Overly, *J. Am. Chem. Soc.* **2005**, *127*, 11146.

50. S. B. Falloon, A. M. Arif, J. A. Gladysz, *Chem. Commun.* **1997**, 629.

51. J. R. Berenguer, J. Fornies, E. Lalinde, F. Martinez, *J. Organomet. Chem.* **1994**, *470*, C15; J. R. Berenguer, J. Fornies, E. Lalinde, F. Martinez, *Organometallics* **1996**, *15*, 4537.

52. J. R. Berenguer, J. Fornies, E. Lalinde, F. Martinez, *J. Chem. Soc., Chem. Commun.* **1995**, 1227.

53. I. Ara, J. R. Berenguer, E. Eguizabal, J. Fornies, E. Lalinde, A. Martin F. Martinez, *Organometallics* **1998**, *17*, 4578; J. R. Berenguer, J. Fornies, E. Lalinde, F. Martinez, E. Urriolabeita, A. J. Welch, *J. Chem. Soc., Dalton Trans.* **1994**, 1291.

54. J. A. Casares, P. Espinet, J. M. Martìn-Alvarez, V. Santos, *Inorg. Chem.* **2004**, *43*, 189.

55. T. Gädt, K. Eichele, L. Wesemann, *Organometallics* **2006**, *25*, 3904.

Chapter 2

Metal coordination chemistry of the R_2AFA^- ligands via N atoms

2.1 Background

A study on the chemistry of the *N*,*N*'-diaryl-6-aminofulvene-2-aldimines was conducted, in particular its coordination chemistry towards late transition metal centres. The focus of the investigation was to establish the capability of these ligand systems to form zwitterionic metal complexes. Such species should be formed upon complexation of the deprotonated ligand and delocalization of the negative charge onto the cyclopentadienyl moiety. Three resonance forms of the anionic ligand may be drawn (Fig. 2.1) and the ability of the cyclopentadienyl portion of the ligand to symmetrically coordinate to a metal in a pentahapto-mode indicates that form **B** makes a significant contribution.

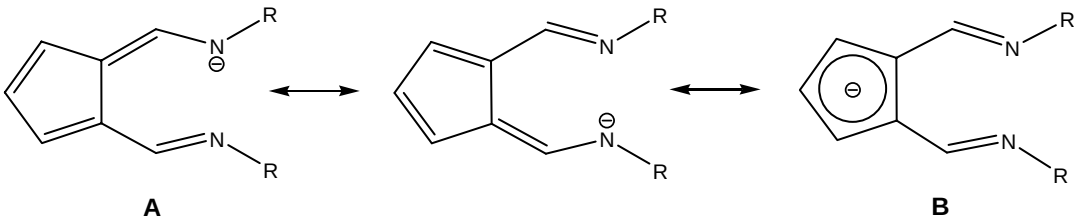

Figure 2.1. Resonance forms for the 6-aminofulvene-2-aldiminate ligand.

The zwitterioninc character of complexes of this ligand is of great interest in relation to homogeneous catalysis involving electrophilic metal centres. One such case is the class of square-planar group 10 transition-metal alkene polymerization catalysts formed by Lewis acid activation of [(1,2-diimine)MMe_2] (M = Ni, Pd) complexes.[1] Replacement of the 1,2-diimine ligand in these systems with an AFA ligand would provide a neutral complex which retains significant positive charge at the metal by virtue of the

contribution from resonance form **B** to the ligand electronic structure (Fig. 2.2), and furthermore would provide catalysts which would not require Lewis acid activation.

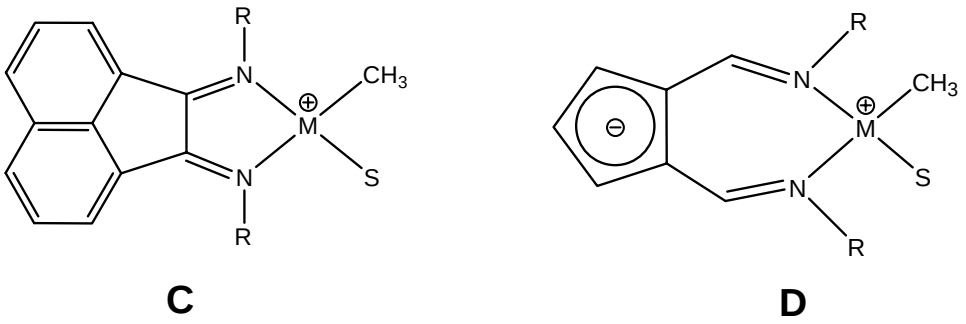

Figure 2.2. 1,2-diimine group-10 metal alkene polymerization catalysts (C, M = Ni, Pd; S = solvent) and the possible neutral zwitterionic analogue containing an AFA ligand (D).

Although the 6-aminofulvene-2-aldimine system (AFAH) was first prepared in 1963,[2] little attention has been given to its properties as a ligand. The bis-phenyl derivative was studied by X-ray crystallography by Mueller-Westerhoff.[3, 4] More recently, Sanz *et al*. isolated six other aromatic derivatives and studied the tautomerism in the solid state and in solution.[5] What emerged was that aminofulvene are the only representatives of a pseudo seven-membered ring compounds with the proton leaving a nitrogen atom that is five bonds separated from the other nitrogen that receives it (Fig. 2.3):

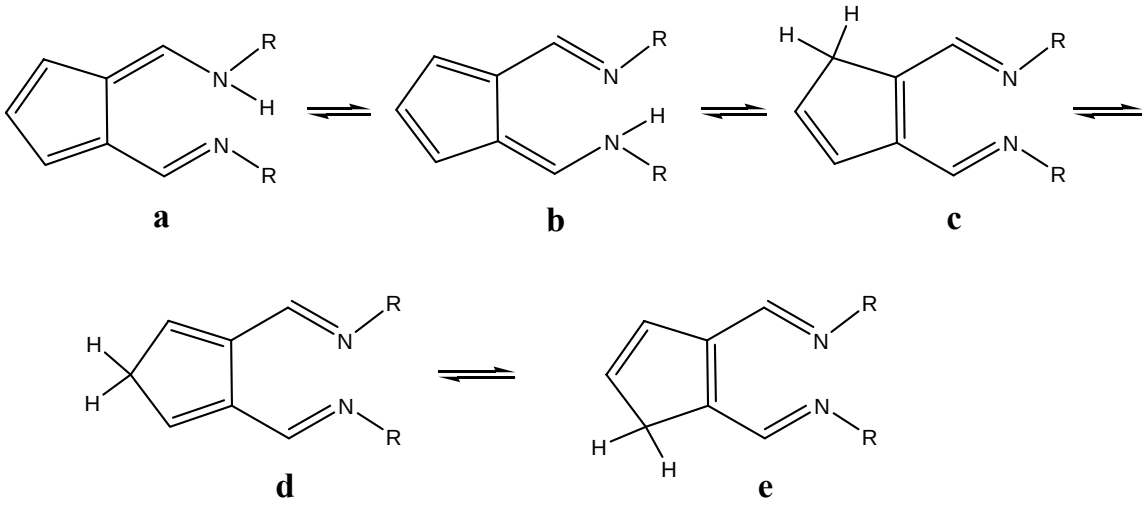

Figure 2.3. Tautomerism of the 6-aminofulvene-2-aldimine.

Of these tautomers, **a** and **b** are the most stable and equivalent; the molecule can therefore be regarded as having an intramolecular hydrogen bond, which has been considered to produce extra stability.[3,6] A double potential energy well results from the proton jumping between the two nitrogen atoms [N-H···N $\rightleftharpoons$ N···H-N].[3] However, if the two donor nitrogen atoms have the same affinity for the proton, a single potential energy well can be observed where the proton is centred between the nitrogen atoms [N···H···N].[3] This behavior can be related to that class of compounds known as Proton-Sponges, such as 1,8-bis(dimethylamino)naftalenes,[7] where the two nitrogen atoms are forced into proximity with the hydrogen jumping between both atoms; aromaticity of the system can provide additional stabilization of a favorable symmetric planar structure.

The same principle can be used to describe compounds of the type of 1-amino-7-imino-1,3,5-cycloheptatrienes,[8] β-diketiminate ligands,[9] and 6-aminopentafulvene-2-aldimine, where the N-H···N moiety provides the structural environment for either facile tautomers or symmetrical hydrogen bonding. The structures of these molecules have been postulated to exhibit non-classical aromaticity in the sense of cyclic delocalized π-electron systems (with ten and six π-electrons, Fig. 2.4).

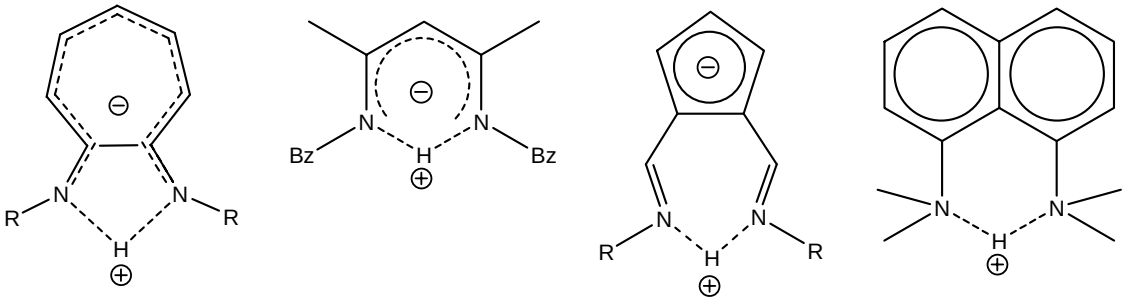

a **b** **c** **d**

Figure 2.4. Proton-Sponge molecules: a) 1-amino-7-imino-1,3,5-cycloheptatrienes ligand; b) β-diketiminate ligand; c) *N,N'*-diaryl-6-aminofulvene-2-aldimine; d) Protonated 1,8-bis(dimethylamino)naftalene.

In the molecular structure of the *N,N'*-diphenyl-6-aminofulvene-2-aldimine, all the C-C and C-N bond distances are approximately halfway between a single and a double bond, with the exception of C(1)-C(2), and the 6-pentafulvene-2-aldimine portion of the molecule (excluding the phenyls) has close symmetry to C_{2v}. Crystallographic studies also showed that the five-membered ring and the two phenyl groups are individually planar, with the two dihedral angles being respectively 19.6 and 7.6°. Coplanarity of the phenyl rings with the 6-aminofulvene-2-aldimine moiety is presumably restricted by steric interaction between the "inside" ortho hydrogens.[3] Hence, it can be predicted that the presence of bulkier ortho-substituents on the aryl rings would increase the non-planarity of the Cp and Ar planes.

Subsequently, Jackman measured the deuteron spin-lattice relaxation times and calculated the deuteron quadrupole coupling constants, in order to probe electrostatic environment of the deuteron in the this type of situation and consequently to provide a qualitative strength for the hydrogen bond.[10] These studies are consistent with either a C_{2v} symmetry or with the existence of rapidly equilibrating C_s tautomers.

A related compound was reported by Stephan *et al.*,[11] who prepared and characterized the $H[1,2\text{-}C_5H_3\text{-}(C(Ph)NH)_2]$. The synthetic approach is the inverse of the one used in the present investigation, with the final diimine ligand afforded upon protonation of the ligand anion coordinated to a magnesium centre (Fig. 2.5).

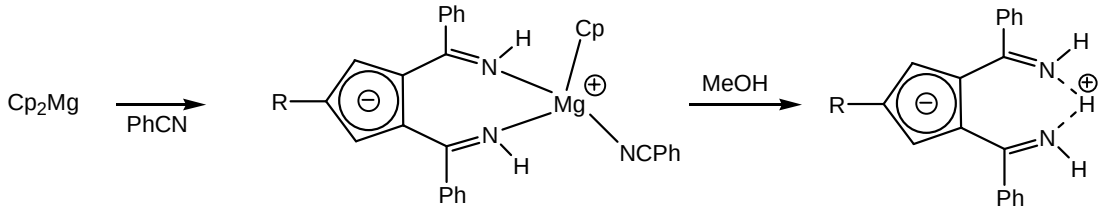

E

Figure 2.5. Reaction of benzonitrile with Cp_2Mg leads to the magnesium complex E, which after demetallation affords the free ligand H[1,2-C_5H_3-(C(Ph)NH)$_2$].

The zwitterionic character of the H[1,2-C_5H_3-(C(Ph)NH)$_2$] was postulated in view of the NMR signals and confirmed by X-ray crystallography, which revealed the planarity of the molecule and the 2-fold symmetry, with one hydrogen atom bridging the two nitrogen atoms. The molecular crystal structure of the related (benzonitrile)magnesium complex (**E**) was also determined, showing a pseudo-tetrahedral geometry of the metal centre, with the ligand coordinated via the N donors. The cyclopentadienyl ring and the CN moieties are individually planar, but not coplanar to each other, with the dihedral angle of 22.30°. However, the C-N and C(Cp)-C(CN) distances are 1.304(2) and 1.436(2) Å respectively, which indicate some degree of π-conjugation. The metal centre lies 0.818 Å out of the plane defined by the two C=N bonds, and this plane forms a dihedral angle of 36.17° with the N-Mg-N plane. The N-Mg-N bond angle is 94.97(7)°, considerably narrower than 109° for an ideal tetrahedral geometry.

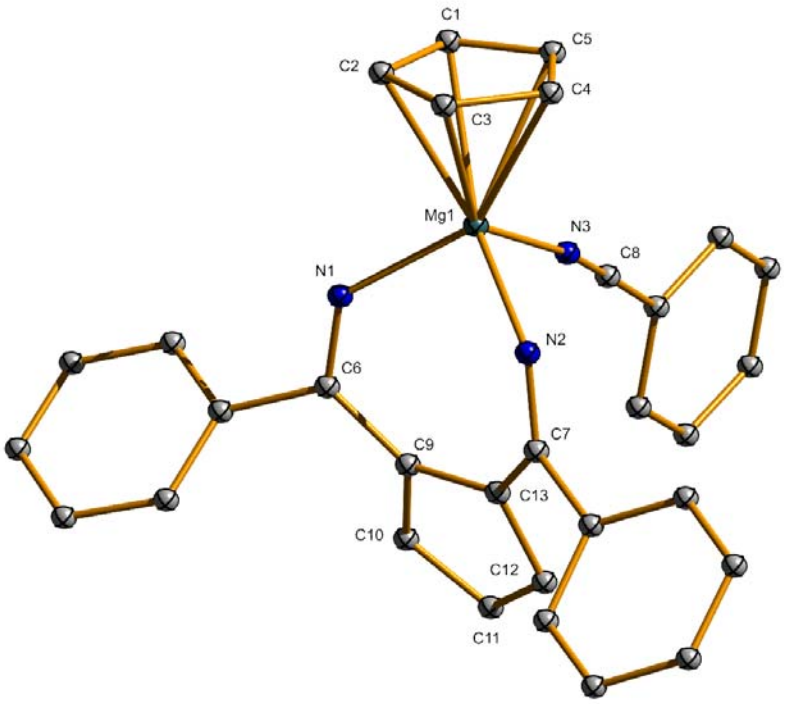

Figure 2.6. Molecular structure of [(1,2-$C_5H_3(C(Ph)NH)_2$)Mg(Cp)(PhCN)].

The same ligand is also able to coordinate to Zr(IV) centres, and the two species [(1,2-$C_5H_3(C(Ph)NH)_2$)$ZrCl_3$(thf)] (**F**) and [(1,2-$C_5H_3(C(Ph)NH)_2)_3$ZrCl] (**G**) were isolated after reaction of the ligand with 1 and 3 equivalents of [$ZrCl_4(thf)_2$] respectively.

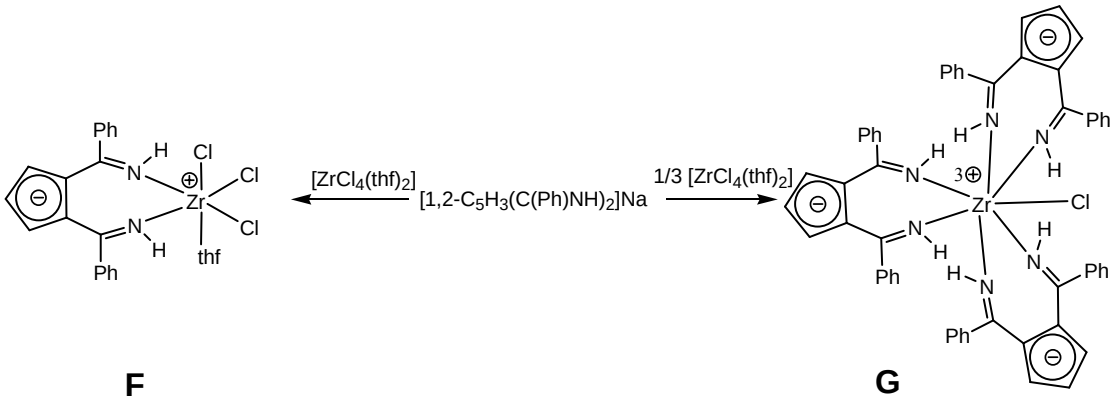

Figure 2.7. Reaction of the deprotonated ligand with 1 and 3 equivalent of $ZrCl_4(thf)_2$ affords isolation of (1,2-C_5H_3-$(C(Ph)NH)_2$)$ZrCl_3$(thf) (F) and (1,2-C_5H_3-$(C(Ph)NH)_2)_3$ZrCl (G) respectively.

Remarkably, any attempts to specifically prepare the L_2ZrCl_2 complex were unsuccessful, leading always to a mixture of **F** and **G**. This observation was interpreted in terms of redistribution of the ligand due to the lack of substitution on the nitrogen donors.[11] The molecular structures of the two complexes are shown in Fig. 2.8 and 2.9.

While the structural parameters within the ligand in **F** and **G** do not differ much from the magnesium analogue, different values are observed in the metal-nitrogen bond distances and angles. Furthermore, the steric congestion present in the seven-coordinate zirconium complex, adds further differences in comparison with the less crowded complex **F**. For example the Zr-N bond lengths of **G**, ranging from 2.218(3) to 2.257(3) Å, are longer than in **F**, whose values are 2.190(9) Å. Also, the average value of the N-Zr-N bite angles for the the three chelating diimines in **G** (79.68(12)°) is slightly smaller than the value in **F** (81.6(3)°).

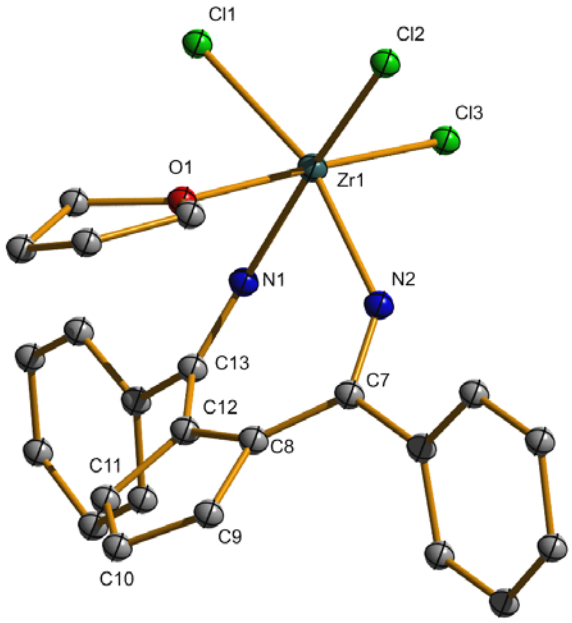

Figure 2.8. Molecular structures of [(1,2-C_5H_3-(C(Ph)NH)$_2$)$ZrCl_3$(thf)]

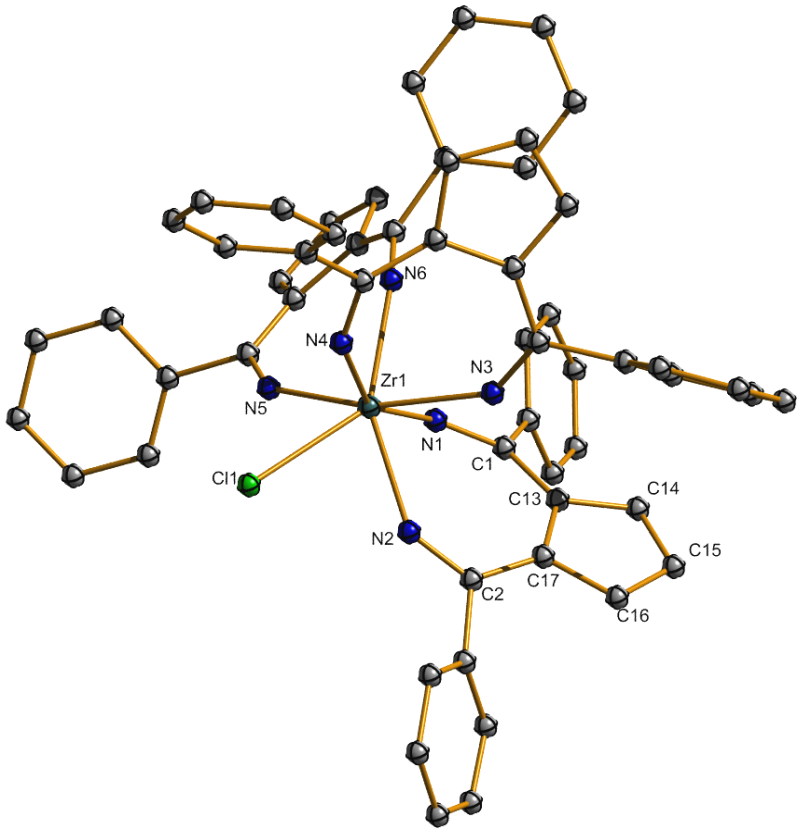

Figure 2.9. Molecular crystal structure of $[(1,2\text{-}C_5H_3\text{-}(C(Ph)NH)_2)_3ZrCl]$.

As observed in the magnesium derivative, in both the zirconium species, the metal centre is not coplanar with the C=N plane. Whilst this might be expected for the sterically crowded complex **G**, where deviation from planarity could occur in order to avoid collision of the phenyl substituents, it is quite remarkable that the same structural feature is present in complexes **E** and **F**, where the low steric demand should not be an issue for the planarity of the metallacycle. In the zirconium species **F**, the dihedral angle between the C=N plane and the N-Zr-N plane is 30.84º, and this observation suggests that other factors need to be considered to explain such distortion. One of these factors might be viewed in terms of coordination geometry around the metal centre and ligand bite angle. Due to the octahedral environment of the zirconium centre, the ligand bite angle must be close to 90º in order to have a suitable orbital overlap. By simple geometrical considerations, such a narrow angle is highly unlikely to be found in

perfectly planar seven-membered ring systems, so that the metal has to be accommodated out of the ligand plane. However, geometry restrictions would still not explain the narrow bite angle present in the tetrahedral magnesium species **E**.

A different explanation for the observed non-planarity of the metallacycles is based on electronic factors. As shown in Fig. 2.10, in analogy with the 6-aminofulvene-2-aldimine systems described before, two more resonance forms for Stephan's ligand system can be drawn, where contribution from fulvene-amide forms might be relevant.

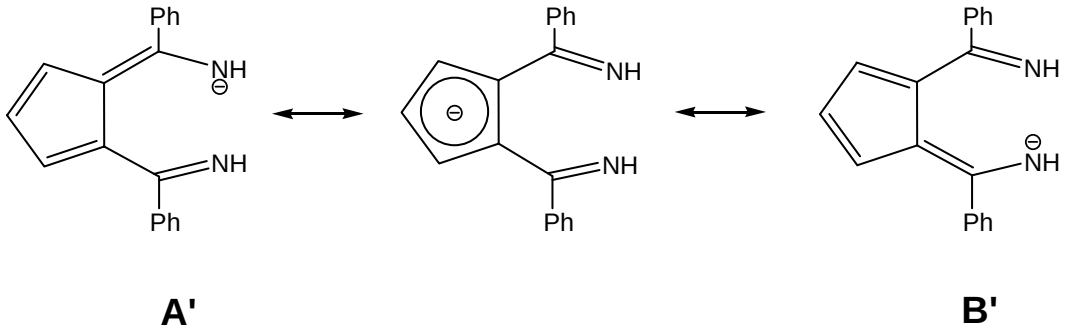

Figure 2.10. Resonance forms for the $[1,2\text{-}C_5H_3\text{-}(C(Ph)NH)_2]^-$ anion.

With this in mind, a more accurate interpretation can be attempted by relating the binding mode of the ligand to one of the other two canonical resonance forms. Because of the high electropositivity of both magnesium and zirconium, the resonance forms **A**' and **B**' have probably much importance, and the ligation can be depicted as having contribution from an amide-metal type bond, with the N atoms having an intermediate hybridization between sp^2 and sp^3. As in complex **E**, deviations from planarity between the cyclopentadienyl ring and the C_2N_2 plane are also observed, with dihedral angles of 20.14° for complex **F** and an average of 18.73° for complex **G**.

The studies of these 1,2-cyclopentadienyl diimine systems were also expanded to group 13 species and complexes featuring the ligand coordinated to Ga(III) (**H**) and Al(III) (**I**) were synthesized.[12]

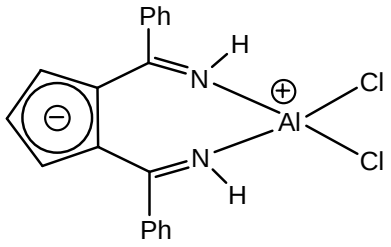

H

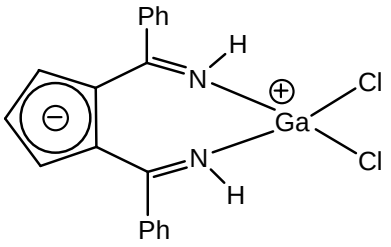

I

Figure 2.11. Group 13 complexes with the ligand $[1,2\text{-}C_5H_3\text{-}(C(Ph)NH)_2]^-$.

The solid-state structures of **H** and **I** are isostructural, with the anion binding the metal via the N donors and the chloride atoms completing a pseudotetrahedral coordination sphere (Fig 2.12 and 2.13).

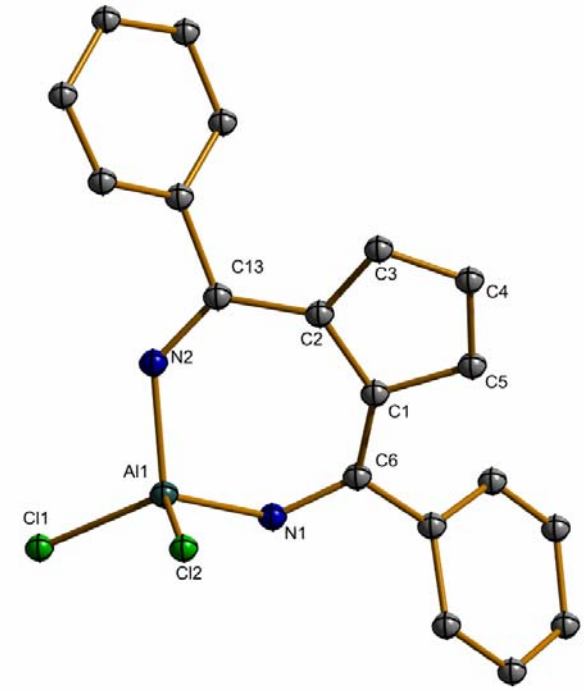

Figure 2.12. Molecular crystal structure of $[(1,2\text{-}C_5H_3\text{-}(C(Ph)NH)_2)AlCl_2]$.

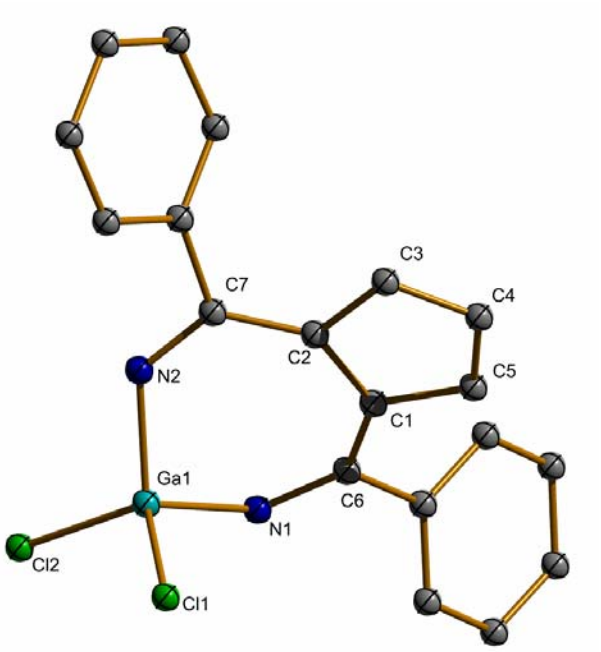

Figure 2.13. Molecular crystal structure of [(1,2-C_5H_3-$(C(Ph)NH)_2$)$GaCl_2$].

The C=N bond distances (1.321(12) and 1.314(12) Å) are similar to those in **F** and **G,** and only slightly longer than in **E** (1.302(2) and 1.306(2) Å). The N-Al-N and N-Ga-N angles are 104.3(4) and 105.06(13)°, larger than the corresponding magnesium complex **E**. Despite these values being closer to the ideal tetrahedral coordination geometry, the metallacycles retain their non-planarity, supporting the hypothesis that electronic factors are more important than geometry restrictions. Moreover, the non-coplanarity of the cyclopentadienyl group and the N_2C_2 plane is even more pronounced than in **E**, **F** and **G**, with values of 28.4 and 33.5º. This feature for the [1,2-C_5H_3-$(C(Ph)NH)_2$]$^-$ ligand is in contrast to many of the related ligands such as aminidinates,[13] diketiminates,[14] and aminotroponiminates,[15]where planarity of the ligand always occurs. This has potentially important repercussions on the formulation of these systems as zwitterionic species. Computational studies of the frontier orbitals of the model [(1,2-C_5H_3-$(C(Ph)NH)_2$)$ZrCl_3$(thf)], where the N_2C_2Cp fragment is assumed as perfectly planar, had revealed that the HOMO is basically identified with the π-orbitals system of the C_5 ring, while the LUMO is mostly located on the metal, very much resembling an empty d-

orbital.[11] As a consequence of the more severe deviation from co-planarity of the C_5 ring and the C_2N_2 plane of the aluminium and gallium derivatives in comparison with the zirconium complexes **F** and **G**, the π-conjugation is more dramatically disrupted.

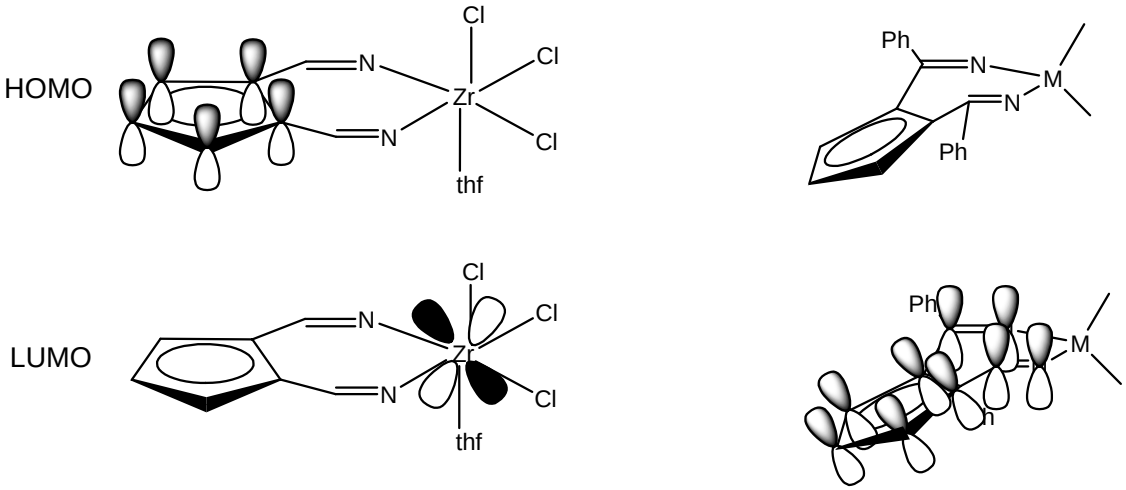

Figure 2.14. HOMO and LUMO molecular orbitals of [(1,2-C_5H_3-$(C(Ph)NH)_2$)$ZrCl_3$(thf)]. Loss of planarity results in a less efficient overlap of the p orbitals.

It can be speculated that this would result in a more effective charge separation between the cyclopentadienyl, where the HOMO is located, and the metal centre, implying an enhanced electrophilicity of the metal atom, and consequently the suitability of these systems for olefin polymerization catalysis.

Another related ligand system was reported by Erker *et al*., who prepared and characterized a series of carbamoyl-substituted cyclopentadienyl zirconium complexes. In this case, the coordination of the ligands occurs via oxygen atoms. Although similar to Stephan's ligands, the resulting products were formulated by taking into account a significant contribution from a fulvenoid mesomeric resonance structure.[16]

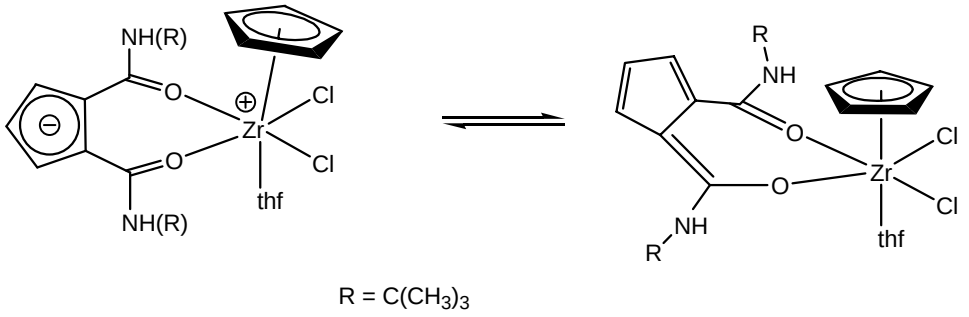

Figure 2.15. [1,2-Bis(*N-tert*-butylcarbamoyl)-cyclopentadienyl]zirconium complex.

2.2 Results and discussion

2.2.1 Synthesis of the ligands

As demonstrated by Hafner *et al*., reaction between dimethylformamide and dimethyl sulfate leads to the formation of the *N*,*N*'-dimethylformamide-dimethylsulfate complex, whose reaction with one equivalent of sodium cyclopentadienide produces the 6-dimethylaminofulvene (Scheme 2.1-2.2).[2]

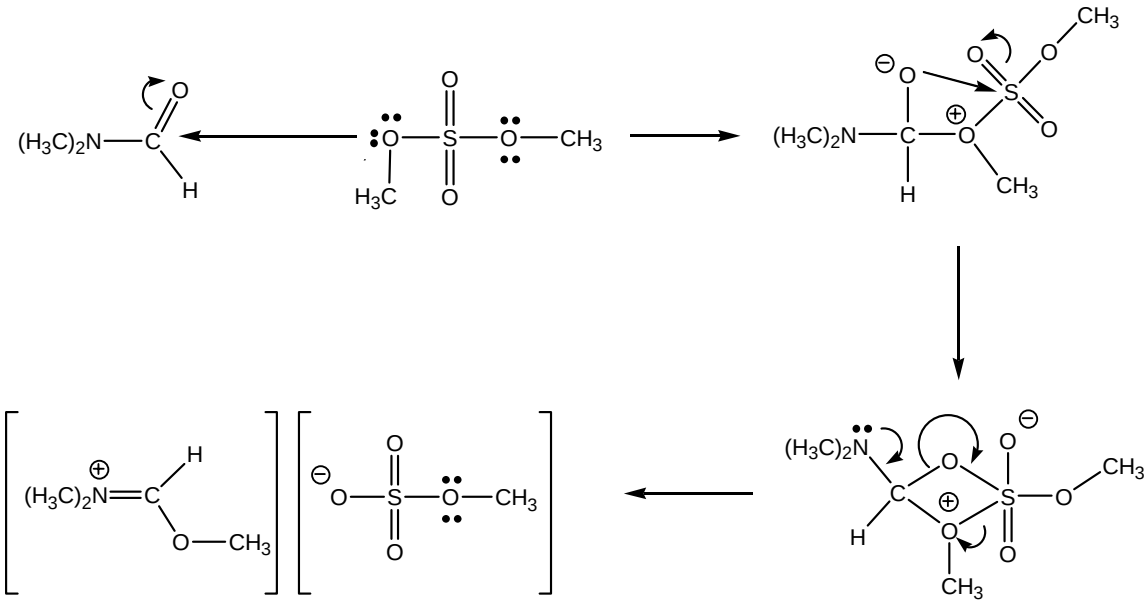

Scheme 2.1. Reaction of of N,N'-dimethylformamide with dimethylsulfate.

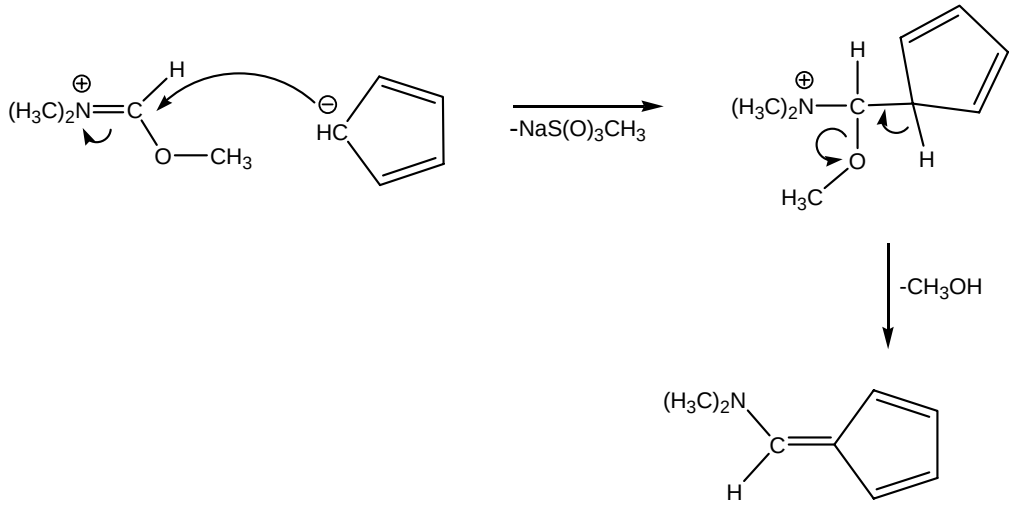

Scheme 2.2. Synthesis of 6-dimethylaminofulvene.

By reaction of the 6-aminofulvene with the product from oxalyl chloride and dimethylformamide, electrophilic substitution takes place to form 6-aminofulvene-2-*N*,*N*'-dimethylaldimmonium chloride, which can be isolated in good yields. Treatment of the aldiminium salt with ammonia, primary aliphatic or aromatic amine leads to the formation of the final *N*,*N*'-diaryl-6-aminofulvene-2-aldimine (Scheme 2.3).

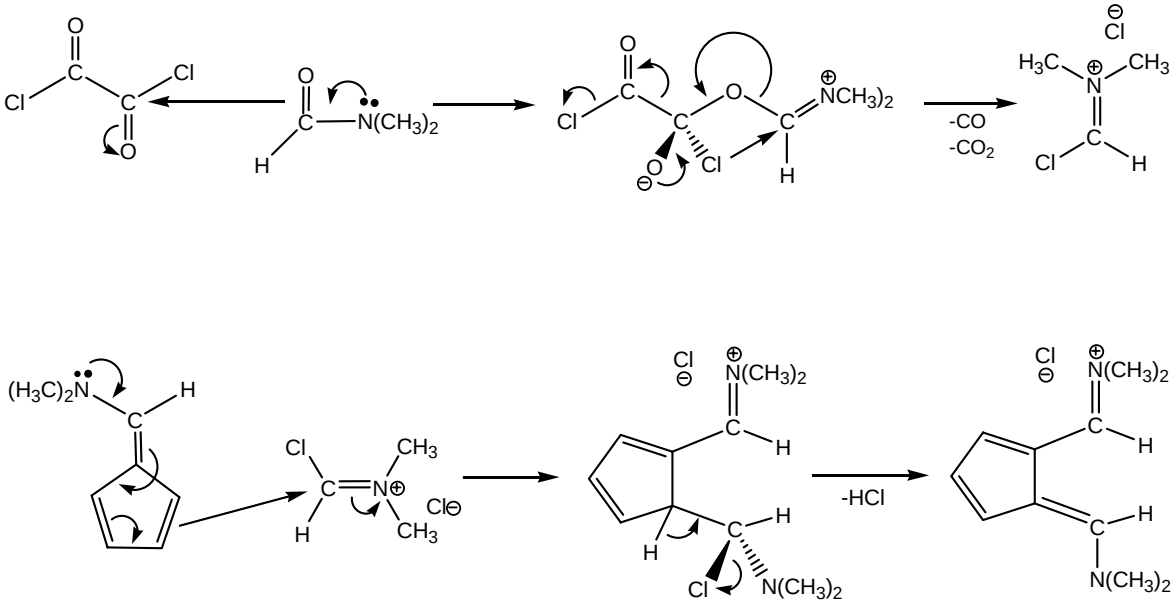

Scheme 2.3. Synthesis of 6-aminofulvene-2-*N,N'*-dimethylaldimonium chloride.

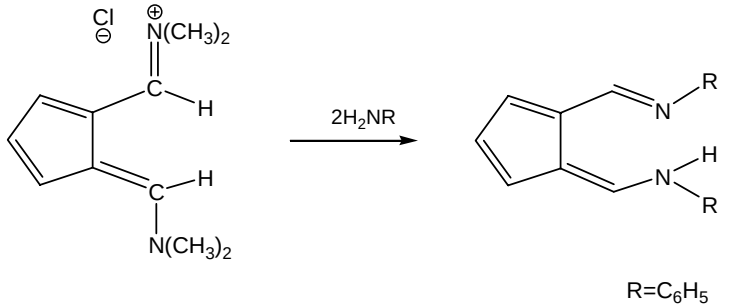

Scheme 2.4. Synthesis of N,N'-diaryl-6-aminofulvene-2-aldimine.

In the present studies, other than the classical *N,N*'-diphenyl-substituted aminofulvene, 3 more ligands with different substituents on the N atoms have been prepared and characterised. The classical Müller-Westerhoff's compound featuring phenyl groups turned out to be the one with highest yield (Fig 2.16).

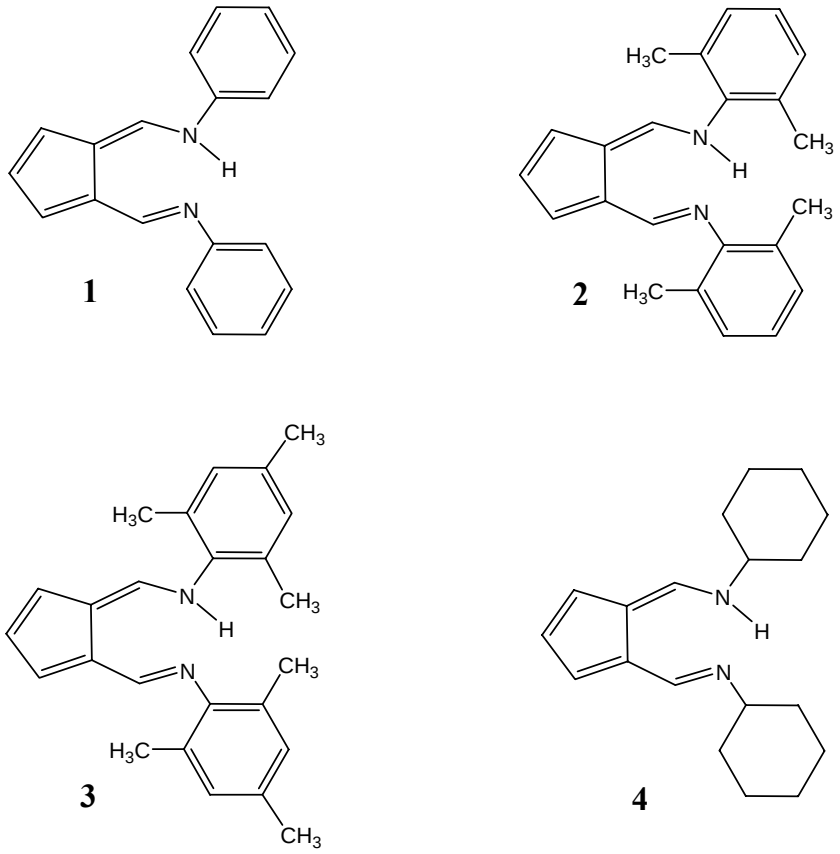

Figure 2.16. The 4 ligands synthesised: 1) *N,N*'-diphenyl-6-aminofulvene-2-aldimine; 2) *N,N*'-di(2,6-dimethyl)phenyl-6-aminofulvene-2-aldimine; 3) *N,N*'-di(2,4,6-trimethyl)phenyl-6-aminofulvene-2-aldimine; 4) *N,N*'-dicyclohexyl-6-aminofulvene-2-aldimine.

The X-ray crystal structures of the ligands reveal that the AFA moiety is almost planar, with the C-C and C-N bond lengths having values which lie in between single and double bonds (1.453(5) and 1.293(5) Å respectively).

In the synthesis of **2**, the reaction led to the formation of a mixture of two species which were separable via chromatography. The other species was characterized via X-ray (Fig 2.17) and NMR and turned out to be the novel compound *N*-(2,6-dimethyl)phenyl-6-aminofulvene-2-aldehyde (**5**), formed by hydrolysis of the ligand.

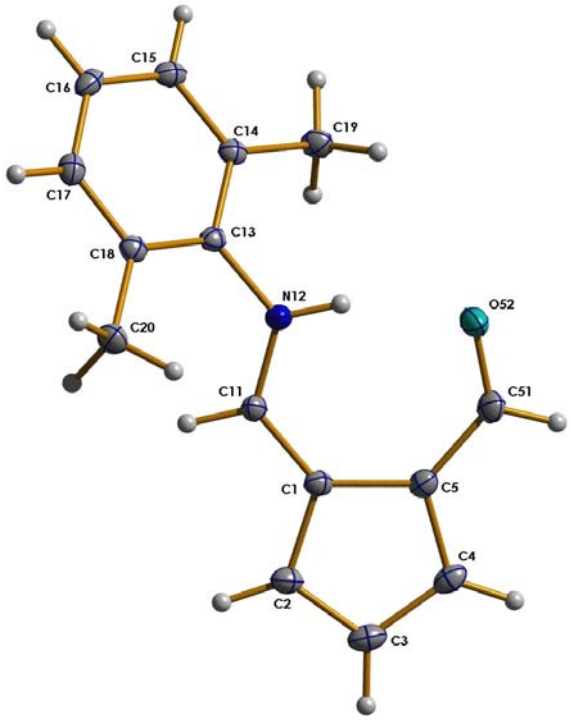

Figure 2.17. Crystal structure of *N*-(2,6-dimethyl)phenyl-6-aminofulvene-2-aldehyde.

Table 2.1. Selected bond lengths and angles for *N*-(2,6-dimethyl)phenyl-6-aminofulvene-2-aldehyde.

Bond	*Bond length (Å)*	*Bond*	*Bond angle (deg)*
C(51)-O(52)	1.2405(19)	O(52)-C(51)-C(5)	127.46(14)
C(5)-C(51)	1.418(2)	C(51)-C(5)-C(1)	130.05(14)
C(4)-C(5)	1.403(2)	C(5)-C(1)-C(11)	130.81(14)
C(3)-C(4)	1.402(2)	C(1)-C(11)-N(12)	125.61(13)
C(2)-C(3)	1.388(2)	C(11)-N(12)-C(13)	125.64(12)
C(1)-C(2)	1.424(2)	C(4)-C(5)-C(51)	123.44(14)
C(1)-C(5)	1.458(2)	C(2)-C(1)-C(11)	122.57(14)
C(1)-C(11)	1.392(2)	C(18)-C(13)-N(12)	121.69(12)
N(12)-C(11)	1.3224(18)	C(14)-C(13)-N(12)	116.48(12)

Such a result was also obtained by Mueller-Westerhoff for the parent compound 6-dimethylaminofulvene-2-aldimine,[3] where the ligand could hydrolyze in boiling aqueous methanol to yield 6-methylaminofulvene-2-aldehyde. Similar considerations for the two systems can be made. As observed in the crystal structure of the novel molecule, the aldehyde tautomeric form is energetically much more stable and the proton is practically bound only to the nitrogen atom. This is consistent with the ^{1}H NMR spectrum, where the N-*H* appears as a doublet (J = 14 Hz for the *trans*-enamine coupling), where a sharp singlet is present for the aldehyde proton.

2.2.2 Synthesis of the complexes: generalities

Attempts to prepare transition metal complexes were made with all the ligands, although not always successfully. As far as catalysis is concerned, the presence of aryl groups on the nitrogen atoms turns out to be of greater interest, due to their closer proximity to the metal centre. Driven by the ultimate desire to utilize such species for alkene

polymerization catalysis, special attention was given to the diaryl-substituted ligands. This is in view of the importance of introducing steric bulk on the nitrogen atoms, which has been proved to be the key feature for late transition metal catalysts bearing diimine ligands.[17] The possibility of selecting aryl amines with bulkier groups in the aromatic ring therefore makes the R_2AFA ligands more appealing.

The common strategy for the synthesis of the complexes involves the deprotonation of the ligand with a base such as NaH, BuLi or CH_3Li to form the metallated ligand, which is not isolated but reacted directly with the appropriate transition metal precursor. Quite surprisingly, this approach led to the formation of bis-chelate species, even though an equimolar ratio of the ligand and the metal precursor was used. Bis-chelated complexes of the ligand **1** with Ni(II), Co(II), Zn(II), and Pd(II) were isolated and characterized. An exception is the reaction of the deprotonated ligand with "$(PPh_3)CuCl$", where monoligation is found. In this case, the oxidation state +1 of the Cu metal centre limits the double coordination of the anionic Ph_2AFA^-. Bis-chelate formation is also avoided by reacting $LiPh_2AFA$ with one equivalent of the metal preursor $[(C_3H_5)PdCl]_2$; in this case only mono-substitution occurs, with formation of one equivalent of LiCl, whereas the second coordination does not take place due to the energetically unfavoured formation of C_3H_5Li. While the diphenyl-substituted ligand turns out to be the most reactive, forming complexes with all the metal precursors so far explored, the same does not seem to happen for ligands **2** and **3**, where probably the steric bulk present on the N atoms hinders the coordination.

A schematic picture of all the synthetic routes to the complexes with the N,N'-diphenyl-6-aminofulvene-2-aldimine ligand is shown in Scheme 2.5. Syntheses of complexes with the ligand **5** were also attempted, although no product was isolated.

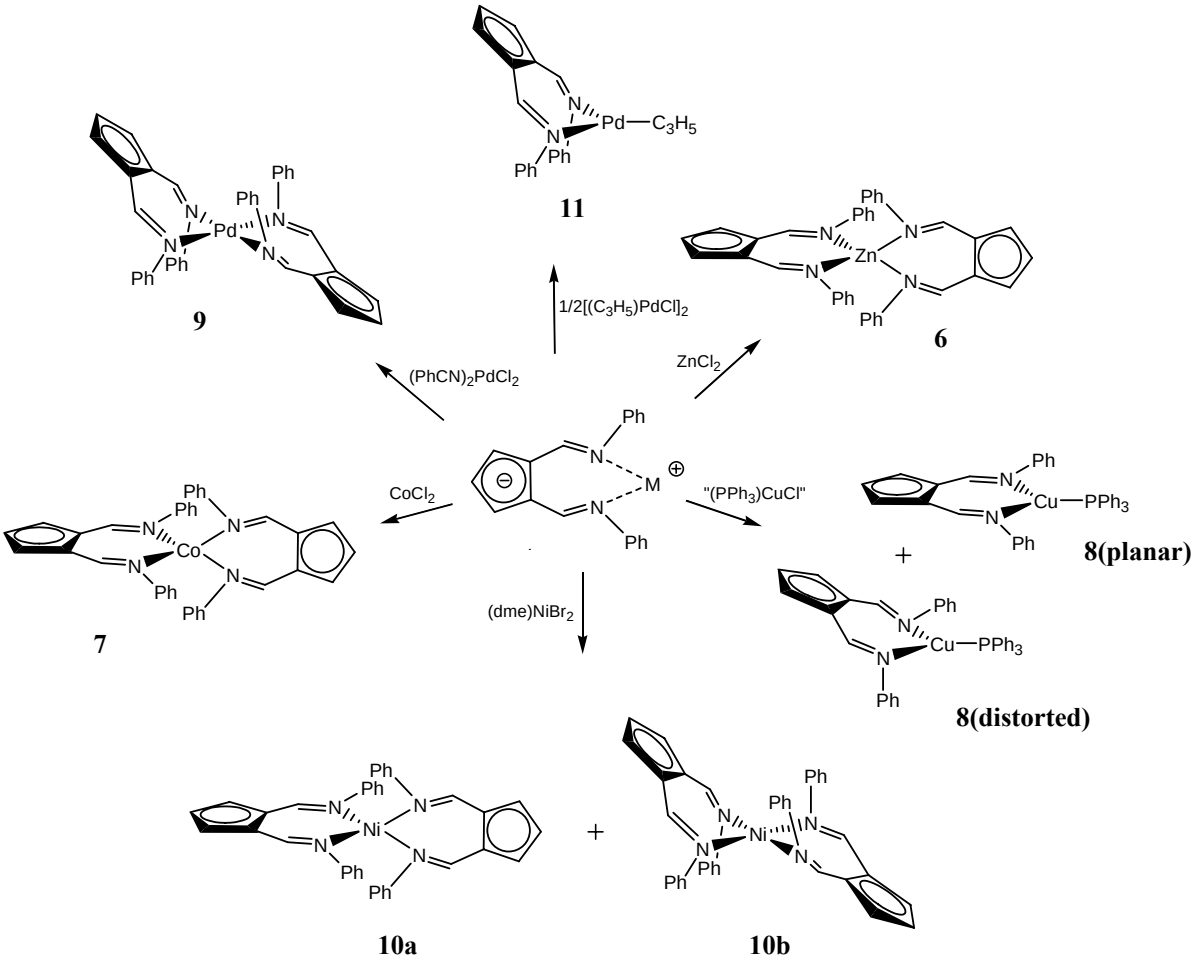

Scheme 2.5. Reactions leading to all the isolated metal complexes

All the compounds were structurally characterised, showing interesting differences. Within the same binding mode of the ligand, it is found that the dihedral angle (***θ***) between the N-M-N plane and the C_2N_2 plane, and the displacement of the metal from this plane (***δ***), vary by remarkable amounts according to the metal used and its coordination geometry. As a general trend, the complexes can substantially be included into three main ranges of the ***θ***, ***δ*** window: 1) molecules where the metallocycle is almost planar, 2) molecules where the distortion from planarity is extreme, 3) molecules falling somehow in between (Fig. 2.18).

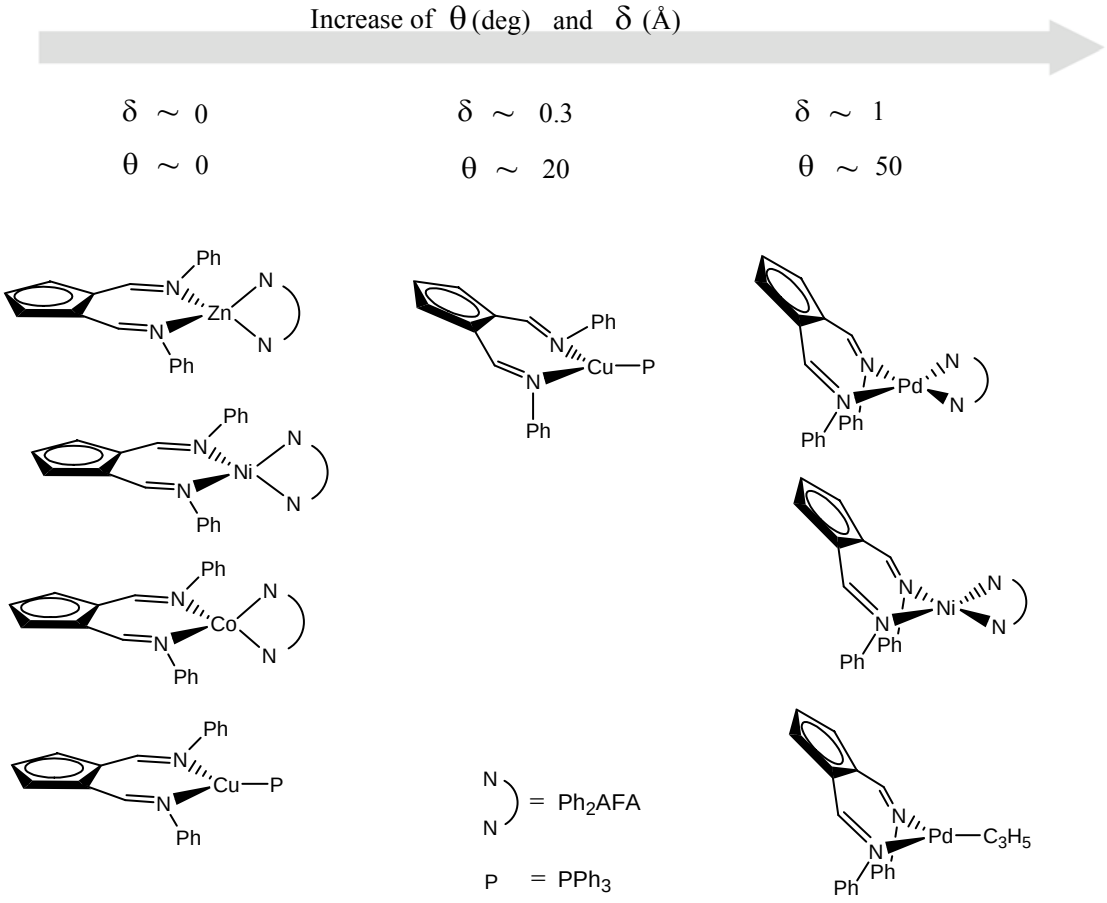

Figure 2.18. The three different areas of the θ, δ window.

These two parameters seem to be associated with the geometry adopted by the metal centre, with the deviation from planarity increasing and the N-M-N bite angle decreasing. For example, almost perfect planarity is found in the tetrahedral species (**6**, **7**, **10b**) whereas the highest displacements occur in the square-planar complexes (**9**, **10a**) where values are 57.09 and 53.60°. However, this interpretation is complicated by the fact that the same complex $LCuPPh_3$ (L = Ph_2AFA) is found into two different areas of the ***θ***, ***δ*** window. It appears therefore that other factors need to be taken into account, such as the steric bulk introduced by the aryl substituents on the nitrogen atoms. Values of ***θ*** and ***δ*** for each complex are reported in Table 2.2.

Table 2.2. Values of the dihedral angle between the C_2N_2 and N-M-N planes (θ) and of the displacement of the metal from the C_2N_2 plane (δ).

Complex	*Θ (deg)*	*δ (Å)*
6	7.63	0.150
7	8.21	0.161
8(planar)	9.17	0.177
8(distorted)	17.82	0.347
9	53.60	1.127
10a	7.00	0.142
10b	57.09	1.106
11	40.77	0.901

Deviations from planarity of the seven-membered metallacyles seem to be in relation with a loss of planarity of the AFA fragment, too. The dihedral angles between the C_5 ring and the C_2N_2 planes change from the negligible values of 1.17, 1.45 and 1.82º for the cobalt, nickel and zinc tetrahedral complexes respectively to the more significant values of 4.38, 5.72 and 10.74º for the **11**, **10a** and **9** square-planar species.

These distortions from planarity of both the seven-membered metallocycle and the AFA fragment had also been observed for the complexes obtained with the ligand H[1,2-C_5H_3-$(C(Ph)NH)_2$] previously discussed. The two ligand systems seem to possess many similarities, even though the presence of the substituents in a closer proximity to the metal centre in the AFA system presumably determines a more direct effect on the conformation that the ligand assumes when coordinated, which is reflected in the wider window of the $\boldsymbol{\theta}$ and $\boldsymbol{\delta}$ values. For example, the maximum values for these two parameters in Stephan's systems are found in complex **F**, where $\boldsymbol{\theta}$ = 31.22º and $\boldsymbol{\delta}$ = 0.859 Å. These values are considerably lower than those found for the square-planar nickel and palladium complexes. Similarly, the aryl groups on the N atoms determine the perfect planarity of the tetrahedral complexes, which is the most sterically favoured conformation. In contrast, deviations from co-planarity of the cyclopentadienyl ring and

the C_2N_2 plane in the *N,N*'-disubstituted AFA fragment are less marked than those found in Stephan's systems, where dihedral angles have values as high as 33.5°.

Despite the exceptional differences in terms of ligand conformation, all the deviations from planarity which have been just discussed are not accompanied by significant changes in bond lengths in the ligand fragment, whereas variations are observed in the angles of the metallacycles.

2.2.3 Structural studies on non-distorted complexes: [$(Ph_2AFA)_2Zn$], [$(Ph_2AFA)_2Co$], [$(Ph_2AFA)Cu(PPh_3)$]

Crystals suitable for X-ray analysis were obtained for complexes **6**, **7**, **8**. Deprotonation of Ph_2AFAH with NaH in THF and reaction with $ZnCl_2$ (1:1 ratio) afforded [$(Ph_2AFA)_2Zn$] (**6**).

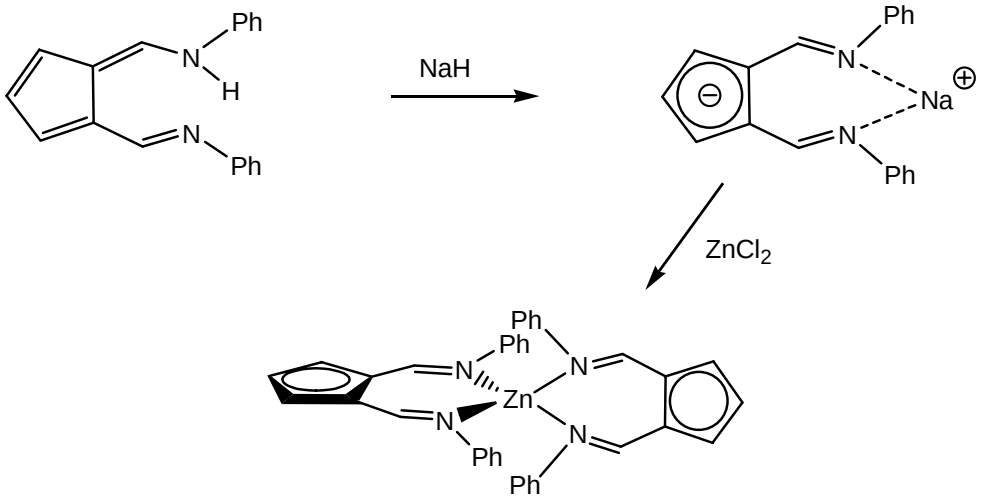

Scheme 2.6. Reaction leading to [$(Ph_2AFA)_2Zn$].

Crystals of **6** suitable for X-ray analysis were obtained by slow evaporation of the solvent from hexane solutions of the complex (Fig 2.19). Selected bond lengths and angles are shown in Table 2.3.

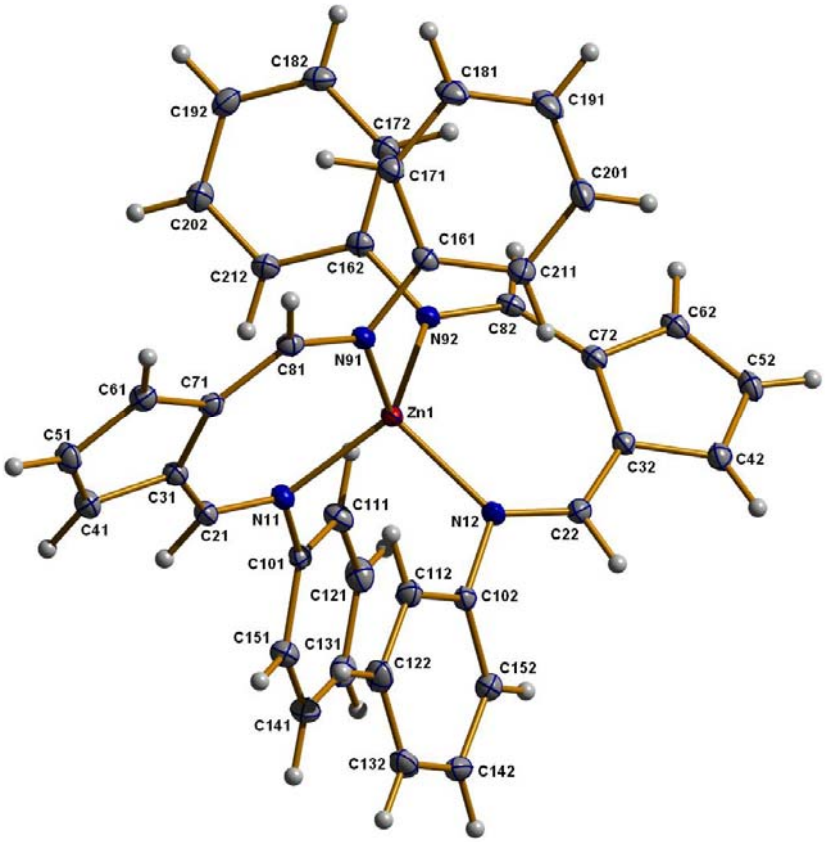

Figure 2.19. Crystal structure of $[(Ph_2AFA)_2Zn]$.

Table 2.3. Selected bond lengths and angles for $[(Ph_2AFA)_2Zn]$ (6).

Bond	*Bond length (Å)*	*Bond*	*Bond angle (deg)*
Zn-N(11)	1.9962(16)	N(11)-Zn-N(91)	111.62(6)
Zn-N(91)	1.9981(16)	Zn-N(91)-C(81)	127.75(13)
N(11)-C(21)	1.313(2)	N(91)-C(81)-C(71)	130.14(18)
C(21)-C(31)	1.411(3)	C(81)-C(71)-C(31)	135.58(18)
C(31)-C(71)	1.459(3)	C(71)-C(31)-C(21)	136.16(18)
C(71)-C(81)	1.410(3)	C(31)-C(21)-N(11)	129.99(18)
N(91)-C(81)	1.132(2)	C(21)-N(11)-Zn	127.68(13)

The molecular structure reveals a slightly distorted tetrahedral geometry around the zinc centre, with the two N-Zn-N angles for the chelate almost equal [111.62(6) and 111.33(7)°] and narrower angles of 100.45 and 101.07° for the non-chelate N-Zn-N Interestingly, all the angles of the seven-membered metallacycle are larger than in the free ligand. Comparing the angles C(72)-C(82)-N(92) and C(32)-C(22)-N(12) with the corresponding angles in the free ligand there is a variation from 130.87(19) and 130.46(19)° for the complex to 126.6(3) and 127.0(3)° for the free ligand, as well as a difference in the angles C(82)-C(72)-C(32) and C(22)-C(32)-C(72), with angles values increasing from 131.6(2)° and 131.0(2)° to 136.04(18)° and 135.40(18)°. Overall, the ligand is "stretching out" by a substantial amount in order to accommodate the larger zinc atom.

Regardless of this distortion in the angles, the aldimine moiety remains on the whole planar, with the metal centre lying only 0.198 Å out of the plane of the ligand and with the N-Zn bond lengths showing values ranging from 1.9962 to 2.0046 Å. The two phenyl groups are tilted by 44.13 and -47.66° relative to the AFA plane. No changes are observed for the C-C bond lengths in the Cp ring in comparison with the protonated free ligand,[4] with distances falling approximately halfway between a single and a double bond. The only exception is the bond C(71)-C(31), whose value is considerably larger [1.459(3) Å]. Similarly, the C-N distances suggest a bond intermediate between single and double.

The behavior in solution of **6** was studied by NMR. Differences with the free ligand are reflected in the shift to higher fields of the Cp protons, which appear as a triplet (*H*4) and a doublet (*H*3, *H*5) respectively at 6.39 and 7.01 ppm, where in the free ligand these signals are found at 6.47 and 7.07. As expected, no signal for the N*H* proton is present, also reflected in the absence of any coupling for the *H*C=N hydrogen atoms, which appear as a sharp singlet at 8.05 ppm. A similar synthetic approach was used for the synthesis of the cobalt analogue (**7**), which was obtained in 78% yield (relative to the moles of ligand) as red crystals from hexane solution .

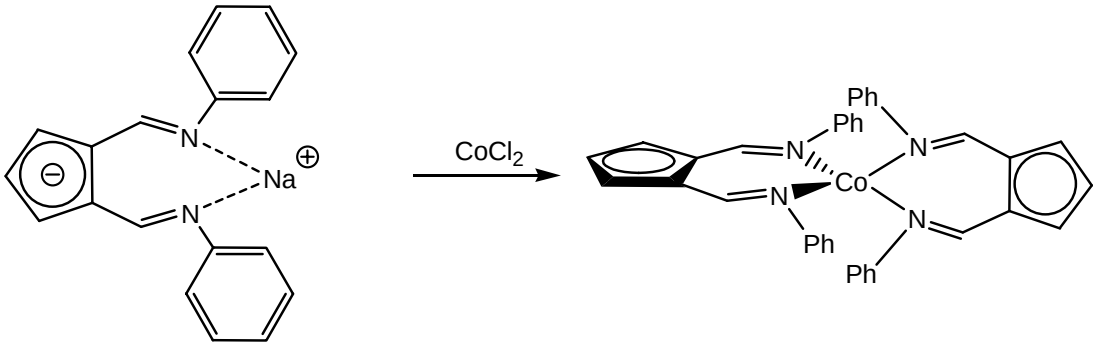

Scheme 2.7. Reaction leading to $[(Ph_2AFA)_2Co]$.

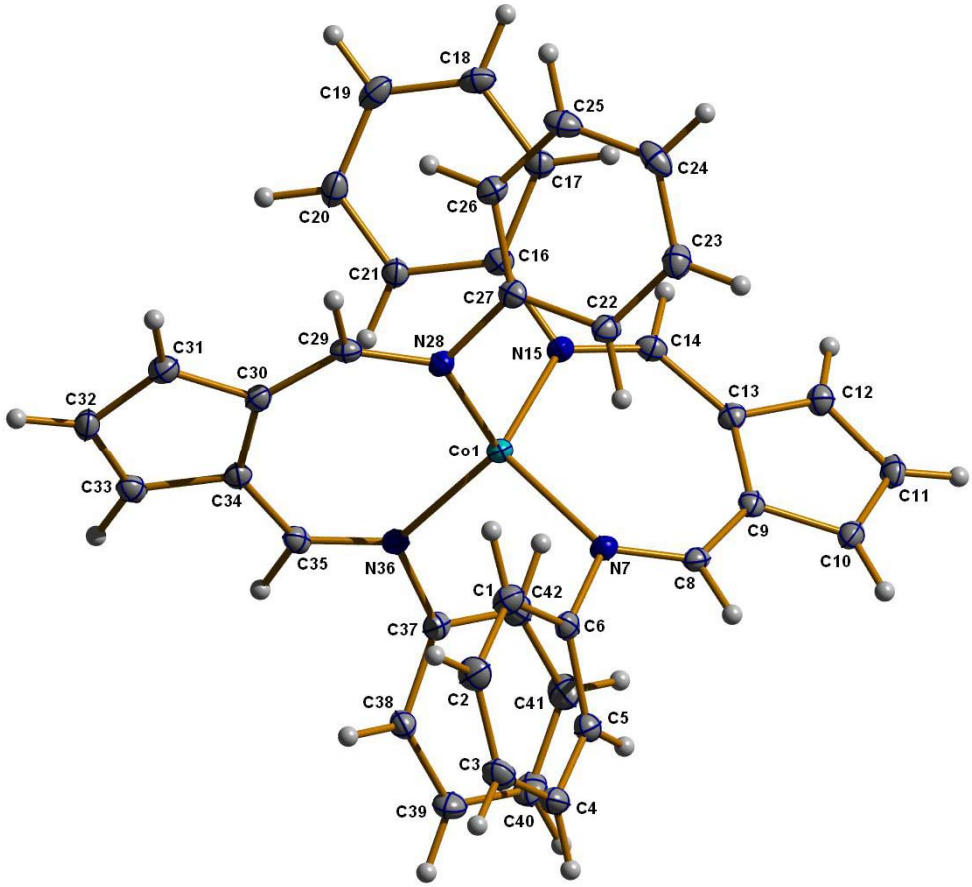

Figure 2.20. Molecular crystal structure of $[(Ph_2AFA)_2Co]$.

Table 2.4. Selected bond lengths and angles for [$(Ph_2AFA)_2Co$] (7).

Bond	*Bond length (Å)*	*Bond*	*Bond angle (deg)*
Co-N(28)	1.982(2)	N(28)-Co-N(36)	110.93(10)
Co-N(36)	1.984(2)	Co-N(28)-C(29)	128.3(2)
N(28)-C(29)	1.310(4)	N(28)-C(29)-C(30)	130.3(3)
C(29)-C(31)	1.411(4)	C(29)-C(30)-C(34)	135.4(3)
C(30)-C(34)	1.459(4)	C(30)-C(34)-C(35)	135.4(3)
C(34)-C(35)	1.403(4)	C(34)-C(35)-N(36)	130.2(3)
N(36)-C(35)	1.314(4)	C(35)-N(36)-Co	128.4(2)

The crystal structure is very similar to the zinc complex, showing a distorted tetrahedral environment of the metal centre (Fig. 2.20). The ligand framework is on the whole planar, and planarity is also present in the metal chelate.

The N-Co distances are more similar to each other than in the zinc analogue, ranging from 1.982(2) to 1.986(2) Å, whereas the N-Co-N angles are just slightly narrower [(110.05(10) and 110.70(10)°]. All the angles of the metallacycle do not significantly differ from those in **6**, and so do the C-C bond lengths, which are similar to each other, with the exclusion of the remarkably longer C(30)-C(35) bond.

As expected for a d^7 transition metal with tetrahedral geometry, the complex is paramagnetic, having three unpaired electrons, therefore NMR spectra only showed broaden signals not easily assignable.

In conclusion, the two complexes show many similarities and can be discussed by using the same structural framework, thus allowing to draw a common description of the ligand electronic environment and consequently bonding mode. From the bond distances it appears that a partial double bond is present within the whole ligand moiety. Because the differences in C-C and C-N bond lengths between complexes **6** and **7** and Stephan's complexes are not significant, a depiction of the ligand can be made in analogy with the species **E**, **F**, **G**, **H** and **I** described above, considering the possible different resonance forms. However, due to the greatly enhanced planarity of the

complexes **6** and **7** in comparison with Stephan's complexes, the view is more consistent with a fully delocalised π-system. Where the contribution from a cyclopentadienyl-diimino form is consistent with the C-N bond distances, these distances are longer than in neutral diimine systems, where values normally range between 1.25-1.28 Å. Moreover, the C(Cp)-N distances in both complexes are shorter than a normal Csp^2-Csp^2 single bond (typically 1.47-1.49 Å), indicating that there is some double bond character in these connections. The only distances that remain appreciably longer are the C-C bonds between the two aldimine-cyclopentadienyl carbon atoms.

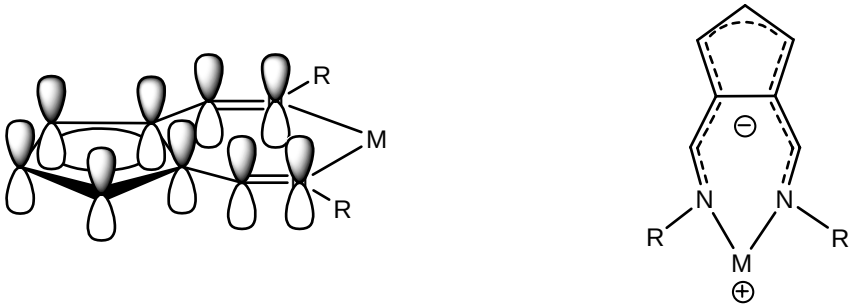

Figure 2.21. Planarity of the system in 6 and 7 suggests an effective delocalization of the negative charge into the AFA moiety.

The planarity of the ligand fragment and the C-C and C-N bond distances are therefore consistent with the view of a diiminate system for complexes **6** and **7**, where the negative charge is delocalised over the whole AFA moiety (Fig. 2.21). Alternatively, as indicated by the similarity of the structural parameters with the protonated free ligand, the complexes can be depicted as a superimposition of the two unsymmetrical structures featuring imino-amide chelates (Fig. 2.22).

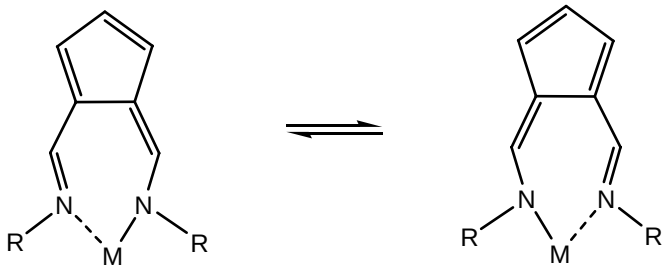

Figure 2.22. The possible two asymmetric resonance forms of the metal-coordinated Ph_2AFA ligand.

As described above, in both complexes **6** and **7**, the only C-C distances that remain appreciably longer are the C-C bonds between the two aldimine-cyclopentadienyl carbon atoms, suggesting that π-delocalisation is less effective in this connection. However, the values of such distances (1.459 Å for both **6** and **7**) indicate that some double bond character is present. In addition, the C-C distances between the non-substituted Cp carbons are slightly shorter than the others. This data can be interpreted by taking into account an additional contribution from a diimino-allyl structure.

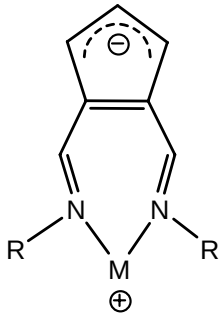

Figure 2.23. Possible allyl-diimino form of the metal-coordinated Ph_2AFA ligand.

Such a depiction can not be used to describe the situation in the related 2-aminotroponiminate systems (R_2ATI). These ligands are normally described as either being the superimposition of the two unsymmetrical resonance forms or as bearing the negative charge delocalised on the whole ligand (Fig. 2.24).

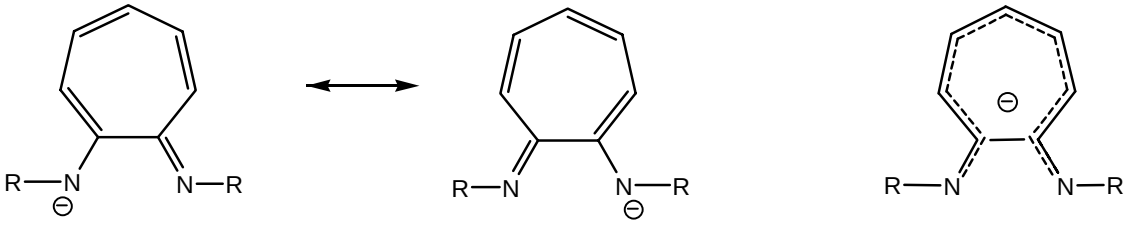

Figure 2.24. Resonance forms for the anionic aminotroponiminate. The alternative view is that of a fully delocalized π-system.

All the crystal structures of aminotroponiminate complexes obtained with main group and transition metals, show that the ligand is invariably planar, and the metal sits on the same plane, presumably due to the more rigid 5-membered metallocycle.[18] Analysis of the bond lengths in these complexes reveals that the C(1)-C(7) is remarkably longer than all the other C-C bonds and is consistent with a Csp^2-Csp^2 single bond. For example, the crystal structure of the cobalt derivative $[(i\text{-Pr})_2ATI]_2Co$ shows values of 1.501 Å for this particular bond, which is considerably longer than the corresponding value found in $[(Ph_2AFA)_2Co]$ (1.457 Å), providing the evidence of the absence of any double bond in these connection.[19]

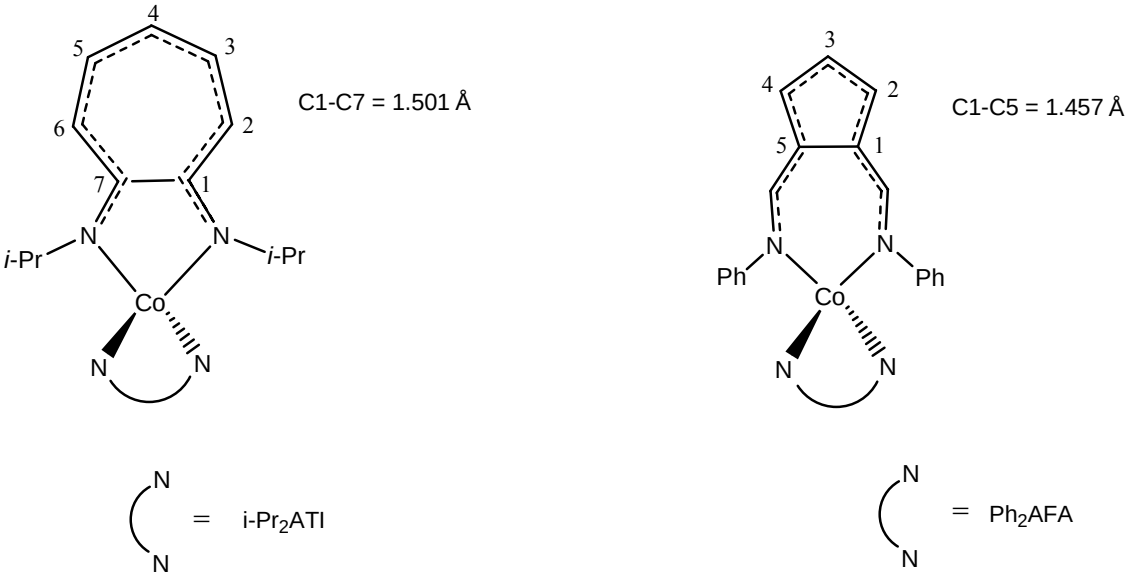

Figure 2.25. Comparison of the cobalt complexes with aminotroponiminate and aldiminate.

As previously mentioned, bis-chelation is avoided by using a metal precursor in a +1 oxidation state, thus limiting the double substitution of the halide ligand. Reaction of the sodium salt of the ligand with ¼ equivalents of $[(PPh_3)CuCl]_4$ in THF, leads to the isolation of $[(Ph_2AFA)Cu(PPh_3)]$ (**8**). The complex is fairly stable, although if not kept under an inert atmosphere slowly decomposes with release of free ligand and free phosphine.

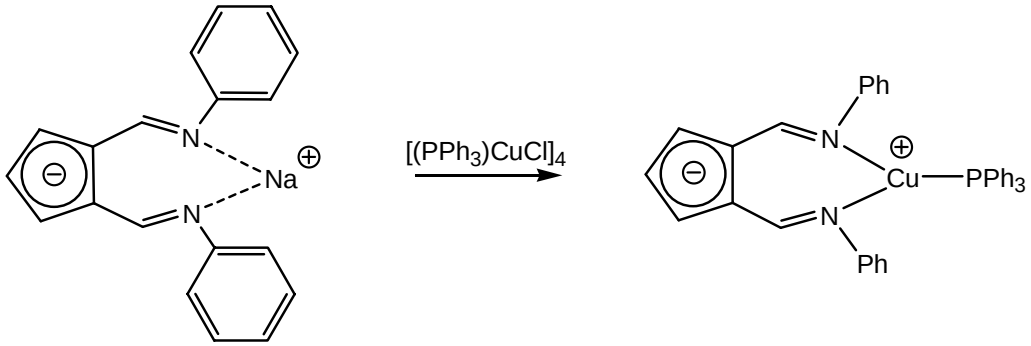

Scheme 2.8. Reaction leading to[(Ph_2AFA)Cu(PPh_3)].

Crystals suitable for X-ray analysis were obtained upon slow evaporation of the solvent from hexane solutions. Selected bond lengths and angles are reported in Table 2.5.

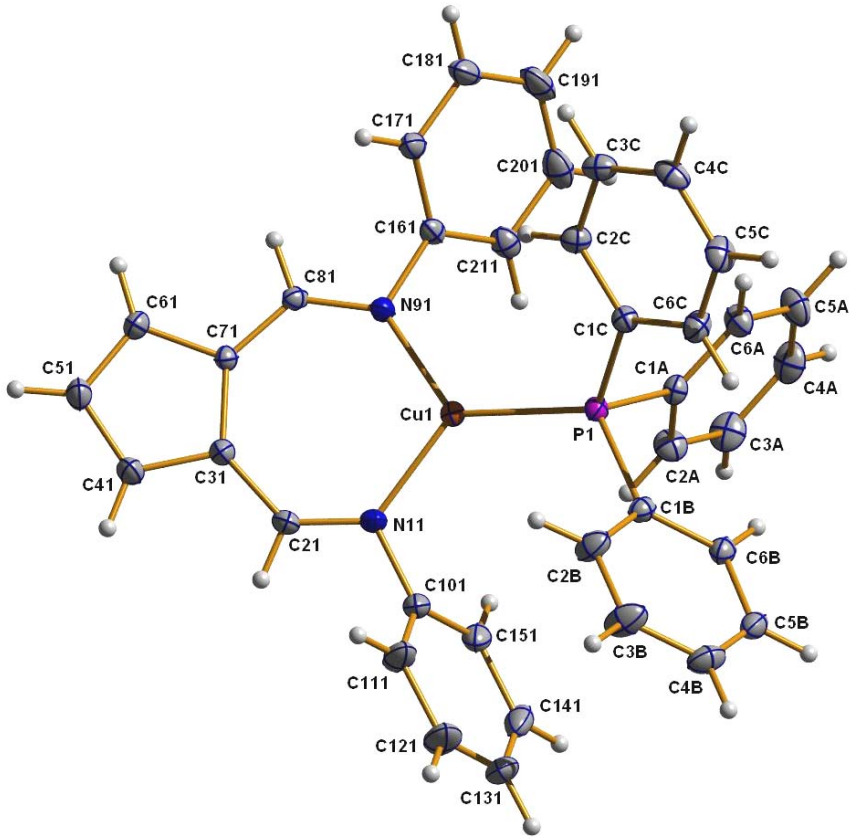

Figure 2.26. Molecular crystal structure for [(Ph_2AFA)Cu(PPh_3)].

Table 2.5. Selected bond lengths and angles for [(Ph_2AFA)Cu(PPh_3)].

Bond	*Bond length (Å)*	*Bond*	*Bond angle (deg)*
Cu-N(11)	1.9847(19)	N(11)-Cu-N(91)	110.29(8)
Cu-N(91)	1.9986(16)	Cu-N(91)-C(81)	126.39(15)
Cu-P(1)	2.2136(6)	N(11)-Cu-P(1)	124.67(6)
N(11)-C(21)	1.301(3)	N(91)-C(81)-C(71)	130.8(2)
C(21)-C(31)	1.411(3)	C(81)-C(71)-C(31)	135.5(2)
C(31)-C(71)	1.449(3)	C(71)-C(31)-C(21)	135.0(2)
C(71)-C(81)	1.409(3)	C(31)-C(21)-N(11)	130.1(2)
N(91)-C(81)	1.311(3)	C(21)-N(11)-Cu	127.73(16)

Although very similar to **6** and **7**, the presence of only one Ph_2AFA ligand on the copper(I) centre introduces some interesting differences. The compound crystallizes with two individual molecules in the asymmetric unit cell (indicated for clarity as **8(planar)** and **8(distorted)**), which differ in the values of the dihedral angle ($\boldsymbol{\theta}$) between the metal mean plane $PCuN_2$ and the plane defined by the two C=N bonds of the ligand. While one of the molecules is essentially planar, in the second molecule such an angle is 17.82°, with the metal displaced of 0.347 Å from the C_2N_2 plane. The difference in these two parameters must be most certainly due to the different orientation of the phosphine ligand relative to the AFA ligand, and distortion occurs to avoid contact between the aryl substituents on the N atoms and the phenyl groups of the phosphine. As a consequence of the deviation from planarity, the N-Cu bond lengths of the non-planar molecule (1.985 and 1.989 Å) are slightly longer than in the planar one, where values are 1.973 and 1.980 Å, and the N-Cu-N angle (110.29) is 1.14° narrower, giving evidence for the existence of a relationship between the values of $\boldsymbol{\theta}$ and $\boldsymbol{\delta}$ and the N-M-N angles.

Despite the different values of $\boldsymbol{\theta}$ and $\boldsymbol{\delta}$ the metal adopts a trigonal planar geometry in both molecules and the C-C and C-N bond lengths are substantially identical, as are the Cu-P bond lengths, which are however longer than the metal chelate. Remarkably, the

N-Cu-N angles are significantly smaller than 120º, which is the value expected for a trigonal-planar geometry, signifying that the ligand can not adopt such a wide bite angle.

All the bond lengths for both molecules, however, are very similar to the zinc and cobalt tetrahedral complexes and the N-Cu-N angle is not much different either, with a value of 110.3°. The only bond which shows some difference is C(31)-C(71) [1.449(3) Å], probably meaning that the diimino-allyl form gives more contribution than in **6** and **7**. No significant differences are observed concerning the strain added into the metallocycle in terms of angle enlargement. Similar to **6** and **7**, the C(31)-C(71)-C(81) and C(71)-C(31)-C(21) angles are 135.5 and 135.0°. Other than causing the distortion from planarity, the presence of the phosphine also affects the positions of the phenyl groups on the nitrogen atoms, which are tilted in the same direction, forming dihedral angles of 51.68 and 52.87° with the aldimine plane.

In solution, the structural differentiation is not retained and the two molecules show common spectroscopycal features. The ^{1}H NMR shows a upfield shift for the Cp protons: *H*4 appears as a triplet at 6.38 ppm, *H*3 and *H*5 appear as a doublet at 7.00 ppm. Again, the absence of the N*H* proton turns the original free ligand doublet for the HC=N protons into a sharp singlet, which in contrast with **6** is shifted to lower fields (8.39 ppm), most certainly due to the presence of the phosphine ligand.

2.2.4 Structural studies on the "distorted" complexes: [$(Ph_2AFA)_2Pd$], [$(Ph_2AFA)Pd(C_3H_5)$].

The bis-chelated AFA palladium complex (**9**) was obtained by deprotonation of Ph_2AFAH with BuLi in toluene followed by reaction with $[(PhCN)_2PdCl_2]$.

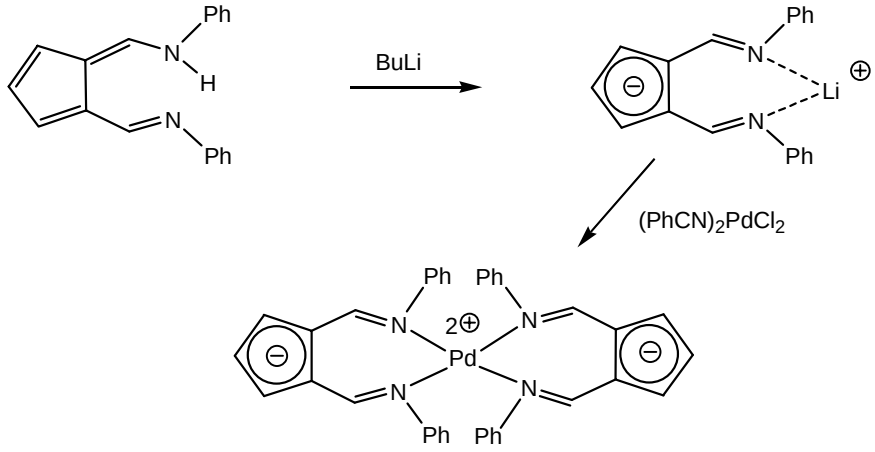

Scheme 2.9. Reaction leading to $[(Ph_2AFA)_2Pd]$.

Crystals suitable for X-ray analysis were grown upon standing of a concentrated toluene solution at -10 °C, or alternatively by slow evaporation of the solvent from a THF solution.

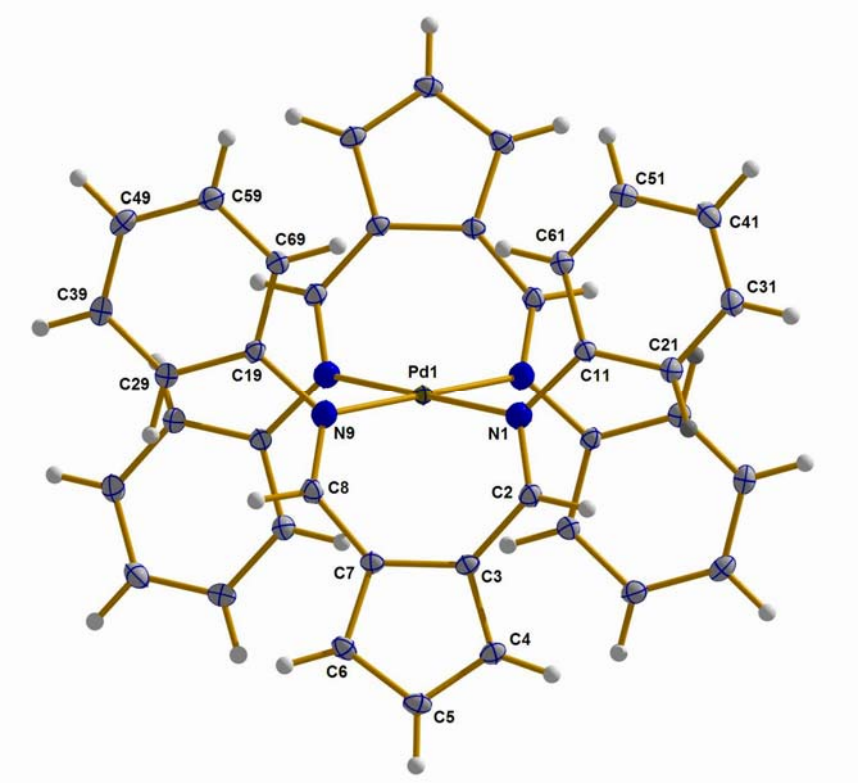

Figure 2.27. Molecular crystal structure of $[(Ph_2AFA)_2Pd]$.

Table 2.6. Selected bond lengths and angles for [$(Ph_2AFA)_2Pd$].

Bond	*Bond length (Å)*	*Bond*	*Bond angle (deg)*
Pd-N(1)	2.028(2)	N(1)-Pd-N(9)	92.89(8)
Pd-N(9)	2.0369(19)	Pd-N(1)-C(2)	121.55(17)
N(1)-C(2)	1.308(3)	N(1)-C(2)-C(3)	127.6(2)
C(2)-C(3)	1.412(3)	C(2)-C(3)-C(7)	131.4(2)
C(3)-C(7)	1.446(3)	C(3)-C(7)-C(8)	130.7(2)
C(7)-C(8)	1.413(3)	C(7)-C(8)-N(9)	127.2(5)
C(8)-N(9)	1.309(3)	C(8)-N(9)-Pd	118.86(16)

Significant differences with the zinc, copper and cobalt analogues are observed. The crystal structure (Fig. 2.27) shows that the complex is centrosymmetric and that the two ligands are therefore equivalent. The geometry of the complex is square-planar, with N-Pd-N angles of 92.89º; as discussed above, coordination occurs with a high distortion of the ligand, which is tilted 53.6º towards an axial position relative to the PdN_4 plane, and the metal is sitting 1.295 Å out of the ligand mean plane. Such distortion, however, is not accompanied by any substantial variation of the bond lengths, whose values approximately fall into the same range as those found in **6**, **7**, **8**. However, as expected for a second row transition metal, the N-Pd distances are longer (2.028 and 2.0369 Å). The distortion of the ligand determines differences in the angles of the chelate, which, in comparison with the planar tetrahedral species, are closer to those found in the free ligand. In particular, the Pd-N-C angles are close to 120°, as it should be in sp^2 hybridized N atoms, where in **6**, **7** and **8** such values average *ca*. 128°. Furthermore, the C(Cp)-C-N angles are about 5° narrower, determining a considerable decrease of the intra ligand N-N distance, which moves from the 3.305 and 3.267 Å in **6** and **7** to 2.946 Å in **9**. As mentioned above, the distortion of the ligand fragment is likely attributable to two distinct factors. The copper complex **8** was previously shown to crystallize with two molecules in the asymmetric unit cell, one of which exhibits a significant displacement from planarity; such a displacement was related to the presence the phosphine ligand,

which places two of the three phenyl groups into different orientations relative to the metal chelate. As a response, the ligands undergo distortion in order to avoid collision of the phenyl N-substituents, which are moved towards the opposite axial position relative to the AFA moiety, and therefore far from the phosphine phenyl groups. Distortion of the ligand in the palladium complex **9** can therefore be anticipated as a result of the addition of bulk produced by the presence of phenyl substituents of the two AFA ligands. The view of the ligand conformation as being exclusively dependent on steric factors, however, does not find support in the isolation of the mono-chelated species $[(Ph_2AFA)Pd(C_3H_5)]$ (**11**).

This complex was obtained by reacting the metallated ligand with ½ equivalent of $[(C_3H_5)PdCl]_2$ (Scheme 2.10).

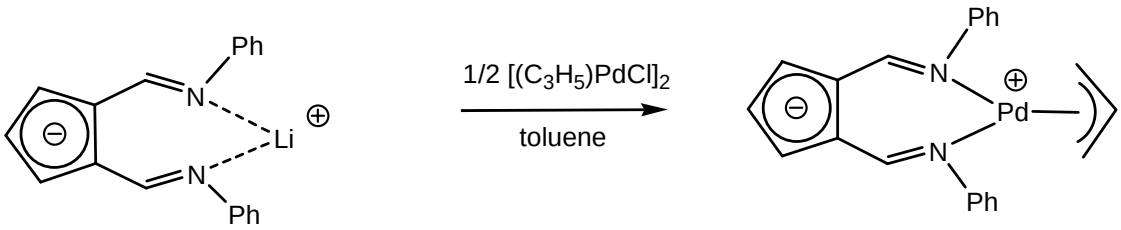

Scheme 2.10. Reaction leading to $[(Ph_2AFA)Pd(C_3H_5)]$.

The product **11** was isolated in 83% yield and crystals suitable for X-ray analysis were obtained as orange blocks by slow evaporation of the solvent from hexane solution.

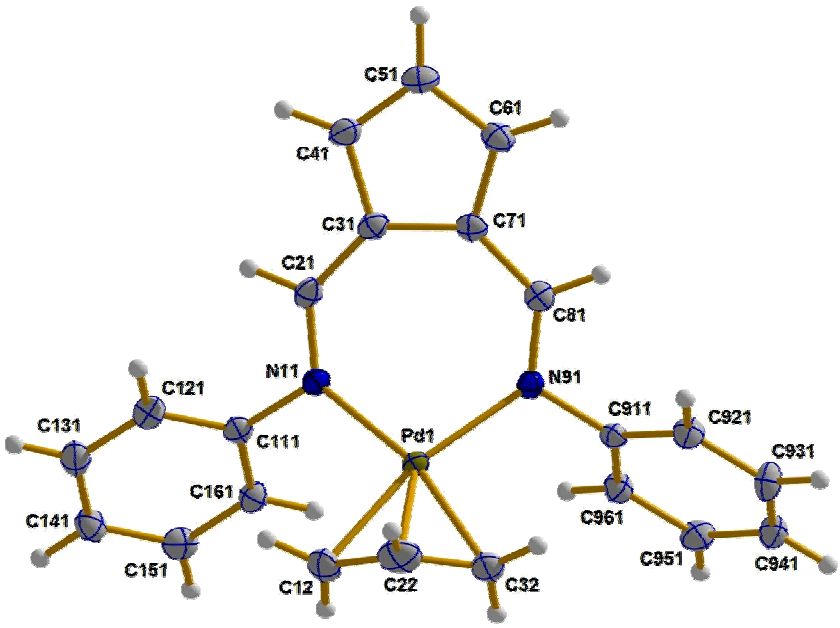

Figure 2.28. Molecular crystal structure of [(Ph_2AFA)Pd(C_3H_5)].

Table 2.7. Selected bond lengths and angles for [(Ph_2AFA)Pd(C_3H_5)].

Bond	*Bond length (Å)*	*Bond*	*Bond angle (deg)*
Pd-N(11)	2.090(2)	N(11)-Pd-N(91)	97.38(9)
Pd-N(91)	2.092(2)	Pd-N(11)-C(21)	124.22(19)
Pd-C(12)	2.126(3)	C(12)-Pd-C(32)	68.69(12)
Pd-C(32)	2.133(3)	C(12)-C(22)-C(32)	120.5(4)
Pd-C(22)	2.107(3)	Pd-N(11)-C(111)	116.5(2)
N(91)-C(81)	1.294(3)	Pd-N(91)-C(911)	116.6(2)
N(11)-C(21)	1.298(4)	N(11)-C(21)-C(31)	130.6(3)
C(21)-C(31)	1.411(4)	C(21)-C(31)-C(71)	134.1(3)
C(31)-C(41)	1.429(5)	C(31)-C(71)-C(81)	132.8(3)
C(41)-C(51)	1.378(4)	C(71)-C(81)-N(91)	129.9(3)
C(51)-C(61)	1.402(5)	C(81)-N(91)-Pd	125.04(19)

The crystal structure reveals a square-planar geometry of the metal centre, with the ligand undergoing the same type of distortion occurring in **9**. Such distortion is of a minor degree in comparison with the bis-chelated complex, but never-the-less quite significant. The dihedral angle between the C_2N_2 plane and the PdN_2 plane is 40.77° and the metal is displaced 0.901 Å from the ligand mean plane. This is quite surprising in view of the extremely lower steric hindrance introduced by the small allyl ligand, and confirms that deviations from planarity are not only dictated by steric factors, although these might be an important component. In the case of the two palladium complexes, it appears that some correlation between the ligand bite angle and the degree of distortion does exist, with the spatial position of the ligand as well as its conformation varying in order to match the required 90º for a square-planar geometry. It emerges, therefore, that the ligand possesses an intrinsic flexibility which can be induced by steric factors or geometrical restrictions. It is tempting to speculate that these two aspects can also be correlated to each other, exerting in combination a greater effect on the resulting structure. More specifically, it is noteworthy that the complexes **9** and **11** differ quite considerably in their chelate angles, with the N-Pd-N angle in the allyl-palladium species (97.38º) larger than in $[(Ph_2AFA)_2Pd]$ (92.89º). Whilst this might be the reason for the inverse trend of the θ values (with narrower N-M-N bite angles causing larger distortions), it can not be ruled out that it is the more hindered environment in **9** that produces some additional distortion of the ligand; such additional distortion is in turn reflected into the narrower N-Pd-N angle.

Apart from the N-Pd-N angle, the presence of the allyl ligand in complex **11** determine a significant difference in the Pd-N distances (2.090 and 2.091 Å), which are longer than in **9**. All the other bond lengths in the metallocycle, instead, remain substantially unaltered. Interestingly, changes in the C-C lengths of the cyclopentadienyl moiety are found. The C41-C51 bond is quite shorter than the others (1.378 Å), whereas C31-C41 is longer (1.429 Å); inversely, the other C-C bond of the unsubstituted carbon atoms (C51-C61) becomes longer (1.403 Å) than the adjacent C61-C71 bond (1.393 Å). This is not in agreement with the symmetry of the bond lengths observed in **6**, **7**, **8**, **9** and suggests some different distribution of the negative charge in

the Cp ring, and of the double bond characters. In addition to the wider N-Pd-N angle, the lower steric congestion of the mono-substituted complex results in an enlargement of all the metallocycle angles, and consequently of the intra-ligand N-N distance (1.314 Å).

The extreme distortion occurring in **9** and **11** also causes effects in the electronic properties of the ligand, as it is observed in the ^{1}H NMR spectrum. The most affected protons are the ones attached to the imino carbon atoms, H-C=N. In complex **9,** shift towards higher fields (7.43 ppm) is more considerable than in the zinc complex (8.05 ppm), whereas for the allyl complex, a considerable downfield shift occurs, with the H-C=N protons found at 8.42 ppm. Interestingly, this value is very close to the other mono-chelate complex **8**, and presumably has to be put in relationship with the absence of the other AFA ligand.

2.2.5 Isomerism of nickel complexes. Studies on the "distorted" and "planar" complexes [$(Ph_2AFA)_2Ni$].

The nickel complex with the Ph_2AFA ligand was prepared by reacting the deprotonated ligand with [(dme)$NiBr_2$] in toluene or THF.

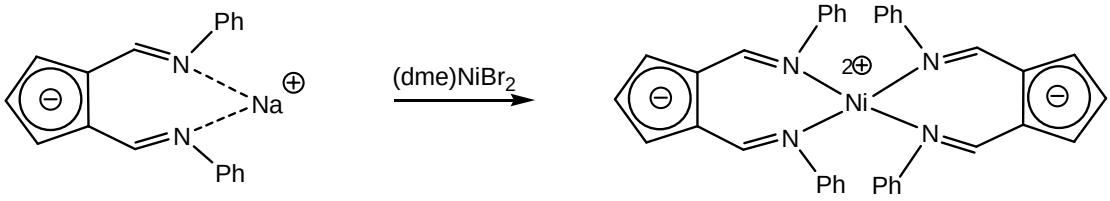

Scheme 2.11. Reaction leading to [$(Ph_2AFA)_2Ni$].

The product can be isolated as a black crystalline solid and its ^{1}H NMR analysis revealed the formation of the diamagnetic bis-chelated [$(Ph_2AFA)_2Ni$] (**10b**) with a square-planar structure. In comparison with the Pd analogue, the shift of *H*4 happened to be at lower fields (6.55 ppm) than in the free ligand, where *H*3 and *H*5 are consistent

with the previous observations, undergoing a rather significant upfield shift to 6.77 ppm. The *H*C=N singlet formed upon N chelation appears at 7.07 ppm, which is the greatest shift observed among all the complexes synthesized. Even more interesting was the discovery in the spectrum of signals attributable to the presence of a paramagnetic species, with broad peaks of the ligand greatly shifted up- and downfield, only visible by expanding the spectrum window.

The situation was greatly clarified from the X-ray analysis conducted on two crystals of the complex, which were obtained via slow diffusion of pentane into CH_2Cl_2 solutions and from storage at -10 °C of toluene solutions. Although very similar in shape and color the two crystals turned out to be different isomers of the same molecule, featuring the nickel centre in two different environments. A square planar species (**10b**) resembling the palladium complex was formed, together with a tetrahedral form (**10a**) similar to the cobalt and zinc structures above discussed. The former (Fig. 2.29) crystallises with a monoclinic unit cell, in which one molecule of toluene is present.

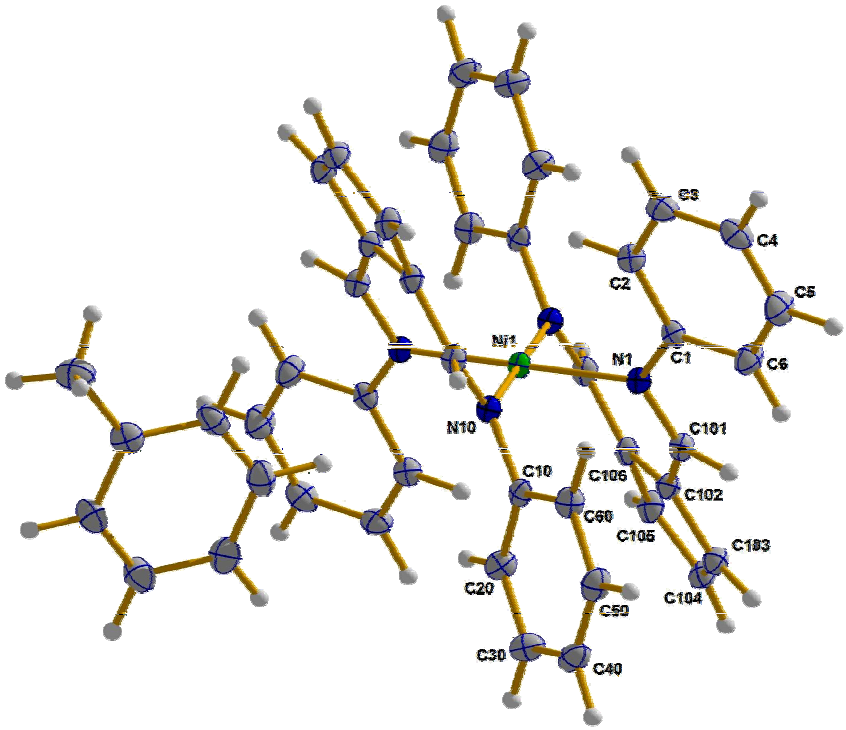

Figure 2.29. Molecular crystal structure of the square-planar complex $(Ph_2AFA)_2Ni$ (10b).

Table 2.8. Selected bond lengths and angles for the square-planar complex [$(Ph_2AFA)_2Ni$] (10b).

Bond	*Bond length (Å)*	*Bond*	*Bond angle (deg)*
Ni-N(1)	1.9170(14)	N(1)-Ni-N(10)	92.97(6)
Ni-N(10)	1.9108(14)	Ni-N(1)-C(101)	118.23(12)
N(1)-C(101)	1.314(2)	N(1)-C(101)-C(102)	127.06(16)
N(10)-C(107)	1.309(2)	C(101)-C(102)-C(106)	129.65(16)
C(101)-C(102)	1.402(2)	C(1)-N(1)-C(101)	119.95(15)
C(102)-C(103)	1.418(2)	C(102)-C(106)-C(107)	129.98(16)
C(103)-C(104)	1.389(3)	C(106)-C(107)-N(10)	126.84(16)
C(104)-C(105)	1.403(3)	Ni-N(1)-C(1)	120.38(11)
C(105)-C(106)	1.409(2)		
C(102)-C(106)	1.453(2)		
C(106)-C(107)	1.408(2)		

In comparison with [$(Ph_2AFA)_2Pd$], the N-Ni distances are shorter, as expected for a first row metal congener, with values of 1.9108 and 1.9170 Å. All the other bond lengths do not show any substantial variation from those in the Pd complex. The N-Ni-N angles are 92.97°, which also does not deviate much from the N-Pd-N angles in **9**.

The other isomer (**10a**, Fig. 2.30) features the nickel atom in a tetrahedral environment, with the metal lying in the same plane as the ligand, which is almost perfectly planar. The N-Ni distances range from 1.969 to 1.978 Å, only ca. 0.01 Å shorter than in the cobalt and ca. 0.02 Å than in the zinc. Analogously, no great deviations in terms of angles are found, with the values for the N-Ni-N angles being 107.9 and 107.6, only 3 degrees smaller than the cobalt counterpart.

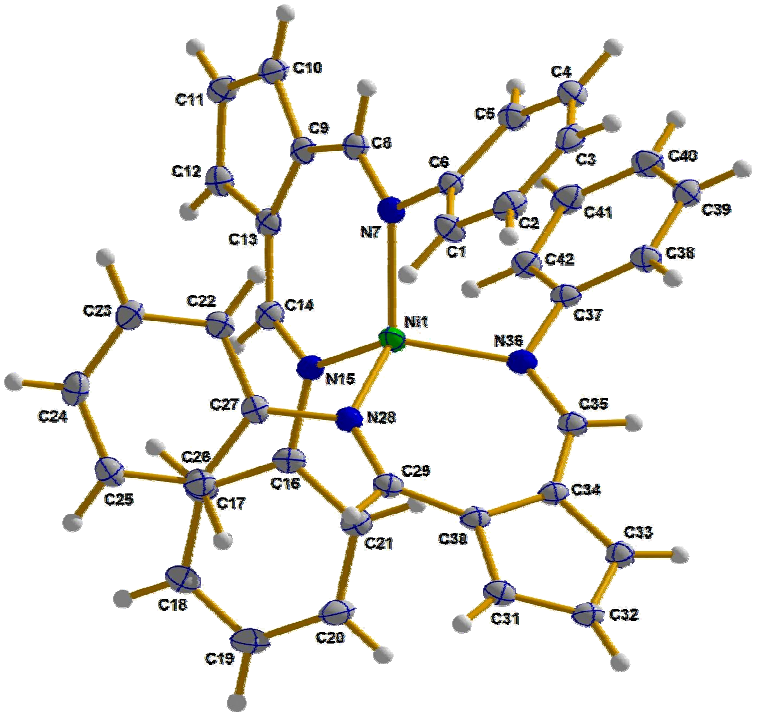

Figure 2.30. Molecular crystal structure of the tetrahedral complex $(Ph_2AFA)_2Ni$ (10a).

Table 2.9. Selected bond lengths and angles for the tetrahedral complex $[(Ph_2AFA)_2Ni]$ (10a).

Bond	*Bond length (Å)*	*Bond*	*Bond angle (deg)*
Ni-N(7)	1.969(2)	N(7)-Ni-N(15)	107.94(9)
Ni-N(15)	1.976(2)	Ni-N(7)-C(8)	130.98(18)
N(7)-C(8)	1.316(3)	N(7)-C(8)-C(9)	130.1(2)
C(8)-C(9)	1.398(3)	C(8)-C(9)-C(13)	134.8(2)
C(9)-C(13)	1.458(3)	C(8)-N(7)-C(6)	116.5(2)
C(13)-C(14)	1.401(4)	C(9)-C(13)-C(14)	134.4(2)
N(15)-C(14)	1.318(3)	C(13)-C(14)-N(15)	130.3(3)
C(9)-C(10)	1.411(4)	Ni-N(7)-C(6)	111.81(15)
C(10)-C(11)	1.387(4)		
C(11)-C(12)	1.383(4)		
C(12)-C(13)	1.413(4)		

Although the adoption of the square planar structure might be initially explained invoking a distortion caused by the presence of a toluene molecule in the crystalline lattice (which is absent in the unit cell of **10b**), this hypothesis is not supported by the NMR studies of the two complexes, which show the presence of both forms in solution. Variable temperature ^1H NMR studies revealed that the two isomers are not interconverting and do not therefore exist in equilibrium. Increasing the temperature from -20° to 40° C is not accompanied by any inter-conversion of the two forms, suggesting that the energy barrier for this process must be too high. Such a process can be formally divided in two steps: the rotation of the ligands around the nickel centre and the subsequent distortion, or vice versa. No matter which step occurs first and which form is transforming into the other one, the presence of the aryl groups on the nitrogen will always cause some degree of hindrance, blocking somehow the interconversion.

It can therefore be argued that the high barrier of inter-conversion is due to the bulk of the two aryl rings. An alternative path for the interconversion could involve a dissociation, or partial dissociation, of one ligand prior to the rotation around the metal centre, but this seems unlikely because of the relatively high thermodynamic stability of both forms.

Probably, kinetic factors must be taken into account to explain the two isomers, whose formation is believed to follow two different reaction paths. Attempts to draw the mechanisms of formation of the two isomers have been made. One hypothesis is that the mechanism leading to the square-planar complex was based on a disproportionation process from the dimer $[Ph_2AFANiCl]_2$. Such a species could form upon pairing of two unsaturated $Ph_2AFANiCl$ fragments resulting from the first substitution of one halide with one Ph_2AFA^- ligand.

Disproportionation of the dimer is presumably a very fast step, since isolation of the hypothized dimeric intermediate was never achieved.

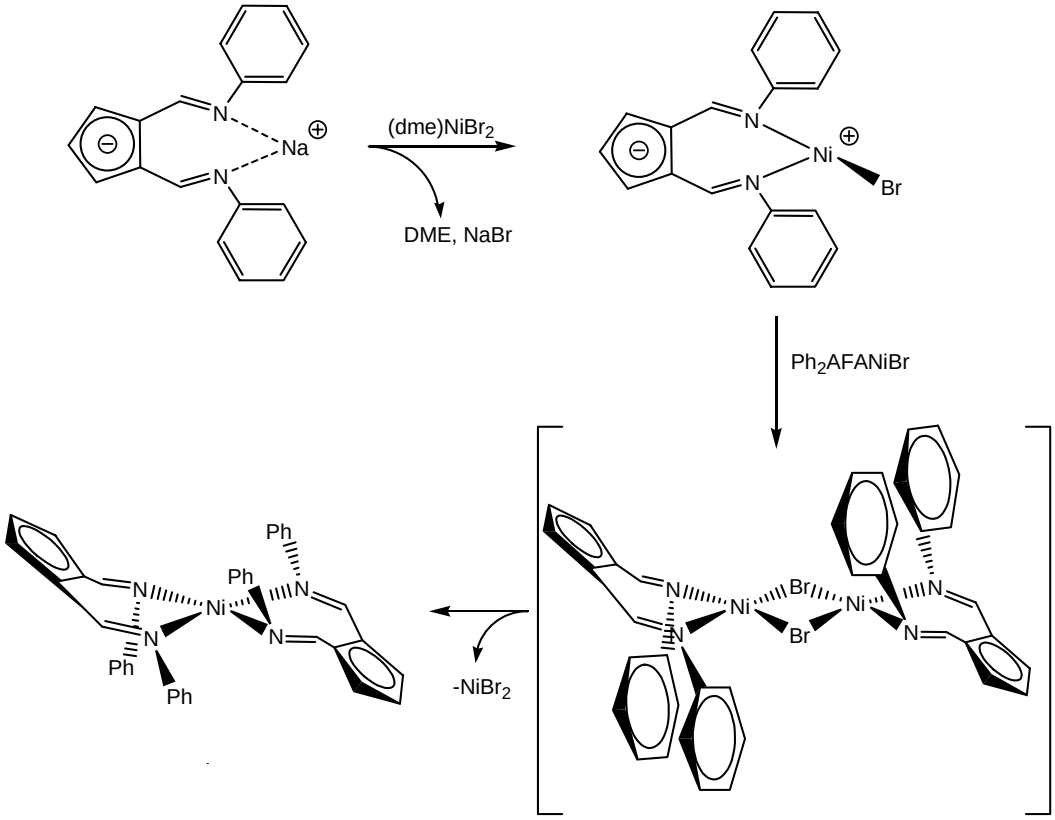

Scheme 2.12. One of the possible mechanisms for the formation of the square-planar $[(Ph_2AFA)_2Ni]$

That the dimeric intermediate is square-planar is suggested by observing that the alternative tetrahedral dimer would place the two aryl substituents in colliding positions.

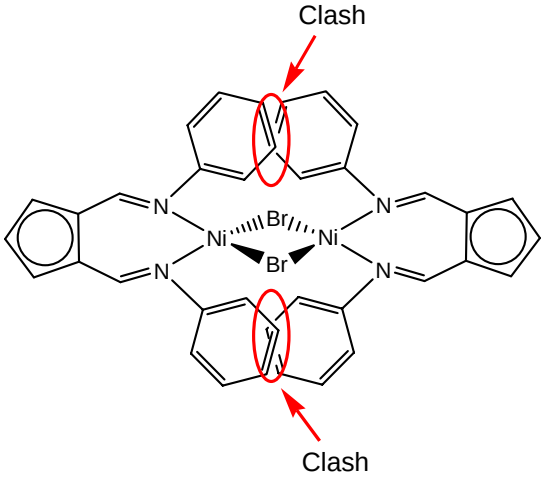

Figure 2.31. The dimeric tetrahedral intermediate would place the phenyl substituents in clashing positions.

On the contrary, the relatively high flexibility of the ligand and the facility of undertaking distortion, renders the square-planar dimer sterically affordable, with the ligands tilted above and below the mean plane, whereas the tetrahedral product is most likely formed with a two step substitution mechanism.

If one of the two complexes is formed after dimerisation, a possible strategy to selectively yield one form would be to prevent the formation of the dimer by using a strongly coordinating molecule, which could lower the rate of dimerisation by binding to the vacant site of the metal centre.

The use of more coordinating solvent such as acetonitrile or an additive such as a phosphine proved not to be useful, since no crystalline product was isolated and analysis was not clear.

Attempts to selectively address the synthesis to one of the two isomers were made by performing the reaction at temperature as low as –78 °C, but the results were unsuccessful and both forms were still formed, suggesting that the ground state energies of the two isomers are very close.

DFT calculations were undertaken for the two crystal structure but they gave inconsistent results. According to what method was used, the energy differences between the square-planar and tetrahedral molecules ground states showed widely different values, and therefore no definite information can be provided at this stage.

2.4 Conclusions

A number of complexes with several transition metals bearing the Ph_2AFA ligand have been prepared and characterized. Although an equimolar ratio between the ligand and the metal di-halide precursor was used, isolation of the mono-substituted complex through the synthetic strategy used in the present work was never achieved. Instead, double coordination always takes place, indicating that ligation of the 6-aminofulvene-2-aldimine to transition metal is a thermodynamically favoured process, despite the distortion of the ligand which must occur in the square-planar bis-chelate complexes.

Mono-coordination was observed by reacting the deprotonated ligand with mono-halide metal precursor, leading to the isolation of the Cu(I)-phosphine complex **8** and the Pd(II)-allyl complex **11**.

Structural analysis was conducted on all the isolated complexes. Of particular interest is the extreme distortion that the ligand is able to undergo in order to bind to the metal. This is unprecedented for chelating diimine ligands which normally favor complexation of the metal within the plane of the ligand.[20] This must be a result of the 1,4-relationship of the imine donors within the AFA ligand framework, which contrasts with the more common 1,2- or 1,3-diimine systems, and the electronic flexibility conferred by the availability of the fulvene form of the ligand.

In the two square-planar complexes with Ni(II) and Pd(II), an extreme distortion occurs in the ligand upon coordination, probably induced by both the narrower ligand bite angle required for a square-planar geometry and the steric hindrance of the aryl rings on the nitrogen atoms. Consistent with this explanation, such a case does not occur in the tetrahedral geometries, where the ligand remains planar, with the phenyl substituents of one ligand able to interdigitate with those of the other ligand. Although there is no strong evidence, the structurally different complexes might be produced via two different mechanisms, and once formed they are not interconvertable. This is in agreement with the observations made for the two nickel complexes **10a** and **10b**. The mechanism for the formation of the square-planar Ni complex was hypothesized to occur with the initial formation of a non-isolable dimeric species, and subsequent disproportionation to yield the $(Ph_2AFA)_2M$ and MX_2.

The relatively easy distortion that the ligand can undergo is in agreement with the high flexibility of these systems, and their ability to coordinate to a wide range of metals with different geometries. By the analysis of the bond lengths and angles it appears that the ligand needs to be described by invoking the contribution of different forms, such as a fulvenoid imine-amide form, a diimino-allyl form and a cyclopentadienyl-diimine form. These last two forms would also give contribution to the overall zwitterionic character of the complexes described and support the formulation of such systems as mainly zwitterions.

1. L. K. Johnson, C. M. Killian, M. Brookhart, *J. Am. Chem. Soc.* **1995**, *117*, 6414; S. D. Ittel, L. K. Johnson, M. Brookhart, *Chem. Rev.*, **2000**, *100*, 1169.
2. K. Hafner, K. H. Vöpel, G. Ploss, C. König, *Justus Liebigs Ann. Chem.* **1963**, *661*, 52; K. Hafner, K. H. Vöpel, G. Ploss, C. König, *Org Synth.* **1967**, *47*, 52.
3. U. Mueller-Westerhoff, *J. Am. Chem. Soc.* **1970**, *92:16*, 4849.
4. H. L. Ammon, U. Mueller-Westerhoff, *Tetrahedron* **1974**, *30*, 1437.
5. D. Sanz, M. Perez-Torralba, S. H. Alarcon, R. M. Claramunt, C. Foces-Foces, J. Elguero, *J. Org. Chem.* **2002**, *67*, 1462; S. P. Brown, M. Perez-Torralba, D. Sanz, R. M. Claramount, L. Emley, *Chem. Commun.* **2002**, 1852.
6. J. Emley, *Chem. Rev.* **1980**, *9*, 1.
7. R. W. Alder, *Chem. Rev.* **1989**, *89*, 1215; H. A. Staab, T. Saupe, *Angew. Chem. Int. Ed. Engl.* **1988**, *27*, 865.
8. W. R. Brasen, H. E. Holmquist, R. E. Benson, *J. Am. Chem. Soc.* **1961**, *83*, 3125.
9. L. C. Dorman, *Tetrahedron Lett.* **1966**, 459; E. Daltrozzo, K. Feldmann, *Tetrahedron Lett.* **1968**, 4983.
10. L. M. Jackman, J. C. Trewella, R. C. Haddon *J. Am. Chem. Soc.* **1980**, *102*, 2519.
11. N. Etkin, C. M. Ong, D. W. Stephan, *Organometallics* **1998**, *17*, 3656.
12. C. M. Ong, D. W. Stephan, *Inorg. Chem.* **1999**, *38*, 5189.
13. M. P. Coles, R. F. Jordan, *J. Am. Chem. Soc.* **1997**, *119*, 8125; M. P. Coles, D. C. Swenson, R. F. Jordan, J. V. G. Young, *Organometallics* **1997**, *16*, 5183.
14. B. Qian, D. L. Ward, M. R. Smith III, *Organometallics*, **1998**, *17*, 3070.
15. E. Ihara, V. G. Young, R. F. Jordan, *J. Am. Chem. Soc.* **1998**, *120*, 8277.
16. K. Klaβ, L. Duda, N. Kleigrewe, G. Erker, R. Frölich, E. Wegelius, *Eur. J. Inorg. Chem.* **1999**,
11.
17. M. Brookart, S. D. Ittel, L. K. Johnson, *Chem. Rev.* **2000**, *100*, 1169.
18. G. M. Villacorta, C. P. Rao, S. J. Lippard, *J. Am. Chem. Soc.* **1998**, *110*, 3175; W. R. Brasen, H. E. Holmquist, R. E. Benson, *J. Am. Chem. Soc.* **1961**, *83*, 3125; B. S. Jaynes, T. Ren, A. Masschelein, S. J. Lippard, *J. Am. Chem. Soc.* **1993**, *115*, 5589; G. M. Villacorta, S. J. Lippard, *Inorg. Chem.* **1988**, *27*, 144; W. M. Davis, M. M. Roberts, A. Zsak, K. Nakanishi, T. Nozoe, S. J.

Lippard, *J. Am. Chem. Soc.* **1985**, *107*, 3864; M. Bartlett, G. J. Palenic, *J. Chem. Soc. D* **1970**, 416; H. V. R. Dias, W. Jin, R. E. Ratcliff, *Inorg. Chem.* **1995**, *34*, 6100.

19. K. J. Franz, N. Singh, B. Spingler, S. J. Lippard, *Inorg. Chem.* **2000**, *39*, 4081.

20. G. Van Koten, K. Vrieze, *Adv. Organomet. Chem.* **1982**, *21*, 151.

Chapter 3

Coordination chemistry of the R_2AFA^- ligand via the C_5 moiety.

3.1 Background

As described in the previous chapter, the anionic form of the 6-aminofulvene-2-aldimine system has proved to be able to coordinate through the nitrogen atoms to a variety of transition metals and a number of novel compounds have been prepared and characterised. Spectroscopycal and structural data seem to support the view of these metal complexes as zwitterionic species, with the separated negative and positive charges localized on the C_5 moiety of the ligand and on the metal centre respectively, although some discrepancies had arisen, indicating that a contribution from other non-zwitterionic structures is also possible.

As found from the X-ray analysis, for example, the C-C bond distances in the cyclopentadienyl moiety turn out to be not all equal, with the C1-C5 distance being considerably longer than the others.

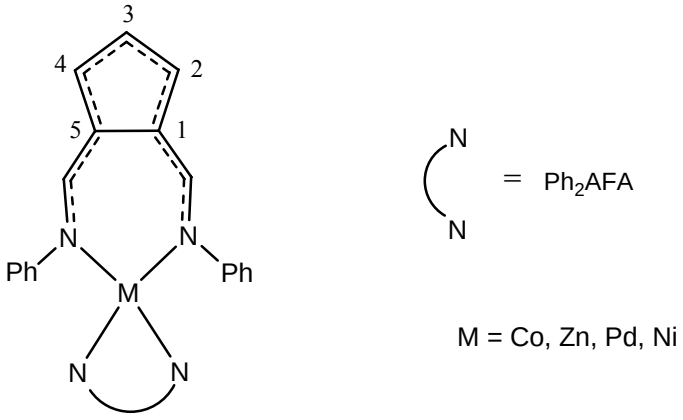

Figure 3.1. Schematic drawing of $(Ph_2AFA)_2M$ complexes. Metals are all in oxidation state +2. In all the structure, the C1-C5 bond is longer than the other C-C bonds

This is in contradiction with the expected bond lengths of an aromatic system, where all the C-C distances are expected to be equal. Moreover, the C-N bonds have values

that are halfway between single and double bond, so that a simple description of the AFA ligand as a diimine-cyclopentadienyl system is not as straight forward as anticipated.

These observations encouraged the enterprise of a study of the coordination chemistry of the ligand via its cyclopentadienyl fragment to transition metals, in order to evaluate the degree of delocalisation of the negative charge and consequently the formulation of these systems as zwitterionic complexes. In theory, in fact, if the zwitterionic form gives the main contribution, it should be possible to symmetrically coordinate the 5-membered aromatic fragment to a further metal centre once the two nitrogen donors have been previously occupied by a first metal.

This investigation not only would provide a better understanding of the electronic properties of the ligand and its tendency to produce zwitterionic species, but it would also allow to devise synthetic approaches to novel bimetallic complexes. Such species are of great interest in a wide range of research fields, from biochemistry, where metallo-enzyme activity is frequently based on bimetallic reactivity patterns,[1] to material chemistry, due to their potential applications in the design of low-dimensional, polymeric materials with novel electrical and/or magnetic properties.[2] A more related field to the current project for the exploitation of bimetallic complexes is that of homogeneous catalysis. The use of the so called "tandem catalysts", systems in which the cooperative action of two or more catalysts in a single reactor is used to yield a product that is not accessible by the individual catalyst, has received a great deal of attention and there are numerous examples from synthetic literature of tandem catalysts used in a range of application. These include metathesis/hydrogenation,[3] ring-opening metathesis/ring-closure metathesis,[4] ring-closing metathesis/trans-annular cyclization,[5] asymmetric ring-opening metathesis/cross metathesis.[6] As far as the present project is concerned, focus on alkene co-polymerisation by the use of tandem catalysts is of particular interest. Such species have the ability to provide polyethylene incorporating alkyl side chains from ethylene homopolymerisations. In these, the first catalyst provides 1-alkene co-monomer for the polymer chain growing at the second polymerisation catalyst employing the same ethylene feed.[7] Ideally, for maximum control of polymer properties, the α-olefin generated by the first catalyst would be of specific chain

length (i.e. 1-butene, 1-hexene, 1-octene etc.), however most oligomerisation catalysts do not have such selectivity and one must usually have to deal with a distribution of chain lengths.[8]

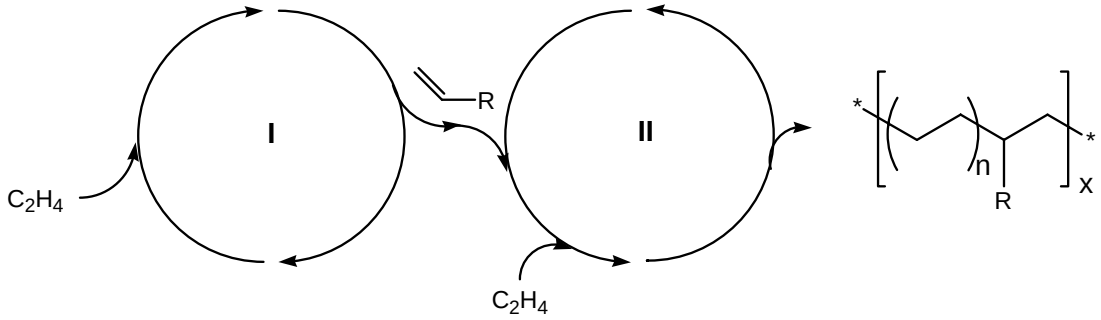

Figure 3.2. Common depiction of a tandem catalyst system. The higher olefin produced in the catalytic cycle I is incorporated in the polymer produced by catalytic cycle II, resulting in branched polyethylenes.

Of course, a number of factors must be taken into account for a successful tandem scheme, the primary being the compatibility of the two catalysts. Best control is achieved when there is no interference between the two catalytic active species.

Due to the high affinity of the 6-aminofulvene-2-aldimine systems towards late transition metal centres, and in view of the general feature of these metals to oligomerise ethylene, a possible further coordination of the Cp moiety of the AFA ligand to a group 4 metal would open the tantalizing prospect of catalyst complexes of the type shown in Fig. 3.3. In principle such a bifunctional catalyst could act as a "tandem catalysts", but with the advantage of being one single molecule, with the two active sites connected but kept well separated by means of a defined spacer. The active sites would therefore be intrinsically compatible, and not interfere between each other. Since this type of polymerisation is performed at low catalysts concentration through intermolecular process, one more advantage would lies in the efficiency of the bimetallic catalyst, with the α-olefin generated in close proximity to the polymerisation site.

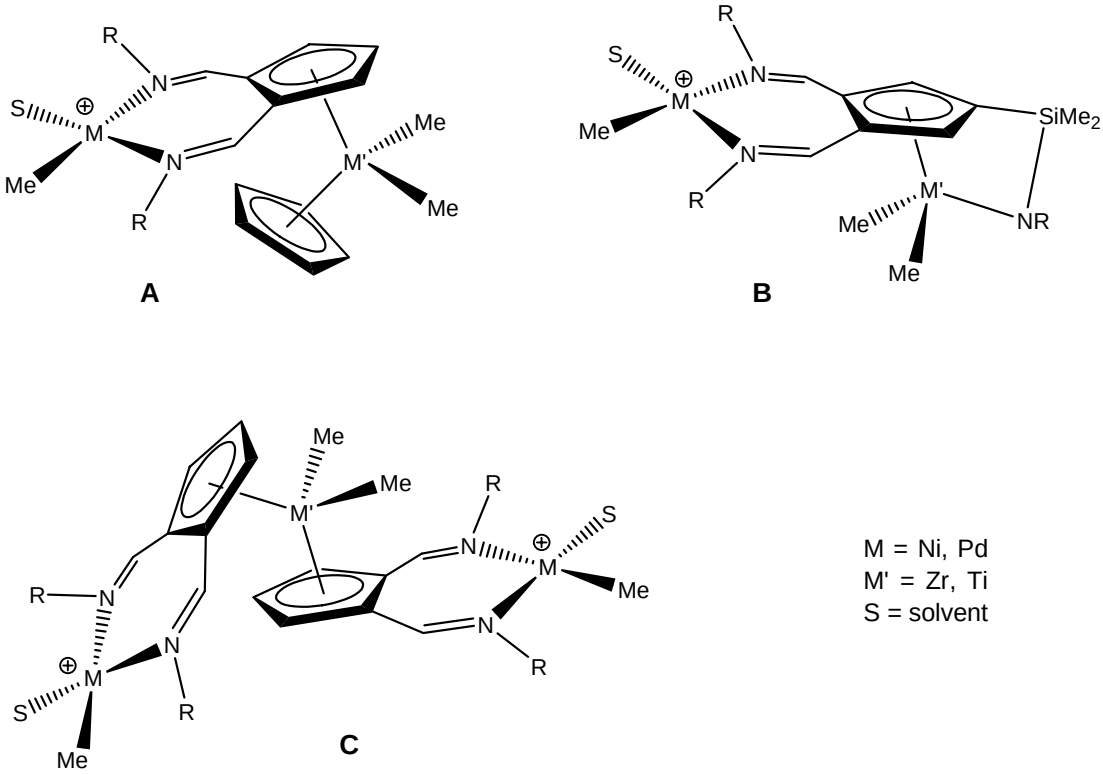

Figure 3.3. Possible bifunctional catalysts based upon the ambidentate ability of the AFA ligand system and incorporating early transition metal metallocene or constrained geometry and late transition metal diimine type catalytic centres within the same molecule.

As demonstrated by Abramo *et al.*, the use of the bifunctional activator $[Ph_3C]_2[1,4\text{-}\{B(C_6F_5)_3\}_2C_6F_4]$ (**B_2**) to spatially confine the two catalyts precursors (η^5-3-ethylindenil)$Me_2Si(\eta^1\text{-}N^tBu)ZrMe_2$ (**Zr**) and ($\eta^5\text{-}C_5Me_4$)$Me_2Si(\eta^1\text{-}N^tBu)TiMe_2$ (**Ti**) (Fig. 3.4) results in a dramatic increase of the efficiency of the homogeneous heterobimetallic olefin enchainment processes for LLDPE synthesis, with polymer products showing narrower molecular weight distributions.[9]

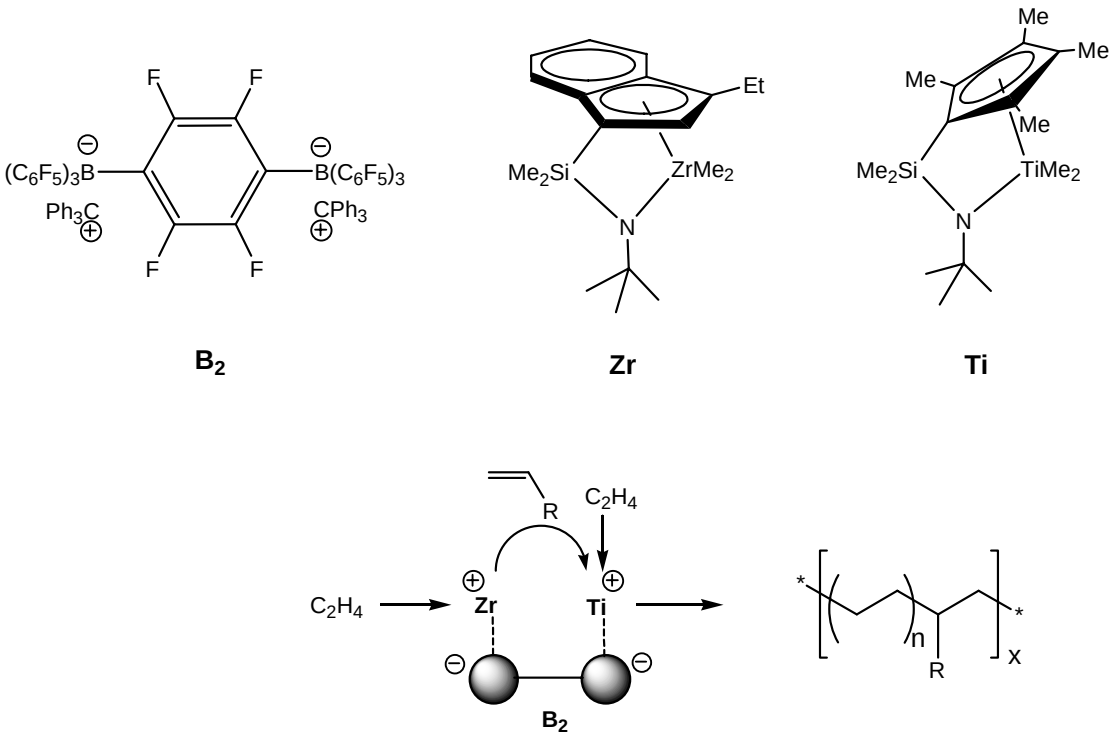

Figure 3.4. Linked tandem catalysts yield polymers with narrower molecular weights distributions.

It is also tempting to speculate that the 1-alkene co-monomer chain length could be modulated by variation of the AFA substituent groups.

The zwitterionic nature of complexes bearing the 6-aminofulvene-2-aldiminates had received first strong evidence by earlier studies on these systems in the chemistry of magnesium. Two novel magnesium complexes had been characterised,[10] one of which showed the 6-aminofulvene-2-aldimine acting as an ambidentate ligand, coordinated to the magnesium centre through both the nitrogen and the C_5 donors (Fig 3.5).

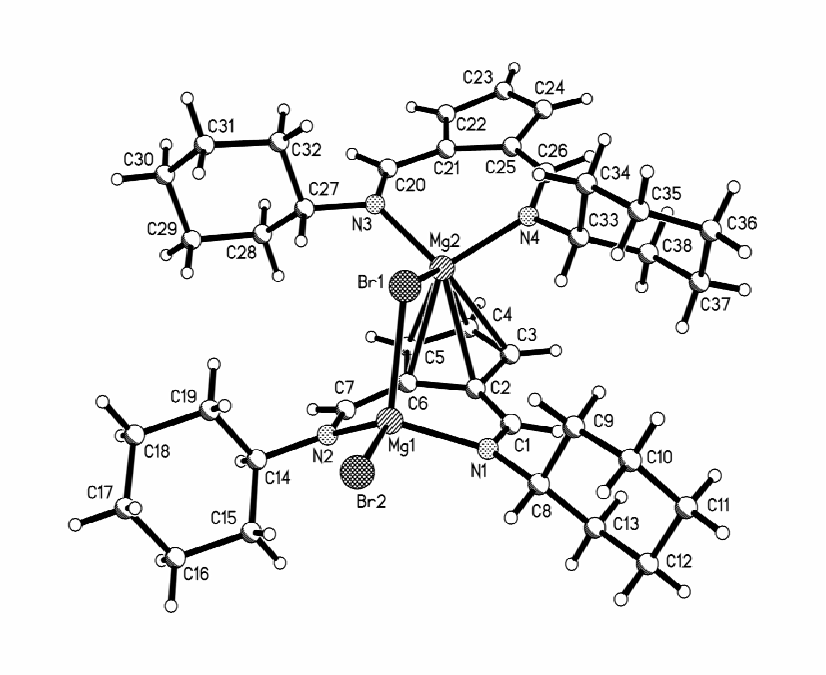

Figure 3.5. Molecular crystal structure of the bimetallic magnesium complex bearing N,N'-dicyclohexyl-6-aminofulvene-2-aldimine acting as an ambidentate ligand.

The C-N bond lengths in the above structure range between 1.280(3) and 1.297(3) Å, indicating that they are probably double bonds. As encountered in the $(Ph_2AFA)_2M$ (M = Co, Ni, Zn, Pd) complexes, the bond lengths within the C_5 ring differ between each other, with the C2-C5 having the biggest value (1.451(4) Å). Furthermore, the C3-C4 and C4-C5 distances (1.393(4) and 1.398(4) Å respectively) are smaller than the C2-C3 and C5-C6 distances (1.413(4) and 1.410(4) Å), consistent with the hypothesis of a major delocalisation of the negative charge into the C3-C4-C5 allyl fragment. Similarly, the coordination of the C_5 moiety to the magnesium centre is not perfectly symmetrical, with bond lengths values ranging from 2.526(3) Å (Mg-C6) to 2.570(3) Å (Mg-C3). However, differences into the Mg-C bonds might be a consequence of the non-symmetrical environment of the metal centre, which is bridged through the bromide to the other magnesium centre, and features another Cy_2AFA ligand coordinated typically through the N donors.

Whilst in the complex just discussed the high electropositivity of the magnesium atom could somehow explain the ability of the ligand to act as an ambidentate ligand and thus use the C_5 moiety as a donor, an analogous behaviour of

the generally less electrophilic late transition metal centres can not be taken for granted.

3.2 Results and discussion

3.2.1 Generalities

As a preliminary study, the reaction of the deprotonated ligand with metal precursors known to be prone to bind aromatic molecules was investigated. Although it has been shown that in the reaction of transition metal complexes with the 6-aminofulvene-2-aldiminate the coordination of the ligand invariably occurs through the nitrogen atoms, such a feature can not be taken as a rule of thumb. The fact that the ligand uses the N atoms for ligation to the zinc, nickel, palladium and copper metals might in theory be attributed to the affinity of these metals for nitrogen-based donors, rather than to a characteristic feature of the 6-aminofulvene-2-aldimine systems. As a matter of fact, the resonance forms which can be drawn for the anionic ligand would not rule out the possibility that a coordination of the 5-membered ring occurs if the reaction is conducted with an appropriate starting material. The choice of the metal precursors becomes therefore a crucial issue.

It is well established that iron and ruthenium metal centres have a high affinity for aromatic molecules and a great number of complexes featuring cyclopentadienyl or arenes as ligands have been synthesized.[11, 12] In particular, the fragment Cp^*Ru^+ has proved to have a very strong interaction with aromatic hydrocarbons.[13] An adapted synthesis of the complex $[Cp^*Ru(MeCN)_3][OTf]$ reported in literature,[1] afforded the isolation of the analogous salt $[Cp^*Ru(MeCN)_3][BF_4]$ which was reacted with $Ph_2AFA^-Li^+$, in order to establish if a coordination via the C5 moiety could be favoured in place of the usual N chelation.

Scheme 3.1. Attempted synthetic route to the synthesis of [Cp*Ru(Ph2AFA)].

However, no single product was isolated. NMR spectra showed that some reaction did take place, but the identity of the species formed could not be clearly established. Most likely, the combined high reactivities of both the deprotonated ligand and the ruthenium precursors compromise the formation of a single product, leading to a mixture of species which are not easily separable. This synthetic approach proved therefore to be not successful.

A different route to investigate the ability of the 6-aminofulvene-2-aldimine ligands to act as an ambidentate ligand was to react the same ruthenium precursor with the $(Ph_2AFA)_2M$ (M = Zn, Pd) complexes discussed in the previous chapter. Such an investigation led to the isolation of three novel complexes, whose structural features are discussed in the following section.

*3.2.2 Synthesis and structural studies of [Cp*Ru(Ph_2AFA)]*

The first attempt to prepare a trimetallic complex was made by treating the zinc complex **6** with the $[Cp^*Ru(MeCN)_3][BF_4]$ in a 1:2 molar ratio. Although ^{1}H-NMR studies showed the expected upfield shifts of the Cp-*H* protons as a consequence of the metal coordination, the mass spectrometry indicated that there was no zinc in the final product and the molecular peak was attributable to the formation of a $[Cp^*Ru(Ph_2AFA)]$ species (**12**).

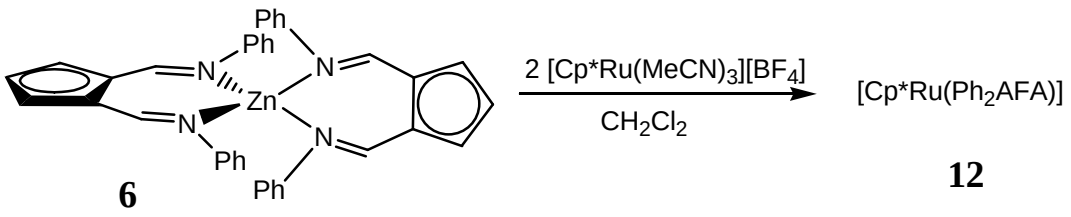

6 **12**

Scheme 3.2. Synthesis of [Cp*Ru(Ph_2AFA)].

Crystals suitable for X-ray analysis were grown from a mixture of CH_2Cl_2/Et_2O and the molecular structure shows that coordination is occurring via the C_5 ring, providing the first example of the cyclopentadienyl coordination of an AFA ligand in which the nitrogen donors are vacant. An analogous 1,2-diminoferrocene species has been prepared by condensation of 1,2-formyl-ferrocene with aniline, but no structural data have been published.[14]

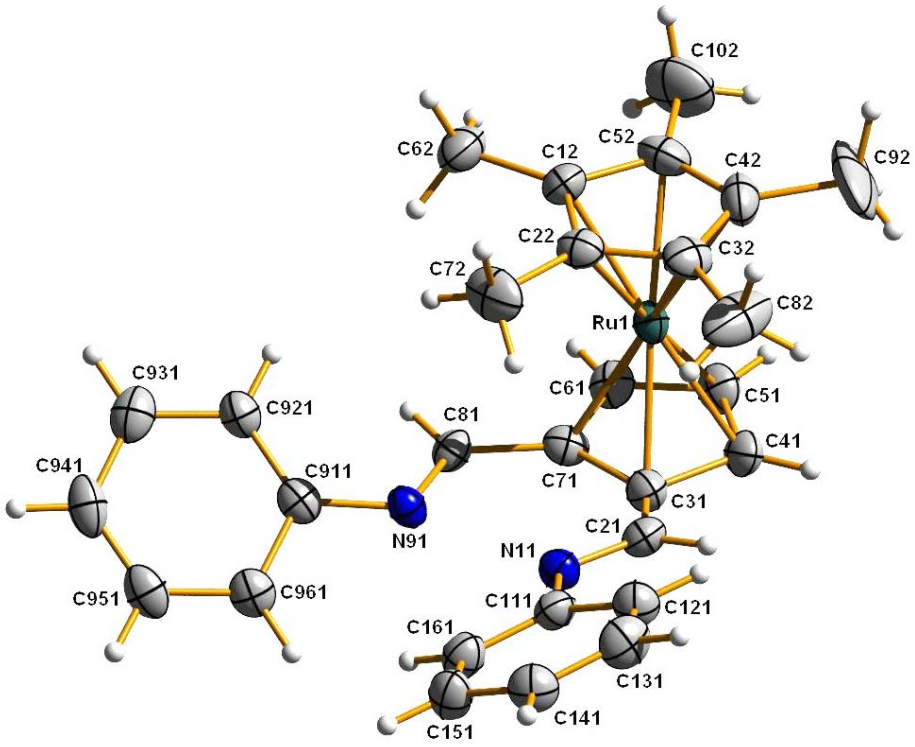

Figure 3.6. Molecular crystal structure of [Cp*Ru(Ph_2AFA)].

Table 3.1a. Selected bond lengths for [Cp*Ru(Ph_2AFA)].

Bond	*Bond length (Å)*	*Bond*	*Bond length (Å)*
Ru-C(31)	2.168(7)	C(81)-N(91)	1.293(6)
Ru-C(41)	2.195(5)	C(71)-C(81)	1.482(9)
Ru-C(51)	2.222(4)	C(31)-C(71)	1.442(6)
Ru-C(61)	2.212(5)	C(21)-C(31)	1.402(8)
Ru-C(71)	2.160(6)	N(11)-C(21)	1.312(6)

Table 3.1b. Selected bond angles for [Cp*Ru(Ph_2AFA)].

Bond	*Bond angle (deg)*
C(31)-C(21)-N(11)	124.5(5)
C(71)-C(31)-C(21)	131.9(7)
C(81)-C(71)-C(31)	128.6(6)
C(71)-C(81)-N(91)	123.7(4)

Although this coordination mode might be expected in view of the high affinity of the Cp*Ru fragment towards π-aromatic molecules, in this case the formation of **12** is believed to occur after fragmentation of a Zn/Ru species initially formed rather than to a real preferred binding mode of the ligand. In other words, the occupation of the N-chelating atoms by the zinc atoms is crucial, leading to an intermediate Zn/Ru bimetallic (or a Ru/Zn/Ru trimetallic) species, which is too unstable and decomposes with release of the [Cp*Ru(η^5-Ph_2AFA)] product. Once formed, such a product is stable and does not undergo redistribution of the ligand to lead to the more usual N-chelation. Such stability can be anticipated in view of the 18 electrons in the valence orbitals of the metal. As consistently observed, no indication of formation of the same product is found when reacting the same Ru precursor with the deprotonated ligand, confirming that occupation of the nitrogen donors prior to reaction with the Cp^*Ru^+ fragment is a main requirement.

Instability of the mixed metal complex with the AFA system behaving as an ambidentate ligand might be due to steric reasons. The tetrahedral geometry of the zinc centre would place one of the two phenyl N-substituents in a congested position

relative to the methyl groups of the C_5Me_5. However, a different explanation might be attempted by invoking a dramatic change of the electronic properties of the ligand after coordination, which would weaken the N coordination to the zinc centre. This view is plausible on the basis of the crystal structure of **12**, where considerable differences in bond distances are found in comparison with the zinc complex **6**. For example, it is surprising to find that the C-C distances within the Cp moiety are significantly dissimilar from those encountered in all the other AFA complexes. In particular the C31-C41 bond length (1.456 Å) turns out to be even longer than the C31-C71 distance (1.443 Å), which was the longest in all the previously discussed complexes and was therefore described as possessing a higher degree of single bond character. Such a difference is one indication that the electronic properties of the ligand have changed and this is emphasized by the even larger value of one of the two C(Cp)-CN bond (C71-C81), which elongates from the value of 1.411 Å in the zinc complex to 1.482 Å, and therefore has to be assumed to be an almost completely single bond. Such an elongation does not occur in the other C(Cp)-CN bond (C21-C31), where the distance is comparable to the one in **6**. A similar observation is found in the C-N bond lengths, where one distance turns out to be slightly shorter (C81-N91 = 1.293 Å) and one basically unaltered (C21-N11 = 1.312 Å) when compared with the zinc derivative. The ligand is apparently losing its C_2 symmetry in the solid state, and it appears that there is a significant contribution from an asymmetric fulvenoid form. Decrease of symmetry is reflected into the loss of planarity of the ligand, where one of the two C-N arms is tilted out of the ligand mean plane and towards the metal. As a consequence, the distance between the Ru centre and the one of the two CN carbon atoms (C21), which is 2.97 Å, indicates that there is possibly some interaction between these two atoms.

Concerning the coordination to the ruthenium centre, the Ru-C distances range between 2.160 and 2.221 Å, considerably shorter than in the magnesium bimetallic complex (Fig 3.5), where the Mg-C bond lengths average 2.548 Å, suggesting that the η^5-AFA coordination is stronger in **12**, as expected for an anionic ligand in place of a zwitterionic one.

*3.2.3 Studies in solution of [Cp*Ru(Ph_2AFA)]*

The symmetry of the AFA fragment seems to be re-established in solution, where fluxionality of the AFA ligand is shown by ^{1}H NMR investigation. When commercial grade $CDCl_3$ is used, a coupling of the two *H*C=N protons is observed, which appear as a doublet with a coupling constant of 7.57 Hz. Similar coupling was also observed in the free protonated ligand, suggesting that the two N donors are actually not proton free. This observation is confirmed by the presence of a broad triplet present at very low field, which is indicative for protons coordinated to the two nitrogen atoms. It therefore emerges that the complex **12** in solution is acting as a proton sponge[15] and the two nitrogen donors are occupied.

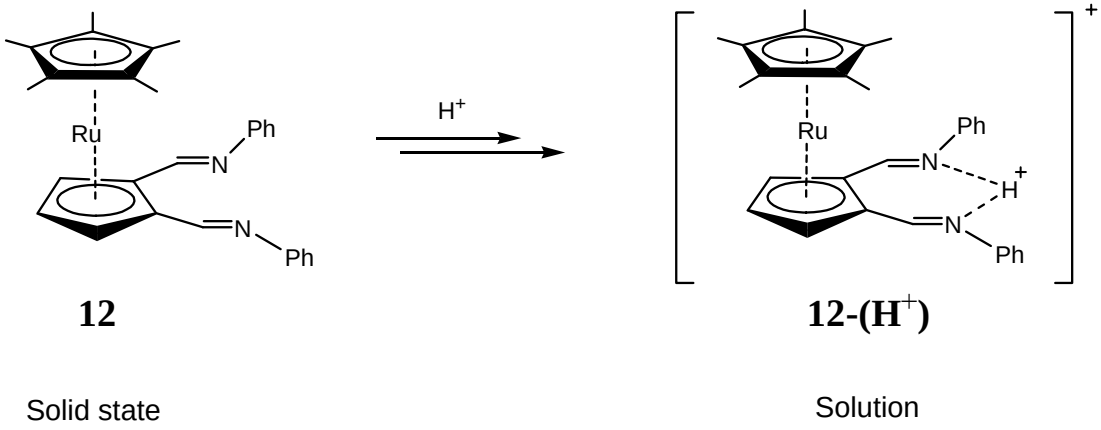

Scheme 3.3. [Cp*Ru(Ph_2AFA)] acts as a proton sponge in non-dry solvents

However, the chemical shift of such a proton occurs at 16.5 ppm, which is at quite lower field than the value found in the free ligand (15.4 ppm), meaning that the acidity of this proton is higher. Assuming the presence of a counteranion to counter balance the extra +1 charge deriving from the presence of the proton, the zwitterionic character of the protonated AFA ligand in **12** is expected to be considerably more pronounced.

The vacancy on the N donors is easily restored by removal of the proton with a base such as NaH. As a result, the downfield signal at 16.5 ppm disappears and the *H*N=C doublet turns into a singlet, proving that the fluxionality of the ligand in solution is occurring in the deprotonated complex, too.

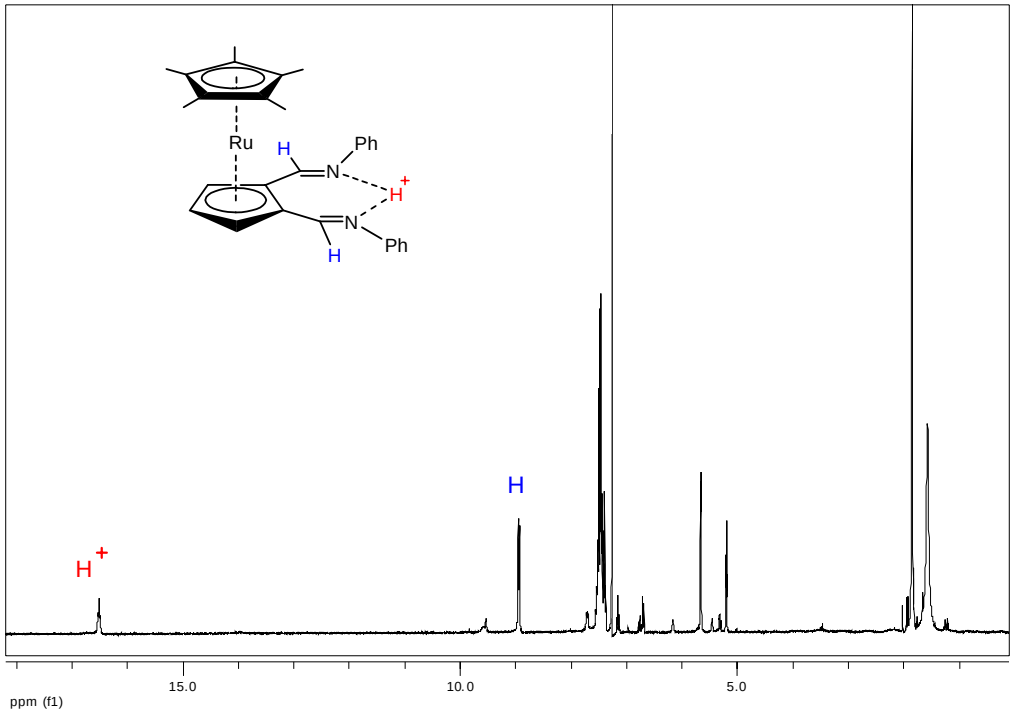

Figure 3.7a. ^{1}H NMR of [Cp*Ru(Ph$_2$AFA)](H$^+$)

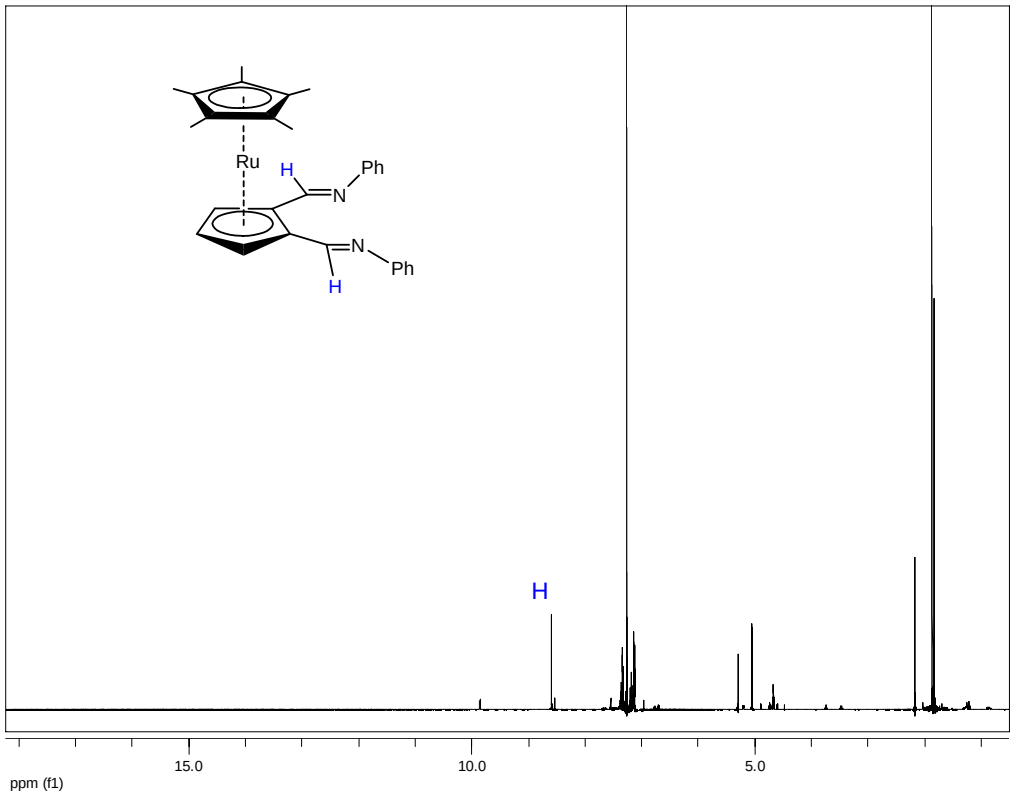

Figure 3.7b. ^{1}H NMR of [Cp*Ru(Ph$_2$AFA)].

It is also found that the addition of the base in presence of water, catalyses the partial hydrolysis of the AFA ligand, leading to the formation of the (*N*-phenyl-6-aminofulvene-2-aldehyde)ruthenium complex **12'** as by-product.

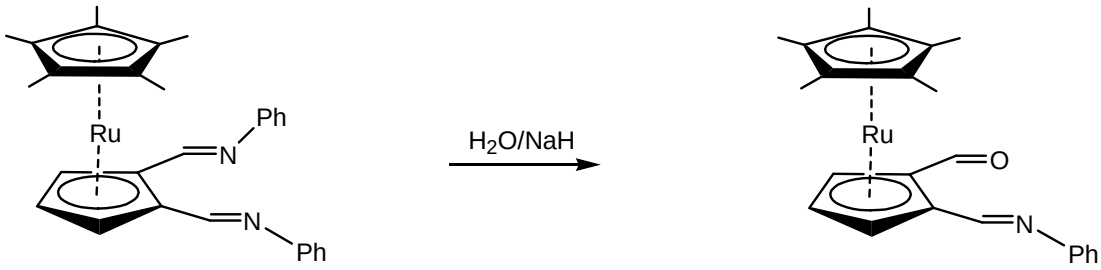

12'

Partial hydrolysis product

Scheme 3.4. Base catalysed partial hydrolysis leading to the imine-aldehyde ruthenium species.

This is suggested by the presence of the aldehyde proton singlet at 9.85 ppm and the singlet for the diimine proton singlet at 8.535 ppm in the ^{1}H NMR spectrum. Because of the asymmetry of the AFA ligand in **12'**, the Cp protons appear as three separate signals between 5.20 and 4.67 ppm. The presence of the carbonyl group is confirmed by IR spectroscopy, where the C=O stretching peak is found at 1667.2 cm^{-1}, which is characteristic for a conjugated carbonyl group, together with the Fermi doublet for the C-H stretching of the aldehyde at 2856.1 cm^{-1}. The imine C=N stretching is observed at 1621.8 cm^{-1}.

Hydrolysis of the AFA ligand can also go to completion, affording the ruthenium-cyclopentadienyl-di-aldheyde derivative, which is obtained as a stable compound by passing solution of **12** through a basic alumina column.

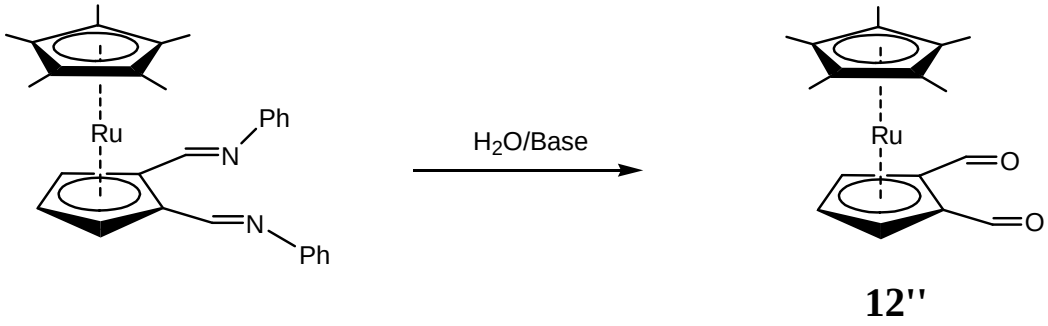

12''

Complete hydrolysis product

Scheme 3.5. Complete hydrolysis leads to the di-aldehyde ruthenium complex.

This is suggested by the ^{1}H NMR spectrum, where the two aldehyde protons appear as a singlet at 9.84 ppm and no signal for the *H*C=N protons are found. Furthermore, the symmetry of the ligand is restored, making the two Cp*H* protons in position 3 and 5 of the AFA carbon frame equivalent, which thus appear as a doublet at 5.02 ppm. As expected, the Cp*H* proton in position 4 appears as a triplet at 4.81 ppm. Formation of the di-aldehyde complex is further supported by IR spectroscopy, where the C=O stretching is present at 1674.9 cm^{-1}, together with the aldehyde C-H stretching at 2855.1 cm^{-1}. Consistently, no band at ~1620 cm^{-1} for the C=N stretching is observed.

The relatively easy deprotonation of **12-(H^+)** is of great interest for the use of **12** as a novel neutral diimine ligand for the synthesis of bimetallic complex. Removal of the acidic proton with a base would make the N donors in principle available for coordination to suitable metal centres.

*3.2.4 Synthesis and structural studies of [{Cp*Ru(Ph_2AFA)}$_2$Pd][BF_4]$_2$*

In a similar synthetic approach, the palladium derivative **9** was reacted with 2 equivalents of the ruthenium precursor [Cp*Ru(MeCN)$_3$][BF_4] in CH_2Cl_2. In contrast to the formation of **12**, in this case the reaction affords isolation of **13** as final product, in which the palladium centre is retained. The product is stable and shows poor solubility in poorly polar organic solvents.

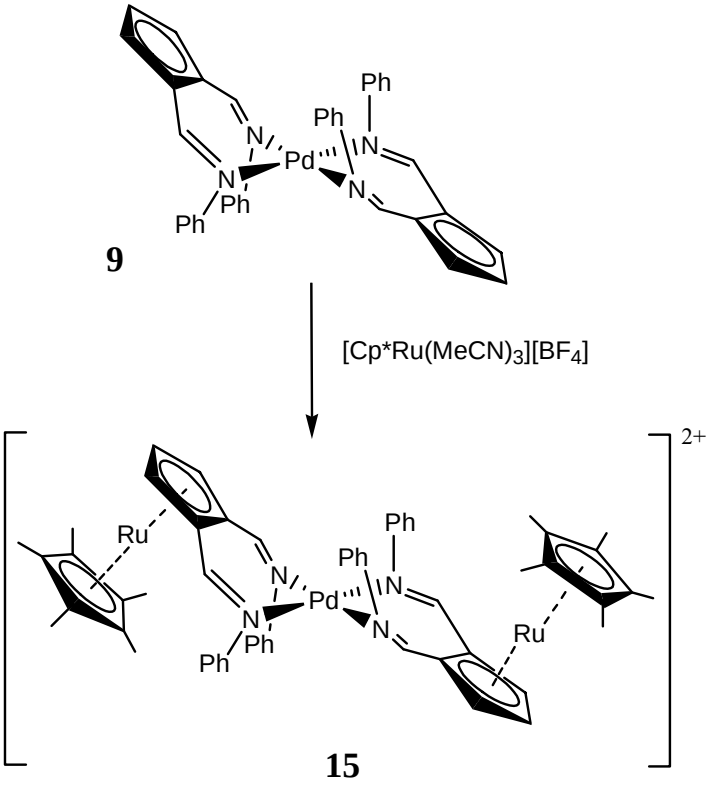

Scheme 3.6. Synthetic route leading to the dication $[\{Cp^*Ru(Ph_2AFA)\}_2Pd]^{2+}$

Crystals suitable for X-ray analysis were obtained from CH_2Cl_2 solution after storage at –10 ºC or alternatively upon slow evaporation of $CHCl_3$ solutions. The crystal structure of **13** shows that the both C_5 rings are now coordinated to the $[Cp^*Ru]^+$ unit and the resulting trimetallic complex has an inversion centre, and the two AFA ligands are therefore equivalent. As found in **12**, the coordination of the Cp moiety to the ruthenium centre is not perfectly symmetrical, and the Ru-C distances follow the same trend, too. The Ru-C51 distance is the longest (2.245 Å), and the two Ru-C31 and Ru-C71 the shortest (2.152 and 2.163 Å respectively). However, the fact that on average the Ru-C distances between **13** and **12** are comparable is perhaps surprising if considering that in the two complexes are positively charged and neutral respectively.

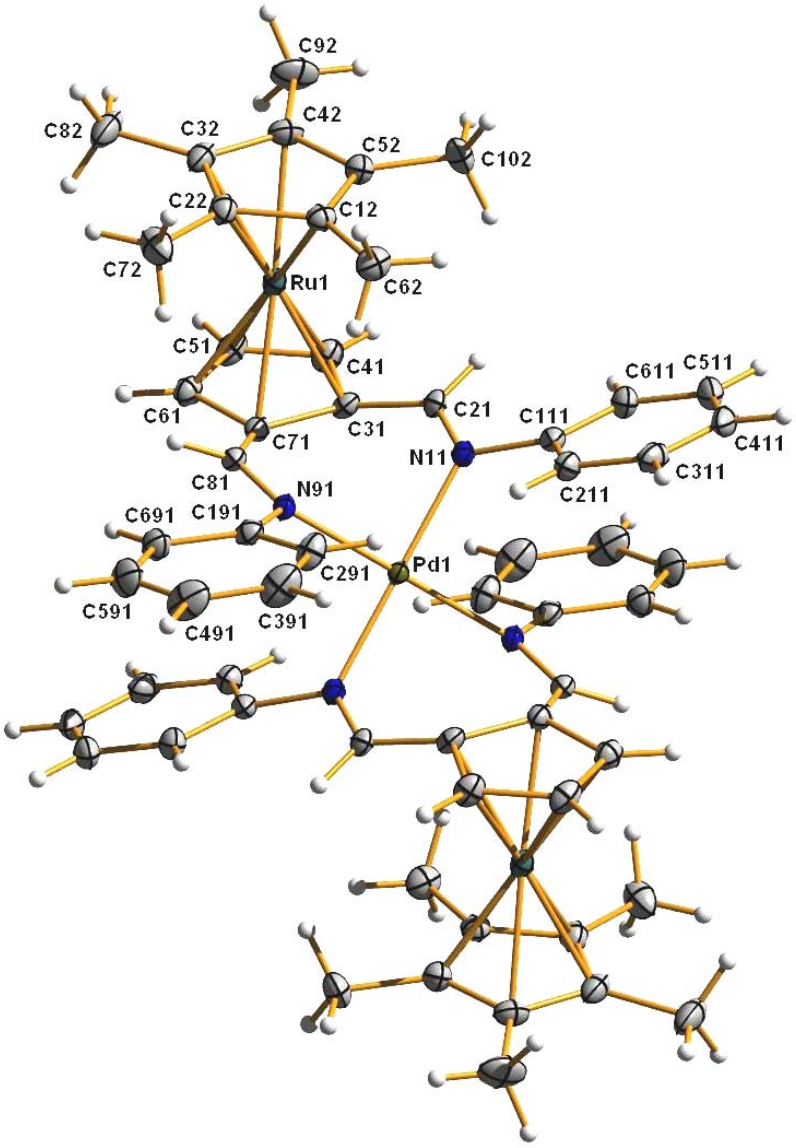

Figure 3.8. Molecular structure of the dication $[\{Cp^*Ru(Ph2AFA)\}_2Pd]^{2+}$.

Table 3.2a. Selected bond lengths for $[\{Cp^*Ru(Ph_2AFA)\}_2Pd][BF_4]_2$.

Bond	*Bond length (Å)*	*Bond*	*Bond length (Å)*
Pd-N(11)	2.030(3)	N(91)-C(81)	1.290(5)
Pd-N(91)	2.034(3)	Ru-C(31)	2.152(4)
N(11)-C(21)	1.296(5)	Ru-C(41)	2.199(4)
C(21)-C(31)	1.434(5)	Ru-C(51)	2.245(4)
C(31)-C(71)	1.472(5)	Ru-C(61)	2.191(4)
C(71)-C(81)	1.430(5)	Ru-C(71)	2.162(4)

Table 3.2a. Selected bond angles for [{Cp*Ru(Ph_2AFA)}$_2$Pd][BF_4]$_2$.

Bond	*Bond angle (deg)*
N(11)-Pd-N(91)	93.05(12)
Pd-N(91)-C(81)	121.5(3)
N(91)-C(81)-C(71)	127.0(3)
C(81)-C(71)-C(31)	130.8(3)
C(71)-C(31)-C(21)	129.5(3)
C(31)-C(21)-N(11)	126.3(4)
C(21)-N(11)-Pd	121.0(3)
C(21)-N(11)-C(111)	119.7(3)
C(81)-N(91)-C(191)	119.3(3)

Quite surprisingly, the Pd-N bond lengths are not affected by the coordination of the Ru centre as well as all the other structural parameters within the (Ph_2AFA)$_2$Pd moiety. The palladium centre is displaced 1.107 Å from the C_2N_2 plane, and such a plane forms a dihedral angle of 52.40˚ with the N-Pd-N plane, which are very similar values to those found in **9**. Furthermore, all the bond lengths and angles of the AFA fragment remain unaltered in comparison with the free Pd complex **9**. The fact that the (Ph_2AFA)$_2$Pd moiety in **13** and the complex **9** are not crystallographically distinguishable supports the view of this latter species as a mainly zwitterionic complex, with the aromatic 5-membered ring prone to coordinate to metal centres. As discussed in chapter 2, this feature can be put in relationship with the distortion occurring in the square-planar AFA-complexes, which produces a disruption on the extended π-conjugation, resulting in a better localization of the negative charge in the C_5 region. Such a distortion is not present in the tetrahedral zinc analogue and after reaction with the Cp* fragment, the zinc atom is not retained. With this in mind, it is noteworthy that the aromatic phenyl substituents do not compete for the coordination to the ruthenium centre, giving further indication of the aromaticity of the 5-membered ring. However, as described for the complex **12**, co-existence of the Pd and Ru atoms in **13** might be due to steric factors. In contrast to the tetrahedral zinc

complex, the square-planar environment of the palladium centre places the phenyl groups of the AFA ligands in opposite directions relative to the Cp* methyl groups.

Although hetero-bimetallic ruthenocenes are known in literature,[16] the synthetic approach used in the present work is completely novel. Rather than functionalizing the ruthenocene via a sequence of cyclopentadienyl substitution reactions and then attaching the palladium atom, the route used is the inverse, starting from a preformed palladium species and then coordinating the ruthenium cyclopentadienyl fragment.

*3.2.5 Synthesis and structural studies of [Cp*Ru(Ph'$_2$AFA)Pd(η^3-C_3H_5)][BF_4]*

The isolation of the trimetallic complex **15** as the product of the reaction between $(Ph_2AFA)_2Pd$ and Cp^*Ru^+ encouraged the use of the same synthetic approach to target complexes which might be of more specific use in homogeneous olefin polymerisation catalysis. Assuming that having the Cp moiety of the AFA ligand metal coordinated results in an increase of the formal positive charge on the Pd atom, such systems would in principle have higher activities towards this type of catalysis.

The synthesis of bimetallic complexes in which the palladium centre has the requisites to act as a catalytic site was therefore attempted. Due to the coordinative saturation of the Pd centre with two AFA ligands, together with the absence of a Pd-C bond to initiate the polyinsertion mechanism, complex **15** is not expected to be an efficient catalyst for olefin polymerisation. A considerably more interesting species would feature a monosubsituted organometallic palladium complex coordinated to the Cp^*Ru^+.

As it will be discussed in the following chapter, one attempt to prepare a zwitterionic alkene polymerization catalyst led to the isolation of [(Ph'$_2$AFA)Pd(η^3-C_3H_5)] (**13**) (Ph'=2,4,6-trimethylphenyl). This complex has in principle all the requirements to catalyse polymerisation of olefins. The presence of bulkier aromatic groups on the nitrogen atoms also adds extra significance in view of the higher catalytic activities which are normally associated for late transition metals (see Chapter 4).

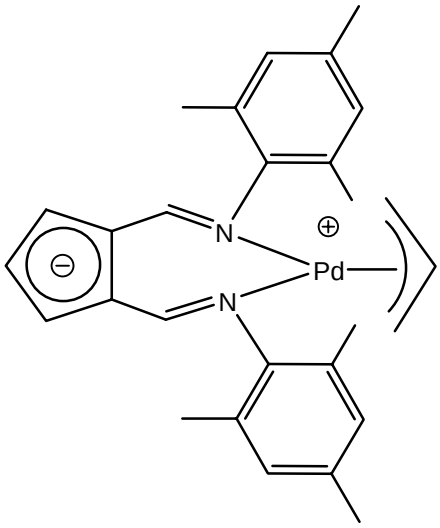

Figure 3.9. Structural formula of [(Ph'$_2$AFA)Pd(η^3-C_3H_5)] (See Chapter 4).

[(Ph'$_2$AFA)Pd(η^3-C_3H_5)] was therefore reacted with one equivalent of [Cp*Ru(MeCN)$_3$][BF_4] in CH_2Cl_2. After 15 minutes the reaction had gone to completion affording [Cp*Ru(Ph'$_2$AFA)Pd(η^3-C_3H_5)][BF_4] (**16**).

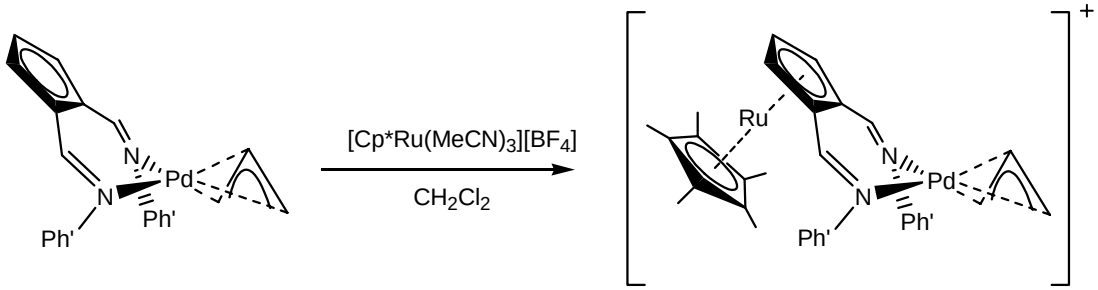

13 **16**

Scheme 3.7. Synthetic route leading to the cation [Cp*Ru(Ph$_2$AFA)Pd(η^3-C_3H_5)]$^+$.

Crystals suitable for X-ray analysis were grown upon slow evaporation of CH_2Cl_2 solutions layered with Et_2O. The crystal structure shows that the coordination of the Cp*Ru$^+$ fragment to the C_5 ring is slightly unsymmetrical, with the shortest Ru-C distance being 2.141 Å and the longest 2.211 Å. These values are shorter than those found in **15**, where the two extremes of the Ru-C distance range were 2.152 and 2.245 Å, suggesting a stronger coordination of the [(Ph'$_2$AFA)Pd(η^3-C_3H_5)] complex.

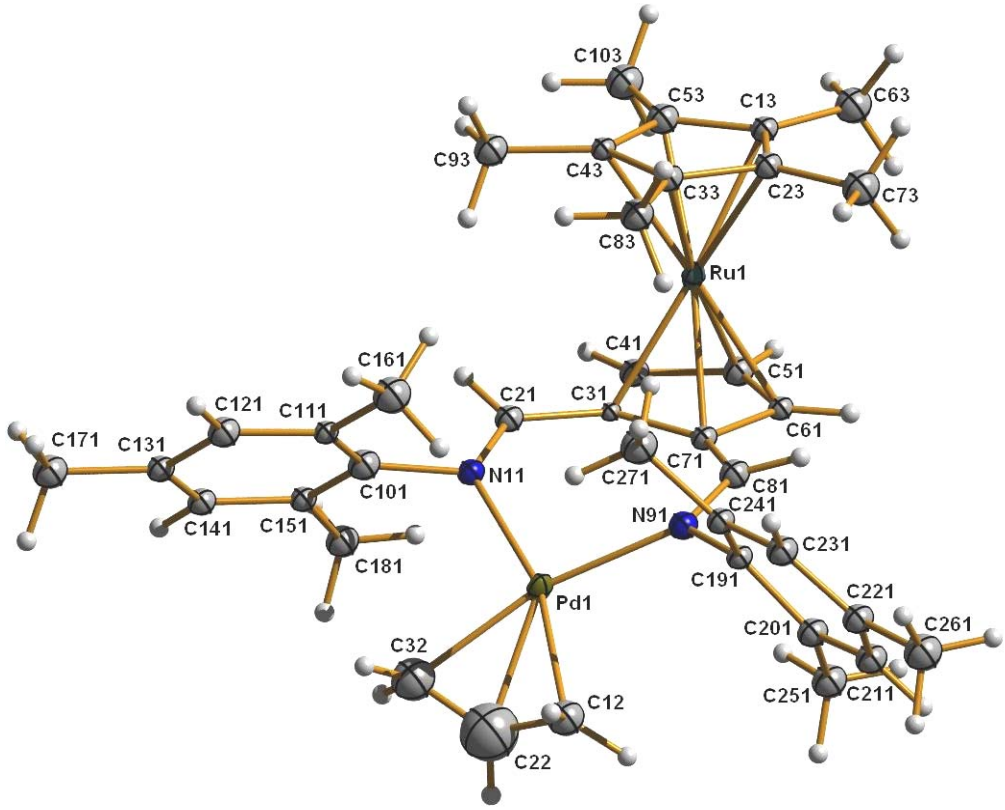

Figure 3.10. Molecular structure of the cation [Cp*Ru(Ph'$_2$AFA)Pd(η^3-C_3H_5)]$^+$.

Table 3.3a. Selected bond lengths for [Cp*Ru(Ph'$_2$AFA)Pd(η^3-C_3H_5)][BF_4].

Bond	*Bond length (Å)*	*Bond*	*Bond length (Å)*
Pd(1)-C(12)	2.124(17)	N(11)-C(21)	1.273(13)
Pd(1)-C(22)	2.08(3)	C(21)-C(31)	1.441(14)
Pd(1)-C(32)	2.097(19)	C(31)-C(71)	1.450(14)
Pd(1)-N(11)	2.125(10)	C(71)-C(81)	1.457(14)
Pd(1)-N(91)	2.111(11)	C(81)-N(91)	1.282(13)
Ru-C(31)	2.141(13)	Ru-C(61)	2.186(13)
Ru-C(41)	2.167(14)	Ru-C(71)	2.203(3)
Ru-C(51)	2.211(14)		

Table 3.3b. Selected bond angles for [Cp*Ru(Ph'$_2$AFA)Pd(η^3-C_3H_5)][BF_4].

Bond	*Bond angle (deg)*	*Bond*	*Bond angle (deg)*
N(11)-Pd-N(91)	100.3(4)	C(31)-C(71)-C(81)	136.0(11)
C(12)-Pd-C(32)	69.2(6)	C(71)-C(81)-N(91)	127.6(12)
Pd-N(11)-C(21)	128.2(9)	C(81)-N(91)-Pd(1)	128.5(9)
N(11)-C(21)-C(31)	130.5(12)	C(21)-C(31)-C(71)	131.5(10)
Pd(1)-N(11)-C(111)	114.99(11)	Pd(1)-N(91)-C(191)	113.02(11)

Coordination to the ruthenium fragment is accompanied by only a small distortion of the Pd complex moiety structure. Values of the dihedral angle (θ) between the N-Pd-N plane and the plane defined by the two C=N bond (27.13˚) and the distance (δ) of the palladium atom from such a plane (0.613 Å) are only slightly bigger than the values found in the free [(Ph'$_2$AFA)Pd(η^3-C_3H_5)] species (23.90˚ and 0.552 Å), indicating that the complex has to undergo only minor adjustments prior to coordination. This is also reflected into the Pd-N bond distances (2.105 and 2.099 Å) and the N-Pd-N angles (100.3˚), which remain substantially unaltered. However, appreciable differences are observed in the other bond distances of the metalla-cycle in **16**. For example, the C=N bond lengths are slightly shorter (1.276 and 1.280 Å) than in **13** (1.299 and 1.305 Å), whereas the C-C(N) distances are considerably longer (1.441 and 1.454 Å). This suggest that there is an increase in double bond character in the C=N connections and a decrease in the C-C(N) connections, which can be regarded as principally single bonds. It appears, therefore, that the ligand in this case resembles more the expected cyclopentadienyl-diimine system. It is intriguing to relate these variations of the bond lengths to the amount of distortion occurring into the AFA-Pd moiety and generated by the Cp coordination. As explained above (and in Chapter 2), it seems to be sensible to state that the larger is the distortion in the AFA fragment, the larger is the disruption of the π-system, signifying that the localisation of the negative charge into the 5-membered ring is more effective and the contribution of the zwitterionic cyclopentadienyl-diimine resonance form is enhanced. The enhancement of the zwitterionic form of the ligand results in turn to an increase of the positive charge on the palladium, which becomes

therefore more electropositive. This interpretation is supported by the Pd-C distances between the metal centre and the allyl ligand, which are significantly shortened (2.059, 2.083 and 2.131 Å) in comparison with the non-coordinated Pd-complex **13** (2.129, 2.147 and 2.154 Å).

3.3 Conclusions

The zwitterionic character of the metal complexes formed with ligands belonging to the class of the 6-aminofulvene-2-aldimine is exploited to provide the synthesis of novel hetero-bi and tri-metallic complexes with ruthenium. The products are all synthesised via the same strategy, using the ruthenium precursor $[Cp^*Ru(MeCN)_3][BF_4]$ and the three AFA complexes $[(Ph_2AFA)_2Zn]$, $[(Ph_2AFA)_2Pd]$ and $[(Ph'_2AFA)Pd(\eta^3\text{-}C_3H_5)]$. The aromatic 5-membered ring in the AFA ligand is coordinated to the highly electrophilic Cp^*Ru^+ fragment affording the isolation of the three new complexes **12**, **15** and **16**, in which the N donors are vacant (**12**) and coordinated (**15**, **16**). The presence of the N-chelate metal is probably dictated by the geometry of the AFA-metal derivative employed. It appears that the use of the square-planar species **9** and **13** leads to the retention of the palladium centre, whereas reaction with the tetrahedral zinc complex **6** follows a fragmentation path which affords the N-vacant ruthenocene **12**. This might depend on the steric hindrance that is generated by the tetrahedral environment of the zinc, with the methyl groups on the Cp* ligand and the phenyl substituents on the nitrogen atoms placed in congested positions. However, a different explanation would invoke electronic redistribution within the aminofulvene-aldimine framework which results in the de-coordination of the zinc atom. Electronic factors may be related to the planarity of the aminofulvene-2-aldimine ligand in the zinc complex, which produces an extended π-delocalisation throughout the whole ligand. Therefore, coordination of the Cp ring might alter the charge distribution, weakening the N-Zn bonds. Along with this hypothesis, the distortion present in the square-planar palladium complexes would be the key feature for retention of the palladium centre by causing the disruption of the p orbitals of the AFA fragment. For this reason, there would be an

enhanced zwitterionic character of the square-planar species, where the negative charge is mainly localised in the Cp ring and hence prone to coordination with no need of charge redistribution.

1. N. Nakajima, K. Tanizawa, K. Tanaka, J. Soda, *J. Biotechnol.* **1998**, *8*, 243; H.-S. Bae, S.-P. Hong, S.-G. Lee, M.-S. Kwak, N. Esaki, M.-H. Sung, *J. Mol. Catal., B: Enzymatic* **2000**, *17*, 223; C. A. Townsend, Chem. Biol. 1997, 4, 721; P. F. Leadlay, *Curr. Opin. Chem Biol.* **1997**, *1*, 162; J. Staunton, B. Wilkinson, *Chem Rev.* **1997**, *97*, 2611; C. Khosla, *Chem. Rev.* **1997**, *97*, 2577.
2. C. Creutz, *Prog. Inorg. Chem.* **1983**, *30*, 1; C. Creutz, H. Taube, *J. Am. Chem. Soc.* **1969**, *91*, 3988; T. J. Meyer, *Prog. Inorg. Chem.* **1983**, *30*, 389; J. E. Miller, *Adv. Chem. Ser.* **1976**, *150*, 18.
3. M. D. Watson, K. B. Wagener, *Macromolecules* **2000**, *33*, 3196.
4. G. S. Weatherhead, J. G. Ford, E. J. Alexanian, R. R. Schrock, A. H. Hoveyda, *J. Am. Chem. Soc.* **2000**, *122*, 1828; W. J. Zuercher, M. Hashimoto, R. H. Grubbs, *J. Am. Chem. Soc*. **2000**, *118*, 6634.
5. J. D. White, P. Hrnciar, A. F. T. Yokochi, *J. Am. Chem. Soc.* **1998**, *120*, 7359.
6. D. S. La, J. G. Ford, E. S. Sattely, P. J. Bonitatebus, R. R. Schrock, A. H. Hoveyda, *J. Am. Chem. Soc.* **1999**, *121*, 11603.
7. Z. J. A. Komon, G. M. Diamond, M. K. Leclerc, V. Murphy, M. Okazaki, G. C. Bazan, *J. Am. Chem. Soc.* **2002**, *124*, 15280; R. Quijada, R. Rojas, G. C. Bazan, Z. J. A. Komon, R. S. Mauler, G. B. Galland, *Macromolecules* **2001**, *34*, 2411; Z. J. A. Komon, X.-H. Bu, G. C. Bazan, *J. Am. Chem. Soc.* **2000**, *122*, 1830; Z. J. A. Komon, X.-H. Bu, G. C. Bazan, *J. Am. Chem. Soc.* **2000**, *122*, 12379.
8. J.-C. Wasilke, S. J. Obrey, T. Baker, G. C. Bazan, *Chem. Rev.* **2005**, *105*, 1001; R. F. De Souza, O. L. Casagrande Jr., *Macromol. Rapid Commun.* **2001**, *22*, 1293; Z. A. J. Komon, G. C. Bazan, *Macromol. Rapid Commun.* **2001**, *22*, 467.
9. G. P. Abramo, L. Li, T. J. Marks, *J. Am. Chem. Soc.* **2002**, *124*, 13966.
10. P. J. Bailey, D. J. Loroño-Gonzàles, S. Parsons, *Chem. Commun.* **2003**, 1426.
11. M. Lacoste, F. Varret, L. Toupet, L. Astruc, *J. Am. Chem. Soc.* **1987**, *109*, 6504; V. Geurchais, D. Astruc, *J. Organomet. Chem.* **1986**, *312*, 97; R. G. Sutherland, M. Iqbal, A. Piorko, *J. Organomet. Chem.* **1986**, *302*, 307; I. W. Robertson, T. A. Stephenson, D. A. Tocher, *J. Organomet. Chem.* **1982**, *228*, 171 and references therein; J.-R. Hamon, D. Astruc, *Organometallics* **1988**, *7*, 1036.

12. J. L. Schrenk, A. M. McNair, F. B. McCormick, K. R. Mann, *Inorg. Chem.* **1986**, *25*, 3501; A. M. McNair, K. R. Mann, *Inorg. Chem.* **1986**, *25*, 2519; A. M. McNair, J. L. Schrenk, K. R. Mann, *Inorg. Chem.* **1984**, *23*, 2633; T. P. Gill, K. R. Mann, *Organometallics* **1982**, *1*, 485; V. S. Kaganovich, A. R. Kudinov, M. I. Rybinskaya, *Izv. Akad. Nauk SSSR, Ser. Khim.* **1986**, 492; J. A. Segal, *J. Chem. Soc., Chem Commun.* **1985**, 1338; N. A. Vol'kenau, I. N. Bolesova, L. S. Shul'pina, A. N. Kitaigorodskii, D. N. Kravtsov, *J. Organomet. Chem.* **1985**, *288*, 341; R. M. Moriarty, Y.-Y. Ku, U. S. Gill, *Organometallics*, **1988**, *7*, 660.

13. P. J. Fagan, M. D. Ward, J. C. Calabrese, *J. Am. Chem. Soc.* **1989**, *111*, 1698.

14. M. Watanabe, T. Okada, *Toso Kenkyu, Giyutsu Hokoku* **2004**, *48*, 15.

15. W. R. Brasen, H. E. Holmquist, R. E. Benson, *J. Am. Chem. Soc.* **1961**, *83*, 3125; L. C. Dorman, *Tetrahedron Lett.* **1966**, 459; E. Daltrozzo, K. Feldmann, *Tetrahedron Lett.* **1968**, 4983.

16. A. J. Arduengo III, D. Tapu, W. J. Marshall, *Angew. Chem. Int. Ed.* **2005**, *44*, 7244; D. Carmichael, L. Ricard, N. Seeboth, J. M. Brown, T. D. W. Claridge, B. Odell, *Dalton Trans.* **2005**, 2173; D. Obendorf, H. Schottenberger, K. Würst, N. Schuler, G. Laus, *J. Organomet. Chem.* **2005**, *690*, 811; T. Meyer-Friedrichsen, H. Wong, M. H. Prosenc, J. Heck, *Eur. J. Inorg. Chem.* **2003**, 936.

Chapter 4

Studies of olefin polymerisation and oligomerisation catalysis

4.1 Introduction

4.1.1 Background

Alkene polymerisation has a long and well documented history, which goes back to the 30s, when ethylene polymerisation had to be performed at high pressure and temperature and provided highly branched polymer of limited use due to its low melting point (<100ºC). It was in 1953 that Karl Ziegler discovered that combinations of $TiCl_4$ and aluminium alkyl compounds were able to polymerise ethylene at low pressure.[1] One year later, Giulio Natta, using Ziegler's heterogeneous systems for propylene polymerisation, observed that the polymers obtained showed a high degree of stereoselectivity or "tacticity": namely all the branches of the polymer were oriented in the same direction relative to the polymeric chain.[2] This new polymer was called "isotactic". These two discoveries opened the doors to a new concept of polymerisation processes and the two scientists received with the Nobel Prize in 1963.

Adequate models were proposed to explain the induction of stereoregular polymer growth by the chiral environment of the catalysts centres.[3]

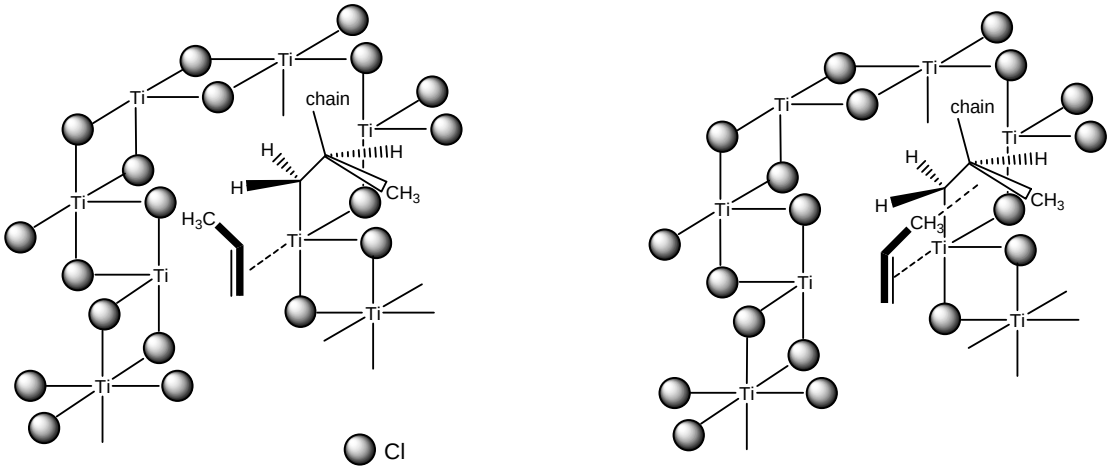

Figure 4.1. Model for the stereospecific polymerisation of propene at chiral Ti centre on the edge of a $TiCl_3$ crystal. The olefin adopts the enantiofacial orientation that places the methyl substituent *trans*- to the polymer chain at the incipient C-C bond (left), being *cis*- orientation disfavoured

The use of a co-catalyst, such as $AlEt_3$, in these systems is essential, its role being to alkylate the titanium atoms on the catalysts surface.[4]

Since those years, the area of alkene polymerisation has been intensively studied and explored, aiming to develop new catalysts with higher activities and stereoselectivity in order to produce polymers with certain desired tacticities and molecular weights, which mean control over the properties of the materials and their applications.

A great advance in the development of these new catalysts occurred in the 1980s with the so called "metallocene revolution" which permitted the use of homogeneous systems, leading to an improvement of all the properties of the polymers obtained.[5] These systems were first discovered by Wilkinson *et al*.[6] and the catalytically active spesies feature predominantly Group 4 metals, although an enormous number of organometallic species with a variety of other metals has been invented and this number is exponentially growing.

The homogeneous nature of these catalysts also helped to elucidate the mechanism of polymerisation, which was proposed by Cossee and is now fully accepted. Scheme 4.1 depicts the basic steps of such mechanism, which is based on sequential olefin insertion into the growing chain.

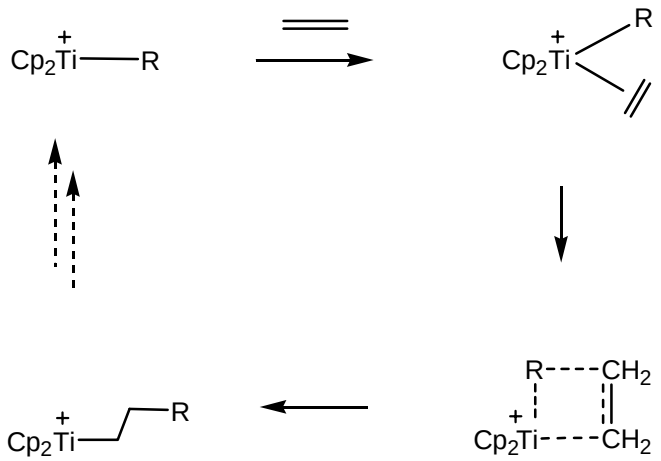

Scheme 4.1. A schematic model of Cossee mechanism for ethylene polymerisation

As shown, the olefin coordinates to the metal prior to insertion, and this is in agreement with the observation that the catalytically active species must have a coordinative unsaturation, as well as an alkyl metal bond in order to undergo the first insertion. "The active species is stabilised by several ligands, which remain bound to the metal throughout the polymerisation and have four important roles: (1) control over the metal coordination number, (2) control over the metal coordination geometry, (3) control over the formal oxidation state of the metal, (4) steric protection of the active site and influence over stereo-selectivity".[7] The choice of the ligand is therefore crucial to provide catalysts able to build up the desired type of polymer.

4.1.2 Catalytic Activation: Generalities

The active species is normally generated in situ using a co-catalyst, as already mentioned, and different routes are possible as shown in Scheme 4.2.

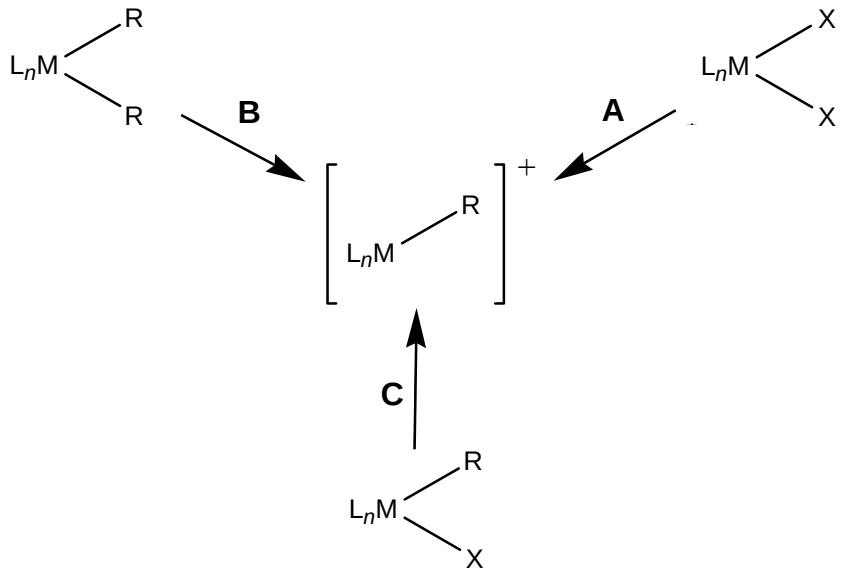

Scheme 4.2. The three possible precursors to the catalytically active species.

In route A, a salt elimination takes place, with an anionic ligand such as a halide being abstracted and substituted by a "non-coordinationg" ligand. Reagents commonly used are $Na[B\{3,5\text{-}(CF_3)_2C_6H_3\}_4]$,[8] or silver salts such as $AgBF_4$ or $AgOSO_2CF_3$ for the later transition metals.

Of greater importance is route B, where catalytic activation is achieved by abstraction of an alkyl ligand. Reagents used for this scope include $[Ph_3C][B(C_6F_5)_4]$,[9] $[PhNHMe_2][B(C_6F_5)_4]$,[10] $[H(OEt_2)][B\{3,5\text{-}(CF_3)_2C_6H_3\}_4]$,[8, 11] or $B(C_6F_5)_3$.[12] Strictly speaking, only the trityl reagent is an abstracting agent, whereas the anilinium salt and the acid remove the alkyl group by protonation. In most cases, the $B(C_6F_5)_3$ only partially abstracts the alkyl ligand leading to "cation-like" species. In this regard, Jordan and co-workers studied the methyl abstraction of Cp_2ZrMe_2 with $B(C_6F_5)_3$ and found that a methyl bridged structure was adopted for the resulting ion pair, with the Zr-Me distance of 2.556(2) Å. [13]

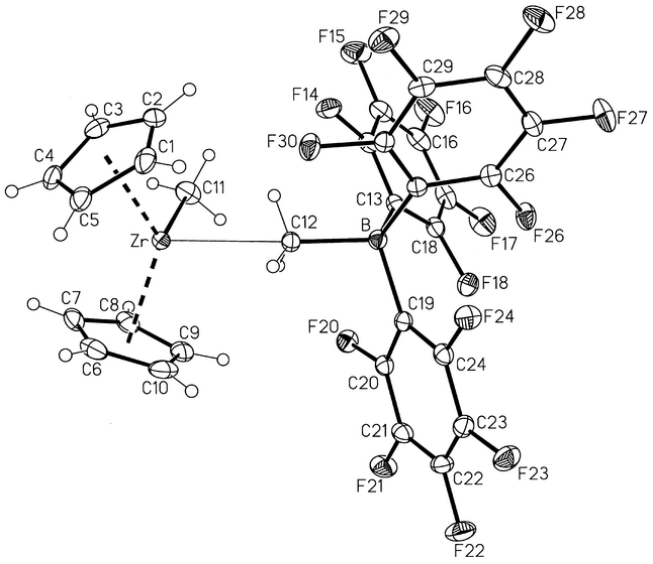

Figure 4.2. Methyl bridged structure of $[Cp_2ZrMe][MeB(C_6F_5)_3]$.

Route C combines alkylation of the metal centre and abstraction of an alkyl group and is normally achieved by treating a dihalide procatalyst with an alkylating species followed by one of the previously mentioned reagents. In this regard, of great impact was the discovery by Reichert and Meyer that addition of water to titanocene systems like $Cp_2Ti(R)Cl/RAlCl_2$ increased the rate of polymerisation, whilst the formation of aluminoxanes was suggested.[14] Sinn and Kaminsky studied the $Cp_2ZrMe_2/AlMe_3$, where a hydrolised form of trimethylaluminium, methylaluminoxane (MAO),[15] afforded extremely active catalysts when combined with zirconocenes. The methylaluminoxane is a poorly characterised species, with a molecular weight range between 900 and 1200 and a core made with $[\{MeAlO\}_n]$ units. Modified methylaluminoxane (MMAO), which is prepared by the controlled hydrolysis of a mixture of trimethylaluminium (TMA) and triisobutylaluminum has emerged as an alternative activator, with the advantages of a better solubility in aliphatic solvents and an enhanced solution storage stability.[16]

Since the active species is highly electron deficient and extremely reactive, their efficiency has been proved to be greatly influenced and limited by the nature of the counteranion. Consequently, a common factor for all the described types of activators is their weak coordinating power. Over the last decades, big emphasis has been put into the coordination energies of different anions, with the ultimate goal of lowering as much as possible their interaction with the metal centre, thus making the

coordination of the olefin a less impeded process. Co-catalysts for metal-catalysed olefin polymerisation have been the subject of several reviews.[17]

4.1.3. Late transition metals in polymerisation catalysis

The high oxophilicity of early transition metal catalysts (titanium, zirconium, chromium) make them unsuitable for the polymerisation of functionalised olefins since they are poisoned by most of these monomers, in particular by the commercially available polar co-monomers, and therefore alternative routes must be used to produce these polymers, such as metathesis reactions of cyclic olefins and successive functionalisation of the resulting unsaturated polymer, or metathesis of polar cycloolefins followed by hydrogenation to remove the resulting unsaturation.[18] Obviously, these multistep processes compromise very often commercialisation of the most valuable polymers which are still produced by free radical polymerisation.

The lower oxophilicity of late transition metals and their presumably higher functional group tolerance make them an interesting target for polymerisation involving polar co-monomers. Despite their potential, for many decades after the discovery of Ziegler-Natta polymerisation, late transition metals were commonly ignored as applicable catalysts. The reason has to be attributed to the lower activities towards olefin insertion that they exhibit in comparison with early transition metals, with the β-hydride elimination step competing with the chain growth, typically leading to the formation of dimers or oligomers.

Group 10 compounds with anionic P,O ligands, for instance, are well known to oligomerize ethylene. Keim *et al*. showed that mixing Ni^0 complexes with phosphorus ylides, for example $Ph_3PCH=C(O)Ph$, produced highly active oligomerisation catalysts.[19] Reaction of the same ylide with $Ni(cod)_2$ in the presence of PPh_3 results in an oxidative addition reaction with cleavage of the P-Ph(ylide) bond and subsequent formation of the phosphanyl-enolato complex **A** (Fig. 4.3) known as Keim's oligomerisation catalyst, [20] which played a central role in the Shell Higher Olefin Process (SHOP).

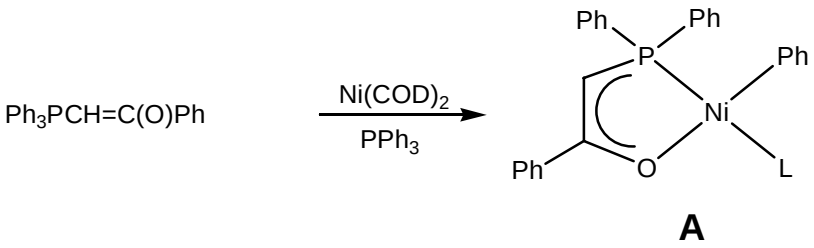

A

Figure 4.3. The traditional Keim's oligomerisation catalyst.

However, under certain conditions, some SHOP-type oligomerisation catalysts were reported to be active polymerisation catalysts. For example, the same compound (**A**) was reported to polymerise ethylene with high activities, producing materials with molecular weights over 100,000.[21] The key to the formation of high molecular weight polymers rather oligomers is the use of a phosphine scavengers such as $Ni(cod)_2$ in order to remove the PPh_3, or alternatively the use of more labile ligands such as pyridine instead of phosphine. These systems have also been shown to be active towards the copolymerisation of ethylene with higher α-olefins.[16]

As rationalized by Grubbs *et al*., replacing the P-O chelate of the SHOP systems with a harder nitrogen-based ligand bearing higher steric demand leads to higher molecular weight polymers.[22] These systems are based on salicylaldimine nickel complexes, and their activity is strongly related to the steric bulk of the substitutents on the aryl ring. Decreasing the steric hindrance in complex 1 (Fig 4.4) results in no activity towards polymerisation. In contrast, use of substituents has the effect of raising not only the M_w of the polymers (> 20,000) but also the catalytic lifetime of the active species; complexes 5 and 8, for example, show M_w of about 350,000 and 532,000 respectively. Moreover, while compounds 1 and 2 require the use of a co-catalyst for activation, the others are neutral, single-component polymerisation catalysts.

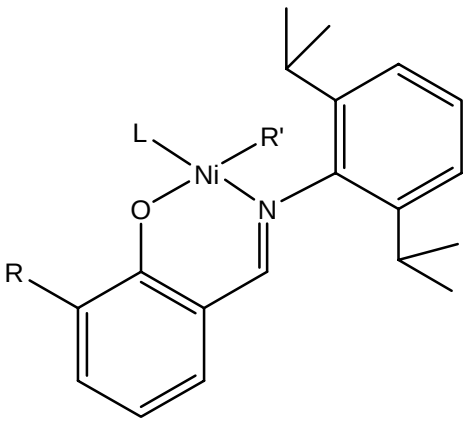

R	R'	L
H	Ph	Ph_3P
^tBu	Ph	Ph_3P
Ph	Ph	Ph_3P
Phen	Ph	Ph_3P
Anth	Ph	Ph_3P
Anth	Me	MeCN
Trityl	Me	MeCN
TPhen	Me	MeCN

Figure 4.4. Ni(II) salicylaldimine complexes. Abbreviations: ^{t}Bu, tert-butyl; Ph, Phenyl; Phen, 9-phenanthroline; Anth, 9-anthracene; Trityl, triphenylmethyl; TPhen, *meta*-terphenyl.

Mecking and co-workers also studied the effect of the introduction of electron-withdrawing substituted aryl groups in the C2 and C6 positions of the aniline aryl ring towards polymerisation, and very recently presented the first examples of structurally characterised neutral methyl nickel complexes which are precursors of active catalysts (Fig. 4.5).[23]

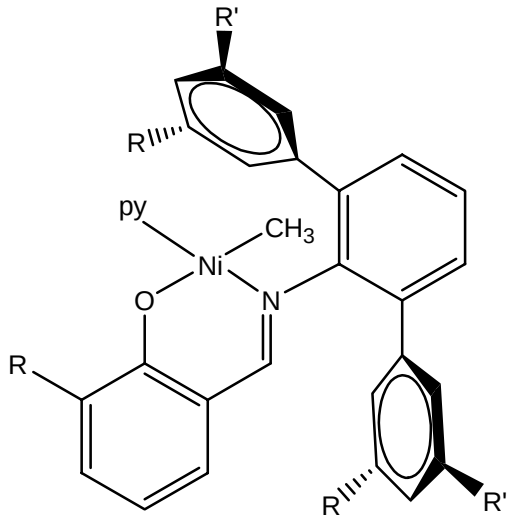

R	R'
CF_3	CF_3
NO_2	H
OCH_3	OCH_3

Figure 4.5. Mecking's catalysts for polymerisation, featuring electron withdrawing substituents on the aryl ring and the Ni-Me bond.

Phosphinophenolate analogues of Grubbs' catalysts have been also receiving attention over the last few years. They can be prepared by reaction of 2-phosphinophenols with diorganonickel, organonickel halide or organonickel-

methoxy precursors, as shown in the example in Fig. 4.6. It has been shown that they undergo direct β-elimination to form nickel hydride complexes which are the actual catalytic species. Presence of additive such as monodentate phosphine can hinder the polymerisation, switching these systems to oligomerisation catalysts.[24]

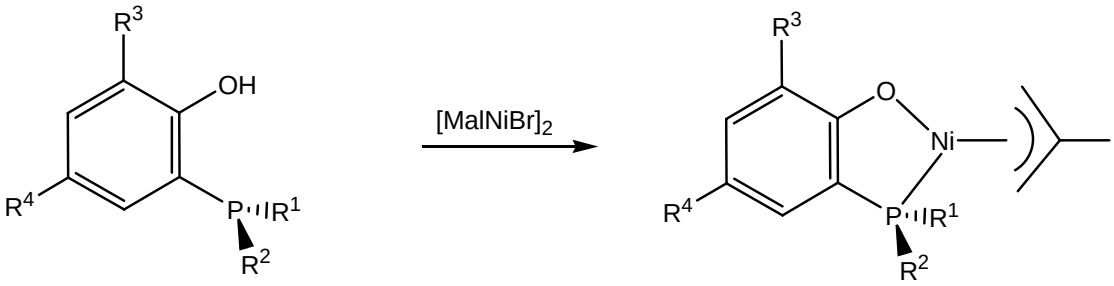

Figure 4.6. Phosphinophenolate complexes. The allyl product is not the actual catalytic species, but it produces a nickel hydride intermediate which is responsible for the polymerisation.

One of the major breakthroughs in late transition metal polymerisation catalysts occurred in 1995 with the discovery by Maurice Brookhart of a new family of compounds exhibiting high activities towards olefin polymerisation.[25] These catalysts are based on neutral chelating nitrogen-based ligands bound to highly electrophilic, cationic nickel and palladium metal centres.[26] One of the key features of these systems is the use of α-diimine ligands containing bulky nitrogen substituents, which are well known to stabilise organometallic complexes. It is possible to prepare a large range of α-diimino ligands by varying the backbone and aryl substituents, and this range can be extended to exhaustive libraries using techniques well developed in the pharmaceutical industry.

Fig. 4.7 shows the traditional Brookhart's catalyst.

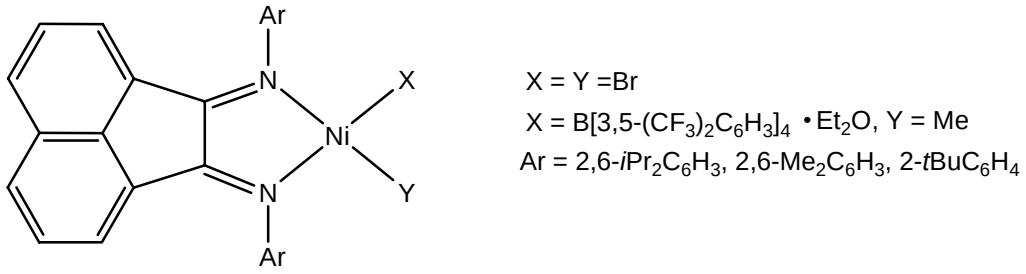

Figure 4.7. The traditional Brookhart's (diimine)nickel complex.

Nickel dibromide complexes have been tested in typical preparative scale polymerisations. Saturation with ethylene of the catalyst precursor suspended in toluene and activation with MAO showed activities with very high activities at 35˚C. Variation of the catalyst structure and polymerisation conditions profoundly influence the molecular weights of the products, which can range from oligomers to high polymers (M_w 30,000 to > 1,000,000).

The palladium catalysts normally yield high molecular weight polyethylene. The products are amorphous material, showing a high content of branches, typically ~100 methyl-ended branches per 1000 methylene groups, which are notably formed by ethylene alone and without the intermediacy of α-olefins. However, the morphology of the polymers is pressure-dependent.

Low temperature NMR spectroscopy provides a powerful method to monitor ethylene chain growth at cationic nickel and palladium centres.[27]

As depicted in Scheme 4.3, the resting state is the alkyl ethylene complex and this is in contrast with early transition metals, where this intermediate is not observed. Barriers to migratory insertion in the range of 17-18 kcal/mol are observed for the palladium based catalyst, whereas for the nickel such barriers are substantially lower, ranging between 13 and 15 kcal/mol.[28] Extensive NMR studies have also shown β-agostic interaction in the formally 14-electron cationic alkyl species generated after the migratory insertion, which turns out to be important to the introduction of branching in the polymers produced. Specifically, if prior to trapping and insertion of the olefin the agostic metal alkyl species undergoes a series of β-hydride elimination and re-additions with a different regiochemistry, the final polymer will have a certain percent of branches. Such phenomenon is called “chain walking” and longer chain walks introduce longer branches.[28]

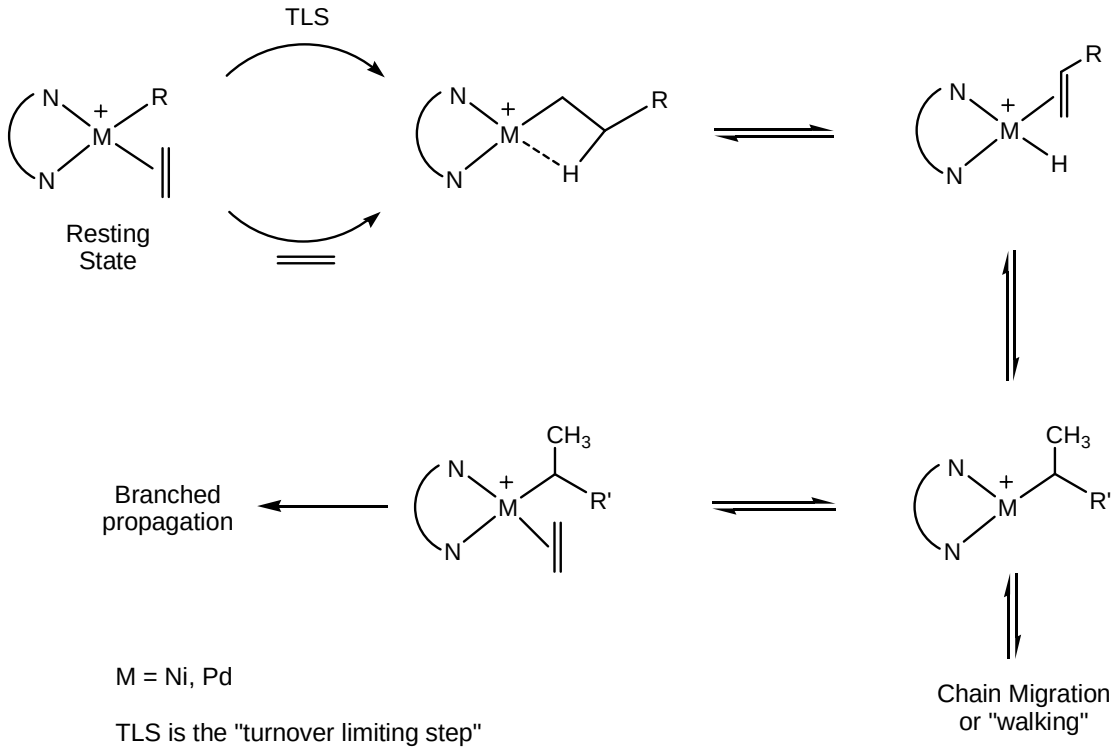

Scheme 4.3. Schematic mechanism for ethylene polymerisation and polymer branch formation with Ni and Pd α-diimine complexes

Chain walking is responsible for high branching in Pd(II) systems under typical ethylene polymerisation conditions, while for Ni(II) systems the microstructure of the polyethylenes also depend on the monomer concentration, reaction temperature and ligand structure. Therefore, the microstructures of the materials produced can be varied from strictly linear to highly branched, resulting in polymers ranging from highly crystalline to totally amorphous.

As previously mentioned, β-hydrogen elimination is generally a faster process in the late transition metals and from the metal-hydride species formed in this step, chain transfer can occur, resulting in the release of the polymer chain and propagation of a new chain, yielding materials with low molecular weights.

Scheme 4.4 illustrates the two proposed mechanisms for the chain transfer. An associative displacement of the unsaturated polymer chain from an olefin hydride intermediate by monomer was firstly invoked; in this regard, the bulky ortho substituents in the Brookhart's systems were proposed to block the approach of the monomer to the axial position of the square-planar intermediate, thus retarding the

rate of displacement. This hypothesis has been supported by alkyl ethylene model systems, which established that exchange of free and bound ethylene does take place by an associative process and the rate of such exchange is dramatically slowed by bulky ortho-substituents.[25]

The other proposed mechanism involves a β-hydrogen transfer to the monomer, with the chain transfer occurring directly from the resting state. The transition state for this process places the olefin axial sites and in this case the role of the bulky substituents is to raise the energy of such transition state, making it increasingly unstable relative to the four-coordinate ethylene alkyl adduct.[29]

A. Associative displacement from the olefin hydride intermediate

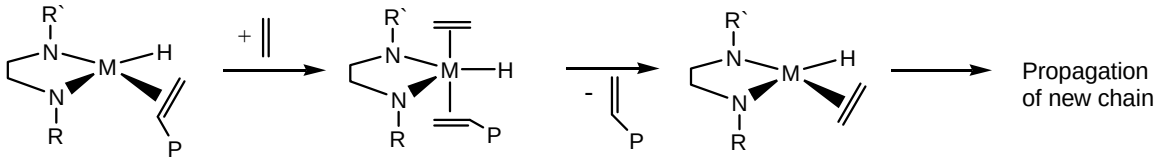

B. Direct ß-hydride transfer to monomer from the alkyl-olefin resting state

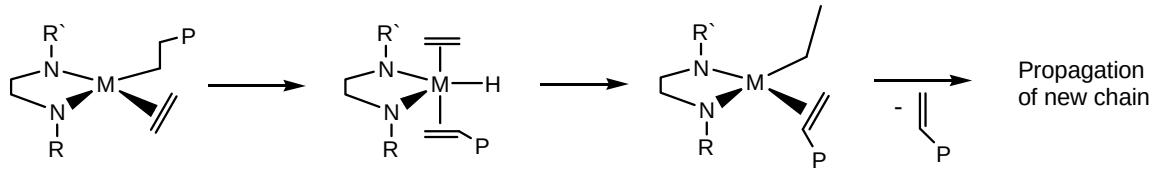

Scheme 4.4. The proposed two possible modes of chain tranfer

Insertion barriers have been accurately modelled using DFT calculations, which indicate that initialization proceeds in a stepwise fashion, with activation barrier for nickel catalysts being in the range of 9-11 kcal/mol, and that formation of high molecular weight polymers can only be explained by suppressing the chain termination transition state due to sterically demanding substituents on the diimine ligand.[30] For palladium complexes, such barriers are higher, ranging between 17 and 18 kcal/mol.[25,27,28]

In agreement with the proposed mechanisms, computational calculations showed that migratory insertion barriers are dramatically lowered by the inclusion of bulky R and Ar ligands.[31]

Although the functionalities on the para position of the aryl ring does not seem to produce any relevant effect in terms of steric hindrance and consequently in terms of catalytic rates, they proved to be useful for tuning the electronic effects free of any contribution from the steric effects. The donating ability of the ligand can indeed be influenced by these subsitutents, leading to polymer with different properties such as molecular weights and branching topology. In general, catalysts bearing electron-donating groups afford polymer with higher molecular weights, whereas electron-withdrawing substituents produce more dendritic polyethylene.[32]

Very recently, diimine systems have also been applied to the preparation of catalysts in combination with other late transition metals. The system shown in Fig 4.8 features a (diimino)copper dichloride which is active in ethylene polymerisation.[33]

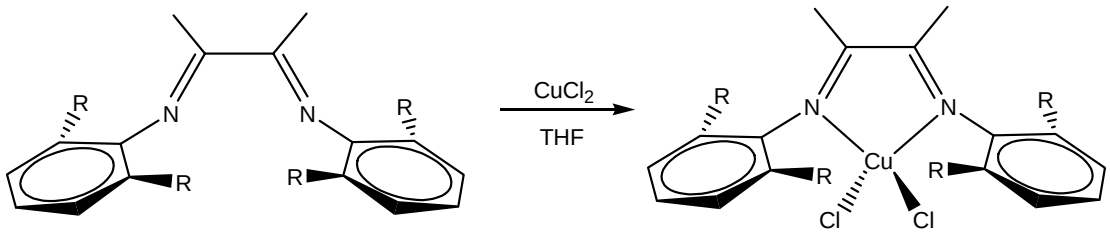

Figure 4.8. (Diimino)copper catalyst active in ethylene polymerisation.

4.1.4. Zwitterionic systems

In 1995 Erker *et al.* introduced an alternative strategy for the generation of the catalytic species.[34] By treating the [Cp_2Zr(butadiene)] complex **A** with $B(C_6F_5)_3$, a metallocene borate-betaine system **B**, highly active in olefin polymerization was formed.

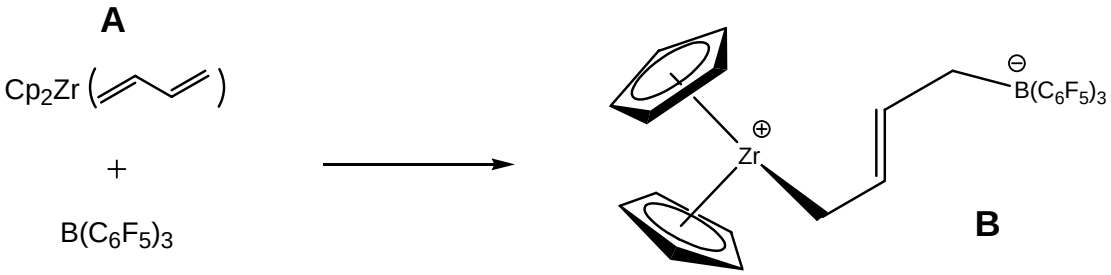

Figure 4.9. Erker's zwitterionic systems

Independently, Devore and co-workers used the same approach for constrained-geometry titanium complexes (**C**).[35] These two systems were called "zwitterionic metallocenes" because the cationic and anionic parts are combined within the same molecule. More recently Piers showed that this method can also be applied to complexes having simple olefin coordinated, as in $Cp_2Zr(C_2H_4)(PPh_2Me)$ (**D**): reaction with $B(C_6F_5)_3$ leads to zwitterionic complexes capable of initiating alkene polymerisation.[36]

Figure 4.10. Devor's constrained geometry titanium complexes and Piers' zirconium complex which capable of reacting with $B(C_6F_5)_3$ to form zwitterionic catalysts.

As for the normal olefin polymerisation processes involving cationic metallocenes, major attention has been focussed on zwitterionic analogues of group 4 metallocenes. They can be divided into three main classes: ring-type zwitterions, girdle-type betaines and bridge-type zwitterions. These three regions available for the counterion are represented in Fig. 4.11.

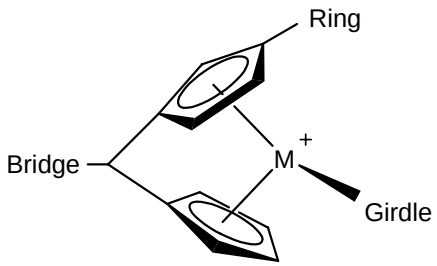

Figure 4.11. The three region normally accessible to the counterion in zwitterionic species.

In the first class the anion, typically a borate, is affixed to one of the Cp-donors. There are a number of different routes for the preparation of this type of species, and examples reported in the literature clearly show that the length of the tether connecting the ring with the borate is a crucial feature for determining the properties of the zwitterions.

Hydroboration of an allyl group attached to a Cp ring using the by reaction with $HB(C_6F_5)_2$ results in a rearrangement of the initially formed zwitterions to a non-zwitterionic species, indicating that a three-carbon tether is too long for the sustenance of a zwitterionic structure.[37]

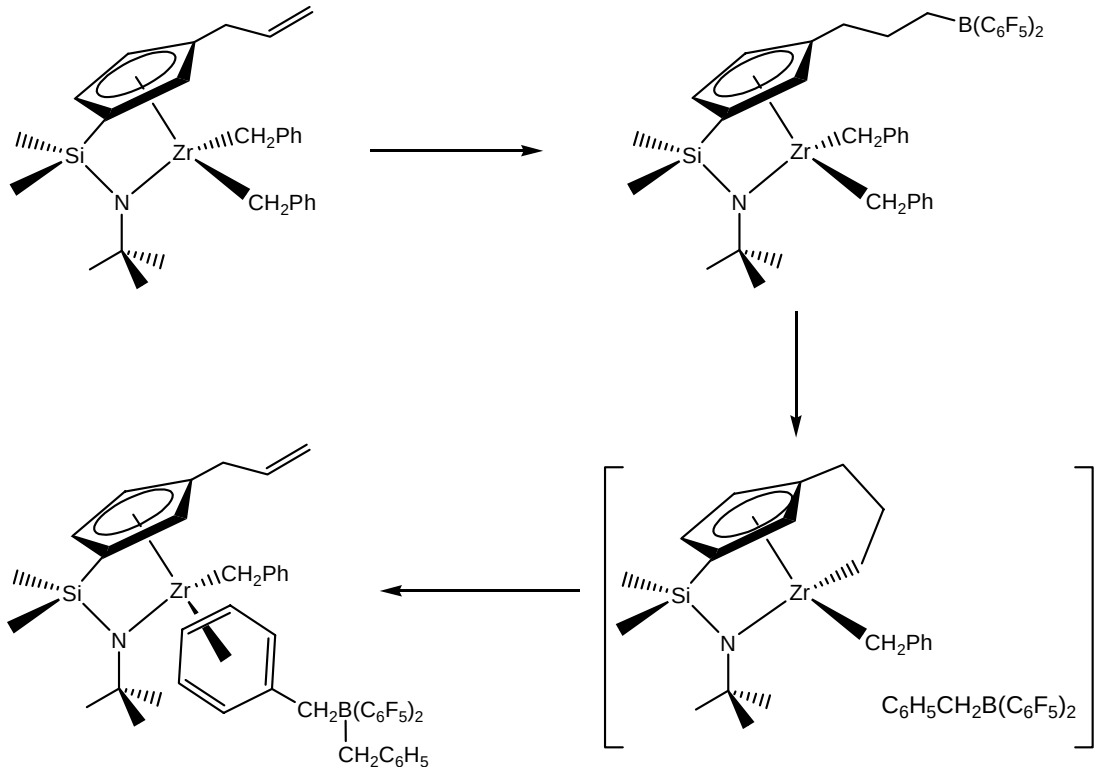

Scheme 4.5. Rearrangement to a non-zwitterionic species for a 3-carbon tethered ring-type zwitterion.

In order to produce ring-zwitterions with a short linker of only one carbon, the so-called "tucked-in" metallocenes, in which one of the methyl groups of the C_5Me_5 has undergone metallation and is σ-bound to the metal, are a common strategy.[38]

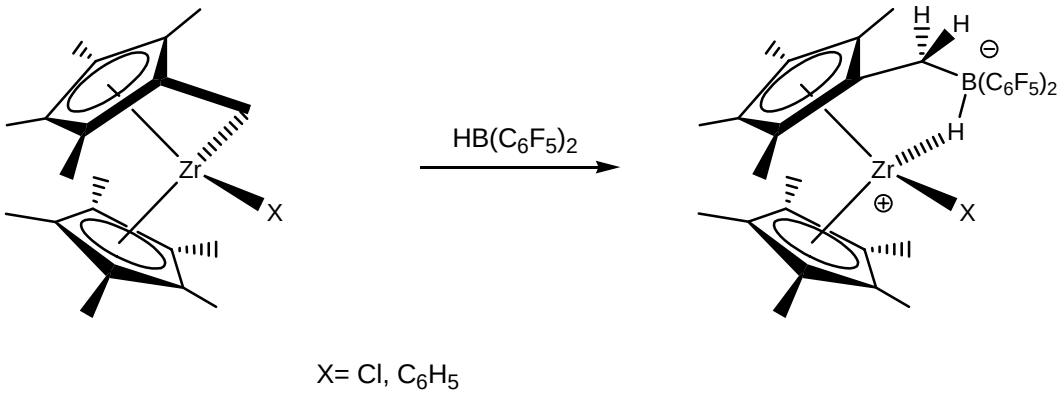

X= Cl, C_6H_5

Figure 4.12. Tuck-in zirconocene/$HB(C_6F_5)_2$-derived zwitterions. The formation of a strong hydroborate-Zr bond renders this species poorly active.

The "base-free" nature of these zwitterions renders them highly active towards ethylene polymerization. To the extent that cationic zirconocenes are never completely "base-free" in condensed media, the metal centres in these compounds are sustained electronically via a variety of intramolecular interactions as shown in the previous paragraph. The hydroborate-Zr chelation shown in Fig 4.12 is particularly strong and therefore damaging for catalysis.

There are also examples of ring-type zwitterions with the borate directly attached to the ring; in this regard, a novel approach developed by Bochmann and Lancaster is the incorporation of the counterion at the beginning of the synthetic route, working with anionic compounds all the way through. With this strategy, the synthetic problems associated with the presence of an electrophilic borane centre are therefore avoided, since the borane is actually masked as a borate.[39]

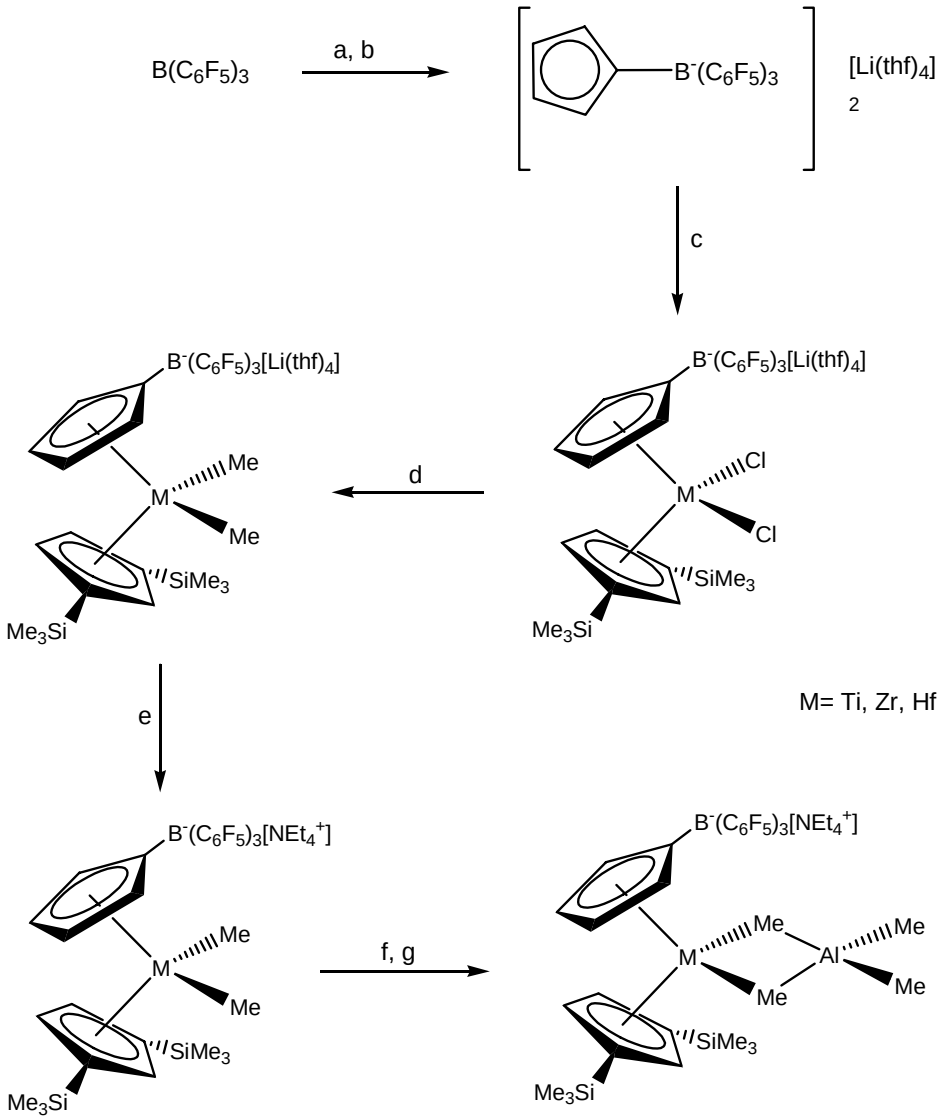

Scheme 4.6. Bochmann's zwitterionic metallocenes. a) C_5H_5Li; b) BuLi; c) $[\{C_5H_3(SiMe_3)_2\}MCl_3]$; d) 2 MeLi; e) $[NEt_4][BF_4]$; f) $[Ph_3C][B(C_6F_5)_4]$, 0.5 Al_2Me_6; g) –[Ph3Me], -$[NEt_4][BF_4]$

In the girdle-type betaines, the counter-anion is located on the alkyl group occupying the active wedge of the metallocene. Differently from the previous type of zwitterions, where the charge separated structure is maintained throughout the polymerization, in this case the separation of charges increases as the polymerisation proceeds and the zwitterionic nature lasts only until the last termination step. Once the β-hydrogen transfer has happened, the reaction continues as in conventional polymerization catalysts. As an example, the above described Erker's zwitterionic

catalyst butadiene/$B(C_6F_5)_3$ zirconium catalyst was proved, by using laser desorption ionization MS analysis, to be short-lived under catalytic conditions.

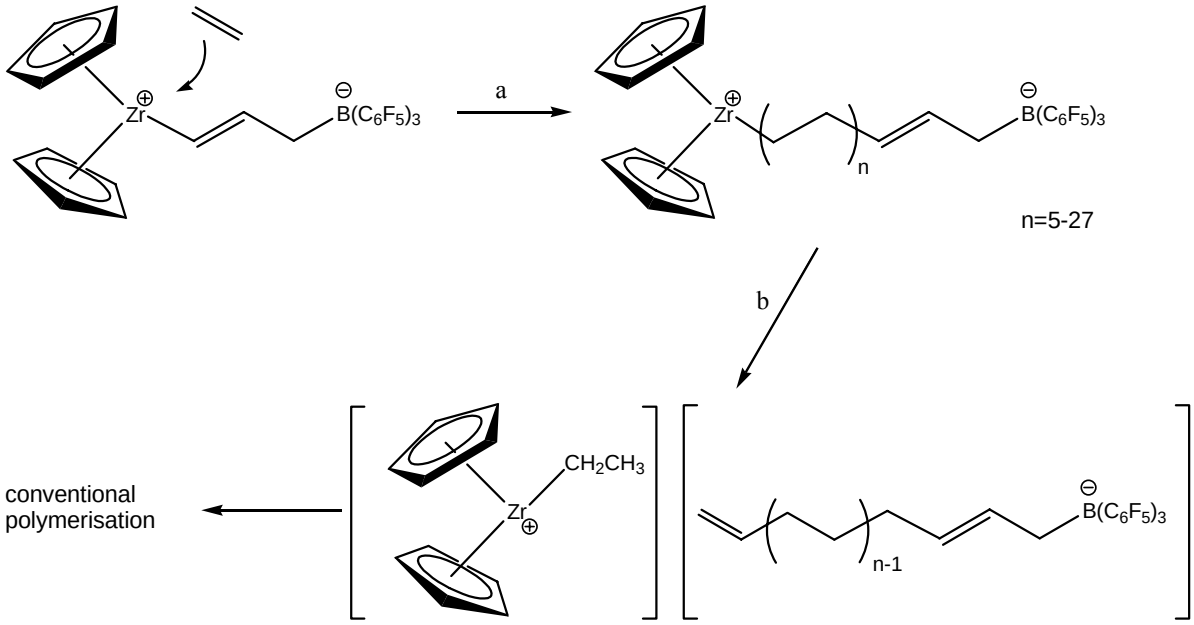

Scheme 4.7. The short lived nature of betaine-type zwitterioinc catalyst. After dissociation of the growing chain, the zwitterions is lost and polymerisation continues in a conventional way.

This new approach has been recently applied to late transition metal catalysts, and the first example of a zwitterionic "butadiene-borate" Ziegler-Natta catalyst system was reported.[40] Treatment of the (η^4-butadiene)nickel complex with $B(C_6F_5)_3$ yields the chelate complex shown below

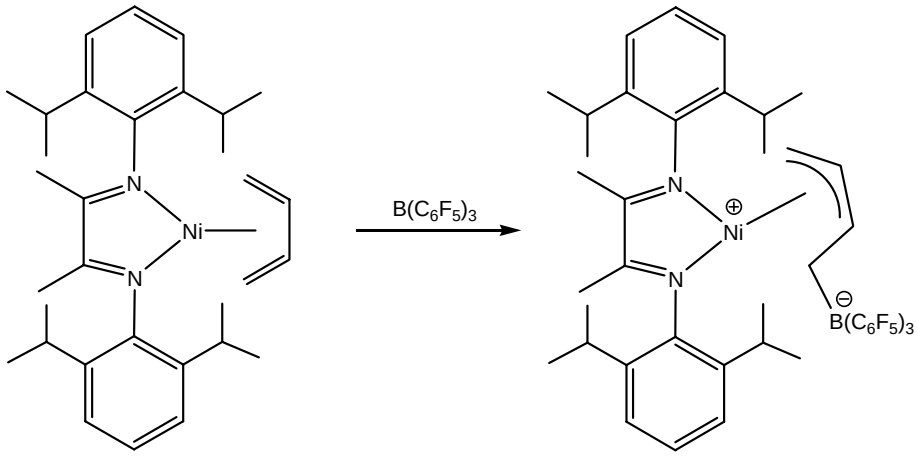

Figure 4.13. Erker's zwitterionic (diimino)nickel complex active in polymerisation.

This development is also important in view of some recent observation made with cobalt-based Ziegler-Natta catalysts. As was independently reported by Budzelaar and Gibson, treatment of bis(imine)halogenocobalt(II) chelate complex shown in Scheme 8 with MAO led to the reduction to the respective Co(I) complexes rather than to alkylation.[41] Alkylation of the Co(I) species and subsequent methyl abstraction must then lead to a σ-alkyl ligand-free cation which can be considered a direct precursor of the active species, although it lacks the necessary metal-carbon bond.

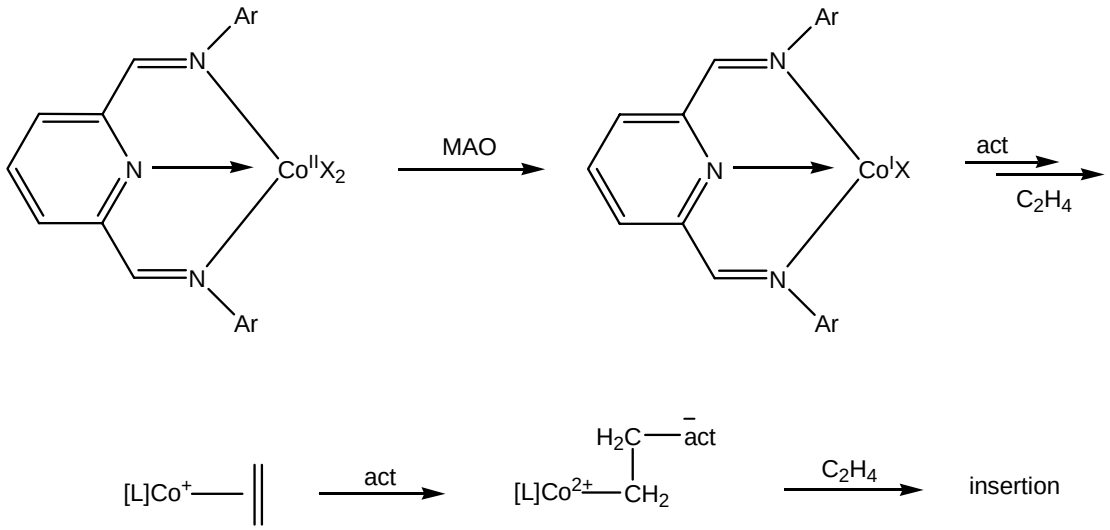

Scheme 4.8. Reduction from the Co(II) to the Co(I) complex and subsequent alkylation.

As reported by Bazan *et al*., addition of one equivalent of $B(C_6F_5)_3$ to Keim's catalyst $[(C_6H_5)_2PC_6H_4C(O))$-κ^2P,O]Ni(η^3-CH_2CMeCH_2) (**E**) yields the complex (**F**) which is considerably more active in ethylene polymerisation than **E** and which can be formulated as an hybrid of two zwitterionic resonance forms:[42]

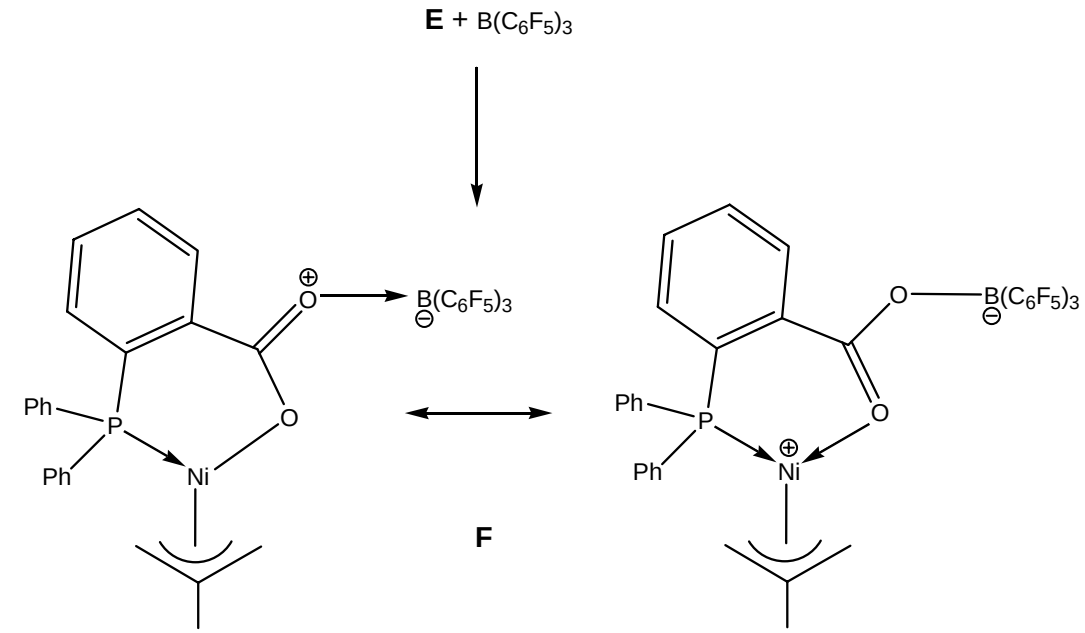

Scheme 4.9. Reaction of E to produce F, which can be formulated to exist in equilibrium of two zwitterionic forms.

Similarly, this approach can be used for the preparation of other neutral zwitterionic catalysts, including Brookhart's type (**G**) and Keim's type (**H**) catalysts:

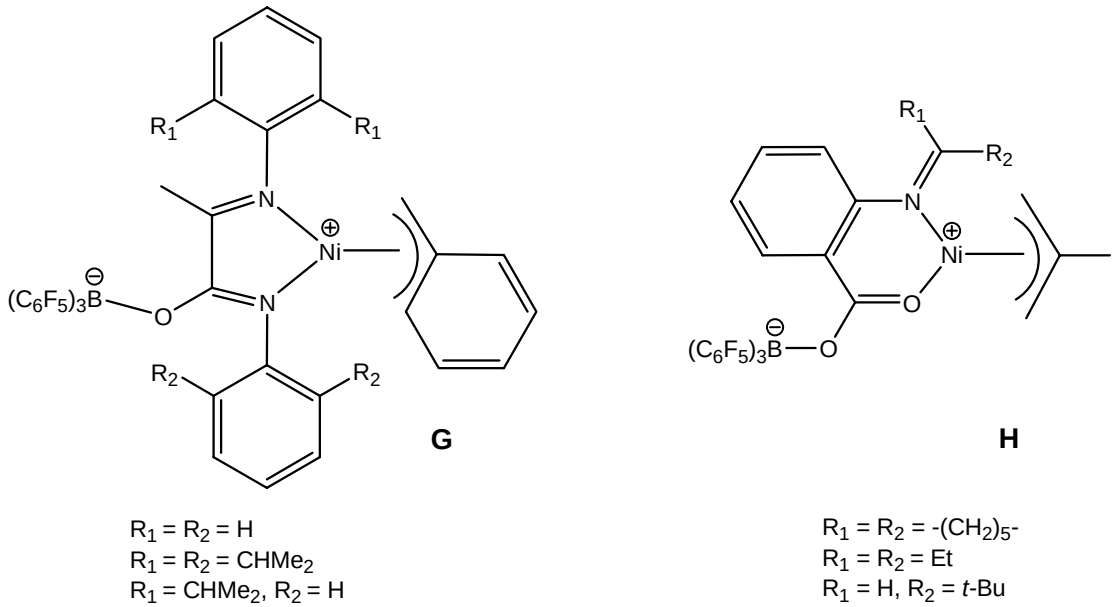

$R_1 = R_2 = H$
$R_1 = R_2 = CHMe_2$
$R_1 = CHMe_2$, $R_2 = H$

$R_1 = R_2 = -(CH_2)_5-$
$R_1 = R_2 = Et$
$R_1 = H$, $R_2 = t\text{-}Bu$

Figure 4.14. Brookhart's type (G) and Keim's type (H) zwitterionic catalysts.

The third class of zwitterionic metallocenes is related to the bridge-type metallocenes and isolation and structural characterisation of these complexes has not yet been achieved. However, recent synthetic methodologies indicate that these systems should be accessible. Potential precursors to zwitterionic bridge-type complexes that have been attracting much attention are based on anionic borate-bridged Group 4 metallocenes of the type shown in Fig 4.15.[43]

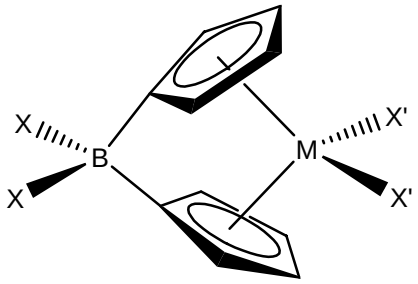

Figure 4.15. Borato-bridged metallocene.

As shown by Bochmann and Lancaster (Scheme 4.10), alkylation and alkyl abstraction leads to *in situ* formation of the zwitterionic species **I**, which is active in ethylene polymerisation.

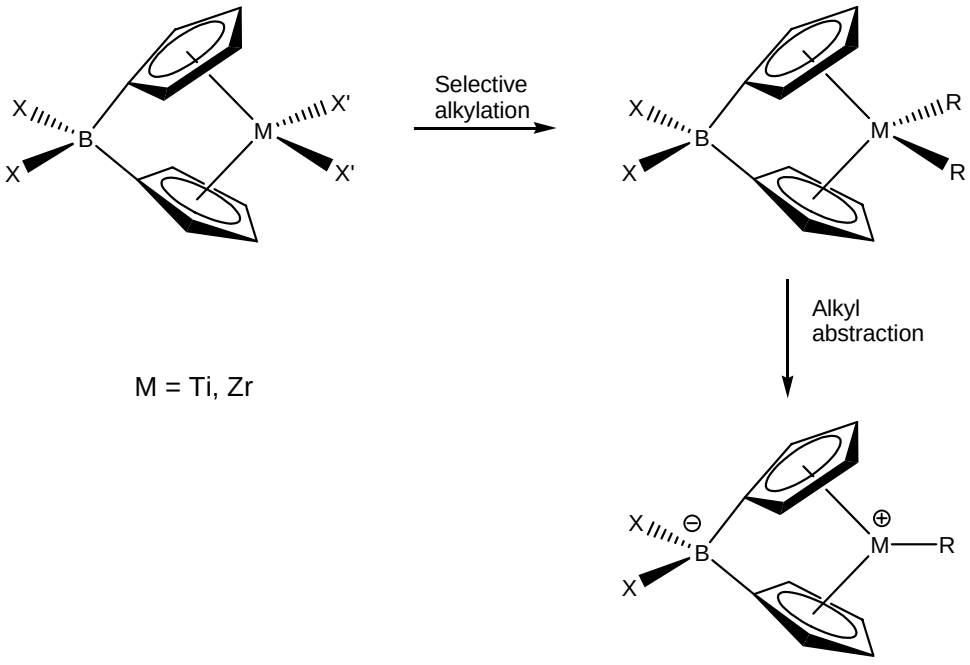

Scheme 4.10. Formation of a bridge-type zwitterionic metallocene.

4.2 Aim of the project

As part of the study on new zwitterionic late transition metal complexes based on 6-aminofulvene-2-aldimine ligands, investigation of these systems as catalysts for olefin polymerisation was one of the objectives of the project.

The design of new zwitterionic analogues of Brookhart's catalyst for homogeneous olefin polymerization arises from the problem of ion pairing effects, which play an important role in terms of catalyst activities. As shown in the general introduction, the formation of the active catalytic species is achieved by the use of a co-catalyst, which is in most cases a Lewis acid and whose function is in general to abstract an alkyl group from the pre-catalyst to form a positively charged metal complex. Although there are different paths of activation depending on the compound employed, the choice of the co-catalyst is invariably dictated by the common feature of providing a weakly coordinating counter anion once the alkyl has been abstracted. After the formation of the positively charged metal centre, it is crucial that the counterion formed after the alkyl abstraction will have the smallest possible interaction with the metal centre, leaving it available for the olefin coordination. To use a rather ambiguous term, a "vacant site" on the metal is the main requirement for any olefin polymerization catalyst. As a matter of fact, the counterion will still have some sort of interaction, affecting the polymerization in different ways. Many efforts have been put into the discovery and design of co-catalysts in which these electrostatic interactions would be minimized.

On the basis of the results obtained with late transition metal with the 6-aminofulvene-2-aldimine ligands, a deeper investigation into these systems was conducted in order to synthesise complexes which could have all the requisites for performing polymerization catalysis.

As far as catalysis is concerned, the main deficiency of the systems discussed in the previous chapters is the saturation of the metal centres, which feature neither the metal-alkyl bond, essential for the first olefin insertion, nor the site available for the coordination of the monomer. The observations that the reactivity of the deprotonated ligand towards metal centres is not easily controlled, led to the

investigation of new strategies to prepare and isolate zwitterionic complexes featuring all the properties needed for being, at least in principle, catalytically active.

4.3 Results and discussion

4.3.1. Generalities

Different strategies were used to prepare complexes suitable for polymerization catalysis. As described in Chapter 1 and Chapter 2, deprotonation of the Ph_2AFAH ligand and reaction with dihalide metal derivatives leads to the formation of di-substituted metal complexes. Attempts to control the stoichiometry of the reaction by varying conditions such as temperature, solvent or metal precursor were all unsuccessful, and isolation of a mono-substituted species was never achieved. Although never experimentally observed, if such a species was formed at some stage during the course of the reaction, its reactivity presumably turned out to be even higher than for the original metal precursor. (Scheme 4.11).

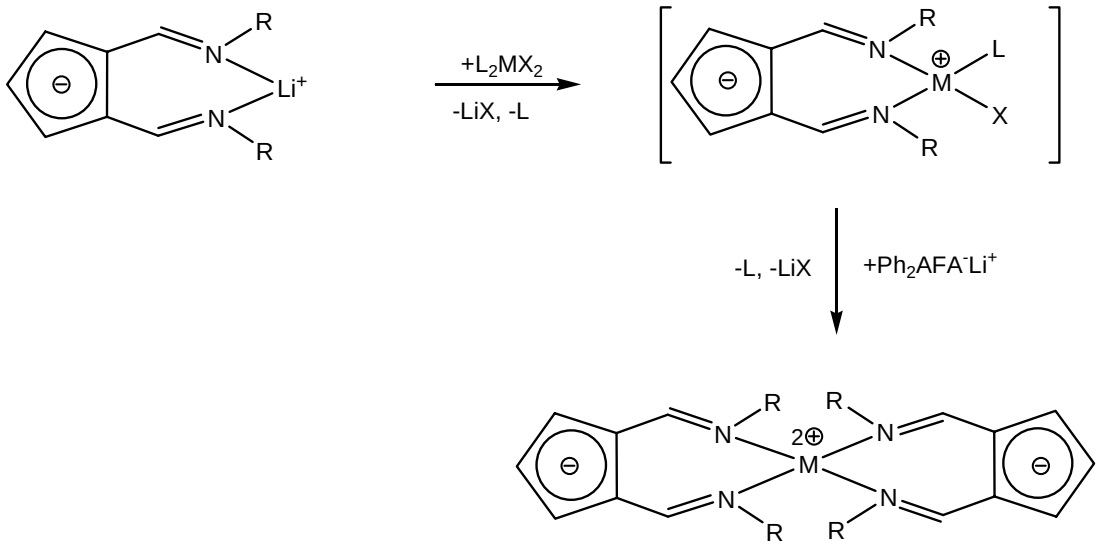

Scheme 4.11. Route to the formation of the bis-substituted metal complexes. If a mono-coordinated intermediate is hypothesised, its reactivity would be higher than the starting metal reactant.

Moreover, the formation of the thermodynamically stable LiX might be the driving force for the bis-ligation. To avoid this problem, another approach was to react the protonated ligand with an organometallic derivative. For example, addition of 1 equivalent of $ZnEt_2$ to a solution of the ligand should result in evolution of ethane upon reaction and possibly isolation of a mono-substituted-ZnEt species (Scheme 4.12).

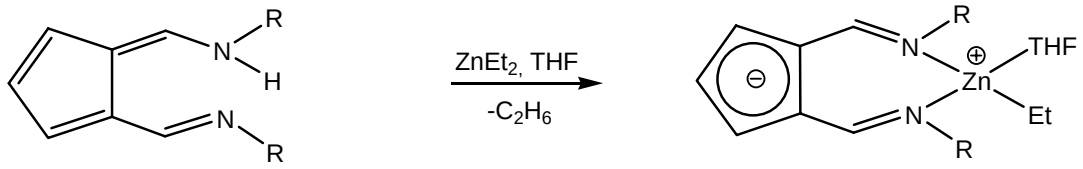

Scheme 4.12. Attempted reaction to the synthesis of a mono-substituted alkylzinc species.

This reaction was performed at different temperatures and in different solvent, but invariably only [Zn $(Ph_2AFA)_2$] was found as final product.

Use of a less reactive starting material such as $[(PPh_3)_2Ni(Ph)(Cl)]$ in combination with the presence of only one metal alkyl bond, should lead to the desired product with formation of benzene.

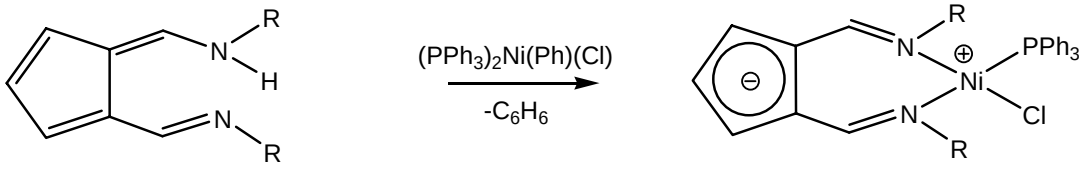

Scheme 4.13. Attempted synthesis of the mono-substituted nickel halide.

In this case, no reaction at all takes place and only free ligand was recovered.

In analogy, the palladium derivative $[(Py)_2Pd(CH_2Ph)_2]$ was reacted with one equivalent of the ligand, but the desired mono-substituted benzyl-palladium species was not formed (Scheme 4.14)

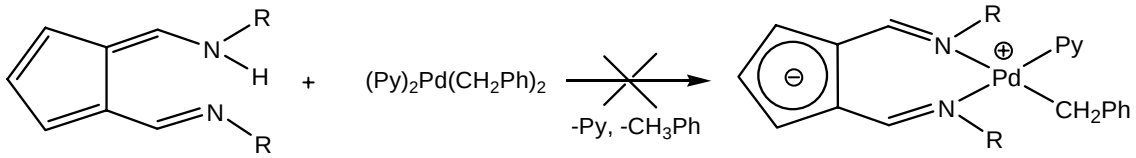

Scheme 4.14. Attempted route to the formation of the mono-substituted benzylpalladium complex.

A different attempted approach was to treat the ML_2 (L = Ph_2AFA, M = Zn, Ni, Pd) with one equivalent of diluted acid solutions, in order to remove one of the ligands by protonation as shown in Scheme 4.15.

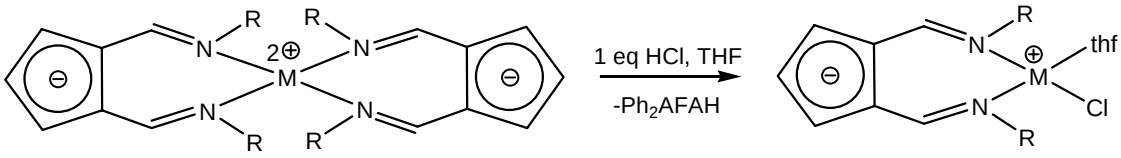

Scheme 4.15. Attempted reaction for the protonation of one of the ligands with one equivalent of diluted acid solution.

Again, this reaction only led to decomposition of the metal complex.

A successful strategy was found to be the reaction between the deprotonated ligand and alkyl-palladium precursors in presence of coordinating molecules. In this case, the alkyl group blocks the second coordination of the ligand, being R^-Li^+ a product not thermodynamically stable.

4.3.2. Synthesis and characterisation of [Ph_2AFAPd(Me)(PPh_3)]

The first complex was prepared by reaction of the deprotonated ligand with [(cod)Pd(CH_3)(Cl)]. The reaction path is shown in Scheme 4.16.

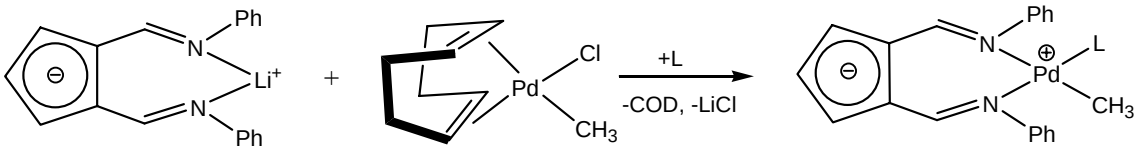

Scheme 4.16. A successful route to the formation of the desired mono-substituted palladium complex, featuring also the metal-alkyl bond.

Use of coordinating solvent such as THF, CH_3CN or PhCN to occupy the fourth coordination site turned out to be unsuccessful, leading to a mixture of species which could not be separated or easily characterised. NMR experiments on these products did show a possible coordination of the ligand, identifiable by the disappearance of the CH=N doublet to two distinct singlets, and an upfield shift of the Cp protons. The

presence of a singlet at negative ppm is also in agreement with the presence of a Pd-CH_3 bond. Despite these observations, such species proved to have a poor stability and slowly decomposed, so that any attempts to isolate single species to be tested for catalysis failed.

By using a more strongly coordinating molecule such as PPh_3, the formation of the stable and isolable complex [Ph_2AFAPd(Me)(PPh_3)] (**14**) was readily achieved. The reaction was performed in different solvents such as DCM, THF and toluene. Slow evaporation from toluene solutions afforded single crystals suitable for X-Ray analysis. The crystallographic structure of the complex is shown in Fig 4.16. The selected bond lengths and angles are shown in Table 4.1 and Table 4.2 respectively.

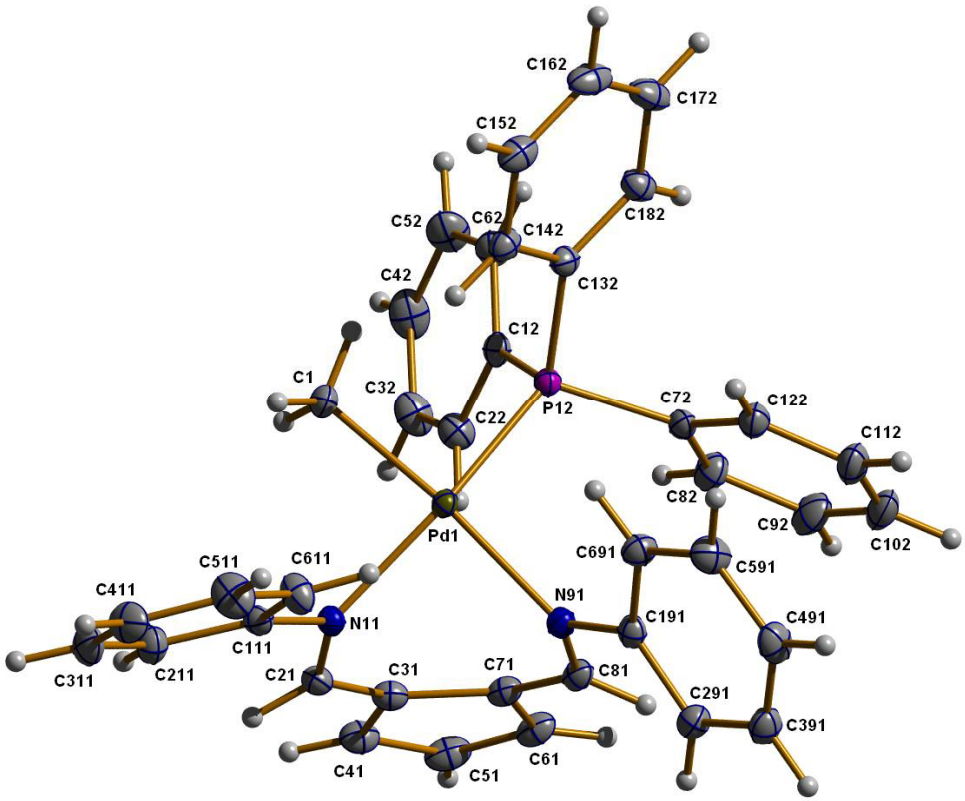

Figure 4.16. Molecular structure of [Ph_2AFAPd(CH_3)(PPh_3)].

Table 4.1. Selected bond lengths for [Ph_2AFAPd(CH_3)(PPh_3)].

Bond	*Bond length (Å)*	*Bond*	*Bond length (Å)*
Pd(1)-C(1)	2.0436(17)	C(71)-C(81)	1.405(3)
Pd(1)-N(11)	2.0945(15)	C(31)-C(71)	1.459(3)
Pd(1)-N(91)	2.1335(14)	C(21)-C(31)	1.424(2)
C(81)-N(91)	1.308(2)	C(31)-C(41)	1.406(3)
N(11)-C(21)	1.300(2)	C(41)-C(51)	1.399(3)
N(91)-C(191)	1.408(2)	C(61)-C(71)	1.419(2)
N(11)-C(111)	1.419(2)	C(51)-C(61)	1.383(3)

Table 4.2. Selected bond angles for [Ph_2AFAPd(CH_3)(PPh_3)].

Bond	*Bond angle (deg)*	*Bond*	*Bond angle (deg)*
N(11)-Pd(1)-N(91)	87.62(2)	N(11)-C(21)-C(31)	126.02(17)
C(1)-Pd(1)-N(11)	87.24(7)	C(21)-C(31)-C(71)	131.07(16)
C(1)-Pd(1)-P(12)	86.49(6)	C(31)-C(71)-C(81)	131.17(16)
P(12)-Pd(1)-N(91)	97.95(4)	C(71)-C(81)-N(91)	125.80(16)
C(21)-N(11)-Pd(1)	114.53(12)	Pd(1)-N(91)-C(191)	126.51(11)
C(81)-N(91)-Pd(1)	111.99(12)	Pd(1)-N(11)-C(111)	122.49(11)

The geometry of the palladium centre is almost square-planar, with the phosphine lying just 0.551 Å above the plane formed by the other three ligands as well as revealing to have the longest distance with the palladium centre (2.216 Å). The ligand itself is not planar, but greatly distorted, almost certainly due to the steric clash between the ligand Ph group and the PPh_3 ligand. These observations had already been encountered in the [(Ph_2AFA)$_2$Pd] complex previously discussed and from a ligand perspective the two compounds show many common features, even though interesting differences are present. The N-Pd-N angle has the value of 87.62Å, significantly smaller than in the bis-substituted palladium complex, whereas the Pd-N distances are longer, which presumably reflects the extreme distortion of the ligand coordination geometry forced by the bulk of the PPh_3 ligand. The Pd-N bond trans- to the methyl ligand [2.1335(14) Å] is substantially longer than that

trans- to the phosphine [2.0945(15) Å] reflecting the greater trans-influence of the alkyl. This longer bond is also that cis- to the PPh_3 ligand so steric effects may also make a contribution to this difference in Pd-N bond distances. The C-N bond lengths are 1.300(2) Å and 1.308(2) Å and therefore a large double bond character can be assumed. With the exception of the C(1)-C(2) length, all the C-C distances in the cyclopentadienyl ring are approximately half way between the usual single and double bond values, suggesting an electron delocalization in the C_5 ring system. This indicates some grade of aromaticity of the Cp moiety since the ligand is anionic. The two aromatic groups on the nitrogen atoms are tilted towards different direction in order to minimize the interaction between the two hydrogen atoms in the ortho position.

The NMR data of **14** also give interesting information. Upon coordination of the ligand onto the metal centre, the original doublet coming from the two HC=N protons which were coupling to the NH proton in the free ligand, split into two different signals with quite different chemical shift (δ = 8.53 and δ = 8.00 ppm) as expected. More interestingly, the more downfield signal is split into a doublet with coupling constant J = 8.34 Hz. This observation is consistent with a large coupling of the imino CH proton with the phosphorus of the PPh_3 ligand, as also confirmed by H-P correlated NMR experiments. Most likely, the presence of the phosphorus nucleus exerts a trans effect on the nitrogen atom, which is reflected into the large splitting of the HC=N proton. The other HC=N proton is not affected and is found as a singlet. Coupling with the phosphorus is also observed for the methyl group which appears at -0.06 ppm and is split into a doublet with coupling constant J = 3.65 Hz. The smaller value of this latter coupling constant is rationalized by its cis position relative to the phosphine. Other interesting information is the upfield shift of the C_5-ring protons, which can be expected if considering a negative charge delocalized on the cyclopentadienyl system.

4.3.3. Synthesis and characterisation of [Ph'$_2$AFAPd(η^3-C_3H_5)] (Ph'= 2,4,6-trimethylphenyl-)

Driven by the observation that introducing steric bulk on the nitrogen atoms results in an enhancement of the catalyst activity, another potential catalyst featuring methyl substituents on the ortho and para positions of the phenyl rings was prepared. The complex [Ph'$_2$AFAPd(η^3-C_3H_5)] (**13**) was prepared by reacting the deprotonated ligand and half equivalent of [(η^3-C_3H_5)PdCl]$_2$ in toluene.

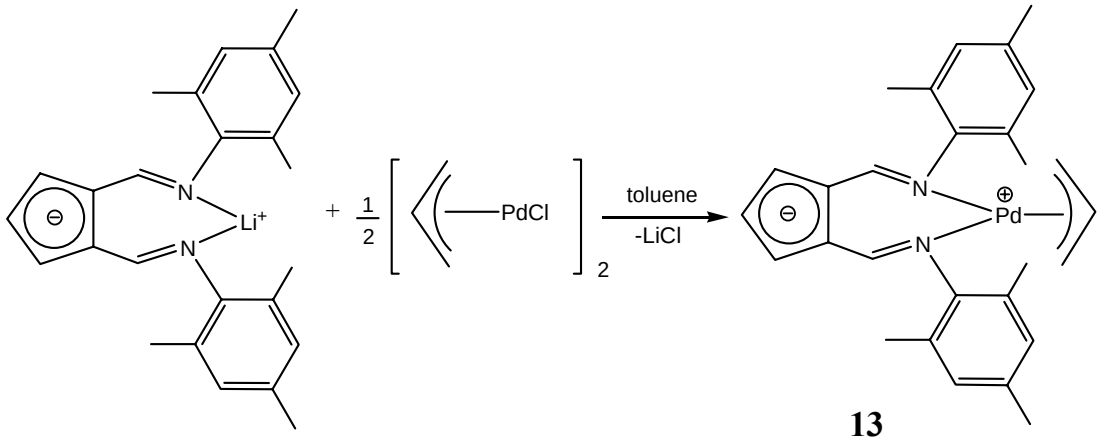

13

Scheme 4.17. Reaction leading to the allylpalladium complex.

The product is light- and air-stable and it is obtained in good yields. Single crystals of the desired product were obtained by slow evaporation of the solvent from hexane solutions, allowing X-ray analysis. The complex shows a square planar geometry and, very interestingly, in this case the ligand does not undergo any remarkable distortion, with the aminofulvene moiety remaining substantially planar. Selected bond lengths and angles are reported in Tables 4.3 and 4.4 respectively.

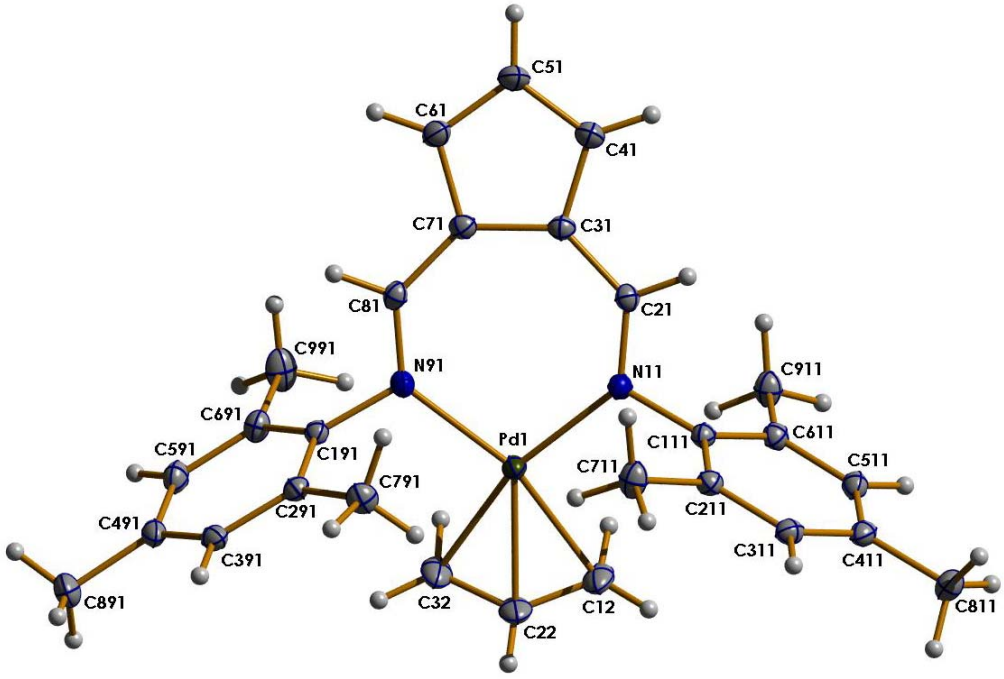

Figure 4.17. Molecular crystal structure of [Ph'$_2$AFAPd(η^3-C_3H_5)].

Table 4.3. Selected bond lengths for [Ph'$_2$AFAPd(η^3-C_3H_5)].

Bond	*Bond length (Å)*	*Bond*	*Bond length (Å)*
Pd(1)-C(12)	2.129(2)	N(11)-C(21)	1.305(2)
Pd(1)-C(22)	2.147(4)	C(21)-C(31)	1.411(3)
Pd(1)-C(32)	2.154(2)	C(31)-C(71)	1.445(2)
Pd(1)-N(11)	2.1009(14)	C(71)-C(81)	1.409(2)
Pd(1)-N(91)	2.0968(15)	C(81)-N(91)	1.299(2)
C(12)-C(22)	1.402(5)	C(41)-C(51)	1.387(3)
C(22)-C(32)	1.324(5)	C(51)-C(61)	1.390(3)
C(31)-C(41)	1.416(2)	C(61)-C(71)	1.412(3)
N(11)-C(111)	1.442(2)	N(91)-C(191)	1.441(2)

Table 4.4. Selected bond angles for [Ph'$_2$AFAPd(η^3-C_3H_5)].

Bond	*Bond angle (deg)*	*Bond*	*Bond angle (deg)*
N(11)-Pd(1)-N(91)	99.04(6)	C(21)-C(31)-C(71)	133.84(16)
C(12)-Pd(1)-C(32)	68.03(9)	C(31)-C(71)-C(61)	106.37(16)
C(12)-Pd(1)-N(11)	96.49(7)	C(71)-C(81)-N(91)	130.75(17)
C(32)-Pd(1)-N(91)	96.54(7)	C(81)-N(91)-Pd(1)	131.49(12)
N(11)-C(21)-C(31)	131.21(16)	C(12)-C(22)-C(32)	123.0(4)

The two mesityl groups are almost perfectly axial to the square plane, whereas the palladium centres lies slightly above the ligand plane; the angle between the ligand pseudo-plane and the metal square plane is 22.58˚. This lack of distortion in comparison with the three previously discussed palladium complexes **9**, **11** and **14** is reflected in the considerably larger N-Pd-N angle (99.04˚), and can be rationalized in terms of the bulkier mesityl groups which limit the distortion. Never-the-less, the N-Pd distances are 2.0968(15) and 2.1009(14) Å, values comparable with the ones found in **14**, although the difference between them is significantly less, as well as no dramatic changes have occurred in the C=N bonds (1.305(2) and 1.299(2) Å) which can still be regarded as somewhere in between double and single bonds. The C-C distances in the C_5-ring have remained unaltered, with the exception of the C(31)-C(71) bond which is shorter (1.445(2) Å).

As in all the other complexes prepared, NMR experiments show a shift to high fields of the Cp protons upon coordination of the ligand. The doublet appearing in the free ligand at 7.96 ppm due to the coupling of the two *H*-CN with the N-*H* proton turns into a singlet as expected from the coordination of the anionic form of the ligand. Spectra recorded in CD_2Cl_2 suggest that in solution the allyl ligand retains the η^3 coordination: two different doublets with coupling constants of 12.40 and 6.49 Hz for the protons in endo and exo position relative to the metal centre are found at 2.42 and 2.20 ppm. In agreement, the proton on the central carbon of the allyl moiety appears as triplet of triplets with the same coupling constants. The use of a coordinating solvent such as CD_3CN or d_6-DMSO does not seem to affect the behaviour in solution of the complex.

4.3.4. Synthesis and characterisation of [Ph'$_2$AFAPd(Me)(Py)].

Several attempts were made at the synthesis of analogous complexes of [Ph_2AFAPd(CH_3)(PPh_3)] with the di-(2,4,6-trimethyl)phenyl-6-aminofulvene-2-aldiminate ligand (Ph'$_2$AFA). Surprisingly, reaction of Ph'$_2$AFA$^-$Li$^+$ with [(cod)Pd(Me)(Cl)] in presence of triphenylphosphine did not result in the formation of [Ph'$_2$AFAPd(CH_3)(PPh_3)] and only the starting materials were recovered. Most likely, the presence of the three methyl groups on the aryl ring brings additional bulk which is preventing the large phosphine from coordinating. On the other hand, as for the diphenyl-substituted ligand, carrying out the same reaction at room temperature in coordinating solvents such as CH_3CN and PhCN, a mixture of species was obtained. Coordination of the ligand is observed via NMR, where the upfield shifts of the C_5-ring protons, the change of the doublet of the *H*C-N protons into two distinct singlets and the presence of a singlet at -0.45 ppm attributable to the Pd-CH_3 bond, support the formation of the desired product (Scheme 4.18).

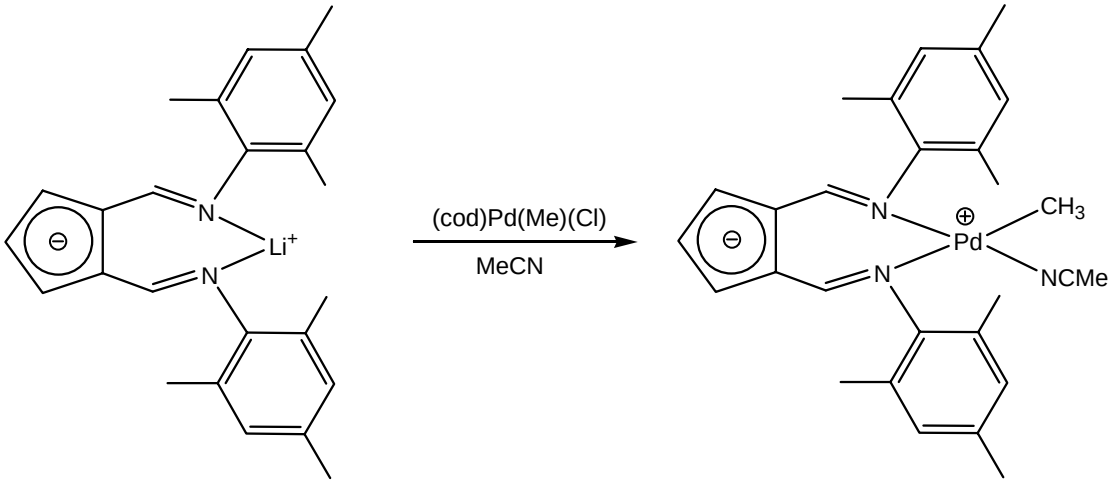

Scheme 4.18. Reaction leading to the Ph'$_2$AFAPd(Me)(MeCN). Isolation of the product was not achieved.

However, the above reaction never went to completion and together with the main product, free ligand was always found. Isolation of one single species was not achieved, and the main product could not be fully characterised. After storing

solutions of the mixture at temperature as low as -10˚C, gradual decomposition of the product was observed, with release of free ligand.

A more encouraging result was obtained by performing the reaction in toluene and using a more coordinating molecule like pyridine. Analysis of the crude product by ^{1}H-NMR gives strong evidence for the formation of desired [Ph'$_2$AFAPd(CH$_3$)(Py)] (**17**) as main product (Scheme 4.19), with no free ligand present.

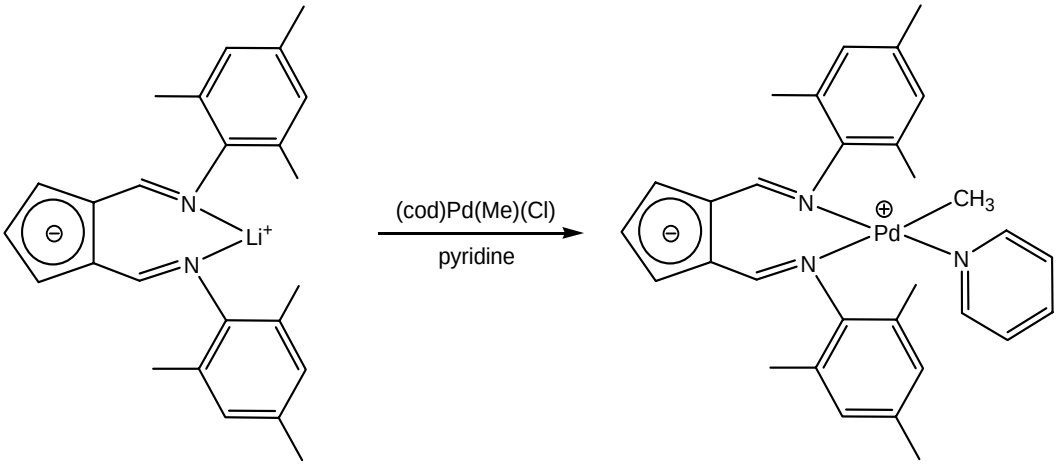

Scheme 4.19. Reaction leading to the [Ph'$_2$AFAPd(Me)(Py)]. ^{1}H NMR shows the formation of the desired complex as main product.

The Pd-CH$_3$ bond appears as a singlet at -0.29 ppm, whereas a shift towards higher fields for the pyridine ring is found. The signals coming from the ligand are consistent with a chelation around the palladium centre: the Cp protons are shifted upfield (6.31 and 6.51 ppm) and the HC=N protons appears as two singlets at 6.97 and 7.94 ppm. The spectrum also shows the coordinated pyridine.

The product shows fair stability, even though ^{1}H NMR shows a gradual dissociation of the pyridine upon standing at room temperature.

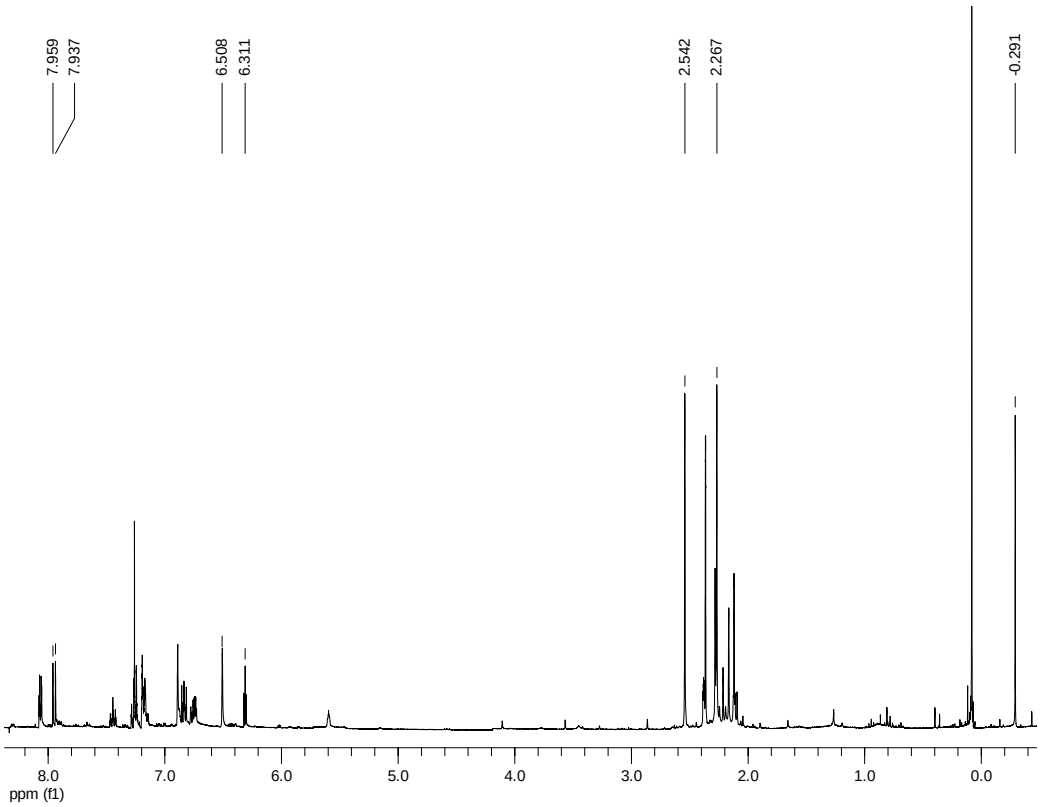

Figure 4.18. ^{1}H NMR of the crude product Ph'$_2$AFAPd(Me)(Py).

Formation of the desired product is also supported by MS. Peaks for M^+ are found at 556.03. The same peak pattern is found at 476.9, consistent with the loss of the pyridine ligand to form $[(Ph'_2AFA)Pd(Me)]^+$.

4.4 Polymerisation tests

Tests of ethylene polymerisation with the pre-catalyst $[(Ph_2AFA)Pd(Me)(PPh_3)]$ were carried out at different temperatures in an autoclave at a pressure of 7 atm. The autoclave was charged with an equimolar ratio of the catalyst and $Ni(cod)_2$ was used as phosphine scavenger in toluene. The mechanism hypothesised for eventual formation of polymer should follow the traditional Cossee polyinsertion, with formation of branching deriving from the chain walking process.

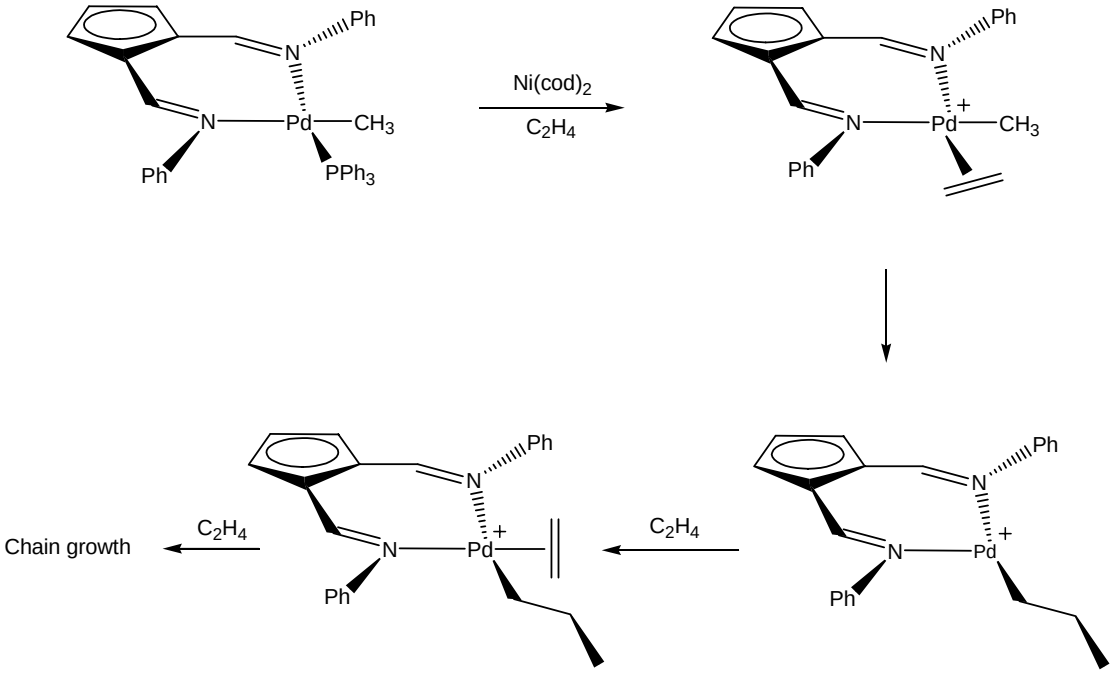

Scheme 4.20. Mechanism of polymerisation by the catalyst [(Ph_2AFA)Pd(Me)(PPh_3)]. The use of [$Ni(cod)_2$] should facilitate the displacement of PPh_3 by the monomer.

The methyl complex showed no reactivity towards ethylene in toluene solution, however this is not unexpected given the coordinative saturation of the complex provided by the PPh_3 ligand. For neutral nickel(II)-based ethylene polymerization catalysts, [$(cod)_2$Ni] has been used as an effective phosphine scavenger,[44] and the addition of 2 molar equivalents of this complex to a solution of catalyst in toluene solution provided a system which showed some reactivity towards ethylene. Under the same reaction conditions [$(cod)_2$Ni] showed no reactivity towards ethylene. An EI mass spectrum of the crude mother liquor obtained after 6 h showed the presence of a distribution of oligomers up to a mass of 617 (44 atoms of C). Together with the oligomers, traces of insoluble polymer were also produced. GPC-viscosity analysis of such polymer showed a value of the polydispersity index of *ca.* 17 (M_n = 8400, M_w = 140000), which is rather large if compared with the typical 3-4 values for polymers obtained by using [(diimine)PdR]+ catalysts.[25] However, the molecular weight distribution is monomodal, suggesting that the large value of the polydispersity index is not due to the presence of different catalytic active sites.

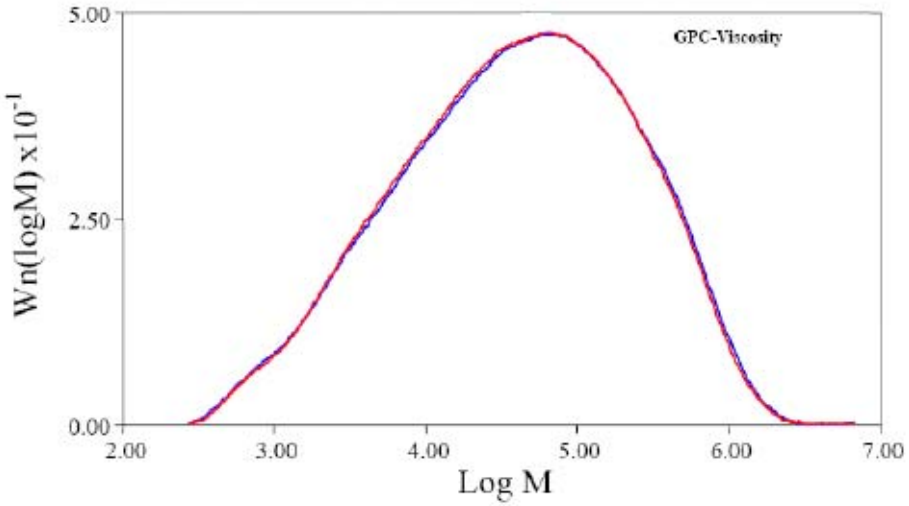

Figure 4.19. Molecular weight distribution of the polyethylene produced by 14/[Ni(cod)$_2$] as determined by GPC-viscosity measurement. Two duplicate runs are shown.

In Fig. 4.20, the intrinsic viscosity plots of the polymer (SRL 8891) are compared with those of known linear and branched polyethylenes, indicating that the polymer is largely linear, with a very low content of branching.

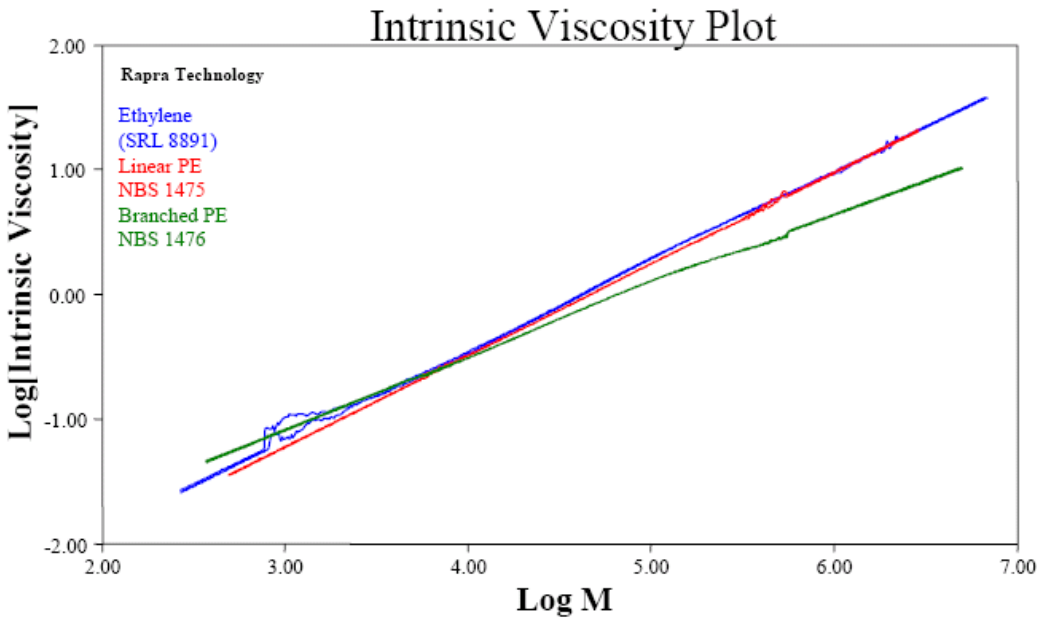

Figure 4.20. Intrinsic viscosity plot of the polyethylene produced by the [Ph$_2$AFAPd(Me)(PPh$_3$)] catalysts, compared with known linear and branched polyethylenes.

This is supported by the ^{13}C NMR spectra of the crude polymer, where in addition to the main peak at 30.0 ppm due to the polymethylene sequence, minor resonances at 37.6, 34.6, 33.3, 27.5 and 20.3 ppm which, indicating the formation of some branching during the course of the reaction (Fig 4.21). On the basis of published analyses of branched polyethylene ^{13}C NMR spectra,[45] these signals are assigned according to the scheme shown in Figure 18. Nomenclature used in this work is that of Usami and Takayama for isolated branches.[46]

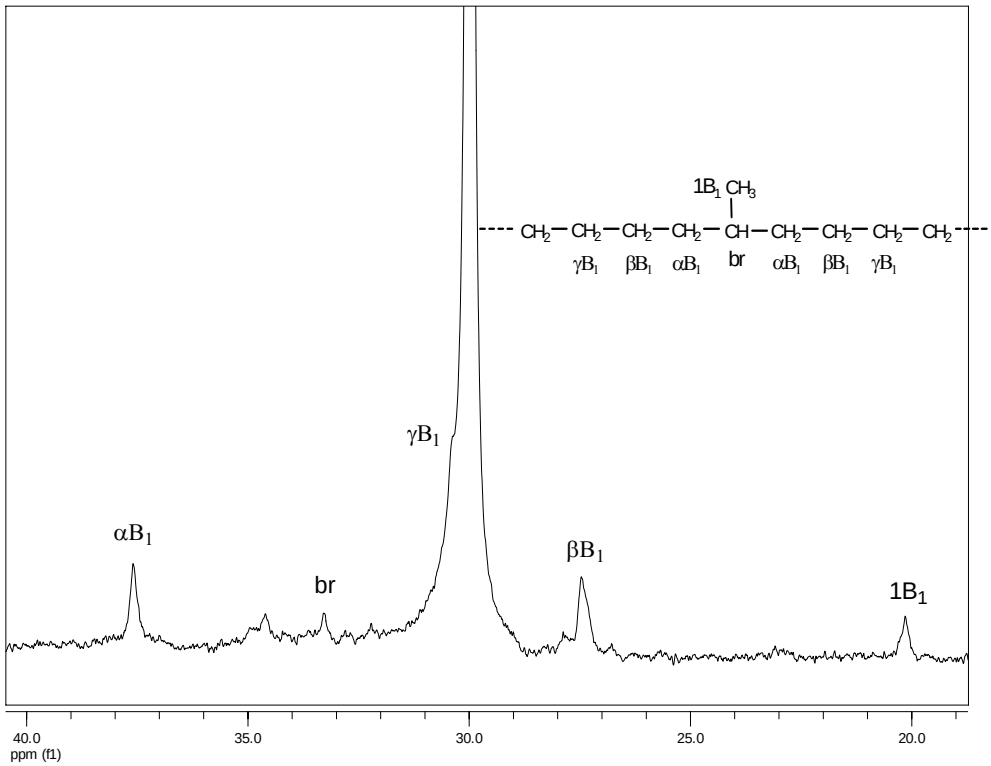

Figure 4.21. $^{13}C\{^1H\}$ NMR spectrum ($C_2D_2Cl_4$, 120 °C, δ in ppm from TMS) of a polyethylene produced by [Ph_2AFAPd(Me)(PPh_3)]/[Ni(cod)$_2$] at room temperature in toluene.

The spectrum is consistent with a predominant formation of methyl branches, with the αB_1 and βB_1 carbon resonances appearing at 37.5 and 27.4 ppm respectively, where the branch point and the methyl group are found respectively at 33.2 and 19.9 ppm. However, due to the low intensities and broadness of the peaks, it can not be ruled out that propyl branch formation is also occurring. This is suggested by the presence of an additional, albeit very small, resonance peak at 34.5 ppm, attributable to the methylene carbon in the α-position of a propyl group. The formation of such branches in the polymer chain may be attributed to the "chain-walking" process

known to occur in polymerisations catalysed by $[(diimine)MR]^+$ catalysts (M = Ni, Pd) (Scheme 4.3).[28] Such a result, however, is not in agreement with the traditional Brookhart's cationic palladium catalysts, which typically produce polyethylene with a much larger number of branches.[26] This suggests a very low rate of chain walking in the $[Ph_2AFAPd(Me)(PPh_3)]$ system, attributable to the reduced electrophilicity (Lewis acidity) of the active species derived from $[Ph_2AFAPd(Me)(PPh_3)]$ compared with the cationic α-diimine ligated catalysts. As a consequence, the β-agostic interaction, shown in Scheme 4.21 (intermediate **I**) becomes weaker, thus retarding the formation of the unsaturated polymer-hydride complex **L**.

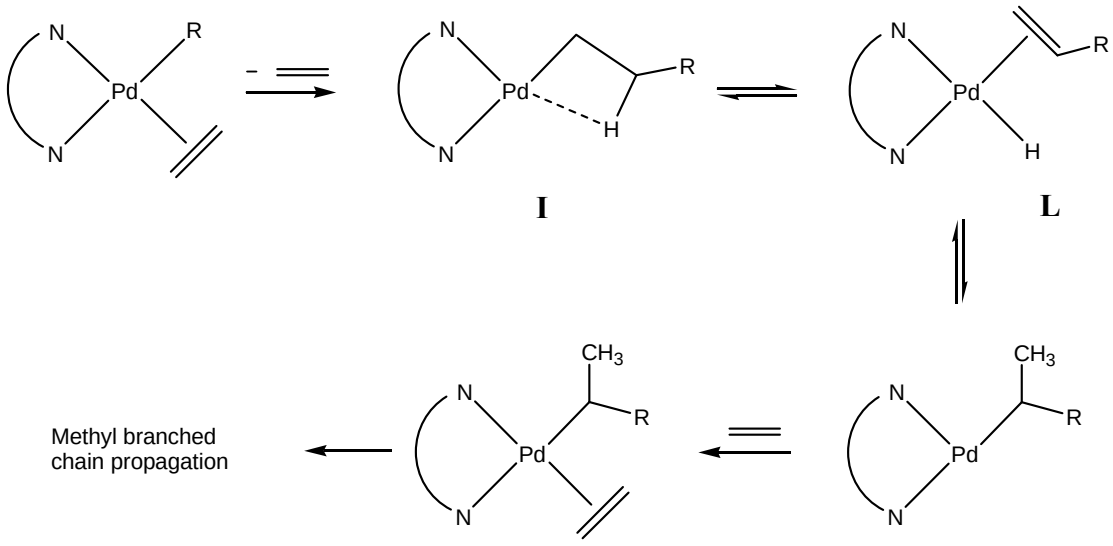

Scheme 4.21. Chain-walking mechanism of methyl branch formation.

The low activity of the system must probably be related to the lack of steric shielding of the axial site, which is the key feature in the Brookhart-type polymerization catalysts. The fact that any polymer is produced seems to indicate a low rate of chain transfer relative to migratory insertion. Whilst this low rate of chain transfer in the catalyst cannot be attributed to steric shielding of the axial sites, it may be attributed to the reduced Lewis acidity of the Pd center compared with the cationic catalysts containing the neutral α-diimine ligands. This will reduce the rate of formation of the 5-coordinate transition state in the associative displacement of unsaturated polymer chain from an olefin-hydride intermediate thought to be responsible for chain transfer (Scheme 4.4).

A number of other factors, such as the absence of charge and the intrinsically higher barriers to insertion in Pd based catalysts in comparison to nickel catalysts would also seem to account for the low activity of this system.

However, it cannot be ruled out that imperfect scavenging of the phosphine by $[Ni(cod)_2]$ results in a high proportion of the catalyst remaining inactive in the form of complex $[Ph_2AFAPd(Me)(PPh_3)]$. Although the $[Ni(cod)_2]$ has proved to be a very effective phosphine scavenger for neutral nickel(II) systems, it has never been utilized for Pd(II) systems. On the basis of the equilibrium shown in Fig, the stronger coordination of PPh_3 by Pd than by Ni would result in a shift towards the left side of the reaction, thus providing a lower concentration of the phosphine-free Pd active species when compared with neutral Ni(II) systems.

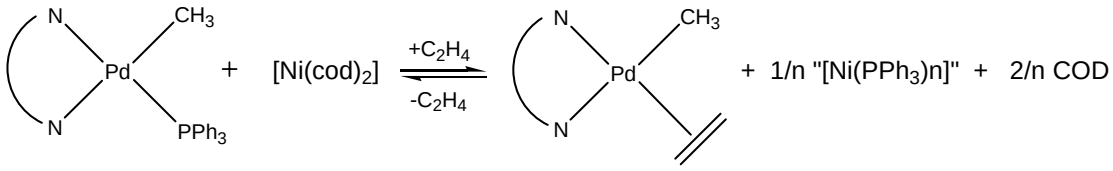

Equation 1

Never-the-less, the formation of any polyethylene by a neutral Pd(II) is unprecedented. Examples of neutral palladium catalysts active in methyl acrylate,[47] norbornene[48] and styrene[49], but none of these catalysts were active in ethylene homopolymerisation.

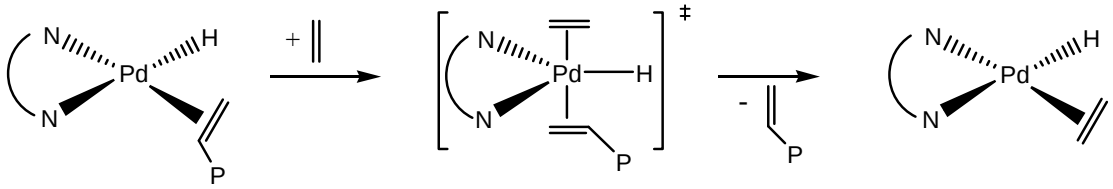

Scheme 4.22. Associative displacement of polymer chain by ethylene monomer (chain transfer).

Tests of polymerisation were also conducted for the complex $(Ph'_2AFA)Pd(\eta^3\text{-}C_3H_5)$ under the same conditions of temperature and pressure. In this case the system is a single component since no use of phosphine scavenger was needed. The mechanism

should be much alike the one above discussed, with the difference that in this case the substituted-phenyl groups introduce more bulk, whereas the AFA molecule, as found in the crystal structure, should remain mainly planar.

After 36 h, no polymer was formed, as well as no oligomers were present in the mother liquors. This total absence of catalysis might be related to the high stability of the Pd-allyl bond, which is most likely not prone to undergo any insertion.

Some preliminary studies of CO insertion into the Pd-alkyl bond were made. Saturating toluene solutions of both complexes with an atmosphere of carbon monoxide results in both cases in a slow decomposition, with release of free ligand and formation of metallic palladium.

A preliminary catalytic study on the not completely characterised [Ph'$_2$AFAPd(Me)(Py)] was conducted for 1-hexene polymerisation. The complex was dissolved in toluene and added to 30 ml of 1-hexene with stirring. However, after 12 h, no polymer was formed at all. Investigation of ethylene polymerisation catalysis has not been carried out yet.

4.5 Future Work

The preliminary studies on polymerisation catalysis have indicated that the use of zwitterionic systems based on 6-aminofulvene-2-aldiminate ligands can potentially open the door to a new class of catalysts for polymerisation. More investigation will have to be carried out to find the best conditions for good performances of such catalysts. Reaching high catalytic activities might also involve modification of the original ligand system. A sensible modification would be the introduction of bulkier substituents on the nitrogen atoms. Although the synthesis of systems with more hindering nitrogen substituents has unsuccessfully been attempted during this project, other synthetic strategies might be devised and therefore more investigation needs to be carried out.

Other changes could be made to the ligand backbone. In this regard, for example, the cyclopentadienyl moiety is a potential site for modifications, such as the introduction of more electron withdrawing groups.

Co-polymerisation of ethylene with higher α-olefins as well as with other polar monomers such as CO and methacrylates have not been thoroughly explored and might be a very fruitful field for future catalysis.

Investigation of the reactivity of the ligand system with early transition metal centres also constitutes a worthwhile subject in view of the higher catalytic activities of these metal centres towards olefin polymerisation.

1. K. Ziegler , E. Hlozkamp, H. Breil, H. Martin, *Angew. Chem.* **1995**, *67*, 541.
2. G. Natta, *Angew. Chem.* **1956**, *68*, 393
3. P. Cosse, *Tetrahedron Letters* **1960**, *12*, 17; P. Cossee, *J. Catal*. **1964**, *3*, 80; A. Zambelli, G. Gatti, C. Sacchi, W. O. Crain, *Macromolecules* **1971**, *4*, 475.
4. C. Elschenbroich, A. Salzer, *Organometallics* **1989**, *423*, VCH publishers.
5. G. J. P. Britovsek, V. C. Gibson, D.F. Wass, *Angew. Chem. Int. Ed.* **1999**, *38*, 428; T. Risse, J. Schmidt, H. Hamann, H-J. Freund, *Angew. Chem. Int. Ed.* **2002**, *41*, 1517; W. Kaminsky, *Stud. Surf. Sci. Catal*. **1999**, *121*, 3; M. Bochmann, *Top. Catal.* **1999**, *7* (1-4), 97.
6. G. Wilkinson, P. L. Pauson, J. M. Birmingham, F.A. Cotton, *J. Am. Chem. Soc.* **1953**, *75*, 1011.
7. J. P. Britovsek, V. C. Gibson, D. F. Wass, *Angew. Chem. Int. Ed.* **1999**, *38*, 428.
8. M. Brookhart, B. Grant, A.F. Volpe, *Organometallics* **1992**, *11*, 3920.
9. J. C. W. Chien, W.-M. Tsai, M. D. Rausch, *J. Am. Chem. Soc.* **1991**, *113*, 8570.
10. A. D. Horton, J. de With, *Organometallics* **1997**, *16*, 5424; A. D. Horton, J. de With, A. J. van der Linden, H. van de Weg, *Organometallics* **1996**, *15*, 2672.
11. H. Nishida, N. Takada, M. Yoshimura, T. Sonoda, H. Kobayashi, *Bull. Chem. Soc., Jpn.* **1984**, *57*, 2600.
12. X. Yang, C. L. Stern, T. J. Marks, *J. Am. Chem. Soc.* **1994**, *116*, 10015; X. Yang, C. L. Stern, T. J. Marks, *J. Am. Chem. Soc.* **1991**, *113*, 3623.
13. I. A. Guzei, R. A. Stockland Jr., R. F. Jordan, *Acta Cryst.* **2000**, *C56*, 635.
14. K. H. Reichert, K.R. Meyer, *Makromol. Chem.* **1973**, *169*, 163.

15. H. Sinn, W. Kaminsky, *Adv. Organomet. Chem.* **1980**, *18*, 99; A. Andresen, H. G. Cordes, J. Herwig, K. Kaminsky, A. Merck, R. Mottweiler, J. Pein, H. Sinn, H. J. Vollmer, *Angew. Chem.* **1976**, *88*, 689; A. Andresen, H.G. Cordes, J. Herwig, K. Kaminsky, A. Merk, R. Mottweiler, J. Pein, H. Sinn, H. J. Vollmer, *Angew. Chem. Int. Ed. Engl.* **1976**, *15*, 630; W. Kaminsky, R. Steiger, *Polyhedron* **1988**, *7*, 2375.
16. A. H. Trullo, *Chem. Eng. News* **2001**, *43*, 38.
17. E. Y.-X. Chen, T. J. Marks, *Chem Rev.* **2000**, *100*, 1391; W. E. Piers, T. Chivers, *Chem. Soc. Rev.* **1997**, *26*, 345.
18. S. J. McLain, E. F. McCord, S. D. Arthur, E. Hauptman, J. Feldman, W. A. Nugent, L. K. Johnson, S. Mecking, M. Brookhart, *Polym. Mater. Sci. Eng.* **1997**, *76*, 246.
19. P.W. Glockner, W. Keim, R. F. Mason, U. S. Patent 3.647.914 Shell Oil Co. **1971** [Chem Abstr. 1971, 75, 88072g].
20. W. Keim, F. H. Kowaldt, R. Goddard, C. Krüger, *Angew. Chem. Int. Ed. Engl.* **1978**, *17*, 466.
21. U. Klabunde, S. D. Ittel, *J. Mol. Catal.* **1987**, *41*, 203; U. Klabunde, R. Mülhaupt, T. Herskovitz, A. H. Janowicz, J. Calabrese, S. D. Ittel, *J. Poly. Sci.* **1987**, 1989.
22. T. R. Younkin, E. F. Connor, J. I. Henderson, S. K. Friedrich, R. H. Grubbs, D. A. Bansleben, *Science* **2000**, *287*, 460.
23. M. A. Zuideveld, P. Wehrmann, C. Röhr, S. Mecking, *Angew. Chem. Int.Ed.* **2004**, *43*, 869.
24. J. Heinicke, N. Peulecke, M. Köhler, M. He, W. Keim, *J. Organomet. Chem.* **2005**, *690*, 2449.
25. L. K. Johnson, C. M. Killian, M. Brookhart, *J. Am. Chem. Soc.* **1995**, *117*, 6414.
26. M. Brookhart, S. D. Ittel, L. K. Johnson, *Chem. Rev.* **2000**, *100*, 1169.
27. R. L. Huff, D. J. Tempel, M. Brookhart, *Book of Abstracts,218th ACS National Meeting,* New Orleans, Aug 22-26, 1999, INOR-139; S. A. Svejda, L. K. Johnson, M. Brookhart, *J. Am. Chem. Soc.* **1999**, *121*, 10634.
28. D. J. Tempel, M. Brookhart, *Organometallics* **1998**, *17*, 2290; L. H. Shultz, D. J. Tempel, M. Brookhart, *J. Am. Chem. Soc.* **2001**, *123*, 11539.
29. D. G. Musaev, R. D. J. Froese, K. Morokuma, *Organometallics*, **1998**, *17*(9), 1850.
30. L. Deng, P. M. Margl, T. Ziegler, *J. Am .Chem. Soc.* **1997,** *119*, 1094.
31. L. Deng, T. K. Woo, L. Cavallo, P. M. Margl, T. Ziegler, *J. Am. Chem. Soc.* **1997**, *119*, 6177; R. D. J. Froese, D. G. Musaev, K. Morokuma, *J. Am. Chem. Soc.* **1998**, *120*, 1581.
32. C. Popeney, Z. Guan, *Organometallics*, **2005**, *24*, 1145.
33. V. C. Gibson, A. Tomov, D. F. Wass, A. J. P. White, D. J. Williams, *J. Chem. Soc.*, *Dalton Trans.*, **2002**, 2261.
34. B. Temme, G. Erker, J. Karl, H. Luftmann, R. Fröhlich, S. Kotila, *Angew. Chem. Int. Ed. Engl.* **1995**, *107*, 1755.
35. D. D. Devore, F. J. Timmers, D. L. Hasha, R. K. Rosen, T. J. Marks, P.A. Deck, C. L. Stern, *J. Am. Chem. Soc.* **1995**, *14*, 3132.

36. Y. Sun, W. E. Piers, S. J. Rettig, *Chem. Commun.* **1998**, 127.
37. R. E. Von H. Spence, W. E. Piers, *Organometallics* **1995**, *14*, 4617.
38. J. Karl, G. Erker, R. Fröhlich, *J. Am. Chem. Soc.* **1997**, *119*, 1116.
39. M. Bochmann, S. J. Lancaster, O. B. Robinson, *J. Chem. Soc. Chem Commun.* **1995**, 2081.
40. J. W. Strauch, G. Erker, G. Kehr, R. Fröhlich, *Angew. Chem. Int Ed.* **2002**, *41*, 14.
41. T. M. Kooistra, Q. Knijnenburg, J. M. M. Smits, A. D. Horton, P. H. M. Budzelaar, A. W. Gal, *Angew. Chem.* **2001**, *113*, 4855; *Angew. Chem. Int. Ed.* **2001**, *40*, 4719; V. C. Gibson, M. J. Humphries, K. P. Tellmann, D. F. Wass, A. J. P. White, D. J. Williams, *Chem. Commun.* **2001**, 2252.
42. Z. J. A. Komon, X. Bu, G. C. Bazan, *J. Am. Chem. Soc.* **2000**, *122*, 1830.
43. C. T. Burns, D. S. Stelck, P. J. Shapiro, V. Ashwani, K. Kunz, G. Kehr, T. Concolino, A. L. Rheingold, *Organometallics* **1999**, *18*, 5432; S. J. Lancaster, M. Bochmann, *Organometallics* **2001**, *20*, 2093, for a review see S. Aldridge, C. Bresner, *Coord. Chem. Rev.* **2003**, *244*, 71.
44. C. Wang, S. Friedrich, T. R. Younkin, R. T. Li, R. H. Grubbs, D. A. Bansleben, M. W. Day, *Organometallics* **1998**, *17*, 3149; U. Klabunde, S. D. Ittel, *J. Mol. Catal.* **1987**, *41*, 23; U. Klabunde, R. Mulhaupt, T. Herskovitz, A. H. Janowicz, J. Calabrese, S. D. Ittel, *J. Polym. Sci., Part A: Polym. Chem.* **1987**, *25*, 1989.
45. G. B. Galland, R. F. De Souza, R. S. Mauler, F. F. Nunes, *Macromolecules* **1999**, *32*, 1620.
46. T. Usami, S. Takayama, *Macromolecules* **1984**, *17*, 1756.
47. G. Tian, H. W. Boone, B. M. Novak, *Macromolecules* **2001**, *34*, 7656.
48. B. M. Novak, A. L. Safir, Polymer Preprints *(American Chemical Society, Division of Polymer Chemistry)* **1996**, *37*, 335.
49. H. Sun, Q. Shen, M. Yang, *European PolymerJjournal* **2002**, *38*, 2045.

Chapter 5

Experimental section

5.1 General procedures

All reactions and manipulations of moisture- and air-sensitive compounds were carried out in an atmosphere of dry nitrogen using Schlenk techniques or in a conventional nitrogen-filled GloveBox (Saffron Scientific), fitted with oxygen and water scavenging columns. All the solvents were purified and dried by means of distillation over an appropriate drying agent prior to use. Toluene, THF, diethyl ether, hexane, benzene were all distilled from Na/benzophenone under a nitrogen atmosphere. NMR solvents were degassed using freeze-thaw cycles and stored over 4Å molecular sieves. Column chromatography was performed on silica gel (Merck 60, 7-120 mesh).

All solvents and reagents were purchased from Sigma-Aldrich, Fischer or Acros and used as received unless otherwise stated.

5.2 Instrumentation

NMR spectra were recorded on a Brucher AC 250 MHz and 360 MHz spectrometers operating at room temperature. ^{1}H and ^{13}C chemical shifts are reported in ppm relative to $Si(CH_3)_4$ (δ=0) and were referred internally with respect to the protio solvent impurity or ^{13}C resonances respectively. Elemental analyses were performed using a Perkin-Elmer 2400 CHN Analyzer. Infrared spectra were obtained using a Perkin-Elmer 1600 Paragon Series FT-IR spectrometer as liquid thin films. Electron impact (EI) mass spectra were obtained either on a Finnigan MAT 4600 quadrupole

spectrometer or on a Kratos MS50TC spectrometer. Fast atom bombardment (FAB) mass spectra were obtained on a MS50TC spectrometer.

GPC analyses for the molecular weight distribution of polymers were obtained at Rapra Technologies, on a Polymer Laboratories GPC220, using a PLgel guard plus 2 x mix bed-B 30cm, 10μm column and a refractive index dectector (& Viskotec differential pressure. The solvent was 1,2,4-trichlorobenzene and the flow rate 1.0 ml/min.

5.3 General procedure for sample preparation for GPC analysis (Rapra Technologies)

A single solution of the sample was prepared by pipetting 15 ml of solvent to 15 mg of sample and heating at 190˚C for 60 min with shaking to dissolve. The sample solution was then filtered through 2 μm metal sinter into glass sample vials. The vials were placed in a heated autosampler compartment and after an initial delay of thirty minutes to allow the samples to equilibrate thermally, injection of part of the content of each vial was carried out automatically.

5.4 Labelling for compounds 6, 8, 9, 10, 11, 13, 14, 15.

The labelling of all protons and carbons for the NMR characterization are referred as shown in the figure below:

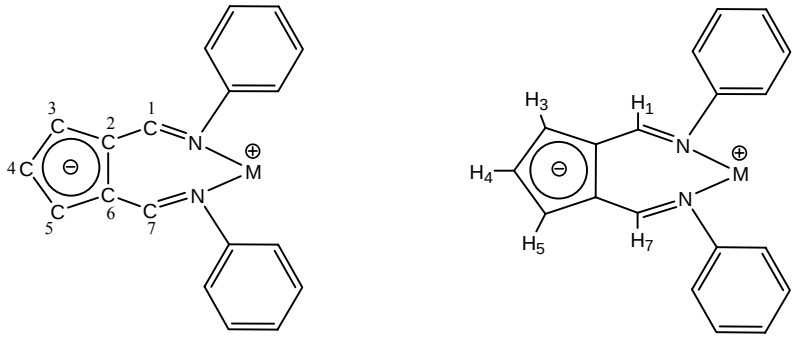

Figure 5.1. Labelling for carbons and protons in the ligand

5.5 Synthesis of the metal precursors

5.5.1 [(dme)$NiBr_2$][1]

$NiBr_2 \cdot xH_2O$ (100 mg, ca. 400 mmol), absolute ethanol (160 ml) and triethyl orthoformate (134 ml, 800 mmoles) were placed in a 1-litre 3-necked flask equipped with a mechanical stirrer and reflux condenser. The mixture was refluxed for 1h under nitrogen. Another 50 ml of triethyl orthoformate was added and the mixture refluxed for 2 more hours. The volume was reduced until crystallisation at the boiling point and 250 ml of 1,2-dimethoxy ethane were added. Another 70 ml of triethyl orthoformate was added and the mixture was refluxed for 2 h. The volume was reduced and the precipitate collected on a Schlenk frit. The salmon-pink solid was washed with 1,2-dimethoxy ethane (50 ml) and with hexane (80 ml) and dried. Yield 44.27 g (40%).

5.5.2 [(cod)$PdCl_2$][2]

Palladium(II) chloride (1g) was dissolved in 5 ml of concentrated hydrochloric acid by warming the mixture. The cool solution was diluted with 150 ml of absolute ethanol, filtered, and the residue and filter paper washed with 20 ml of ethanol. To the combined filtrate and washings were added 3.0 ml of 1,5-cyclooctadiene with stirring. The yellow product precipitated immediately, and after 10-min storage was separated and washed with three 30-ml portions of diethyl ether. Yield was 3.10 g (96% based on $PdCl_2$)

5.5.3 [(cod)Pd(CH_3)(Cl)][3]

In a 100-ml Schlenk tube, 2.0 g (7.0 mmol) of [(cod)$PdCl_2$] was dissolved in 50 ml of CH_2Cl_2. Then 1.16 ml (1.3 equiv) of [$Sn(CH_3)_4$] were added and stirred at room temperature until the bright yellow colour of the precursor had vanished, which normally took *ca.* 1 day. In some cases addition of more tetramethyltin was necessary if the colour of the mixture had not disappeared yet. The solution was

filtered off celite, and the solvent was removed under reduced pressure from the nearly colourless solution, while the temperature was kept at 0 ˚C using an ice bath. The off-white powder was washed with several small portions of diethyl ether in order to remove the [$(CH_3)_3SnCl$] formed. Yield was 90%

5.5.4 $[(PhCN)_2PdCl_2]$[4]

Palladium(II) chloride (2.0 g, 11.3 mmol) was loaded into a 200-ml round-bottom flask, equipped with stirring bar. Benzonitrile (60 ml) was added, and the mixture was stirred magnetically while being heated to 100 ˚C. After 20 min most of the palladium chloride had dissolved to give a red-brown solution. The solution was filtered while still hot, and the filtrate was poured into a 500-ml Erlenmeyer flask containing 350 ml of petroleum ether. A precipitate was formed immediately. The yellow-orange product was filtered through a fine frit, washed with 3 portions of 15 ml of petroleum ether and dried *in vacuo*. Yield was 95%.

5.5.5 $[(\eta^3\text{-}C_3H_5)_2Pd_2Cl_2]$[5]

A 200-ml, two-necked, round-bottomed flask equipped with a magnetic stirring bar, a gas inlet tube, and a condenser topped with a bubbler was charged with an aqueous solution of palladium(II) chloride (4.44 g, 25 mmol) and sodium chloride (2.95 g, 50 mmol) in 10 ml of H_2O, followed by methanol (60 ml) and allyl chloride (6.0 g, 67 mmol). Carbon monoxide was passed slowly (2-2.5 L h^{-1}) under stirring through the reddish-brown solution for 1h. The bright yellow suspension thus obtained was poured into water (300 ml) and extracted with 2 x 100 ml of chloroform. The extract was washed with water (two 150-ml portions) and dried over calcium chloride. Evaporation under reduced pressure gave yellow crystals of the desired complex. Yield: 93%.

5.5.6 $[Cp^*RuCl_2]_2$[6]

All operations were carried out in a 500-ml round-bottomed flask under an inert atmosphere.

To a filtered solution of 8.0 g (31.6 mmol) of $RuCl_3 \cdot 3H_2O$ in 200 ml of CH_3OH was added 9.6 g (72 mmol) of C_5Me_5H, and the mixture was refluxed for 4h. the brown solution, which contains part of the product as a microcrystalline precipitate, was chilled to -80 ˚C for 12 h and filtered cold through a porous frit. The solid was dried *in vacuo* and washed twice with 30 ml of pentane in order to remove the decamethylruthenocene. Yield was 80% of the theoretical based on Ru.

In case the methanolic mother liquor was still green, the reaction had not gone to completion. It can be refluxed for a second time, and more product can be recovered using the above work-up procedure.

5.5.7 $[Cp^*Ru(\mu_3\text{-}Cl)]_4$[7]

A 100-ml round-bottomed flask was charged with 2.08 g (6.60 mmol) of Cp^*RuCl_2 and 15 ml of THF. Then 6.6 cm^3 of 1 M lithium triethylborohydride in THF (6.60 mmol) were added all at once to the solution via syringe. The reaction mixture turned to a dark blue-green colour initially during the addition, and gas evolution was observed. After 45 minutes of stirring, the crystalline orange precipitate which formed was isolated by filtration and rinsed twice with small amounts (ca.2 ml) of THF. It was then dried *in vacuo* to yield 1.42 g (79%) of crystalline orange product.

5.5.8 $[Cp^*Ru(CH_3CN)_3][BF_4]$

An adaptation of the reported synthesis was used. A 100-ml round-bottomed flask was charged with 3.00 g (2.76 mmol) of $[Cp^*Ru(\mu_3\text{-}Cl)]_4$ and 20 ml of acetonitrile. The mixture was refluxed for 1 h and then allowed to cool to room temperature. To the stirred mixture were added 2.14 g (11.0 mmol) of silver tetrafluoroborate and the mixture stirred for 1 h. After filtration, the solvent was removed *in vacuo*. Diethyl ether (10 ml) was added to the residue, and the yellow-orange crystalline solid was

isolated via filtration with a filtered-capped cannula. After another 3 x 2-ml washings with diethyl ether, the solid was dried *in vacuo* to yield 4.5 g of the desired product

5.5.9 $[(PPh_3)_2Ni(Ph)Cl]$[8]

A Schlenk flask was charged with anhydrous $NiCl_2$ (1.30g, 10mmol), zinc dust (0.66 g, 10 mmol), PPh_3 (11.02 g, 0.42 mmol) and were suspended in 100 ml of DMF. The reaction mixture was heated to 50 ˚C for 2 h and stirred for additional 15h at room temperature whereupon a brick red precipitate was formed. The solvent was evaporated and toluene (200 ml) was added. After adding chlorobenzene (3.10 ml, 25 mmol) the solution was stirred for 3 h at 0 ˚C. The colour changed to a deep brown. After filtration the solution was concentrated to about 70 ml and hexane (100 ml) was added. A yellow solid precipitated which was isolated by filtration, washed twice with hexane (50 ml) and thoroughly dried under vacuum. The yield was 5.01 g (72%).

5.6 Synthesis of the ligands

5.6.1 6-(dimethylamino)fulvene[9]

Dimethylformamide (31.2 ml, 200mmol) was placed in a 500-ml 3-necked flask equipped with mechanical stirrer, dropping funnel and reflux condenser and was heated to 55 ˚C. Dimethyl sulphate (400 ml, 200 mmol) was added dropwise while stirring during 30 minutes. After the addition was completed, the mixture was stirred for additional 2 hours at 70-80 ˚C. A colourless oil of dimethylformamide-dimethylsulphate was obtained in 97%yield

The DMF-DMS oil (99.85 g, 200mmol) was slowly added to a solution of sodium cyclopentadienide (100 ml, 2.0 M in THF, 200 mmol) at -10 ˚C under a nitrogen atmosphere. When the addition was completed, the mixture was stirred at 20 ˚C for 2 h. The solvent and volatiles were removed *in vacuo.* Activated charcoal and petroleum ether 60-80 ˚C (100 ml) were added, the mixture refluxed for 4 h and

filtered while hot. Other 2 portions of 50 ml of hot petroleum ether 60-80 ˚C were added to the solid to extract more product.

The combined solutions were concentrated under vacuum and stored at -18 ˚C to yield 15.51 g (64%) of the 6-(dimethylamino)fulvene as yellow flakes.

^{1}H-NMR ($CDCl_3$, 250 MHz, 20 ˚C): δ 7.15 (s, 1H, *H*2), 6.62 (m, 1H, *H*7, *J*= 8.4 Hz), 6.56 (m, 1H, *H*6, *J*= 10.1 Hz), 6.44 (m, 1H, *H*5, *J*= 8.6 Hz), 6,35 (m, 1H, *H*4, *J*= 8.4 Hz), 3.29 (s, 6H, CH_3). ^{13}C NMR ($CDCl_3$, 62.9 MHz, 20 ˚C): δ 148.70 (*C*2), 125.30 (*C*6), 124.50 (*C*5), 119.62 (*C*4), 116.92 (*C*3), 114.00 (*C*7), 30.41 (*C*H_3). MS (EI, *m*/*z*): 122 (M^+), 107 (M^+- CH_3). Elemental analysis for $C_8H_{11}N$: C, 79.27; H, 9.17; N, 11.56. Found: C, 78.98; H, 9.10; N, 11.46.

5.6.2 6-dimethylaminofulvene-1-*N,N'*-dimethylaldimmonium chloride

DMF (6.6 ml, 85 mmol) were dissolved in 100 ml of THF in a 3-necked flask equipped with dropping funnel. A solution of oxalyl chloride (7.4 ml, 85 mmol) in THF (20 ml) was slowly added while keeping the temperature at 0 ˚C. After the addition was complete, the mixture was stirred for 1 h. The suspension was carefully added under nitrogen to a solution of 6-(dimethylamino)fulvene (10.22 g, 84.5 mmol) in THF (150 ml). The temperature was kept below -60 ˚C throughout the addition. After the addition, the mixture was stirred for additional 2 h at room temperature. The solvent and volatiles were removed *in vacuo* and the crude product washed with 100 ml hexane/ether (50:50) to give 17.54 g (98%) of the product as a dark green solid.

^{1}H-NMR ($CDCl_3$, 250 MHz, 20 ˚C): δ 9.76 (s, 2H, C*H*N), 7.35 (d, 2H, Cp*H*), 6.78 (t, 1H, Cp*H*), 3.83 (s, 6H, CH_3), 3.42 (s, 6H, CH_3). ^{13}C-NMR ($CDCl_3$, 62.9 MHz, 20 ˚C): δ 160.60 (*C*2), 130.30 (*C*6), 125.81 (*C*5), 119.32 (*C*3), 48.81 (*C*H_3), 42.13 (*C*H_3).

5.6.3 *N,N'*-diphenyl-6-aminofulvene-2-aldimine (1)

A solution of 6-dimethylaminofulvene-1-*N,N*'-dimethylaldimmonium chloride (15 g, 85 mmol) in 150 ml of ethanol was refluxed with aniline (15.5 ml, 170 mmol) for 12

h. The solvent and volatiles were removed *in vacuo*, activated charcoal was added and the residue refluxed in 250 ml of hexane for 12 h. The mixture was filtered while still hot and 2 portions of 50 ml of hot hexane were used to extract more product from the solid. The solutions were combined and the volume reduced to about 1/4. Storage at -20 ˚C afforded 14.58 g (63%) of the desired product as orange crystalline powder.

^{1}H-NMR ($CDCl_3$, 250 MHz, 20 ˚C): δ 15.59 (br, 1H, N*H*), 8.29 (d, 2H, *H*1/*H*7, *J*= 6.9 Hz), 7.38 (m, 4H, C_6H_5), 7.23 (m, 4H, C_6H_5), 7.16 (t, 2H, C_6H_5), 7.05 (d, 2H, *H*3/*H*5, ^{3}J= 3.7 Hz), 6.47 (t, 1H, *H*4, ^{3}J= 3.7 Hz). ^{13}C-NMR ($CDCl_3$, 62.9 MHz, 20 ˚C): δ 150.63 (*C*1/*C*7), 145.25 (*C*, ipso-Ar), 134.68 (*C*3/*C*5), 129.56 (*m*-*C*, Ar), 124.84 (*p*-*C*, Ar), 122.08 (*C*2/*C*6), 120.96 (*C*4), 119.12 (*o*-*C*, Ar). MS (EI, *m/z*): 273 (M^+). Elemental analysis for $C_{19}H_{16}N_2$: C, 83.78; H, 5.73; N, 10.29. Found: C, 82.25; H, 5.87; N, 10.20.

5.6.4 *N,N'*-di-(2,6-dimethyl)phenyl-6-aminofulvene-2-aldimine (2)

A solution of 6-dimethylaminofulvene-1-*N,N'*-dimethylammonium chloride (15 g, 85 mmol) in 100 ml was refluxed with 2,6-dimethylaniline (20.9 ml, 170 mmol) for 3 days. The solvent and volatiles were removed *in vacuo*, activated charcoal was added and the residue refluxed in 250 ml of hexane for 24 h. The mixture was filtered while still hot and 2 portions of 50 ml of hot hexane were used to extract more product from the solid. Evaporation of the solvent led to a mixture of two species as an orange oil. Purification by column chromatography (1:50 ethyl acetate-hexane) and removal of the eluent afforded the isolation of the desired product as yellow crystalline powder in 10% yield.

^{1}H-NMR ($CDCl_3$, 250 MHz, 20 ˚C): δ 14.82 (br, 1H, N*H*), 7.91 (d, 2H, *H*1/*H*7, *J* = 6.9 Hz), 7.10-6.97 (m, 6H, $C_6H_3Me_2$), 7.00 (d, 2H, *H*3/*H*5, ^{3}J = 3.7 Hz), 6.46 (t, 1H, *H*4, ^{3}J= 3.7 Hz), 2.20 (s, 12H, $C_6H_3Me_2$). ^{13}C-NMR ($CDCl_3$, 62.9 MHz, 20): δ 156.63 (*C*1/*C*7), 144.91 (*C*, ipso-Ar), 134.82 (*C*3/*C*5), 131.11 (*o*-*C*), 128.83 (*m*-*C*), 125.40 (*p*-*C*), 122.12 (*C*2/*C*6), 120.43 (*C*4), 18.74 (*o*-*C*H_3). MS (FAB, *m/z*): 328 (M^+). Elemental analysis for $C_{23}H_{24}N_2$: C, 84.11; H, 7.37; N, 8.53. Found: C, 83.78; H, 7.27; N, 8.475.

5.6.5 *N*-(2,6-dimethyl)phenyl-6aminofulvenealdehyde (5)

From the above procedure, isolation of the second species was possible via chromatography as a pale yellow crystalline powder. Recrystallisation from hexane solution afforded the formation of yellow crystals suitable for X-ray analysis in 15% yield.

The labelling for all protons and carbons for the NMR characterization are referred as shown in the figure below:

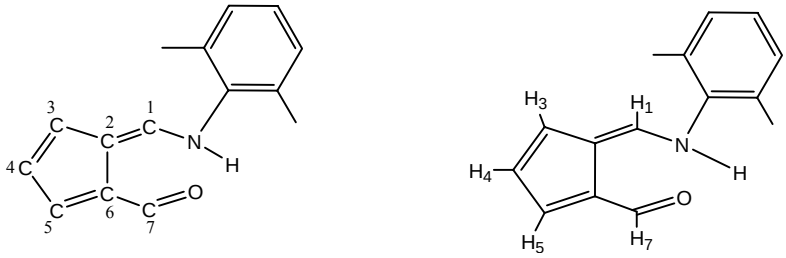

Figure 5.2. Labelling for carbons and protons in compound 5.

^{1}H-NMR ($CDCl_3$, 360 MHz, 20 ˚C): δ 13.32 (br, 1H, N*H*), 9.64 (s, 1H, *H*7), 7.72 (d, 1H, *H*1, ^{3}J = 13.77 Hz), 7.53 (m, 1H, *H*5), 7.37 (s, 3H, $C_6H_3Me_2$), 7.18 (m, 1H, *H*3), 6.58 (dd, 1H, *H*4, ^{3}J = 4.05 Hz, ^{3}J = 3.44 Hz), 2.48 (s, 6H, $C_6H_3Me_2$). ^{13}C-NMR ($CDCl_3$, 90.6 MHz, 20): δ 184.63 (*C*7), 153.15 (*C*1), 140.94 (N-$C_6H_3Me_2$), 137.70 (*C*6), 135.2 (*C*2), 132.7 ($C_6H_3Me_2$), 129.0 ($C_6H_3Me_2$), 128.3 (*C*4), 127.7 ($C_6H_3Me_2$), 120.8 (*C*5), 116.6 (*C*3), 18.6 ($C_6H_3Me_2$). Elemental analysis for $C_{15}H_{15}NO$: C, 79.97; H, 6.71; N, 6.22. Found: C, 79.88; H, 6.71; N, 6.15.

5.6.6 *N,N'*-di-(2,4,6-trimethyl)phenyl-6-aminofulvene-2-aldimine (3)

A solution of 6-dimethylaminofulvene-1-*N,N'*-dimethylaldimmonium chloride (9.24 g, 43.42 mmol) in absolute ethanol (150 ml) was refluxed with an excess of 2,4,6-trimethylaniline (18.29 ml, 130.26 mmol) for 4 days. The solvent and volatiles were removed under *vacuum*, activated charcoal was added and the product refluxed in hexane (200 ml) overnight. The solution was filtered while still hot and the solid

residue extracted with another 3x30 ml portions of hot hexane. The combined solutions were concentrated *in vacuo* and stored at -20˚C for 1 day to produce the final product as a yellow crystalline solid, which was separated and dried *in vacuo*. Yield (10.22 g, 66%).

^{1}H-NMR ($CDCl_3$, 250 MHz, 20 ˚C): δ 14.96 (br, 1H, N*H*), 7.89 (d, 2H, *H*1/*H*7, $^{3}J_{N\text{-}H}$= 7.0 Hz), 7.00 (d, 2H, *H*3/*H*5, ^{3}J= 3.7 Hz), 6.88 (s, 4H, Ar-*H*), , 6.44 (t, 1H, *H*4, ^{3}J= 3.7 Hz), 2.27 (s, 6H, *p*-CH_3), 2.16 (s, 12H, Ar-CH_3). ^{13}C-NMR ($CDCl_3$, 62.9 MHz, 20): δ 156.81 (*C*1/*C*7), 141.68 (*C*, ipso-Ar), 134.65 (*o*-*C*), 132.71 (*C*3/*C*5), 130.73 (*p*-*C*), 129.91 (*m*-*C*), 120.85 (*C*2/*C*6), 119.14 (*C*4), 20.65 (*p*-*C*H_3), 18.44 (*o*-*C*H_3). MS (EI, *m/z*): 357 (M^+), 238 (M^+-C_9H_{11}). Elemental analysis for $C_{25}H_{28}N_2$: C, 84.21; H, 7.93; N, 7.86. Found: C, 84.19; H, 7.88; N, 7.66.

5.6.7 *N,N'*-dicyclohexyl-6-aminofulvene-2-aldimine (4)

A solution of 6-dimethylaminofulvene-1-*N,N'*-dimethylaldimmonium chloride (15 g, 85 mmol) in 150 ml of ethanol was refluxed with cyclohexylamine (19.4 ml, 170 mmol) for 12 h. The solvent and volatiles were removed *in vacuo*, activated charcoal was added and the residue refluxed in 250 ml of hexane for 12 h. The mixture was filtered while still hot and 2 portions of 50 ml of hot hexane were used to extract more product from the solid. The solutions were combined and the volume reduced to about 1/4. Storage at -20 ˚C afforded 16.67 g (69.2%) of the desired product as yellow needles.

^{1}H-NMR ($CDCl_3$, 250 MHz, 20 ˚C): δ 14.04 (br, 1H, N*H*), 7.94 (d, 2H, *H*1/*H*7, *J*= 6.6 Hz), 6.81 (d, 2H, *H*3/*H*5, ^{3}J= 3.5 Hz), 6.34 (t, 1H, *H*4, ^{3}J= 3.5 Hz), 3.25 (p, 2H, ipso-Cy*H*), 1.20-2.01 (m, 20H, Cy*H*). ^{13}C-NMR ($CDCl_3$, 62.9 MHz, 20 ˚C): δ 154.78 (*C*1/*C*7), 129.86 (*C*3/*C*5), 120.08 (*C*2/*C*6), 117.65 (*C*4), 64.19 (ipso-*C*, Cy), 35.39 (*o*-*C*, Cy), 26.00 (*p*-*C*, Cy), 25.49 (*m*-*C*, Cy). MS (FAB, *m/z*): 284 (M^+), 201 (M^+ - C_6H_{11}). Elemental analysis for $C_{19}H_{28}N_2$: C, 80.21; H, 9.94; N, 9.85. Found: C, 80.00; H, 9.86; N, 9.80.

5.7 Synthesis of the complexes

5.7.1 [(Ph$_2$AFA)$_2$Zn] (6)

To a solution of Ph$_2$AFAH (0.40 g, 1.47 mmol) in THF (30 ml), NaH was added as an excess (2-3 equivalents) and immediately a gas evolution was observed. The mixture was stirred for 1 h and a solution of anhydrous $ZnCl_2$ (0.197 g, 1.47 mmol) in THF (30 ml) was added via cannulation. After stirring for 3 h, the solution was filtered through celite and the solvent was removed *in vacuo*. The solid was extracted with CH_2Cl_2 and the solvent removed to yield a yellow crystalline solid. Crystals suitable for X-ray analysis were obtained by slow evaporation of the solvent from hexane solutions.

^{1}H-NMR ($CDCl_3$, 360 MHz, 20 ˚C): δ 8.05 (s, 4H, *H*1/*H*7), 7.01 (d, 4H, *H*3/*H*5, ^3J= 3.65 Hz), 7.00-6.97 (m, 12H, C_6H_5), 6.84-6.80 (m, 8H, C_6H_5), 6.39 (t, 2H, *H*4, ^3J= 3.65 Hz). ^{13}C-NMR ($CDCl_3$, 90.6 MHz, 20 ˚C): δ 162.94 (*C*=N), 150.69 (N-C_6H_5), 139.82 (C_6H_5), 128.87 (C_6H_5), 125.05 (*C*3/*C*5), 122.19 (C_6H_5), 118.67 (*C*2/*C*6), 117.99 (C4). Anal. Calcd. For $C_{38}H_{30}N_4Zn$: C, 75.06; H, 4.97; N, 9.21. Found: C, 75.33; H, 4.58; N, 8.86.

Crystal Data

Crystal Description	Yellow needle	***β* (deg)**	93.1990(10)
Empirical Formula	$C_{38}H_{30}N_4Zn$	***γ* (deg)**	90
M_w	608.03	***V* (Å^3)**	2952.68(10)
***T* (K)**	150(2)	***Z***	4
Crystal system	Monoclinic	***μ* (Mo Kα) (mm^{-1})**	0.866
Space group	$P2_1/c$	**No. of independent reflections**	7091 [R(int) = 0.0323]
***a* (Å)**	10.0520(2)	**No. of data with $\|F\| > 4\sigma(\|F\|)$**	6313
***b* (Å)**	19.0001(4)	**Absorption Correction**	Multiscan (T_{min} = 0.810, T_{max} = 1)
***c* (Å)**	15.4841(3)	***R***	0.0437
***α* (deg)**	90	R_w	0.0981

5.7.2 [$(Ph_2AFA)_2Co$] (7)

To a solution of Ph_2AFAH (0.40 g, 1.47 mmol) in THF (30 ml), NaH was as an excess (2-3 equivalents) added as an excess (2-3 equivalents) and immediately a gas evolution was observed. The mixture was stirred for 1 h and anhydrous $CoCl_2$ (0.189 g, 1.47 mmol) was added as a solid. After stirring for 3 h, the solution was filtered through celite and the solvent was removed *in vacuo*. The solid was extracted with hexane (250 ml) and the solvent slowly evaporated to afford isolation of red crystals suitable for X-ray analysis.

MS (FAB, *m/z*): 601 (M^+). Elemental analysis for $C_{38}H_{30}N_4Co$: C, 75.86; H, 5.03; N, 9.31. Found: C, 75.69; H, 4.72; N, 9.30.

Crystal Data

Crystal Description	Red Lath	***β* (deg)**	92.857(2)
Empirical Formula	$C_{38}H_{30}N_4Co$	***γ* (deg)**	90
M_w	601.59	***V* (Å^3)**	2934.7(3)
***T* (K)**	150(2)	***Z***	4
Crystal system	Monoclinic	***μ* (Mo Kα) (mm^{-1})**	0.619
Space group	$P2_1/c$	**No. of independent reflections**	7214 [R(int) = 0.0740]
***a* (Å)**	10.0207(6)	**No. of data with $\|F\| > 4\sigma(\|F\|)$**	5342
***b* (Å)**	18.9775(11)	**Absorption Correction**	Semi-empirical (T_{min} = 0.705, T_{max} = 1.000)
***c* (Å)**	15.4515(9)	***R***	0.0622
***α* (deg)**	90	R_w	0.1282

5.7.3 [$(Ph_2AFA)CuPPh_3$] (8)

To a solution of anhydrous CuCl (0.060 g, 0.612 mmol) in THF (20 ml), PPh_3 (0.160 g, 0.306 mmol) were added and the mixture was stirred for 1 h to afford the formation of a white suspension of $[(PPh_3)CuCl]_4$. In a Schlenk flask, to a solution of Ph_2AFAH (0.166 g, 0.612 mmol) in THF (25 ml), NaH was added as an excess (2-3 equivalents) and the mixture stirred for 1 h. The $[(PPh_3)CuCl]_4$ suspension was added via cannulation and the mixture stirred for 2 h. The deep red solution obtained was filtered through celite and the solvent removed. The solid residue was extracted with

200 ml of hexane. Slow evaporation from the hexane solution afforded the isolation of red crystals suitable for X-ray analysis in 55% yield.

^{1}H-NMR ($CDCl_3$, 360 MHz, 20 ˚C): δ 8.39 (s, 4H, *H*1/*H*7), 7.00 (d, 4H, *H*3/*H*5, ^{3}J= 3.58 Hz), 7.31-6.89 (m, 25H, C_6H_5), 6.38 (t, 2H, *H*1, ^{3}J= 3.58 Hz). ^{13}C-NMR ($CDCl_3$, 90.6 MHz, 20 ˚C): δ 162.36 (*C*=N), 154.91 (N-C_6H_5), 135.16 (*C*3/*C*5), 133.93 (P-C_6H_5), 133.61 (P-C_6H_5), 129.91 (P-C_6H_5), 129.55 (P-C_6H_5), 128.64 (*m*-C_6H_5), 124.03 (*p*-C_6H_5), 122.42 (*o*-C_6H_5), 118.21 (*C*2/*C*6), 116.36 (*C*4). Anal. Calcd. For $C_{37}H_{30}N_2CuP$: C, 74.42; H, 5.06; N, 4.69. Found: C, 74.22; H, 4.87; N, 4.51.

Crystal Data

Crystal Description	Red Block	***β* (deg)**	92.5700(10)
Empirical Formula	$C_{37}H_{30}N_2PCu$	***γ* (deg)**	105.7550(10)
M_w	597.14	***V* (Å^3)**	2966.1(3)
***T* (K)**	150(2)	***Z***	4
Crystal system	Triclinic	***μ* (Mo Kα) (mm^{-1})**	0.819
Space group	$P\text{-}_1$	**No. of independent reflections**	14028 [*R*(int) = 0.0231]
***a* (Å)**	10.7960(6)	**No. of data with $\|F\| > 4\sigma(\|F\|)$**	12257
***b* (Å)**	14.0838(8)	**Absorption Correction**	Multiscan (T_{min} = 0.887, T_{max} = 1.000)
***c* (Å)**	20.3173(11)	***R***	0.0448
***α* (deg)**	92.1710(10)	R_w	0.1100

5.7.4 [$(Ph_2AFA)_2Pd$] (9)

To a solution of Ph_2AFAH (0.40 g, 1.47 mmol) in toluene (25 ml), 0.92 ml of CH_3Li (1.6M in THF) were added and the mixture stirred for 1 h. A solution of $(PhCN)_2PdCl_2$ (0.421 g, 1.10 mmol) in toluene (50 ml) was stirred at 50 ˚C for 1 h and then added via cannulation. The mixture was stirred at room temperature for 2 h and then filtered through celite. Concentration of the solution and storage at -5 ˚C afforded the isolation of $(Ph_2AFA)_2Pd$ as a dark purple solid. Crystals suitable for X-ray analysis were obtained from THF solutions upon slow evaporation of the solvent.

^{1}H NMR (360 MHz, CD_2Cl_2): δ 7.44 (s, 2H, *H*1/*H*7), 7.45-7.42 (d, 4H, *o*-C_6H_5), 7.29-7.25 (t, 4H, *m*-C_6H_5), 7.20-7.15 (t, 2H, *p*-C_6H_5), 6.70 (d, 2H, *H*3/*H*5, ^{3}J=

3.63 Hz), 6.38 (t, 1H, *H*4, ^3J= 3.63 Hz). $^{13}C\{^1H\}$ NMR ($CDCl_3$, 90.6 MHz, 20 ˚C): δ 160.44 (*C*=N), 149.03 (N-C_6H_5), 135.16 (C_6H_5), 128.53 (C_6H_5), 125.35 (*C*3/*C*5), 122.87 (C_6H_5), 120.56 (*C*2/*C*6), 117.39 (*C*4).

Crystal Data

Crystal Description	Red Block	***β* (deg)**	90.412(2)
Empirical Formula	$C_{42}H_{38}N_4OPd$	***γ* (deg)**	90
M_w	721.16	***V* (Å^3)**	3339.7(3)
***T* (K)**	150(2)	***Z***	4
Crystal system	Monoclinic	***μ* (Mo Kα) (mm^{-1})**	0.596
Space group	*I*2/a	**No. of independent reflections**	4725 [*R*(int) = 0.0332]
***a* (Å)**	16.7396(7)	**No. of data with $\|F\| > 4\sigma(\|F\|)$**	3997
***b* (Å)**	19.2569(8)	**Absorption Correction**	Multiscan (T_{min} = 0.769, T_{max} = 0.910)
***c* (Å)**	10.3606(5)	***R***	0.0401
***α* (deg)**	90	R_w	0.1002

5.7.5 [$(Ph_2AFA)_2Ni$] (10)

To a solution of Ph_2AFAH (0.40 g, 1.47 mmol) in toluene (30 ml), 0.92 ml of BuLi (1.6M in hexanes) was added and the mixture was stirred for 1 h. [(dme)$NiBr_2$] (0.450 g, 1.47 mmol) was added as a solid. After stirring for 3 h, the solution was filtered through celite and the volume reduced to *ca.* 1/3. Upon storage at -10 ˚C, black crystals also suitable for X-ray analysis had formed, which turn out to be a mixture of tetrahedral and square-planar $(Ph_2AFA)_2Ni$ in 40% yield.

Square-planar $(Ph_2AFA)_2Ni$: ^{1}H-NMR ($CDCl_3$, 360 MHz, 20 ˚C): δ 7.85 (d, 4H, *o*-C_6H_5), 7.33-7.17 (m, 6H, *p*-C_6H_5, *m*-C_6H_5), 7.08 (s, 2H, *H*1/*H*7), 6.78 (d, 2H, *H*3/*H*5, ^3J = 3.55 Hz), 6.56 (t, 1H, *H*5, ^3J = 3.55 Hz). MS (electrospray, *m/z*): 602 (M^+).

Crystal Data for the tetrahedral species

Crystal Description	Red Block	***β* (deg)**	90.8290(10)
Empirical Formula	$C_{38}H_{30}N_4Ni$	***γ* (deg)**	90
M_w	601.37	***V* (Å^3)**	2932.45(17)
***T* (K)**	150(2)	***Z***	4
Crystal system	Monoclinic	***μ* (Mo Kα) (mm^{-1})**	0.696
Space group	$P2_1/c$	**No. of independent reflections**	5137 [R(int) = 0.0505]
***a* (Å)**	10.0629(3)	**No. of data with $\|F\| > 4\sigma(\|F\|)$**	4258
***b* (Å)**	18.9890(6)	**Absorption Correction**	Semiempirical (T_{min} = 0.717, T_{max} = 1.000)
***c* (Å)**	15.3651(6)	***R***	0.0424
***α* (deg)**	90	R_w	0.0922

Crystal Data for the square-planar species

Crystal Description	Red Block	***β* (deg)**	90.121(3)
Empirical Formula	$C_{52}H_{46}N_4Ni$	***γ* (deg)**	90
M_w	785.67	***V* (Å^3)**	2007.3(2)
***T* (K)**	150(2)	***Z***	2
Crystal system	Monoclinic	***μ* (Mo Kα) (mm^{-1})**	0.526
Space group	$P2_1/c$	**No. of independent reflections**	4904 [R(int) = 0.038]
***a* (Å)**	10.3205(7)	**No. of data with $\|F\| > 4\sigma(\|F\|)$**	3598
***b* (Å)**	19.8426(12)	**Absorption Correction**	Semiempirical (T_{min} = 0.63, T_{max} = 0.94)
***c* (Å)**	9.8018(6)	***R***	0.0402
***α* (deg)**	90	R_w	0.1051

5.7.6 [(Ph_2AFA)Pd(η^3-C_3H_5)] (11)

To a solution of Ph_2AFAH (0.30 g, 1.10 mmol) in toluene (25 ml), 0.7 ml of CH_3Li (1.6M in THF) were added and the mixture stirred for 1 h. A solution of [(η^3-C_3H_5)PdCl]$_2$ (0.200 g, 0.55 mmol) in toluene (25 ml) was added via a cannula and the mixture stirred for 2h. After filtration through celite, the solvent was removed and the solid residue was extracted with 250 ml of hexane; slow evaporation from this solution afforded isolation of yellow crystals suitable for X-ray analysis.

^{1}H-NMR ($CDCl_3$, 360 MHz, 25˚C): δ 8.35 (s, 2H, *H*1/*H*7), 7.41-7.33 (m, 8H, *m*-, *o*-C_6H_5), 6.85 (d, 2H, *H*3/*H*5, ^3J = 3.59 Hz), 6.31 (t, 1H, *H*4, ^3J = 3.59 Hz), 5.28 (tt, 1H, Allyl C*H*, ^3J = 12.39, 6.95 Hz), 2.45 (s, 6H, Ph-CH_3), 2.85 (d, 2H, Allyl C*H*H, ^3J = 6.95 Hz), 2.44 (d, 2H, Allyl C*H*H, ^3J = 12.39 Hz). ^{13}C{^{1}H} NMR ($CDCl_3$, 90.6 MHz, 20 ˚C): δ 162.73 (*C*=N), 157.06 (N-C_6H_5), 134.72 (*p*-C_6H_5), 128.86 (*o*-C_6H_5), 124.64 (*C*3/*C*5), 121.88 (*m*-C_6H_5), 119.25 (*C*2/*C*6), 117.68 (C_3H_5), 116.27 (*C*4) 61.26 (C_3H_5).

Crystal Data

Crystal Description	Orange Block	***β* (deg)**	90
Empirical Formula	$C_{22}H_{20}N_2Pd$	***γ* (deg)**	90
M_w	418.80	***V* (Å^3)**	1838.95(7)
***T* (K)**	150(2)	***Z***	4
Crystal system	Orthorhombic	***μ* (Mo Kα) (mm^{-1})**	1.015
Space group	*Pna*2$_1$/c	**No. of independent reflections**	3831 [*R*(int) = 0.0297]
***a* (Å)**	19.8592(4)	**No. of data with $\|F\| > 4\sigma(\|F\|)$**	3407
***b* (Å)**	10.3053(2)	**Absorption Correction**	Multiscan (T_{min} = 0.607, T_{max} = 0.872)
***c* (Å)**	8.9856(2)	***R***	0.0247
***α* (deg)**	90	R_w	0.0567

5.7.7 [(Ph'$_2$AFA)Pd(η^3-C_3H_5)] (13) (Ph'= 2,4,6-trimethyl-phenyl)

To a solution of Ph'$_2$AFAH (0.40 g, 1.11 mmol) in toluene (25 ml), 0.7 ml of CH_3Li (1.6M in THF) were added and the mixture stirred for 1 h. A solution of [(η^3-C_3H_5)PdCl]$_2$ (0.200 g, 0.55 mmol) in toluene (25 ml) was added via a cannula and the mixture stirred for 2h. After filtration through celite, the solvent was removed and the solid residue was extracted with 250 ml of hexane; slow evaporation from this solution afforded isolation of yellow crystals suitable for X-ray analysis.

^{1}H-NMR (CD_2Cl_2, 360 MHz, 25˚C): δ 7.89 (s, 2H, *H*1/*H*7), 6.90 (s, 2H, $C_6H_2Me_3$), 6.89 (s, 2H, $C_6H_2Me_3$), 6.73 (d, 2H, *H*3/*H*5, ^3J = 3.56 Hz), 6.19 (t, 1H, *H*4, ^3J = 3.56 Hz), 5.41 (tt, 1H, Allyl C*H*, ^3J = 12.39, 6.94 Hz), 2.45 (s, 6H, Ph-*Me*$_3$), 2.43 (d, 2H, Allyl C*H*H, ^3J = 12.39 Hz), 2.28 (s, 6H, Ph-*Me*$_3$), 2.27 (s, 6H, Ph-*Me*$_3$), 2.21 (d, 2H, Allyl C*H*H, ^3J = 6.94 Hz). ^{13}C{^{1}H} NMR (CD_2Cl_2, 90.6 MHz, 20 ˚C): δ

165.51 (*C*=N), 155.85 (N-$C_6H_2Me_3$), 134.02 (*m*-$C_6H_2Me_3$), 133.68 (*o*-$C_6H_2Me_3$), 129.81 (*p*-$C_6H_2Me_3$), 128.84 (*C*3/*C*5), 128.78 (*o*-$C_6H_2Me_3$), 128.72 (*m*-$C_6H_2Me_3$), 117.60 (*C*4), 116.11 (Allyl *C*H), 115.63 (*C*2/*C*6), 63.09 (Allyl CH_2), 20.57 (C_6H_2-CH_3), 19.00 (C_6H_2-CH_3), 18.93 (C_6H_2-CH_3). Anal. Calcd. For $C_{28}H_{32}N_2PPd$: C, 66.86; H, 6.41; N, 5.57. Found: C, 66.72; H, 6.42; N, 5.48.

Crystal Data

Crystal Description	Yellow Block	***β* (deg)**	80.0450(10)
Empirical Formula	$C_{28}H_{32}N_2Pd$	***γ* (deg)**	85.9600(10)
M_w	502.96	***V* (Å^3)**	1219.13(5)
***T* (K)**	150(2)	***Z***	2
Crystal system	Triclinic	***μ* (Mo Kα) (mm^{-1})**	0.778
Space group	*P*-1	**No. of independent reflections**	6749 [*R*(int) = 0.0272]
***a* (Å)**	8.6841(2)	**No. of data with |*F*| > 4σ(|*F*|)**	6055
***b* (Å)**	10.7538(2)	**Absorption Correction**	Multiscan (T_{min} = 0.764, T_{max} = 0.910)
***c* (Å)**	13.8393(4)	***R***	0.0295
***α* (deg)**	73.3250(10)	R_w	0.0765

5.7.8 [(Ph_2AFA)Pd(PPh_3)(CH_3)] (14)

To a solution of Ph_2AFAH (0.30 g, 1.10 mmol) in toluene (25 ml), 0.7 ml of CH_3Li (1.6M in THF) were added and the mixture stirred for 1 h. To a solution of [(cod)Pd(CH_3)(Cl)] (0.290 g, 1.10 mmol), PPh_3 (0.288 g, 1.10 mmol) was added and the resulting suspension was cannulated into the solution of the deprotonated ligand and the mixture was stirred for 3 h. After filtration through celite, the solvent was slowly evaporated, affording the isolation of [(Ph_2AFA)Pd(PPh_3)(CH_3)] as red crystals suitable for X-ray analysis.

^{1}H-NMR ($CDCl_3$, 360 MHz, 25°C): δ 8.53 (d, 1H, *H*1, ^3J = 8.20 Hz), 8.00 (s, 1H, *H*7), 7.52 (d, 2H, C_6H_5), 7.31-7.39 (m, 9H, P-C_6H_5), 7.25-7.20 (m, 6H, P-C_6H_5), 7.12 (t, 1H, C_6H_5), 7.01 (t, 1H, C_6H_5), 6.93 (dd, 1H, *H*3, ^3J = 3.57 Hz), 6.77 (dd, 1H, *H*5, ^3J = 3.57 Hz), 6.45 (t, 1H, *H*4, ^3J = 3.57 Hz), -0.021 (d, 3H, CH_3, *J* = 3.57 Hz). $^{13}C\{^1H\}$ NMR ($CDCl_3$, 90.6 MHz, 25°C): δ 160.71 (*C*1), 158.43 (*C*7), 150.80 (*C*8),

150.10 (*C*12), 134.16 (*C*17, $^{2}J_{C\text{-}P}$ = 11.7 Hz), 131.79 (*C*15), 131.39 (*C*11), 130.89 (*C*16, $^{1}J_{C\text{-}P}$ = 48.9 Hz), 130.09 (*C*19), 128.77 (*C*14), 128.30 (*C*10), 127.94 (*C*18, $^{3}J_{C\text{-}P}$ = 10.3 Hz), 124.39 (*C*3), 123.84 (*C*5), 122.96 (*C*13), 121.16 (*C*9), 119.28 (*C*2), 119.13 (*C*6), 118.06 (*C*4), 3.55 (*C*H$_3$, $^{2}J_{C\text{-}P}$ = 8.5 Hz). Anal. Calcd. For $C_{38}H_{33}N_2PPd$: C, 69.67; H, 5.08; N, 4.28. Found: C, 69.36; H, 4.97; N, 4.15.

Crystal Data

Crystal Description	Dark Red Block	***β* (deg)**	99.393(3)
Empirical Formula	$C_{38}H_{33}N_2PPd$	***γ* (deg)**	90
M_w	655.03	***V* (Å^3)**	3060.4(2)
***T* (K)**	150(2)	***Z***	4
Crystal system	Monoclinic	***μ* (Mo Kα) (mm^{-1})**	0.688
Space group	$P2_1/n$	**No. of independent reflections**	9135 [*R*(int) = 0.0333]
***a* (Å)**	9.0131(3)	**No. of data with $\|F\| > 4\sigma(\|F\|)$**	7534
***b* (Å)**	19.7765(8)	**Absorption Correction**	Multiscan (T_{min} = 0.682, T_{max} = 0.810)
***c* (Å)**	17.4028(8)	***R***	0.0313
***α* (deg)**	90	R_w	0.0826

5.7.9 [Cp*Ru(Ph$_2$AFA)] (12)

[Cp*Ru(CH$_3$CN)$_3$][BF$_4$] (0.250 g, 0.559 mmol) and [(Ph$_2$AFA)$_2$Zn] (0.339, 0.559 mmol) were dissolved in CH_2Cl_2 (30 mL) and the mixture stirred for 1 h. After filtration with a filter-capped cannula, 30 mL of diethyl ether were slowly layered. Upon standing for 1 day, crystals suitable for X-ray had formed, which were isolated and dried under vacuum.

^{1}H-NMR ($CDCl_3$, 360 MHz, 25˚C): δ 8.59 (s, 2H, *H*1/*H*7), 7.37-7.12 (m, 10H, C$_6$*H*$_5$), 5.05 (d, 2H, *H*3/*H*5, ^{3}J = 2.83 Hz), 4.67 (t, 1H, *H*4, ^{3}J = 2.83 Hz), 1.87 (s, 15H, CpC*H*$_3$). ^{13}C{^{1}H} NMR ($CDCl_3$, 90.6 MHz, 20 ˚C): δ 159.36 (*C*=N), 153.09 (N-*C*$_6$H$_5$), 129.07 (*m*-*C*$_6$H$_5$), 124.99 (*p*-*C*$_6$H$_5$), 120.67 (*o*-*C*$_6$H$_5$), 88.09 (*C*$_5$Me$_5$), 83.83 (*C*3/*C*5), 77.20 (*C*2/*C*6), 76.02 (*C*4), 11.83 (C$_5$*Me*$_5$).

Crystal Data

Crystal Description	Red Block	***β* (deg)**	114.164(2)
Empirical Formula	$C_{31}H_{34}Cl_2N_2Ru$	***γ* (deg)**	90
M_w	606.57	***V* (Å^3)**	1512.75(9)
***T* (K)**	220(2)	***Z***	2
Crystal system	Monoclinic	***μ* (Mo Kα) (mm^{-1})**	0.716
Space group	$P2_1$	**No. of independent reflections**	5391 [R(int) = 0.0311]
***a* (Å)**	11.1538(4)	**No. of data with $\|F\| > 4\sigma(\|F\|)$**	5090
***b* (Å)**	11.6438(4)	**Absorption Correction**	Multiscan (T_{min} = 0.698, T_{max} = 0.880)
***c* (Å)**	12.7666(4)	***R***	0.0337
***α* (deg)**	90	R_w	0.0900

5.7.10 [Cp*Ru(Ph$_2$AFA)](H$^+$) (12-(H$^+$))

If **12** is dissolved in non-dry CH_2Cl_2, the protonated species is formed, which can be isolated from CH_2Cl_2 solutions as deep red crystals upon slow evaporation of the solvent. Although the shape and size of the crystals were suitable for X-ray analysis, they did not diffract and molecular structure could not be obtained.

^{1}H-NMR ($CDCl_3$, 360 MHz, 25˚C): δ 16.51 (bt, N-*H*$^+$-N), 8.95 (d, 2H, *H*1/*H*7, ^3J = 7.57), 7.52-7.39 (m, 10H, C_6H_5), 5.66 (d, 2H, *H*3/*H*5, ^3J = 2.99 Hz), 4.20 (t, 1H, *H*4, ^3J = 2.99 Hz), 1.85 (s, 15H, CpC*H*$_3$). ^{13}C{^{1}H} NMR (CD_2Cl_2, 90.6 MHz, 20 ˚C): δ 161.37 (*C*=N), 142.66 (N-*C*$_6$H$_5$), 130.59 (*m*-*C*$_6$H$_5$), 128.45 (*p*-*C*$_6$H$_5$), 119.91 (*o*-*C*$_6$H$_5$), 92.57 (*C*$_5$Me$_5$), 85.47 (*C*3/*C*5), 84.91 (*C*2/*C*6), 79.47 (*C*4), 11.50 (C$_5$*Me*$_5$). MS (FAB, *m/z*): 309 (M$^+$).

5.7.11 [(Cp*Ru)$_2$(Ph$_2$AFA)$_2$Pd][BF$_4$]$_2$ (15)

[Cp*Ru(CH$_3$CN)$_3$][BF$_4$] (0.250 g, 0.559 mmol) and [(Ph$_2$AFA)$_2$Pd] (0.181 g, 0.280 mmol) were stirred in CH_2Cl_2 (40 ml) for 1 h, and the solution filtered with a filter-capped cannula. After storage at -5 ˚C for 2 days, X-ray quality crystals of the desired compound had formed as orange blocks. More crystals suitable for X-ray analysis were obtained from $CHCl_3$ solution via slow evaporation of the solvent.

^{1}H-NMR (CD_3OD, 360 MHz, 25˚C): δ 7.91 (s, 4H, *H*1/*H*7), 7.70-7.67 (m, 8H, m-C_6H_5), 7.56-7.53 (m, 12H, C_6H_5), 5.66 (t, 2H, *H*4, ^3J = 2.80 Hz), 5.40 (d, 4H, *H*3/*H*5, ^3J = 2.80 Hz), 1.58 (s, 30H, CpCH_3). ^{13}C-NMR (CD_3OD, 90.6 MHz, 25˚C): δ 168.47 (*C*=N), 147.91 (N-C_6H_5), 131.02 (C_6H_5), 130.32 (C_6H_5), 123.81 (C_6H_5), 96.01 (*C*4), 88.11 (*C*2-*C*6), 86.18 (C_5Me_5), 77.58 (*C*3-*C*5), 11.57 (C_5Me_5). Anal. Calcd. For $C_{58}H_{60}N_4B_2F_8Ru_2Pd$: C, 53.78; H, 4.67; N, 4.33. Found: C, 53.39; H, 4.43; N, 4.13.

Crystal Data

Crystal Description	Orange Block	***β* (deg)**	104.6070(10)
Empirical Formula	$C_{60}H_{62}B_2Cl_6F_8N_4PdRu$	***γ* (deg)**	90
M_w	767.02	***V* (Å^3)**	3139.21(11)
***T* (K)**	150(2)	***Z***	2
Crystal system	Monoclinic	***μ* (Mo Kα) (mm^{-1})**	1.079
Space group	$P2_1/c$	**No. of independent reflections**	8342 [R(int) = 0.039]
***a* (Å)**	11.0330(2)	**No. of data with $\|F\| > 4\sigma(\|F\|)$**	7050
***b* (Å)**	15.3253(3)	**Absorption Correction**	Semi-empirical (T_{min} = 0.66, T_{max} = 0.87)
***c* (Å)**	19.1861(4)	***R***	0.0489
***α* (deg)**	90	R_w	0.1188

5.7.12 [(Cp*Ru) (Ph'$_2$AFA)Pd(η^3-C_3H_5)][BF_4] (16)

[Cp*Ru(CH_3CN)$_3$][BF_4] (0.100 g, 0.224 mmol) and [(Ph'$_2$AFA)Pd(η^3-C_3H_5)] (0.112 g, 0.224 mmol) were dissolved in 20 ml of CH_2Cl_2 and the mixture stirred for 30 min. After filtration with a filter-capped cannula, the volume was reduced to *ca.* 7 ml and Et_2O (10 ml) was added. After standing for 1 day at room temperature, some yellow crystals had formed which were characterised via X-ray.

^{1}H-NMR (CD_2Cl_2, 360 MHz, 20˚C): δ 7.97 (s, 1H, *H*1/*H*7), 7.89 (s, 1H, *H*1/*H*7), 7.03 (s, 3H, $C_6H_2Me_3$), 6.99 (s, 1H, $C_6H_2Me_3$), 5.61 (m, 1H, Allyl C*H*), 5.14 (d, 1H, *J* = 2.9 Hz, *H*3/*H*5), 5.10 (dd, 1H, *H*4, *J* = 2.9, 2.9 Hz,), 5.05 (d, 1H, *H*3/*H*5, *J* = 2.9 Hz,), 3.08 (d, 1H, Allyl C*H*H, *J* = 12.6 Hz,), 2.88 (d, 1H, Allyl C*H*H, *J* = 6.8 Hz,), 2.69 (s, 3H, $C_6H_2Me_3$), 2.51 (s, 3H, $C_6H_2Me_3$), 2.48 (d, 1H, Allyl C*H*H, *J* = 12.6 Hz,), 2.40 (d, 1H, Allyl C*H*H, *J* = 6.8 Hz,), 2.37 (s, 3H, $C_6H_2Me_3$),

2.36 (s, 3H, $C_6H_2Me_3$), 2.31 (s, 3H, $C_6H_2Me_3$), 2.21(s, 3H, $C_6H_2Me_3$), 1.96 (s, 9H, Cp* CH_3), 1.94 (s, 6H, Cp* CH_3). $^{13}C\{^1H\}$ NMR (CD_2Cl_2, 90.6 MHz, 20˚C): δ 173.3 (*C*1), 173.1 (*C*7), 153.9 (N-$C_6H_2Me_3$), 153.0 (N-$C_6H_2Me_3$), 137.3-121.7 (10C, $C_6H_2Me_3$), 121.0 (Allyl *C*H), 91.74-91.72 (C_5Me_5), 85.77 (*C*3), 85.71 (*C*5), 82.3 (*C*4), 76.73 (*C*2), 76.69 (*C*6), 67.16 (Allyl CH_2), 66.19 (Allyl CH_2), 21.5-19.8 (6C, $C_6H_2Me_3$), 12.74 and 12.72 (C_5Me_5). MS (EI, *m/z*): 739 (M^+).

Crystal Data

Crystal Description	Yellow Plate	***β* (deg)**	95.609(15)
Empirical Formula	$C_{39}H_{49}BCl_2F_4N_2PdRu$	***γ* (deg)**	90
M_w	910.98	***V* (Å^3)**	7871(3)
***T* (K)**	150(2)	***Z***	8
Crystal system	Monoclinic	***μ* (Mo Kα) (mm^{-1})**	1.025
Space group	$P2_1$	**No. of independent reflections**	7520 [*R*(int) = 0.2559]
***a* (Å)**	15.532(3)	**No. of data with $\|F\| > 4\sigma(\|F\|)$**	4049
***b* (Å)**	18.155(4)	**Absorption Correction**	Multiscan (T_{min} = 0.013, T_{max} = 0.930)
***c* (Å)**	28.048(7)	***R***	0.0782
***α* (deg)**	90	R_w	0.2081

5.7.13 [(Ph'$_2$AFA)Pd(Py)(CH$_3$)] (17)

Ph'$_2$AFAH (0.235g, 0.66 mmol) was dissolved in 20 ml of toluene; 0.45 ml of BuLi (1.6 M in hexanes) were added and the mixture stirred for 1 h. Into another Schlenk flask, [(cod)Pd(Me)Cl] (0.175g, 0.66 mmol) was dissolved in toluene (10 ml) and 0.053 ml of dry pyridine was added with a syringe; after 1 min, a white suspension had formed, which was immediately cannulated into the solution of the deprotonated ligand. The mixture was stirred for 12 h and filtered through celite. The solvent was removed, and the black solid obtained was extracted with several 20 ml portions of hexane. By storage of the hexane extraction solutions at -10 ˚C, several amounts of brown solid were obtained, which were isolated and combined. The solid was washed with 5 ml of hexane and dried under vacuum.

5.8 General procedure for ethylene polymerisation

A Büchi autoclave (100 ml) was heated at 80 ˚C under vacuum for 3 h and then cooled to room temperature under an ethylene atmosphere. The autoclave was charged with 20 ml of toluene and then sealed. The pressure of ethylene was set to the desired value and the desired temperature was established by means of an oil bath. After releasing the pressure, a solution of 75 μmol in 5 ml of toluene of the appropriate catalyst (**12-13**) was added. For catalyst **12**, [Ni(cod)$_2$] (150 μmol in 5 ml of toluene) was also added in sequence via cannula. The reactor was sealed and pressurized with ethylene to the desired reaction pressure. The reaction mixture was stirred under constant pressure for 6 h, after which time the pressure was released and the catalyst quenched with acidified methanol. An aliquot of the mother liquor were analyzed by EI-MS to detect formation of oligomers, whereas the polymer produced was collected by filtration and dried overnight under vacuum.

1. F. A. Cotton, *Inorg. Synth.* **1971**, *13*, 160.
2. D. Drew, J. R. Doyle, *Inorg. Synth.* **1990**, *28*, 346.
3. R. E. Rulke, J. M. Ernsting, A. L. Spek, C. J. Elsevier, P. W. N. M. Van Leeuwen, K. Vrieze, *Inorg. Chem.* **1993**, 32, 5769.
4. G. K. Anderson, M. Lin, *Inorg. Synth.* **1990**, *28*, 60.
5. Y. Tatsuno, T. Yoshida, S. Otsuka, *Inorg. Synth.* **1990**, *28*, 342.
6. U. Koelle, J. Kossakowski, *Inorg. Synth.* **1992**, *29*, 225.
7. P. J. Fagan, M. D. Ward, J. C. Calabrese, *J. Am. Chem. Soc.* **1989**, *111*, 1698.
8. A. Zeller, E. Herdtweck, T. Strassner, *Eur. J. Inorg. Chem.* **2003**, 1802.
9. K. Hafner, K. H. Vöpel, G. Ploss, C. König, *Org. Synth.* **1967**, *47*, 52